Journal of Immunology Research

Vascular Macrophages as a Target for Modulation in Vascular Diseases

Lead Guest Editor: Nivin Sharawy
Guest Editors: Mohammad A. Khan and Heather Medbury

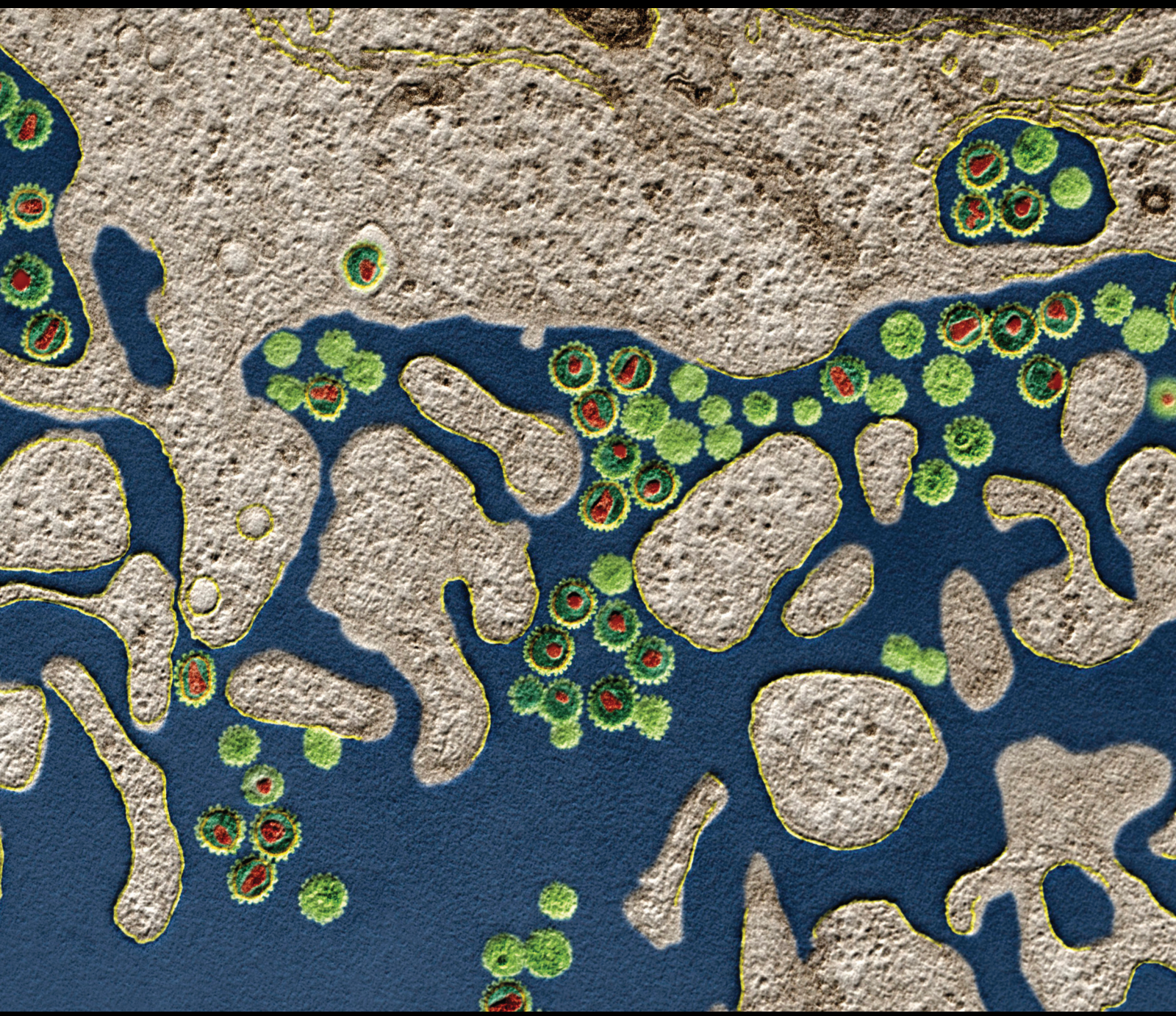

Vascular Macrophages as a Target for Modulation in Vascular Diseases

Journal of Immunology Research

Vascular Macrophages as a Target for Modulation in Vascular Diseases

Lead Guest Editor: Nivin Sharawy
Guest Editors: Mohammad A. Khan and Heather Medbury

Contents

Characterization and Significance of Monocytes in Acute Stanford Type B Aortic Dissection
Li Lu, Yuanhao Tong, Wenwen Wang, Yayi Hou, Huan Dou, and Zhao Liu
Research Article (15 pages), Article ID 9670360, Volume 2020 (2020)

Inhibition of the Ubiquitin-Activating Enzyme UBA1 Suppresses Diet-Induced Atherosclerosis in Apolipoprotein E-Knockout Mice
Jiawei Liao, Xiaolei Yang, Qiuyue Lin, Shuang Liu, Yunpeng Xie, Yunlong Xia, and Hui-Hua Li
Research Article (10 pages), Article ID 7812709, Volume 2020 (2020)

Involvement of lncRNAs and Macrophages: Potential Regulatory Link to Angiogenesis
Yang Jia and Yedi Zhou
Review Article (9 pages), Article ID 1704631, Volume 2020 (2020)

Nε-Carboxymethyl-Lysine Negatively Regulates Foam Cell Migration via the Vav1/Rac1 Pathway
Zhengyang Bao, Lili Zhang, Lihua Li, Jinchuan Yan, Qiwen Pang, Zhen Sun, Yue Geng, Lele Jing, Chen Shao, and Zhongqun Wang
Research Article (10 pages), Article ID 1906204, Volume 2020 (2020)

Galectin-3 Is a Potential Mediator for Atherosclerosis
Ziyu Gao, Zhongni Liu, Rui Wang, Yinghong Zheng, Hong Li, and Liming Yang
Review Article (11 pages), Article ID 5284728, Volume 2020 (2020)

Macrophage-Based Therapies for Atherosclerosis Management
Renyi Peng, Hao Ji, Libo Jin, Sue Lin, Yijiang Huang, Ke Xu, Qinsi Yang, Da Sun, and Wei Wu
Review Article (11 pages), Article ID 8131754, Volume 2020 (2020)

Vascular Macrophages in Atherosclerosis
Hailin Xu, Jingxin Jiang, Wuzhen Chen, Wenlu Li, and Zhigang Chen
Review Article (14 pages), Article ID 4354786, Volume 2019 (2019)

Distinct Redox Signalling following Macrophage Activation Influences Profibrotic Activity
Caitlin V. Lewis, Antony Vinh, Henry Diep, Chrishan S. Samuel, Grant R. Drummond, and Barbara K. Kemp-Harper
Research Article (15 pages), Article ID 1278301, Volume 2019 (2019)

Urinary NGAL and RBP Are Biomarkers of Normoalbuminuric Renal Insufficiency in Type 2 Diabetes Mellitus
Aimei Li, Bin Yi, Yan Liu, Jianwen Wang, Qing Dai, Yuxi Huang, Yan Chun Li, and Hao Zhang
Research Article (11 pages), Article ID 5063089, Volume 2019 (2019)

Monocyte Subsets, Stanford-A Acute Aortic Dissection, and Carotid Artery Stenosis: New Evidences
Noemi Cifani, Maria Proietta, Maurizio Taurino, Luigi Tritapepe, and Flavia Del Porto
Research Article (6 pages), Article ID 9782594, Volume 2019 (2019)

Promiscuous Chemokine Antagonist (BKT130) Suppresses Laser-Induced Choroidal Neovascularization by Inhibition of Monocyte Recruitment
Shira Hagbi-Levi, Michal Abraham, Liran Tiosano, Batya Rinsky, Michelle Grunin, Orly Eizenberg, Amnon Peled, and Itay Chowers
Research Article (12 pages), Article ID 8535273, Volume 2019 (2019)

Functions of Exosomes in the Triangular Relationship between the Tumor, Inflammation, and Immunity in the Tumor Microenvironment
Tiantian Wang, Moussa Ide Nasser, Jie Shen, Shujuan Qu, Qingnan He, and Mingyi Zhao
Review Article (10 pages), Article ID 4197829, Volume 2019 (2019)

Hindawi
Journal of Immunology Research
Volume 2020, Article ID 9670360, 15 pages
https://doi.org/10.1155/2020/9670360

Research Article

Characterization and Significance of Monocytes in Acute Stanford Type B Aortic Dissection

Li Lu,[1,2] Yuanhao Tong,[1] Wenwen Wang,[1] Yayi Hou,[2,3,4] Huan Dou,[2,3,4] and Zhao Liu[1]

[1]*Department of Vascular Surgery, Nanjing Drum Tower Hospital, The Affiliated Hospital of Nanjing University Medical School, Nanjing 210008, China*
[2]*The State Key Laboratory of Pharmaceutical Biotechnology, Division of Immunology, Medical School, Nanjing University, Nanjing 210093, China*
[3]*Department of Rheumatology and Immunology, Nanjing Drum Tower Hospital, The Affiliated Hospital of Nanjing University Medical School, Nanjing 210008, China*
[4]*Jiangsu Key Laboratory of Molecular Medicine, Nanjing University, Nanjing 210093, China*

Correspondence should be addressed to Yayi Hou; yayihou@nju.edu.cn, Huan Dou; dg1930026@smail.nju.edu.cn, and Zhao Liu; liuzhao83@gmail.com

Received 21 October 2019; Accepted 5 February 2020; Published 15 May 2020

Guest Editor: Nivin Sharawy

Acute aortic dissection (AAD) is one of the most common fatal diseases noted in vascular surgery. Human monocytes circulate in dynamic equilibrium and display a considerable heterogeneity. However, the role of monocytes in AAD remains elusive. In our recent study, we firstly obtained blood samples from 22 patients with Stanford type B AAD and 44 age-, sex-, and comorbidity-matched control subjects. And the monocyte proportions were evaluated by flow cytometry. Results showed that the percentage of total $CD14^+$ monocytes in the blood samples of Stanford AAD patients was increased significantly compared with that of normal volunteers ($P < 0.0005$), and the absolute numbers of $CD14^{bright}CD16^+$ and $CD14^{bright}CD16^-$ monocytes both increased significantly regardless of the percentage of PBMC or $CD14^+$ cells, while $CD14^{dim}CD16^+$ monocytes displayed the opposite tendency. However, the percentage of $CD14^+$ cells and its three subsets demonstrated no correlation with D-dimer (DD) and C-reactive protein (CRP). Then, blood mononuclear cell (PBMC) samples were collected by Ficoll density gradient centrifugation, followed with $CD14^+$ magnetic bead sorting. After the purity of $CD14^+$ cells was validated over 90%, AAD-related genes were concentrated in $CD14^+$ monocytes. There were no significant differences observed with regard to the mRNA expression levels of *MMP1* ($P = 0.0946$), *MMP2* ($P = 0.3941$), *MMP9* ($P = 0.2919$), *IL-6* ($P = 0.4223$), and *IL-10* ($P = 0.3375$) of the $CD14^+$ monocytes in Stanford type B AAD patients compared with those of normal volunteers. The expression levels of *IL-17* ($P < 0.05$) was higher in Stanford type B AAD patients, while the expression levels of TIMP1($P<0.05$), TIMP2($P<0.01$), *TGF-β1* ($P < 0.01$), *SMAD3* ($P < 0.01$), *ACTA2* ($P < 0.001$), and *ADAMTS-1* ($P < 0.001$) decreased. The data suggested that monocytes might play an important role in the development of Stanford type B AAD. Understanding of the production, differentiation, and function of monocyte subsets might dictate future therapeutic avenues for Stanford type B AAD treatment and can aid the identification of novel biomarkers or potential therapeutic targets for decreasing inflammation in AAD.

1. Introduction

Acute aortic dissection (AAD) is one of the most common emergencies of vascular surgery. A recent study demonstrated that the incidence of AAD was increased during the past decades [1, 2]. During the development of AAD, blood transfuses aorta through the ruptured aortic or blood vessels and separates the normal structure of the aorta, spreading into the media. This process results in the gradual expansion of the axial ends to form the true and false two-chamber state of the aorta, which is one of the most typical characteristics of AAD [3, 4]. In a recent study, AAD was divided into two types according to whether the ascending aorta was involved (type A) or not (type B) according to the Stanford system,

which is a widely accepted classification system for AAD [5, 6]. Patients with Stanford type B AAD account for 25% to 40% of all aortic dissections and remain more likely to present with hypertension than those with Stanford type A AAD [7]. Furthermore, the majority of patients presenting with Stanford type A AAD are managed surgically (86% overall), while Stanford type B AAD is treated medically (63%), which makes our preclinical research of Stanford type B AAD more meaningful [8]. It has been also suggested that inflammation plays an important role in the development of AAD, which is receiving attention gradually [9, 10]. Several studies demonstrated that local inflammation was enhanced following the development of AAD, which was mainly reflected by the infiltration of large numbers of mononuclear macrophages, multinuclei leukocytes, and T/B lymphocytes [11, 12]. These inflammatory cells aggregate in the aorta and secrete inflammatory mediators to degrade the extracellular matrix, resulting in weakening of the aortic wall and reduced ability for gradual stress resistance [13]. In addition to the degradation of the extracellular matrix, local inflammation further causes ischemia, degeneration, and necrosis of aortic smooth muscle cells [14]. Flow dynamics (usually hypertension) eventually lead to rupture or dilation of the aortic intima, which in turn induces AAD [15]. Although several studies have been reported on the pathogenesis of AAD, it is well established that inflammation plays an important role in the development of this disease [16]. However, little is known with regard to the specific way by which inflammation participates in the development of Stanford type B AAD, especially the role of monocytes.

Monocytes are important cells of the innate immunity that are present in the circulation system. Based on the expression of the surface markers CD14 and CD16, a new nomenclature for dividing monocytes into three subgroups has been approved by the International Society of Immunology's Nomenclature Committee. This classification is the following: $CD14^{bright}CD16^{-}$ monocytes, $CD14^{bright}CD16^{+}$ monocytes, and $CD14^{dim}CD16^{+}$ monocytes [17]. The aforementioned cells circulate in dynamic equilibrium, and the kinetics underlying their production, differentiation, and disappearance are critical to understanding both homeostasis and inflammatory responses. Different monocyte subsets have different biological functions. $CD14^{bright}CD16^{-}$ monocytes are also known as classical monocytes, having superior phagocytosis activities. $CD14^{bright}CD16^{+}$ monocytes are also known as inflammatory monocytes, which are the inflammatory effector cells that stimulate the proliferation of T cells, the production of excessive reactive oxygen species (ROS), and the promotion of angiogenesis. $CD14^{dim}CD16^{+}$ monocytes are also known as nonclassical monocytes, used mainly for patrol of exogenous pathogens, as well as for antiviral defense [18, 19]. It was reported that monocytes recruited to areas of inflammation could differentiate into macrophages, which were involved in local aortic inflammatory responses in a mouse atherosclerosis model [20]. The inhibition of the differentiation of monocytes and the recruitment of mononuclear-macrophages to the aorta significantly improved the progression of atherosclerosis [21]. In addition, in abdominal aortic aneurysm (AAA), the accumulation of macrophages and the expression levels of the monocyte chemoattractant protein-1 (MCP-1) were both increased in the AAA wall [22, 23]. However, a limited number of studies have been performed with regard to the characteristics of monocytes in AAD. The specific mechanism of monocyte subsets with regard to the pathogenesis of AAD remains unclear. The purpose of the present study was to investigate the monocytic population and mediators on blood samples from patients with AAD.

2. Materials and Methods

2.1. Patient Eligibility Criteria. In the present study, 22 patients with AAD (Stanford type B) and 44 healthy volunteers were included. The acute Stanford type B aortic dissections are aortic dissections that arise when the entry tear is distal to the subclavian artery. The included criteria include the Acute Stanford type B aortic dissections which are one of the aortic dissections, which happened in 2 weeks and arise when the entry tear is distal to the subclavian artery. Acute Stanford B-type aortic dissection exclusion criteria are as follows: (1) Stanford B-type aortic dissection over 2 weeks, (2) aorta dissection involving the start of the left subclavian artery above the aorta, (3) the combination of immune diseases of Stanford type B aortic dissection, (4) Stanford type B aortic dissection patients with genetic diseases (such as Marfan syndrome), and (5) Stanford B-type aortic dissection after thoracic endovascular aortic repair (TEVAR) operation. In the parameters, gender, age, and history of hyperlipidemia did not exhibit a significant difference ($P > 0.05$) between the two groups, while significant differences were noted with regard to the variable history of diabetes ($P < 0.05$), smoking ($P < 0.01$), and hypertension ($P < 0.001$). All samples were collected from Nanjing Drum Tower Hospital, the Affiliated Hospital of Nanjing University Medical School. All volunteers provided written informed consent, and all studies were conducted according to the principles of the Declaration of Helsinki following approval by the relevant institutional review boards.

2.2. Flow Cytometry Analysis. All blood samples were transferred to the EDTA collecting tubes (Becton Dickinson). A total of 50 μl blood was obtained and transferred into the corresponding flow tubes. The blood samples were treated with FC blocker (Miltenyi Biotec, Germany) at room temperature for 15 min and subsequently stained with Alexa Fluor 488-labeled anti-human CD14 (Miltenyi Biotec, Germany) and APC-labeled anti-human CD16 (Miltenyi Biotec, Germany). The aforementioned antibodies were incubated at 4°C for 30 min in the dark. Subsequently, the blood samples were treated with 1x FACS™ lysis solution for approximately 10 min, and FACS buffer was added. The samples were finally centrifuged at 300 g for 5 min at 4°C, rinsed again with FACS buffer, and finally resuspended in 150 μl FACS buffer for subsequent testing by flow cytometry (BD Accuri™ C6, BD Biosciences, USA). All the antibodies were used according to the manufacturer's instructions. Classical monocyte cells were defined as $CD14^{bright}CD16^{-}$, whereas inflammatory

monocyte cells were defined as $CD14^{bright}CD16^{+}$ and nonclassical monocyte cells as $CD14^{dim}CD16^{+}$.

2.3. Magnetic Bead Sorting. Blood samples were collected from 8 patients with AAD (Stanford type B) and 8 healthy volunteers. Total blood was isolated by a Ficoll density gradient centrifugation step in order to obtain peripheral blood mononuclear cells (PBMCs). The cell number was determined, and the cell suspension was centrifuged at 300 g for 10 min. The supernatant was aspirated completely, and the pellet was resuspended in 80 μl buffer per 10^7 of total cells. Subsequently, 20 μl CD14 Microbeads (Miltenyi Biotec, Germany) was added per 10^7 total cells, mixed, and incubated for 15 min at 2-8°C. The cells were washed by addition of 1-2 ml buffer per 10^7 total cells and centrifuged at 300 g for 10 min. The supernatant was removed completely, and the cell pellet (10^7 cells) was resuspended in 500 μl buffer and further processed for magnetic separation. An appropriate MACS column and a MACS separator were selected according to the number of total cells and the number of $CD14^{+}$ cells. LS columns (Miltenyi Biotec, Germany) were used for separation. Initially, the column was placed in the magnetic field of a suitable MACS separator (Miltenyi Biotec, Germany) and prepared by rinsing with 3 ml FACS buffer. The cell suspension was applied onto the column, and new FACS buffer was added when the column reservoir was empty. Subsequent washing steps were performed by adding 3 ml FACS buffer three times, and the column was removed from the separator following removal of the content in the column reservoir. The cell suspension was transferred to a suitable collection tube, and 5 ml FACS buffer was pipetted onto the column. The magnetically labeled cells were immediately removed by pushing the plunger into the column, and the collected cells were $CD14^{+}$ cells. A minor fraction of the $CD14^{+}$ cells was centrifuged at 300 g for 5 min at 4°C and resuspended in 100 μl FACS buffer. The cells were stained with Alexa Fluor 488-labeled anti-human CD14 antibody (Alexa Fluor 488-CD14, Miltenyi Biotec, Germany) and incubated at 4°C for 30 min in the dark. The cells were further centrifuged at 300 g for 5 min at 4°C, resuspended in 150 μl FACS buffer, and subsequently detected by flow cytometry (BD Accuri™ C6, BD Biosciences, USA). The remaining $CD14^{+}$ cells were centrifuged at 300 g for 5 min, and following aspiration of the supernatant, they were subsequently tested.

2.4. Quantitative Polymerase Chain Reaction (RT-qPCR). Total RNA from $CD14^{+}$ cells were extracted by the TRIzol reagent (Invitrogen, USA) and reverse-transcribed by a reverse transcription kit (HiScript® II Q RT SuperMix for qPCR, Vazyme Biotech, Nanjing, China). Subsequently, the cDNAs were used as templates for RT-qPCR analysis performed on the BIOER Line Gene 9640 detection system (Hangzhou, China). The Ct value and the relative expression levels of each gene were calculated according to the $2^{-\Delta\Delta Ct}$ formula. The relative amount of the target gene and that of the reference gene *GAPDH* were obtained. All the reactions were repeated three times. All RNA samples exhibited a 260/280 ratio of ≈2.0. The primer sequences used are shown in Table 1.

2.5. Statistical Analysis. The data were expressed as the mean ± SEM. Statistical analyses were performed by GraphPad Prism 5 (San Diego, CA, USA). Multigroup comparisons were analyzed by Student's *t*-test or the one-way ANOVA test. A P value less than 0.05 ($P < 0.05$) was considered for significant differences. The experiments were repeated at least three times.

3. Results

3.1. Clinical Characteristics of the Patients with AAA. The D-dimer values and the CRP values in Stanford type B AAD patients were higher than those noted in healthy control subjects ($P < 0.001$), while there was significant difference in history of diabetes ($P < 0.05$), smoking ($P < 0.01$), and hypertension ($P < 0.001$). In addition, apparent differences were noted in the percentage of neutrophils ($P < 0.01$), lymphocytes ($P < 0.001$), WBC count, and monocytes ($P < 0.001$) between these two groups (Table 2).

3.2. The Behaviors of Monocyte Subsets in Stanford Type B AAD. Currently, numerous studies have demonstrated that aortic inflammation is inseparable for the development of aortic disease and that monocytes play an important role in inflammation. Following the induction of inflammation in local tissues, monocytes are recruited to the tissues and differentiate into macrophages, which secrete inflammatory mediators and participate in local inflammatory reactions [24–26]. In order to demonstrate the population of monocytes in Stanford type B AAD patients, we performed flow cytometry analysis with human blood samples. The results indicated that the percentage of $CD14^{+}$ cells in AAD patients was significantly higher than that of normal volunteers (Figures 1(a) and 1(b)). To further confirm the biological features of the three monocyte subsets, we analyzed their percentages in PBMCs. The gating strategy is shown in Figure 1(c) [27]. The results indicated that $CD14^{dim}CD16^{+}$ monocytes exhibited a significant decrease in the proportion of PBMCs ($P < 0.05$), while the percentages of the two other monocyte subsets ($CD14^{bright}CD16^{-}$, $CD14^{bright}CD16^{+}$) were increased significantly ($P < 0.001$) (Figure 1(d)). Due to the significant increase caused in the percentage of $CD14^{+}$ cells in PBMC ($P < 0.001$), we analyzed the percentages of the three monocyte subsets in $CD14^{+}$ cells.

3.3. Correlation Analysis between Monocyte and D-Dimer and C-Reactive Protein. DD and CRP were viewed as diagnostic and prognostic tools for AAD. D-dimer is a fibrin degradation product, generated following fibrinolysis of a thrombus [28–30]. C-reactive protein (CRP) is an acute phase reactant, which is a sensitive and a nonspecific inflammatory marker [30–33]. The serum levels of DD and CRP are usually used to assess the overall severity of acute diseases or to predict adverse events [34, 35]. The correlation analysis indicated no significant correlation between DD and the percentages of monocyte subsets in PBMCs (all $R^2 < 0.5$ and $P > 0.05$) (Figure 2(a)). Similar results were observed with regard to the correlation between DD and the percentages of monocyte subsets in $CD14^{+}$ cells (all $R^2 < 0.5$ and $P > 0.05$)

Table 1: Primer sequences for quantitative real-time polymerase chain reaction.

Gene name	Forward primer	Reverse primer
MMP9	GGACGATGCCTGCAACGT	CAAATACAGCTGGTTCCCAATCT
MMP1	CATGAAAGGTGGACCAACAATTT	CCAAGAGAATGGCCGAGTTC
MMP2	TACACCAAGAACTTCCGTCTGT	AATGTCAGGAGAGGCCCCATA
TGF-β1	CTAATGGTGGAAACCCACAACG	TATCGCCAGGAATTGTTGCTG
SMAD3	ACCATCCCCAGGTCCCTGGATGGCC	AACTCGGCCGGGATCTCTGTGTGGCGT
ACTA2	TCAATGTCCCAGCCATGTAT	CAGCACGATGCCAGTTGT
TIMP1	CTTCTGCAATTCCGACCTCGT	ACGCTGGTATAAGGTGGTCTG
TIMP2	AAGCGGTCAGTGAGAAGGAAG	GGGGCCGTGTAGATAAACTCTAT
IL-6	ACTCACCTCTTCAGAACGAATTG	CCATCTTTGGAAGGTTCAGGTTG
IL-10	TCAAGGCGCATGTGAACTCC	GATGTCAAACTCACTCATGGCT
IL-17	TCCCACGAAATCCAGGATGC	GGATGTTCAGGTTGACCATCAC
ADAMTS-1	CAGAGCACTATGACACAGCAA	AGCCATCCCAAGAGTATCACA
GAPDH	AGAAGGCTGGGGCTCATTTG	AGGGGCCATCCACAGTCTTC

Table 2: Clinical data of patients.

Characteristics	Healthy control ($n = 44$)	AAD patient ($n = 22$)	χ^2 or t	P value
Mean age	52.89 ± 15.24	55.33 ± 13.32	0.744	0.459
Gender (M/F)	25/19	15/7	2.652	0.103
Smoking history	10 (22.73%)	12 (54.55%)	6.682	0.009**
Hypertension (%)	9 (20.45%)	14 (63.64%)	12.05	<0.001***
Hyperlipidemia (%)	12 (27.27%)	9 (40.91%)	1.257	0.262
Diabetes (%)	2 (4.54%)	6 (27.27%)	4.991	0.026*
DD (mg/l)	0.26 ± 0.15	3.73 ± 2.54	8.875	<0.001***
CRP (mg/l)	2.18 ± 1.27	30.57 ± 24.76	7.478	<0.001***
WBC (10^9/l)	6.38 ± 1.42	10.48 ± 2.02	9.368	<0.001***
NE (%)	59.92 ± 6.81	67.21 ± 10.63	3.319	0.002**
LY (%)	33.12 ± 6.93	24.25 ± 6.83	4.853	<0.001***
MO (%)	5.64 ± 1.12	9.21 ± 2.32	8.276	<0.001***

DD: D-dimer; CRP: C-reactive protein; NE (%): neutrophil percentage; LY (%): lymphocyte percentage; MO (%): monocyte percentage. Values were expressed as the mean ± SD or as indicated. The data of D-dimer was detected by an automatic blood coagulation analyzer (CA7000, Sysmex, Inc., Japan), and the data of CRP was analyzed by an automatic biochemical analyzer (C8000, Abbott, Inc., USA). The data were means ± SEM. $^*P < 0.05$, $^{**}P < 0.01$, and $^{***}P < 0.005$ vs. healthy control.

(Figure 2(b)), while a weaker correlation between CRP and the percentages of monocyte subsets was noted in the present study (all $R^2 < 0.5$ and $P > 0.05$) (Figures 2(c) and 2(d)).

3.4. CD14$^+$ Monocyte Gene Detection. To further explore the characteristics of monocytes in Stanford type B AAD patients, we attempted to obtain human CD14$^+$ monocytes by magnetic bead sorting. The percentage of CD14$^+$ monocytes was approximately 5% of the total cells (Figure 3(a)). Following gradient density centrifugation, the percentage of CD14$^+$ monocytes in PBMCs increased to approximately 30% (Figure 3(b)). Finally, the purity of CD14$^+$ monocytes was higher than 90% following magnetic bead sorting (Figure 3(c)). On this basis, we detected several genes by RT-qPCR, which were important for the development of AAD in CD14$^+$ monocytes. The results indicated that the expression levels of the matrix metalloproteinase family genes (*MMP1*, *MMP2*, and *MMP9*) were not significantly different between Stanford type B AAD patients and normal volunteers (Figure 4(a)). The expression levels of the tissue inhibitor matrix metalloproteinase genes (*TIMP1* and *TIMP2*) were decreased ($P < 0.05$) (Figure 4(b)). Similarly, the levels of transforming growth factor-β1 (*TGF-β1*), SMAD3, alpha-actin (*ACTA2*), and a disinterring and metalloproteinase with thrombospondin motifs 1 (*ADAMTS-1*) were decreased (Figure 4(c)). The mRNA expression levels of *IL-6* and *IL-10* indicated no significant difference between Stanford type B AAD patients and normal volunteers, while *IL-17* levels were apparently increased (Figure 4(d)).

4. Discussion

Acute aortic dissection (AAD) is the most serious clinical emergency in aortic disease. It exhibits an acute onset, rapid

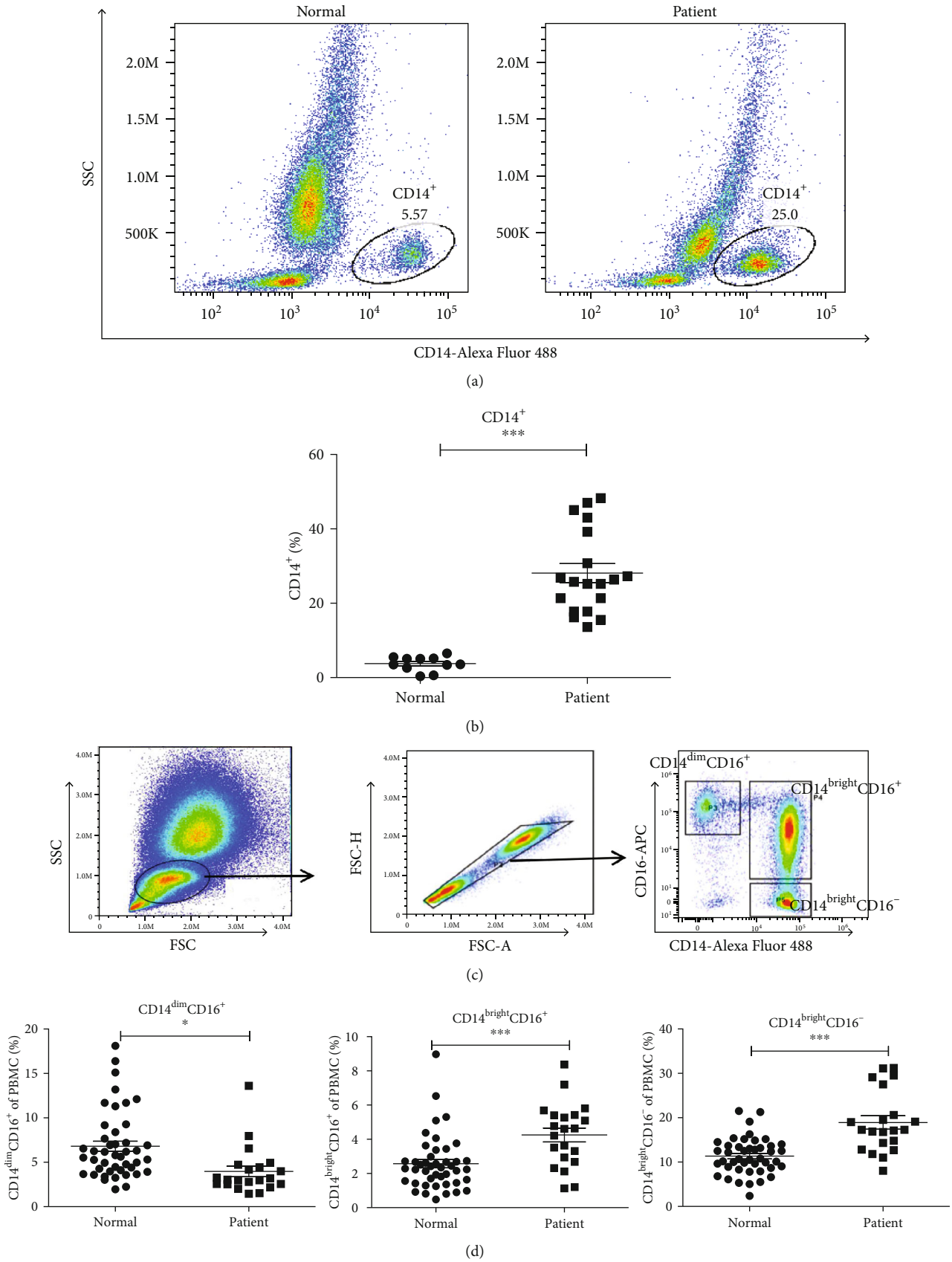

Figure 1: Continued.

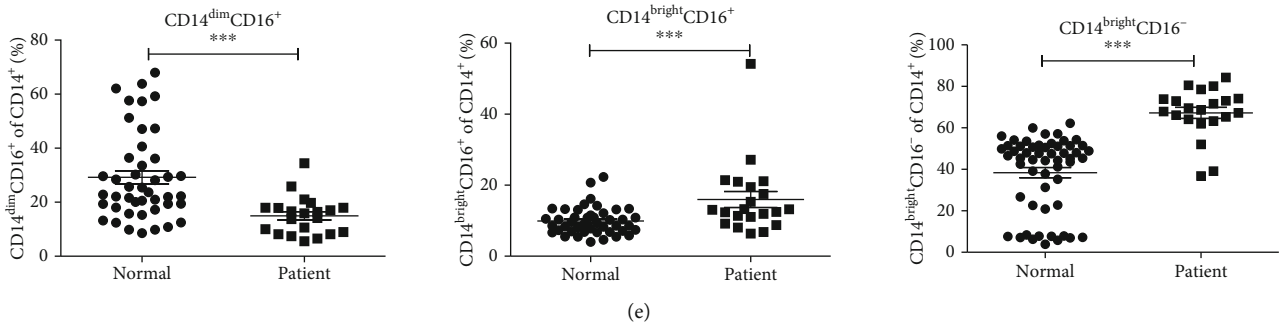

Figure 1: (a) Flow cytometry analysis of $CD14^+$ monocytes in blood of normal control and Stanford type B AAD patients; (b) the statistical graph of (a); (c) gating strategy of monocyte subsets via flow cytometry: $CD14^{bright}CD16^-$ (classic monocytes), $CD14^{bright}CD16^+$ (intermediate), and $CD14^{dim}CD16^+$ (nonclassical); (d) the statistical graph in the percentage of three monocyte subsets in PBMC; (e) the statistical graph in the percentage of three monocyte subsets in $CD14^+$ monocytes; data were shown as the mean ± SEM (standard error of the mean). Stanford type B AAD patient: $n = 22$; normal control $n = 44$. The data were means ± SEM. $^*P < 0.05$, $^{**}P < 0.01$, and $^{***}P < 0.005$ vs. normal group.

development, morbidity complications, a high mortality rate, and an increased misdiagnosis rate [4, 5, 36]. Additional studies have contributed significantly to the prevention, diagnosis, and treatment of AAD diseases. In the present study, we demonstrated that the percentages of total monocytes and the subsets in the blood samples of Stanford type B AAD patients were markedly altered, although no apparent correlation with DD and CRP was noted. However, several genes associated with AAD (*TIMP1*, *TIMP2*, *TGF-β1*, *SMAD3*, *ACTA2*, *ADAMTS-1*, and *IL-17*) demonstrated significant changes in their levels in Stanford type B AAD patients. The investigation of the number of $CD14^+$ monocytes is required to further understand the characteristics of monocytes in AAD.

It is well known that the aorta is composed of a large number of extracellular matrix components for the maintenance of the arterial blood flow and the blood pressure. Following degradation of these structures, the arterial wall is dilated and ruptures [3, 37]. Recent studies have demonstrated that multiple inflammatory cells are involved in the remodeling of aortic vascular tissues, such as activated T and B cells and mononuclear-macrophages [38–40], indicating that inflammation participates in the development of AAD by regulating the number, location, and functional balance of the inflammatory cells. As one of the most important inflammatory cells, monocytes can participate in the vascular remodeling process via different mechanisms of action. However, a limited number of studies have explored these pathways. Previous studies have reported that the percentage of monocytes in blood of Stanford A AAD patients was increased [41], while there were no related reports in patients with Stanford type B AAD. The results of the present study indicated by flow cytometry that the percentage of $CD14^+$ cells in the blood of Stanford type B AAD patients was higher than that of normal volunteers. The findings indicated that monocytes were multiplied and recruited to areas of inflammation where they differentiated and acted as effector cells to respond to various biological changes [42].

From 2010, a new nomenclature for classifying monocytes into three subgroups has been approved by the International Society of Immunology's Nomenclature Committee. This classification is based on the expression levels of the surface markers CD14 and CD16 and is the following: $CD14^{bright}CD16^-$, $CD14^{bright}CD16^+$, and $CD14^{dim}CD16^+$ [16]. $CD14^{bright}CD16^-$ monocytes comprise 80–90% of the monocyte pool with the remaining 10-20% being shared by $CD14^{bright}CD16^+$ and $CD14^{dim}CD16^+$ monocytes [43]. The features of these three types of monocytes were examined in Stanford type B AAD patients. The monocytes were gated according to their CD14 and CD16 expression, and the results demonstrated that the percentages of $CD14^{dim}CD16^+$ monocytes in PBMC and in $CD14^+$ cells were significantly decreased in AAD patients, while the percentages of the other two subsets ($CD14^{bright}CD16^-$ and $CD14^{bright}CD16^+$) were markedly increased. Similar results were observed in other types of diseases. For example, the number of $CD14^{bright}CD16^+$ monocytes in patients with coronary heart disease was higher and exhibited a positive correlation with atherogenic plaque formation [44]. A higher increase of $CD14^{bright}CD16^+$ monocytes and lower levels of $CD14^{bright}CD16^-$ monocytes in patients with acute takotsubo cardiomyopathy has been previously shown [45]. Tsujioka et al. demonstrated that the peak levels of $CD14^{bright}CD16^-$ monocytes exhibited a negative association with the recovery of left ventricular function following acute myocardial infarction [46]. $CD14^{bright}CD16^-$ and $CD14^{bright}CD16^+$ monocytes are inflammatory effectors recruited in inflammatory sites in response to inflammatory stimuli. It has been shown that the $CD14^{bright}CD16^-$ monocytes mature via a continuum to $CD14^{bright}CD16^+$ monocytes and subsequently to $CD14^{dim}CD16^+$ monocytes [47]. We proposed that the decrease of $CD14^{dim}CD16^+$ monocytes might be due to the reduced maturation of $CD14^{bright}CD16^-$ monocytes [18]. Furthermore, we considered that the infiltration of the macrophages detected in the aorta might result from the migration of circulating monocytes, rather than the localization of the resident aorta macrophages. They are involved in the remodeling of aortic blood vessels. Therefore, the increase in the percentages of these two monocytes was cognitively compatible. It was

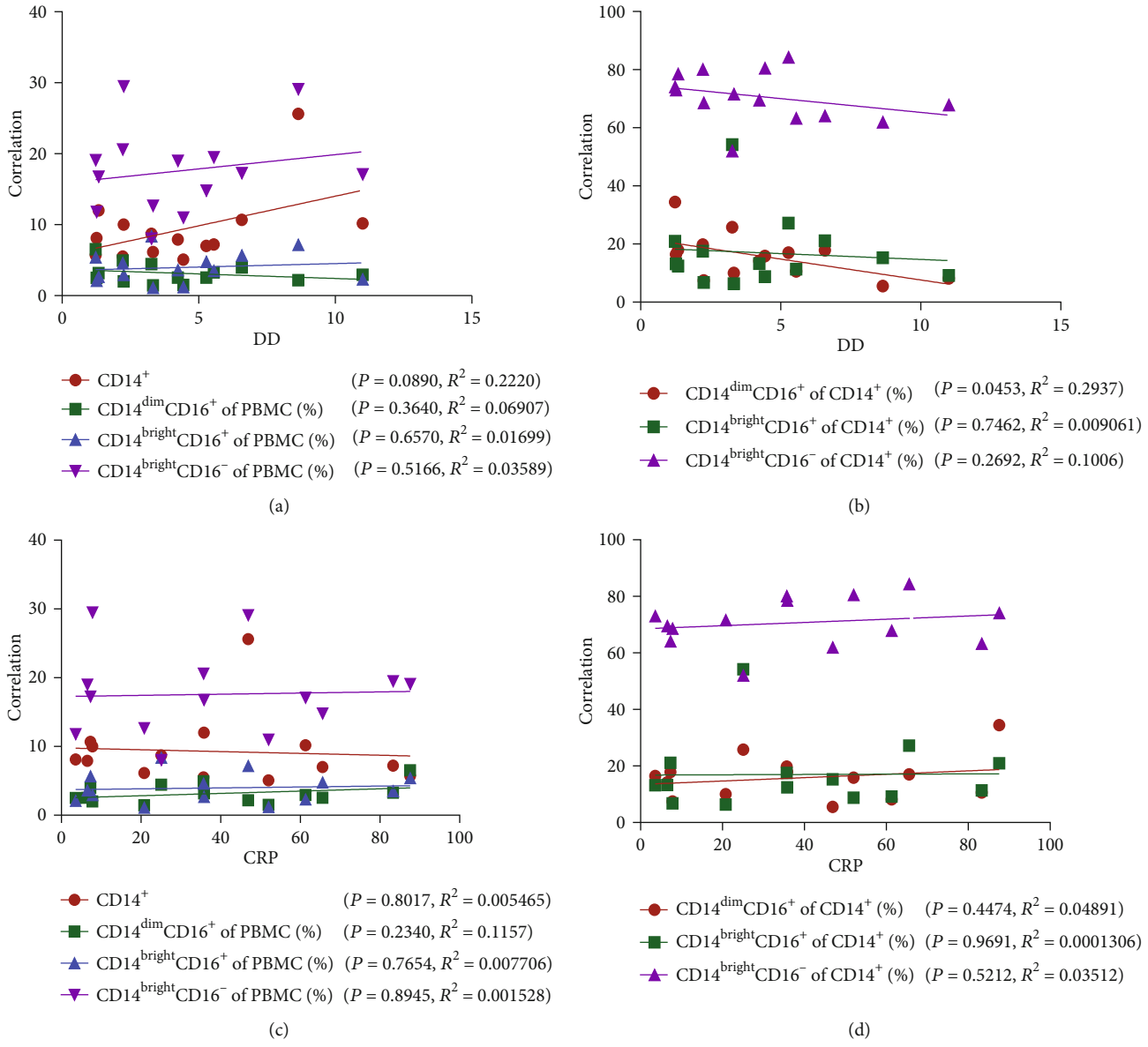

Figure 2: (a) Correlation analysis between the serum levels of DD and the percentage of monocyte subsets ($CD14^{dim}CD16^{+}$, $CD14^{bright}CD16^{+}$, and $CD14^{bright}CD16^{-}$) in PBMC. $P > 0.05$. (b) Correlation analysis between the serum levels of DD and the percentage of monocyte subsets ($CD14^{dim}CD16^{+}$, $CD14^{bright}CD16^{+}$, and $CD14^{bright}CD16^{-}$) in $CD14^{+}$ cells. $P > 0.05$. (c) Correlation analysis between the serum levels of CRP and the percentage of monocytes subsets ($CD14^{dim}CD16^{+}$, $CD14^{bright}CD16^{+}$, $CD14^{bright}CD16^{-}$) in PBMC. $P > 0.05$. (d) Correlation analysis between the serum levels of CRP and the percentage of monocyte subsets ($CD14^{dim}CD16^{+}$, $CD14^{bright}CD16^{+}$, and $CD14^{bright}CD16^{-}$) in $CD14^{+}$ cells. $P > 0.05$; $n = 14$. The data were means ± SEM. $^{*}P < 0.05$, $^{**}P < 0.01$, and $^{***}P < 0.005$ vs. normal group.

hypothesized that the reduction in the number of noncanonical monocytes was mediated by the decreased maturation of classical monocytes. The maturation pathway of monocytes involves the maturation of $CD14^{bright}CD16^{-}$ monocytes to $CD14^{bright}CD16^{+}$ [17, 27]. In summary, the results indicated that these three monocyte subsets might play different roles in the development of Stanford type B AAD.

D-dimer (DD) is a specific protein fiber degradation product that is formed by plasmin hydrolysis. DD is released in large quantities following thrombosis, resulting in elevated levels of this biomarker in the serum [48, 49]. Therefore, the serum levels of DD are considered an optimal diagnostic tool for deep vein thrombosis, pulmonary embolism, and AAD [50–52]. This assessment was well recognized in the diagnosis of acute aortic syndrome (including AAD) [1, 52–54]. In a previous study conducted in 2006, D-dimer testing (DT) was performed in 113 consecutive AAD patients within 24 h of symptom onset in the Osaka Mishima Emergency and Critical Care Center [55]. The results indicated that 104 (92%) AAD patients were positive for DT [55]. In the same year, the University Hospital of Strasbourg in France performed

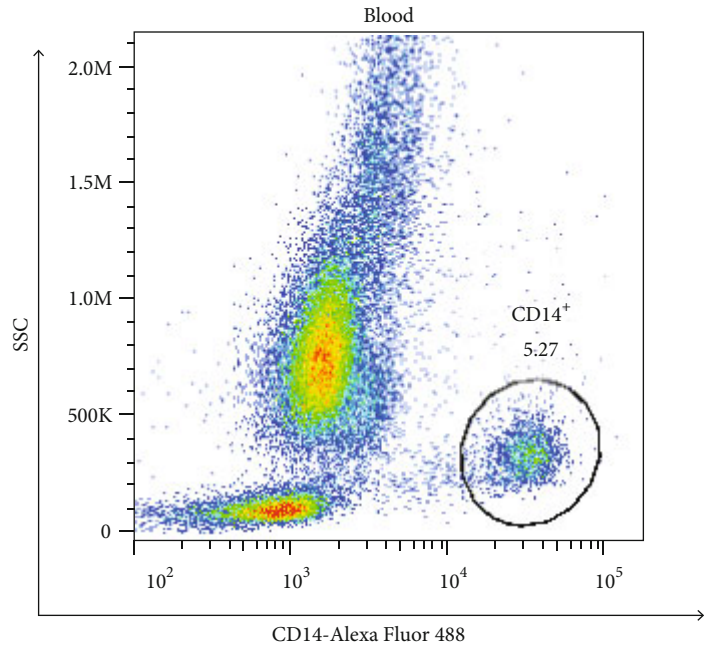

(a)

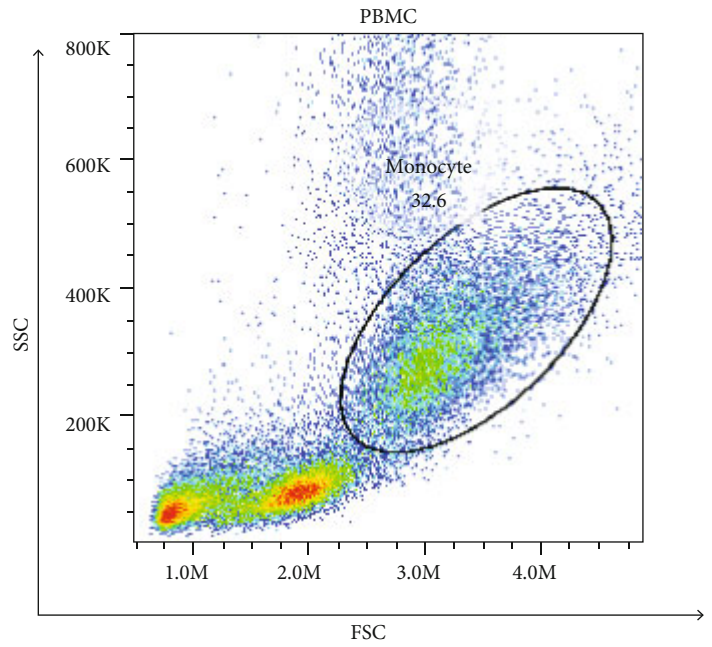

(b)

Figure 3: Continued.

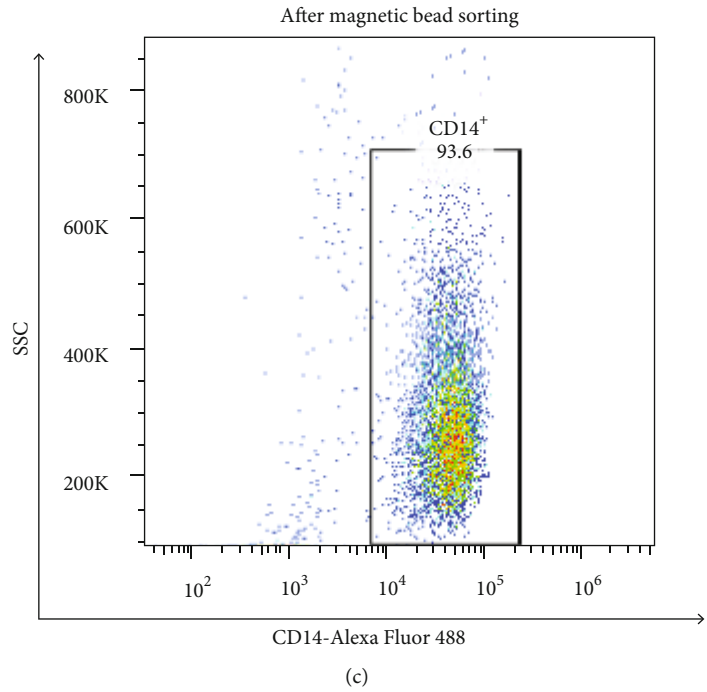

Figure 3: (a) Flow cytometry analysis of $CD14^+$ cells in blood; (b) flow cytometry analysis of $CD14^+$ cells in PBMC; (c) flow cytometry analysis of $CD14^+$ cells after magnetic bead sorting.

DT in 94 consecutive patients admitted to their institution with confirmed AAD, and the results indicated that 93 patients (99%) with AAD exhibited elevated DD (>400 ng/ml) [55]. It has been shown that the serum levels of DD are positively correlated with AAD. However, the present study indicated no significant correlation between DD and the percentages of monocyte subsets. It is possible that the two are independent factors affecting the disease process. In addition, it may be related to the sampling time point. A previous study demonstrated that the positive rate of DT detection was considerably low in patients aged less than 70 years and in patients exhibiting a 120 min time interval from symptom onset to admission [56]. The mean age of the patients of the present study was lower than 70 years, and the time interval from symptom onset to blood sample acquisition and detection was approximately 120 h, suggesting that this may be an important cause of negative results. In addition, we hypothesized that the time point required for the change in the monocyte number in Stanford type B AAD was different from that noted for the increase in the DD levels in other inflammatory diseases. The number of monocytes was increased in response to the changes in the microenvironment occurring during the disease progression. However, the large quantities of DD were released following induction of thrombosis. In addition to DD, C-reactive protein (CRP) is usually used to analyze the prognosis of AAD patients. The results indicated no significant correlation between CRP levels and monocyte subsets. CRP is a nonspecific acute inflammatory response protein produced by hepatocytes and is usually used to assess the overall severity of an acute disease or to predict adverse events [57]. However, it cannot be used as a clinical indicator for the prediction of AAD [57]. Furthermore, the time point required for the monocyte changes to take place may also differ from that noted for the CRP increase in the Stanford type B AAD patients, which remained to be confirmed by further research.

As we can see, diabetes ($P < 0.05$), smoking history ($P < 0.01$), and hypertension ($P < 0.001$) in Stanford type B AAD patients were higher than those noted in healthy control subjects. These might be related to the abnormal expression of monocytes and the occurrence of Stanford type B AAD. Actually, studies have been reported that the occurrence of male abdominal aortic aneurysms is closely related to the lifestyle-related factors, including cigarette smoking, obesity (body mass index (BMI) and waist circumference (WC)), and history of comorbidities (diabetes mellitus, hypercholesterolemia, and hypertension) [58]. What is the relationship between these lifestyle-related factors and the abnormal expression of monocytes? Studies have shown that the number of monocytes was increased in the blood of smokers [59]. Similarly, an increase in circulating monocyte counts has been found in patients with diabetes [60]. It has been reported that humans with hypertension have increasing intermediate and nonclassical monocytes, and increased endothelial stretch enhanced monocyte conversion to $CD14^{bright}CD16^+$ monocytes [61]. Thus, we can speculate that the above lifestyle-related factors may result in high expression of monocytes and induce Stanford type B AAD, which remains to be confirmed further.

To determine the biological changes caused on monocytes other than their percentages and phenotype, we obtained $CD14^+$ monocytes by magnetic bead sorting and analyzed the expression levels of several genes of $CD14^+$ cells. It has been shown that the expression levels of several genes

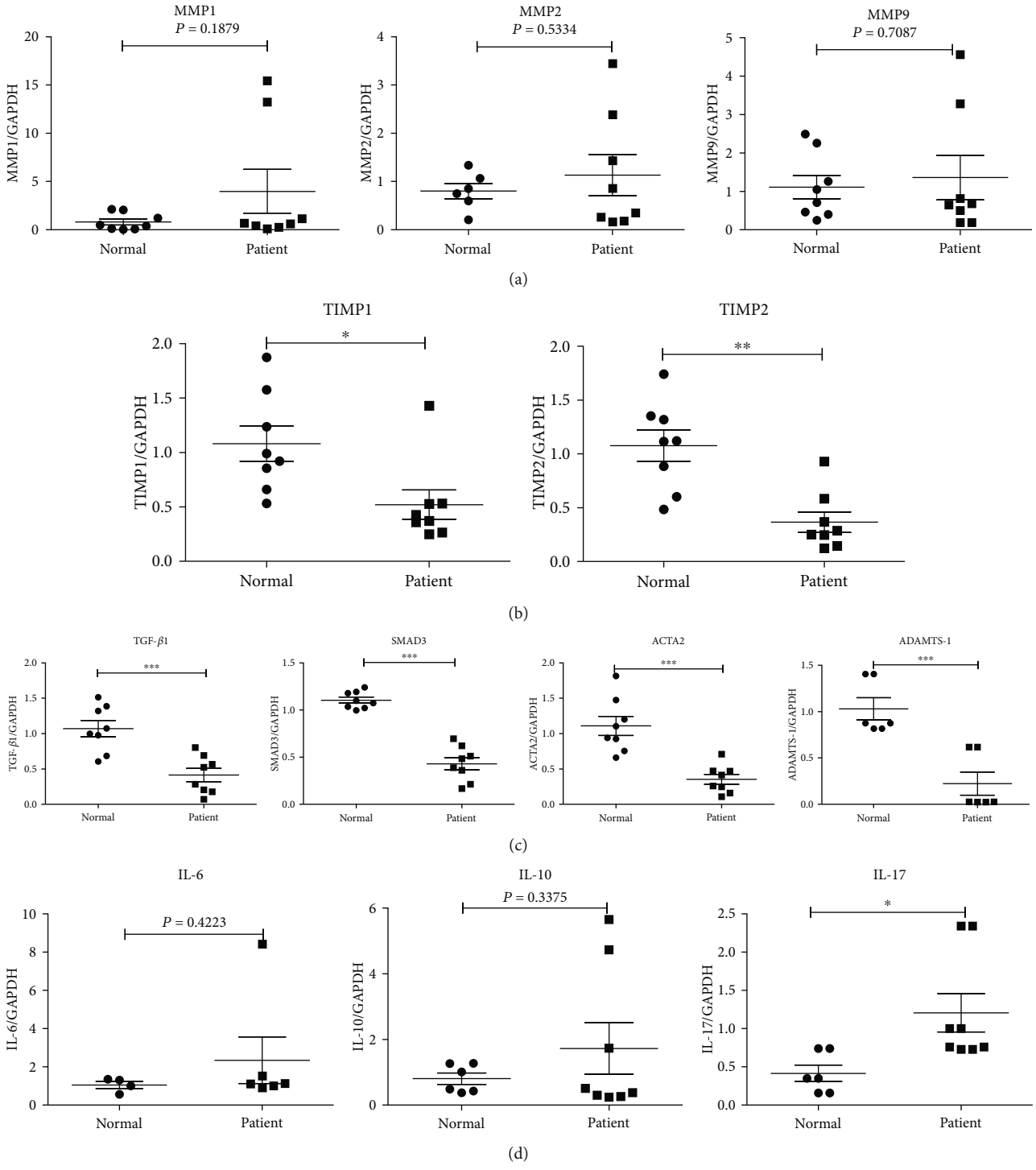

FIGURE 4: (a) The mRNA expression levels of MMP1, MMP2, and MMP9; (b) the mRNA expression levels of TIMP1, TIMP2; (c) the mRNA expression levels of TGF-β1, SMAD3, ACTA2, and ADAMTS-1; (d) the mRNA expression levels of IL-6, IL-10, and IL-17; Stanford type B AAD patient: $n = 8$; normal control: $n = 8$. The data were means ± SEM. $^{*}P < 0.05$, $^{**}P < 0.01$, and $^{***}P < 0.005$ vs. normal group.

are associated with the induction of aortic diseases induced by ANG II, such as *TGF-β* [62, 63], *SMAD3* [64–66], *MMP1* [66–69], *MMP2* [70–72], *MMP9* [72, 73], and *TIMP1*/*TIMP2* [74, 75]. Previous reports have clearly demonstrated that *MMP1*, *MMP2*, and *MMP9* are activated in the aortic disease [66–72]. However, the present study demonstrated that the expression levels of *MMP1*, *MMP2*, and *MMP9* indicated no significant differences between $CD14^{+}$ cells in Stanford type B AAD patients and normal volunteers, while *TIMP1* and *TIMP2* (inhibitor of MMPs) levels were decreased [73–75]. It has been reported that the balance between MMPs/TIMPs regulates ECM conversion and

remodeling, and an imbalance in this proportion may result in an abnormal amount of ECM degradation, leading to the development of severe vascular disease [76]. We speculated that monocytes may exhibit altered levels of TIMPs, but not of MMPs during the development of Stanford type B AAD.

Approximately 10 years ago, a hypothesis was proposed suggesting that aortic lesions were caused by excess TGF-β1 production in the aortic medium [77]. Subsequent studies confirmed this hypothesis and revealed that the downstream pathway of TGF-β1 was mediated by SMAD3. This suggested that excessive TGF-β/SMAD3 signaling stimulated smooth muscle cell uncontrolled and excessive proliferation, resulting in arterial lumen changes and the trigger of a series of aortic diseases [78, 79]. However, the present results indicated that the mRNA expression levels of *TGF-β1* and *SMAD3* were significantly decreased in Stanford type B AAD compared with those of normal volunteers, which was inconsistent with previous reports. Considering that the detection of $CD14^+$ monocytes was obtained from the patient blood, these two genes involved in $CD14^+$ monocyte function may play additional undiscovered roles, which require further investigation.

Alpha-actin (*ACTA2*) is the most common mutated gene in aortic disease, mainly affecting vascular smooth muscle cell (SMC) function. The major function of these cells is to contract in response to the stretch, a process that depends on the cyclic interaction between thin filaments, which are encoded by ACTA2 [80, 81]. The heterozygous mutations in ACTA2 lead to an inherited predisposition for thoracic aortic aneurysms and dissections (TAAD) [80–82]. The recent results of the present study indicated that the expression levels of ACTA2 in $CD14^+$ monocyte were lower in Stanford type B AAD patients, suggesting that *ACTA2* may be mutated in $CD14^+$ monocytes.

The recently discovered extracellular metalloproteinase named ADAMTS-1 is disinterring with a thrombospondin motif and metalloproteinase [83]. It has been reported that ADAMTS-1 inhibits ECM remodeling and participates in vascular disease by inhibiting cell proliferation [84–86]. Its mechanism of action is mediated by the combination of the vascular endothelial growth factor and the fibroblast growth factor [84–86]. Previous studies have demonstrated that the expression levels of ADAMTS-1 are increased significantly in aortic tissues of AAD patients [87, 88]. ADAMTS-1 was also introduced as a major mediator of vascular homeostasis, and ADAMTS-$1^{-/-}$ mice were more susceptible to the AAA phenotype [89]. The results of the present study indicated that the expression levels of ADAMTS-1 in $CD14^+$ cells were lower in Stanford type B AAD patients compared with those of the normal volunteers.

Interleukin-6 (IL-6) is an important stimulator of atherosclerotic lesions, which can aggravate atherosclerosis [90, 91]. However, the results of the current study indicated that the mRNA levels of IL-6 in Stanford type B AAD patient $CD14^+$ cells exhibited no significant difference compared with those of the normal volunteers. In addition to IL-6, IL-10 also played an important role in promoting the development of aortic aneurysm. It has been reported that high levels of IL-10 are detected in the serum of patients with aneurysms and that IL-$10^{-/-}$ counteracts Ang II-induced vascular dysfunction in APOE$^{-/-}$ mice [92]. The results of the present study indicated that in $CD14^+$ monocytes, the mRNA expression levels of IL-10 demonstrated no significant difference between Stanford type B AAD patients and normal volunteers, while interleukin-17 (IL-17) exhibited a significant increase. It has been reported that IL-17 is involved in various autoimmune diseases, including multiple sclerosis, rheumatoid arthritis, and systemic lupus erythematosus [[93–95], and previous studies have also indicated that high expression of IL-17 induces vascular inflammation, endothelial dysfunction, arterial hypertension, hypertension, and aortic aneurysm [96, 97]. In addition, IL-17 affects the basic function of the mononuclear/macrophage lineage and participates in the development of advanced atherosclerosis, promoting the increase of monocyte adhesion and the recruitment of circulating monocytes [98, 99]. We have demonstrated that the expression levels of IL-17 in $CD14^+$ monocytes were increased in Stanford type B AAD patients and that this effect may be inextricably linked to the changes of the monocyte biological characteristics. This requires further investigation in further study.

Although the present study contains several limitations, the results reported that the numbers and phenotypes of monocytes were significantly altered in the blood of Stanford type B AAD patients, suggesting that monocytes may play an important role in promoting the development of Stanford type B AAD. The specific mechanism of this process remains undiscovered. The mRNA expression levels of $CD14^+$ monocytes can aid in identification and prognosis of the disease. Understanding the characteristics of monocyte subset generation, differentiation, and function can dictate the development of future therapeutic avenues for Stanford type B AAD.

Data Availability

The data used to support the findings of this study are included within the article.

Conflicts of Interest

The authors declare no conflict of interest.

Authors' Contributions

Li Lu and Yuanhao Tong contributed equally to this work.

Acknowledgments

The present work was supported by the National Natural Science Foundation of China (81600375), the Six Talent Peaks Project in Jiangsu Province (No. YY-021), the Jiangsu Provincial Medical Youth Talent Foundation (QXRC201621), the Outstanding Youth Project supported by the Nanjing Medical Science and Technology Development Foundation (JQX17003), the Social Development Program of Jiangsu Province (BE2019604), and the Fundamental Research Funds for the Central Universities (No. 021414380342).

References

[1] R. Erbel, V. Aboyans, C. Boileau et al., "2014 ESC Guidelines on the diagnosis and treatment of aortic diseases: Document covering acute and chronic aortic diseases of the thoracic and abdominal aorta of the adult. The Task Force for the Diagnosis and Treatment of Aortic Diseases of the European Society of Cardiology (ESC)," *European Heart Journal*, vol. 35, no. 41, pp. 2873–2926, 2014.

[2] P. G. Hagan, C. A. Nienaber, E. M. Isselbacher et al., "The international registry of acute aortic dissection (IRAD)," *JAMA*, vol. 283, no. 7, pp. 897–903, 2000.

[3] U. K. A. Sampson, P. E. Norman, F. G. R. Fowkes et al., "Global and regional burden of aortic dissection and aneurysms: mortality trends in 21 world Regions, 1990 to 2010," *Global Heart*, vol. 9, no. 1, pp. 171–180.e10, 2014.

[4] G. J. Reul, D. A. Cooley, G. L. Hallman, S. B. Reddy, E. R. Kyger 3rd, and D. C. Wukasch, "Dissecting aneurysm of the descending aorta. Improved surgical results in 91 patients," *Archives of Surgery*, vol. 110, no. 5, pp. 632–640, 1975.

[5] L. G. Svensson, S. B. Labib, A. C. Eisenhauer, and J. R. Butterly, "Intimal tear without hematoma: an important variant of aortic dissection that can elude current imaging techniques," *Circulation*, vol. 99, no. 10, pp. 1331–1336, 1999.

[6] C. A. Nienaber and R. E. Clough, "Management of acute aortic dissection," *The Lancet*, vol. 385, no. 9970, pp. 800–811, 2015.

[7] G. C. Hughes, "Management of acute type B aortic dissection; ADSORB trial," *The Journal of Thoracic and Cardiovascular Surgery*, vol. 149, no. 2, pp. S158–S162, 2015.

[8] L. A. Pape, M. Awais, E. M. Woznicki et al., "Presentation, diagnosis, and outcomes of acute aortic dissection: 17-year trends from the International Registry of Acute Aortic Dissection," *Journal of the American College of Cardiology*, vol. 66, no. 4, pp. 350–358, 2015.

[9] D. Wen, H. Y. Wu, X. J. Jiang et al., "Role of plasma C-reactive protein and white blood cell count in predicting in-hospital clinical events of acute type A aortic dissection," *Chinese Medical Journal*, vol. 124, no. 17, pp. 2678–2682, 2011.

[10] H. Kuehl, H. Eggebrecht, T. Boes et al., "Detection of inflammation in patients with acute aortic syndrome: comparison of FDG-PET/CT imaging and serological markers of inflammation," *Heart*, vol. 94, no. 11, pp. 1472–1477, 2008.

[11] R. He, D. C. Guo, W. Sun et al., "Characterization of the inflammatory cells in ascending thoracic aortic aneurysms in patients with Marfan syndrome, familial thoracic aortic aneurysms, and sporadic aneurysms," *The Journal of Thoracic and Cardiovascular Surgery*, vol. 136, no. 4, pp. 922–929.e1, 2008.

[12] K. Kin, S. Miyagawa, S. Fukushima et al., "Tissue- and plasma-specific microRNA signatures for atherosclerotic abdominal aortic aneurysm," *Journal of the American Heart Association*, vol. 1, no. 5, article e000745, 2012.

[13] E. Schulz, T. Gori, and T. Münzel, "Oxidative stress and endothelial dysfunction in hypertension," *Hypertension Research*, vol. 34, no. 6, pp. 665–673, 2011.

[14] D. Wen, X. L. Zhou, J. J. Li, and R. T. Hui, "Biomarkers in aortic dissection," *Clinica Chimica Acta*, vol. 412, no. 9-10, pp. 688–695, 2011.

[15] C. U. Chae, R. T. Lee, N. Rifai, and P. M. Ridker, "Blood pressure and inflammation in apparently healthy men," *Hypertension*, vol. 38, no. 3, pp. 399–403, 2001.

[16] M. Zhang, H. Zhu, Y. Ding, Z. Liu, Z. Cai, and M. H. Zou, "AMP-activated protein kinase α1 promotes atherogenesis by increasing monocyte-to-macrophage differentiation," *Journal of Biological Chemistry*, vol. 292, no. 19, pp. 7888–7903, 2017.

[17] L. Ziegler-Heitbrock, P. Ancuta, S. Crowe et al., "Nomenclature of monocytes and dendritic cells in blood," *Blood*, vol. 116, no. 16, pp. e74–e80, 2010.

[18] P. Italiani and D. Boraschi, "From monocytes to M1/M2 macrophages: phenotypical vs. functional differentiation," *Frontiers in Immunology*, vol. 5, 2014.

[19] K. L. Wong, W. H. Yeap, J. J. Tai, S. M. Ong, T. M. Dang, and S. C. Wong, "The three human monocyte subsets: implications for health and disease," *Immunologic Research*, vol. 53, no. 1-3, pp. 41–57, 2012.

[20] W. Xiong, X. Wang, D. Dai, B. Zhang, L. Lu, and R. Tao, "The anti-inflammatory vasostatin-2 attenuates atherosclerosis in ApoE^{-/-} mice and inhibits monocyte/macrophage recruitment," *Thrombosis and Haemostasis*, vol. 117, no. 2, pp. 401–414, 2017.

[21] S. Mellak, H. Ait-Oufella, B. Esposito et al., "Angiotensin II mobilizes spleen monocytes to promote the development of abdominal aortic aneurysm inApoe−/−Mice," *Arteriosclerosis, Thrombosis, and Vascular Biology*, vol. 35, no. 2, pp. 378–388, 2015.

[22] B. L. Hoh, K. Hosaka, D. P. Downes et al., "Monocyte chemotactic protein-1 promotes inflammatory vascular repair of murine carotid aneurysms via a macrophage inflammatory protein-1α and macrophage inflammatory protein-2-dependent pathway," *Circulation*, vol. 124, no. 20, pp. 2243–2252, 2011.

[23] X. Ju, T. Ijaz, H. Sun et al., "Interleukin-6-signal transducer and activator of transcription-3 signaling mediates aortic dissections induced by angiotensin II via the T-helper lymphocyte 17-interleukin 17 axis in C57BL/6 mice," *Arteriosclerosis, Thrombosis, and Vascular Biology*, vol. 33, no. 7, pp. 1612–1621, 2013.

[24] B. C. Tieu, C. Lee, H. Sun et al., "An adventitial IL-6/MCP1 amplification loop accelerates macrophage-mediated vascular inflammation leading to aortic dissection in mice," *Journal of Clinical Investigation*, vol. 119, no. 12, pp. 3637–3651, 2009.

[25] K. Rahman, Y. Vengrenyuk, S. A. Ramsey et al., "Inflammatory Ly6Chi monocytes and their conversion to M2 macrophages drive atherosclerosis regression," *Journal of Clinical Investigation*, vol. 127, no. 8, pp. 2904–2915, 2017.

[26] F. M. van der Valk, S. Bekkering, J. Kroon et al., "Oxidized phospholipids on lipoprotein(a) elicit arterial wall inflammation and an inflammatory monocyte response in humans," *Circulation*, vol. 134, no. 8, pp. 611–624, 2016.

[27] A. A. Patel, Y. Zhang, J. N. Fullerton et al., "The fate and lifespan of human monocyte subsets in steady state and systemic inflammation," *Journal of Experimental Medicine*, vol. 214, no. 7, pp. 1913–1923, 2017.

[28] T. Suzuki, A. Distante, A. Zizza et al., "Diagnosis of acute aortic dissection by D-dimer: the International Registry of Acute Aortic Dissection Substudy on Biomarkers (IRAD-Bio) experience," *Circulation*, vol. 119, no. 20, pp. 2702–2707, 2009.

[29] P. Nazerian, C. Mueller, A. de Matos Soeiro et al., "Diagnostic accuracy of the aortic dissection detection risk score plus D-dimer for acute aortic syndromes: the ADvISED prospective multicenter study," *Circulation*, vol. 137, no. 3, pp. 250–258, 2018.

[30] F. del Porto, M. Proietta, L. Tritapepe et al., "Inflammation and immune response in acute aortic dissection," *Annals of Medicine*, vol. 42, no. 8, pp. 622–629, 2010.

[31] D. Wen, X. Du, J. Z. Dong, X. L. Zhou, and C. S. Ma, "Value of D-dimer and C reactive protein in predicting inhospital death in acute aortic dissection," *Heart*, vol. 99, no. 16, pp. 1192–1997, 2013.

[32] M. B. Pepys, "C-reactive protein fifty years on," *The Lancet*, vol. 317, no. 8221, pp. 653–657, 1981.

[33] G. T. Jones, L. V. Phillips, M. J. A. Williams, A. M. van Rij, and T. D. Kabir, "Two C-C family chemokines, eotaxin and RANTES, are novel independent plasma biomarkers for abdominal aortic aneurysm," *Journal of the American Heart Association*, vol. 5, no. 5, 2016.

[34] S. A. LeMaire and L. Russell, "Epidemiology of thoracic aortic dissection," *Nature Reviews Cardiology*, vol. 8, no. 2, pp. 103–113, 2011.

[35] R. He, D. C. Guo, A. L. Estrera et al., "Characterization of the inflammatory and apoptotic cells in the aortas of patients with ascending thoracic aortic aneurysms and dissections," *The Journal of Thoracic and Cardiovascular Surgery*, vol. 131, no. 3, pp. 671–678.e2, 2006.

[36] S. Wang, S. Unnikrishnan, E. B. Herbst, A. L. Klibanov, F. W. Mauldin Jr., and J. A. Hossack, "Ultrasound molecular imaging of inflammation in mouse abdominal aorta," *Investigative Radiology*, vol. 52, no. 9, pp. 499–506, 2017.

[37] F. Luo, X. L. Zhou, J. J. Li, and R. T. Hui, "Inflammatory response is associated with aortic dissection," *Ageing Research Reviews*, vol. 8, no. 1, pp. 31–35, 2009.

[38] K. L. Andrews, A. K. Sampson, J. C. Irvine et al., "Nitroxyl (HNO) reduces endothelial and monocyte activation and promotes M2 macrophage polarization," *Clinical Science*, vol. 130, no. 18, pp. 1629–1640, 2016.

[39] A. Gaggar, P. L. Jackson, B. D. Noerager et al., "A novel proteolytic cascade generates an extracellular matrix-derived chemoattractant in chronic neutrophilic inflammation," *Journal of Immunology*, vol. 180, no. 8, pp. 5662–5669, 2008.

[40] A. Babelova, K. Moreth, W. Tsalastra-Greul et al., "Biglycan, a danger signal that activates the NLRP3 inflammasome via toll-like and P2X receptors," *Journal of Biological Chemistry*, vol. 284, no. 36, pp. 24035–24048, 2009.

[41] N. Cifani, M. Proietta, M. Taurino, L. Tritapepe, and F. del Porto, "Monocyte subsets, Stanford-A acute aortic dissection, and carotid artery stenosis: new evidences," *Journal of Immunology Research*, vol. 2019, Article ID 9782594, 6 pages, 2019.

[42] A. L. Blomkalns, D. Gavrila, M. Thomas et al., "CD14 directs adventitial macrophage precursor recruitment: role in early abdominal aortic aneurysm formation," *Journal of the American Heart Association*, vol. 2, no. 2, article e000065, 2013.

[43] C. Shi and E. G. Pamer, "Monocyte recruitment during infection and inflammation," *Nature Reviews. Immunology*, vol. 11, no. 11, pp. 762–774, 2011.

[44] B. Passlick, D. Flieger, and H. W. Ziegler-Heitbrock, "Identification and characterization of a novel monocyte subpopulation in human peripheral blood," *Blood*, vol. 74, no. 7, pp. 2527–2534, 1989.

[45] C. Scally, H. Abbas, T. Ahearn et al., "Myocardial and systemic inflammation in acute stress-induced (takotsubo) cardiomyopathy," *Circulation*, vol. 139, no. 13, pp. 1581–1592, 2019.

[46] H. Tsujioka, T. Imanishi, H. Ikejima et al., "Impact of Heterogeneity of Human Peripheral Blood Monocyte Subsets on Myocardial Salvage in Patients With Primary Acute Myocardial Infarction," *American College of Cardiology*, vol. 54, no. 2, pp. 130–138, 2009.

[47] D. W. Williams, K. Anastos, S. Morgello, and J. W. Berman, "JAM-A and ALCAM are therapeutic targets to inhibit diapedesis across the BBB of CD14+CD16+ monocytes in HIV-infected individuals," *Journal of Leukocyte Biology*, vol. 97, no. 2, pp. 401–412, 2015.

[48] C. Ay, R. Vormittag, D. Dunkler et al., "D-dimer and prothrombin fragment 1 + 2 predict venous thromboembolism in patients with cancer: results from the Vienna Cancer and Thrombosis Study," *Journal of Clinical Oncology*, vol. 27, no. 25, pp. 4124–4129, 2009.

[49] J. A. Kline, M. M. Hogg, D. M. Courtney, C. D. Miller, A. E. Jones, and H. A. Smithline, "D-dimer threshold increase with pretest probability unlikely for pulmonary embolism to decrease unnecessary computerized tomographic pulmonary angiography," *Journal of Thrombosis and Haemostasis*, vol. 10, no. 4, pp. 572–581, 2012.

[50] M. Righini, J. van Es, P. den Exter et al., "Age-adjusted D-dimer cutoff levels to rule out pulmonary embolism: the ADJUST-PE study," *JAMA*, vol. 311, no. 11, pp. 1117–1124, 2014.

[51] J. S. Cui, Z. P. Jing, S. J. Zhuang et al., "D-dimer as a biomarker for acute aortic dissection: a systematic review and meta-analysis," *Medicine*, vol. 94, no. 4, article e471, 2015.

[52] S. E. Asha and J. W. Miers, "A systematic review and meta-analysis of D-dimer as a rule-out test for suspected acute aortic dissection," *Annals of Emergency Medicine*, vol. 66, no. 4, pp. 368–378, 2015.

[53] H. Watanabe, N. Horita, Y. Shibata, S. Minegishi, E. Ota, and T. Kaneko, "Diagnostic test accuracy of D-dimer for acute aortic syndrome: systematic review and meta-analysis of 22 studies with 5000 subjects," *Scientific Reports*, vol. 6, no. 1, 2016.

[54] R. Gorla, R. Erbel, P. Kahlert et al., "Accuracy of a diagnostic strategy combining aortic dissection detection risk score and D-dimer levels in patients with suspected acute aortic syndrome," *European Heart Journal: Acute Cardiovascular Care*, vol. 6, no. 5, pp. 371–378, 2017.

[55] H. Hazui, M. Nishimoto, M. Hoshiga et al., "Young adult patients with short dissection length and thrombosed false lumen without ulcer-like projections are liable to have false-negative results of D-dimer testing for acute aortic dissection based on a study of 113 cases," *Circulation Journal*, vol. 70, no. 12, pp. 1598–1601, 2006.

[56] P. Ohlmann, A. Faure, O. Morel et al., "Diagnostic and prognostic value of circulating D-dimers in patients with acute aortic dissection," *Critical Care Medicine*, vol. 34, no. 5, pp. 1358–1364, 2006.

[57] T. Kitai, S. Kaji, K. Kim et al., "Prognostic value of sustained elevated C-reactive protein levels in patients with acute aortic intramural hematoma," *The Journal of Thoracic and Cardiovascular Surgery*, vol. 147, no. 1, pp. 326–331, 2014.

[58] O. Stackelberg, A. Wolk, K. Eliasson et al., "Lifestyle and risk of screening-detected abdominal aortic aneurysm in men," *Journal of the American Heart Association*, vol. 6, no. 5, article e004725, 2017.

[59] E. J. Jensen, B. Pedersen, E. Narvestadt, and R. Dahl, "Blood eosinophil and monocyte counts are related to smoking and lung function," *Respiratory Medicine*, vol. 92, no. 1, pp. 63–69, 1998.

[60] S. A. Kocaman, A. Sahinarslan, A. Akyel, T. Timurkaynak, B. Boyaci, and A. Cengel, "The association of circulating monocyte count with coronary collateral growth in patients with diabetes mellitus," *Acta Diabetologica*, vol. 47, no. 1, pp. 49–54, 2010.

[61] R. Loperena, J. P. van Beusecum, H. A. Itani et al., "Hypertension and increased endothelial mechanical stretch promote monocyte differentiation and activation: roles of STAT3, interleukin 6 and hydrogen peroxide," *Cardiovascular Research*, vol. 114, no. 11, pp. 1547–1563, 2018.

[62] S. N. Angelov, J. H. Hu, H. Wei, N. Airhart, M. Shi, and D. A. Dichek, "TGF-β (transforming growth factor-β) signaling protects the thoracic and abdominal aorta from angiotensin II-induced pathology by distinct mechanisms," *Arteriosclerosis, Thrombosis, and Vascular Biology*, vol. 37, no. 11, pp. 2102–2113, 2017.

[63] E. M. Gallo, D. C. Loch, J. P. Habashi et al., "Angiotensin II-dependent TGF-β signaling contributes to Loeys-Dietz syndrome vascular pathogenesis," *Journal of Clinical Investigation*, vol. 124, no. 1, pp. 448–460, 2014.

[64] D. M. DiRenzo, M. A. Chaudhary, X. Shi et al., "A crosstalk between TGF-β/Smad3 and Wnt/β-catenin pathways promotes vascular smooth muscle cell proliferation," *Cellular Signalling*, vol. 28, no. 5, pp. 498–505, 2016.

[65] A. W. Turner, M. Nikpay, A. Silva et al., "Functional interaction between COL4A1/COL4A2 and SMAD3 risk loci for coronary artery disease," *Atherosclerosis*, vol. 242, no. 2, pp. 543–552, 2015.

[66] I. M. B. H. van de Laar, R. A. Oldenburg, G. Pals et al., "Mutations in *SMAD3* cause a syndromic form of aortic aneurysms and dissections with early-onset osteoarthritis," *Nature Genetics*, vol. 43, no. 2, pp. 121–126, 2011.

[67] N. Fiotti, C. Calvagna, G. Sgorlon et al., "Multiple sites of vascular dilation or aneurysmal disease and matrix metalloproteinase genetic variants in patients with abdominal aortic aneurysm," *Journal of Vascular Surgery*, vol. 67, no. 6, pp. 1727–1735, 2018.

[68] A. Sakowicz, M. Lisowska, L. Biesiada et al., "Association of maternal and fetal single-nucleotide polymorphisms in metalloproteinase (MMP1, MMP2, MMP3, and MMP9) genes with preeclampsia," *Disease Markers*, vol. 2018, Article ID 1371425, 10 pages, 2018.

[69] M. Shen, J. Lee, R. Basu et al., "Divergent roles of matrix metalloproteinase 2 in pathogenesis of thoracic aortic aneurysm," *Arteriosclerosis, Thrombosis, and Vascular Biology*, vol. 35, no. 4, pp. 888–898, 2015.

[70] N. Tzemos, E. Lyseggen, C. Silversides et al., "Endothelial function, carotid-femoral stiffness, and plasma matrix metalloproteinase-2 in men with bicuspid aortic valve and dilated aorta," *Journal of the American College of Cardiology*, vol. 55, no. 7, pp. 660–668, 2010.

[71] A. Ghosh, A. Pechota, D. Coleman, G. R. Upchurch Jr., and J. L. Eliason, "Cigarette smoke–induced MMP2 and MMP9 secretion from aortic vascular smooth cells is mediated via the Jak/Stat pathway," *Human Pathology*, vol. 46, no. 2, pp. 284–294, 2015.

[72] C. F. Lai, V. Seshadri, K. Huang et al., "An osteopontin-NADPH oxidase signaling cascade promotes pro-matrix metalloproteinase 9 activation in aortic mesenchymal cells," *Circulation Research*, vol. 98, no. 12, pp. 1479–1489, 2006.

[73] E. Vianello, E. Dozio, R. Rigolini et al., "Acute phase of aortic dissection: a pilot study on CD40L, MPO, and MMP-1, -2, 9 and TIMP-1 circulating levels in elderly patients," *Immunity & Ageing*, vol. 13, no. 1, 2016.

[74] G. Sangiorgi, S. Trimarchi, A. Mauriello et al., "Plasma levels of metalloproteinases-9 and -2 in the acute and subacute phases of type A and type B aortic dissection," *Journal of Cardiovascular Medicine*, vol. 7, no. 5, pp. 307–315, 2006.

[75] X. Wang and R. A. Khalil, "Matrix Metalloproteinases, Vascular Remodeling, and Vascular Disease," *Advances in Pharmacology*, vol. 81, pp. 241–330, 2018.

[76] J. P. Habashi, D. P. Judge, T. M. Holm et al., "Losartan, an AT1 antagonist, prevents aortic aneurysm in a mouse model of Marfan syndrome," *Science*, vol. 312, no. 5770, pp. 117–121, 2006.

[77] P. A. Suwanabol, S. M. Seedial, X. Shi et al., "Transforming growth factor-β increases vascular smooth muscle cell proliferation through the Smad3 and extracellular signal-regulated kinase mitogen-activated protein kinases pathways," *Journal of Vascular Surgery*, vol. 56, no. 2, pp. 446–454.e1, 2012.

[78] N. Kalinina, A. Agrotis, Y. Antropova et al., "Smad expression in human atherosclerotic lesions," *Arteriosclerosis, Thrombosis, and Vascular Biology*, vol. 24, no. 8, pp. 1391–1396, 2004.

[79] D.-C. Guo, H. Pannu, V. Tran-Fadulu et al., "Mutations in smooth muscle α-actin (*ACTA2*) lead to thoracic aortic aneurysms and dissections," *Nature Genetics*, vol. 39, no. 12, pp. 1488–1493, 2007.

[80] H. Morisaki, K. Akutsu, H. Ogino et al., "Mutation of ACTA2 gene as an important cause of familial and nonfamilial nonsyndromatic thoracic aortic aneurysm and/or dissection (TAAD)," *Human Mutation*, vol. 30, no. 10, pp. 1406–1411, 2009.

[81] E. S. Regalado, D. C. Guo, S. Prakash et al., "Aortic disease presentation and outcome associated with ACTA2 mutations," *Circulation. Cardiovascular Genetics*, vol. 8, no. 3, pp. 457–464, 2015.

[82] K. Kuno, N. Kanada, E. Nakashima, F. Fujiki, F. Ichimura, and K. Matsushima, "Molecular cloning of a gene encoding a new type of metalloproteinase-disintegrin family protein with thrombospondin motifs as an inflammation associated gene," *The Journal of Biological Chemistry*, vol. 272, no. 1, pp. 556–562, 1997.

[83] C. Gendron, M. Kashiwagi, N. H. Lim et al., "Proteolytic activities of human ADAMTS-5: comparative studies with ADAMTS-4," *The Journal of Biological Chemistry*, vol. 282, no. 25, pp. 18294–18306, 2007.

[84] A. Luque, D. R. Carpizo, and M. L. Iruela-Arispe, "ADAMTS1/METH1 inhibits endothelial cell proliferation by direct binding and sequestration of $VEGF_{165}$," *The Journal of Biological Chemistry*, vol. 278, no. 26, pp. 23656–23665, 2003.

[85] A.-C. Jönsson-Rylander, T. Nilsson, R. Fritsche-Danielson et al., "Role of ADAMTS-1 in Atherosclerosis," *Arteriosclerosis, Thrombosis, and Vascular Biology*, vol. 25, no. 1, pp. 180–185, 2005.

[86] P. Ren, L. Zhang, G. Xu et al., "ADAMTS-1 and ADAMTS-4 Levels Are Elevated in Thoracic Aortic Aneurysms and Dissections," *The Annals of Thoracic Surgery*, vol. 95, no. 2, pp. 570–577, 2013.

[87] Y. Gao, W. Wu, C. Yu et al., "A disintegrin and metalloproteinase with thrombospondin motif 1 (ADAMTS1) expression increases in acute aortic dissection," *Science China. Life Sciences*, vol. 59, no. 1, pp. 59–67, 2016.

[88] J. Oller, N. Méndez-Barbero, E. J. Ruiz et al., "Nitric oxide mediates aortic disease in mice deficient in the metalloprotease Adamts1 and in a mouse model of Marfan syndrome," *Nature Medicine*, vol. 23, no. 2, pp. 200–212, 2017.

[89] D. A. Sukovich, K. Kauser, F. D. Shirley, V. DelVecchio, M. Halks-Miller, and G. M. Rubanyi, "Expression of interleukin-6 in atherosclerotic lesions of male apoE-knockout mice," *Arteriosclerosis, Thrombosis, and Vascular Biology*, vol. 18, no. 9, pp. 1498–1505, 1998.

[90] Y. W. Lee, W. H. Lee, and P. H. Kim, "Oxidative mechanisms of IL-4-induced IL-6 expression in vascular endothelium," *Cytokine*, vol. 49, no. 1, pp. 73–79, 2010.

[91] S. Kasashima, A. Kawashima, Y. Zen et al., "Upregulated interleukins (IL-6, IL-10, and IL-13) in immunoglobulin G4-related aortic aneurysm patients," *Journal of Vascular Surgery*, vol. 67, no. 4, pp. 1248–1262, 2018.

[92] V. V. Lima, S. M. Zemse, C. W. Chiao et al., "Interleukin-10 limits increased blood pressure and vascular RhoA/Rho-kinase signaling in angiotensin II-infused mice," *Life Sciences*, vol. 145, pp. 137–143, 2016.

[93] M. Montes, X. Zhang, L. Berthelot et al., "Oligoclonal myelin-reactive T-cell infiltrates derived from multiple sclerosis lesions are enriched in Th17 cells," *Clinical Immunology*, vol. 130, no. 2, pp. 133–144, 2009.

[94] K. Hirota, H. Yoshitomi, M. Hashimoto et al., "Preferential recruitment of CCR6-expressing Th17 cells to inflamed joints via CCL20 in rheumatoid arthritis and its animal model," *The Journal of Experimental Medicine*, vol. 204, no. 12, pp. 2803–2812, 2007.

[95] A. B. Pernis, "Th17 cells in rheumatoid arthritis and systemic lupus erythematosus," *Journal of Internal Medicine*, vol. 265, no. 6, pp. 644–652, 2009.

[96] S. Karbach, A. L. Croxford, M. Oelze et al., "Interleukin 17 drives vascular inflammation, endothelial dysfunction, and arterial hypertension in psoriasis-like skin disease," *Arteriosclerosis, Thrombosis, and Vascular Biology*, vol. 34, no. 12, pp. 2658–2668, 2014.

[97] H. Nguyen, V. L. Chiasson, P. Chatterjee, S. E. Kopriva, K. J. Young, and B. M. Mitchell, "Interleukin-17 causes Rho-kinase-mediated endothelial dysfunction and hypertension," *Cardiovascular Research*, vol. 97, no. 4, pp. 696–704, 2013.

[98] A. K. Sharma, G. Lu, A. Jester et al., "Experimental abdominal aortic aneurysm formation is mediated by IL-17 and attenuated by mesenchymal stem cell treatment," *Circulation*, vol. 126, no. 11, Supplement 1, pp. S38–S45, 2012.

[99] C. Erbel, M. Akhavanpoor, D. Okuyucu et al., "IL-17A influences essential functions of the monocyte/macrophage lineage and is involved in advanced murine and human atherosclerosis," *Journal of Immunology*, vol. 193, no. 9, pp. 4344–4355, 2014.

Hindawi
Journal of Immunology Research
Volume 2020, Article ID 7812709, 10 pages
https://doi.org/10.1155/2020/7812709

Research Article

Inhibition of the Ubiquitin-Activating Enzyme UBA1 Suppresses Diet-Induced Atherosclerosis in Apolipoprotein E-Knockout Mice

Jiawei Liao,[1] **Xiaolei Yang**,[1] **Qiuyue Lin**,[1] **Shuang Liu**,[2] **Yunpeng Xie**,[1] **Yunlong Xia**,[1] **and Hui-Hua Li**[1]

[1]*Department of Cardiology, Institute of Cardiovascular Diseases, First Affiliated Hospital of Dalian Medical University, Dalian 116011, China*
[2]*Department of Occupational and Environmental Health, School of Public Health, Dalian Medical University, Dalian 116011, China*

Correspondence should be addressed to Hui-Hua Li; hhli1935@aliyun.com

Received 30 October 2019; Revised 4 February 2020; Accepted 28 February 2020; Published 20 March 2020

Guest Editor: Heather Medbury

Background. Ubiquitin-like modifier activating enzyme 1 (UBA1) is the first and major E1 activating enzyme in ubiquitin activation, the initial step of the ubiquitin-proteasome system. Defects in the expression or activity of UBA1 correlate with several neurodegenerative and cardiovascular disorders. However, whether UBA1 contributes to atherosclerosis is not defined. *Methods and Results*. Atherosclerosis was induced in apolipoprotein E-knockout (*Apoe*-/-) mice fed on an atherogenic diet. UBA1 expression, detected by immunohistochemical staining, was found to be significantly increased in the atherosclerotic plaques, which confirmed to be mainly derived from lesional $CD68^+$ macrophages via immunofluorescence costaining. Inactivation of UBA1 by the specific inhibitor PYR-41 did not alter the main metabolic parameters during atherogenic diet feeding but suppressed atherosclerosis development with less macrophage infiltration and plaque necrosis. PYR-41 did not alter circulating immune cells determined by flow cytometry but significantly reduced aortic mRNA levels of cytokines related to monocyte recruitment (*Mcp-1*, *Vcam-1*, and *Icam-1*) and macrophage proinflammatory responses (*Il-1β* and *Il-6*). Besides, PYR-41 also suppressed aortic mRNA expression of NADPH oxidase (*Nox1*, *Nox2*, and *Nox4*) and lesional oxidative stress levels, determined by DHE staining. *In vitro*, PYR-41 blunted ox-LDL-induced lipid deposition and expression of proinflammatory cytokines (*Il-1β* and *Il-6*) and NADPH oxidases (*Nox1*, *Nox2*, and *Nox4*) in cultured RAW264.7 macrophages. *Conclusions*. We demonstrated that UBA1 expression was upregulated and mainly derived from macrophages in the atherosclerotic plaques and inactivation of UBA1 by PYR-41 suppressed atherosclerosis development probably through inhibiting macrophage proinflammatory response and oxidative stress. Our data suggested that UBA1 might be explored as a potential pharmaceutical target against atherosclerosis.

1. Introduction

Cardiovascular diseases have now ranked as the top cause of mortality globally, representing 31% of all global deaths in 2016, according to WHO's statistics [1]. Atherosclerosis, a chronic inflammatory disease with abnormal lipid deposition in the large- and median-sized arteries, is the predominant underlying contributor to the majority of fatal conditions, such as myocardial infarction, unstable angina, sudden cardiac death, and stroke [2]. Besides the strong inflammatory nature, atherosclerosis is also characterized by proliferation, apoptosis/necrosis, enhanced oxidative stress, and disturbed protein homeostasis [3].

The ubiquitin-proteasome system (UPS) is the major pathway for intracellular protein degradation within eukaryotic cells, accounting for 80-90% of intracellular protein degradation [4, 5]. Due to the central role of the UPS in maintaining intracellular protein metabolism, it is reported to be involved in a wide variety of biological processes, such as growth and proliferation, inflammation, oxidative stress, and apoptosis/-necrosis, that are crucial for cardiovascular biology and pathology [6, 7]. The UPS includes two independent but

sequential parts: the ubiquitination and proteasome-mediated proteolysis [4, 5]. As the initial step of the UPS, ubiquitination modification starts as ubiquitin activation by forming a thioester linkage with the E1 activating enzyme. Activated ubiquitin was then transferred through a transesterification reaction to an E2 conjugating enzyme, followed by formation of an isopeptide bond with targeted protein substrate via the E3 ligating enzyme [4, 5]. The ubiquitined proteins finally enter the 20S proteasome complex for further degradation into peptides [4, 5]. Previous studies have confirmed abnormal UPS in atherosclerosis, especially in symptomatic plaques, suggesting that the UPS contributes to atherogenesis [8–10]. However, current studies mainly focus on the proteasome and E3 ligating enzyme activities; little is known about the E1 activating enzymes, the apex of the ubiquitination cascade, in atherosclerosis.

Ubiquitin-like modifier activating enzyme 1 (UBA1) is the first identified E1 activating enzyme for ubiquitin activation [11]. It is a highly conserved protein and consists of two main isoforms: UBA1a containing 1058 amino acids and UBA1b containing 1018 amino acids [11]. Besides UBA1, UBA6 is also capable of activating ubiquitin [12]. However, UBA6-mediated ubiquitin activation is currently restricted to specific protein ubiquitination, as only one specific E2 enzyme out of the currently known E2 enzymes can be conjugated with UBA6 [12]. Therefore, UBA1 plays a central role in ubiquitin activation and protein quality. Total loss of UBA1 is lethal, while defects in UBA1 expression or activity contribute to the pathogenesis of several neurodegenerative disorders such as spinal muscular atrophy, Huntington's disease, Parkinson's disease, Alzheimer's disease, and amyotrophic lateral sclerosis [13]. Recent studies also suggested that UBA1 might be essential for maintaining cardiovascular homeostasis and thus contribute to disease progression. For example, Qin et al. reported that inhibition of UBA1 by a small molecular inhibitor PYR-41 effectively attenuated carotid neointimal thickening via suppressing monocyte/macrophage infiltration and smooth muscle cell proliferation in a rat model of balloon injury [14]; Shu et al. demonstrated that cardiac UBA1 was upregulated in a mouse model of angiotensin II-induced cardiac remodeling and UBA1 inhibition by PYR-41 significantly reduced cardiac inflammation and oxidative stress [15]. However, whether UBA1 is involved in atherosclerosis is not defined. Here in this study, we explored this issue in a mouse atherosclerosis model, the apolipoprotein E-knockout mice (*Apoe*-/-) fed on an atherogenic diet.

2. Materials and Methods

2.1. Animals and Experimental Designs. Male *Apoe*-/- mice on C57BL/6 background were purchased from Beijing Vital River Laboratory and housed under specific pathogen-free conditions on a 12-hour light/12-hour dark cycle with free access to water and diet. At the age of 10 weeks old, the mice were fed on an atherogenic diet (0.5% cholesterol and 20% fat) for the next 8 weeks to fast induce atherogenesis. PYR-41(Selleck) was administrated (10 mg/kg body weight) 2 times per week by intraperitoneal injection, with DMSO as control, during atherogenic diet feeding. All experiments were performed according to the guidelines for the care and use of laboratory animals of the National Institute of Health (NIH publication no.85Y23, revised 1996) and approved by the Animal Care and Use Committee of Dalian Medical University.

2.2. Plasma Lipid and Glucose Analysis. Mice were fasted for 4 hours. Blood samples were collected via retroorbital puncture. Plasma total cholesterol, triglycerides, and glucose were measured with commercial kits (BioSino), according to the manufacturer's guidance. Lipoprotein profiles were fractioned by fast protein liquid chromatography (FPLC) and analyzed as we previously described [16]. Insulin resistance was measured by glucose tolerance test (GTT). Briefly, mice were fasted for 4 hours and then challenged with an intraperitoneal injection of glucose (2 g/kg body weight). Blood samples were collected before (time 0) and at 30, 60, and 120 minutes (time 30, 60, and 120, respectively) after glucose injection by retroorbital bleeding. Plasma glucose was measured with commercial kit as described above (BioSino).

2.3. Histological Analysis. Mice were sacrificed and flushed with PBS through the left ventricle. The aorta and the aortic root samples were prepared as previously described [17]. Briefly, the aorta was rid of the adventitia and cut open longitudinally under a dissecting microscope, while the heart was embedded in OCT (Sakura Finetek), snap frozen in liquid nitrogen, and cross-sectioned serially at 7 μm thick throughout the aortic root. Atherosclerosis burden in the *en face* aortas and the aortic root sections was visualized by Oil-red O (Sigma) staining. UBA1 expression in the vessels of the aortic root sections was detected by immunohistochemical staining with anti-UBA1 antibody (ab34711, Abcam) or immunofluorescence costaining using anti-UBA1 (ab34711, Abcam) and anti-CD68 (MCA1957, Bio-Rad) antibodies. Macrophages and smooth muscle cells in the atherosclerotic plaques were visualized by immunohistochemical staining with anti-CD68 antibody (MCA1957, Bio-Rad) and anti-α-SMA antibody (ab5694, Abcam). Necrotic areas in the plaques were visualized by HE staining and designated as eosin-negative acellular areas. All quantifications were determined with ImageJ software.

2.4. Flow Cytometry Analysis. Blood was collected via retroorbital puncture and depleted of erythrocyte by lysing buffer (BD Biosciences). Then cell suspensions were treated with Fc block, washed, and stained with CD45 PerCP-Cy5.5, CD3 FITC, CD11b FITC, F4/80 BV421, and Gr-1 APC (BD Biosciences) accordingly. Circulating monocytes were defined as $CD45^+CD11b^+F4/80^+Gr\text{-}1^-$, neutrophils as $CD45^+CD11b^+Gr\text{-}1^+F4/80^-$, and T cells as $CD45^+CD3^+$. Events were acquired on a live gate on Fortessa flow cytometer (BD Biosciences).

2.5. RNA Isolation and Quantitative Real-Time PCR Analysis. Total RNA was extracted with TRIzol (Invitrogen) and reverse transcripted using a RT kit (MedChem Express). Quantitative real-time PCR was performed using SYBR Green PCR reagents (MedChem Express) and normalized

to *Gapdh*. The primer sequences used in quantitative real-time PCR are described in Table 1.

2.6. Cell Culture. RAW264.7 cells were cultured in RPMI-1640 medium (Gibco) supplemented with 10% fetal bovine serum and 1% antibiotics (100 Units/ml penicillin and 100 μg/ml streptomycin) and maintained in a humidified incubator at 37°C under 5% CO_2. When cells were grown to 80% confluence, they were treated with PYR-41 (5 μM, Selleck) for 2 hours, then washed and subjected to ox-LDL (50 μg/ml, Unionbiol) treatment. After incubation with ox-LDL for 12 hours, cells were harvested for RNA extraction or fixed with 4% paraformaldehyde solution for Oil-red O staining.

2.7. Statistical Analysis. Data were presented as mean or mean ± SEM. Statistical significance was evaluated by Student's *t*-test using Prism software. P value < 0.05 was regarded as significant.

3. Results

3.1. UBA1 Expression Was Upregulated and Mainly Derived from Macrophages in the Diet-Induced Atherosclerosis in Apoe-/- Mice. First, we explored the expression of UBA1 during atherogenesis in *Apoe-/-* mice. As shown in Figure 1(a), UBA1 expression was significantly increased in the diet-induced atherosclerotic plaques, detected by immunochemical analysis. To further identify the origin of UBA1 expression, we costained UBA1 with CD68, a marker of macrophages, which is the main type and also majority of functional cells in atherosclerosis. As shown in Figure 1(b), UBA1 almost fully colocalized with CD68. Together, our data indicated that UBA1 expression was upregulated and mainly derived from macrophage in diet-induced atherosclerosis in *Apoe-/-* mice.

3.2. Inhibition of UBA1 Did Not Alter the Main Metabolic Parameters during Diet-Induced Atherogenesis in Apoe-/- Mice. Next, we examined the role of increased macrophage UBA1 expression in the diet-induced atherosclerosis in *Apoe-/-* mice, using a specific inhibitor PYR-41. We found that PYR-41 treatment did not change plasma total cholesterol (TC) and triglyceride (TG) levels as well as lipoprotein profiles fractioned by FPLC during atherogenic diet feeding (Figures 2(a) and 2(b)). Similarly, PYR-41 treatment did not change plasma glucose levels, insulin resistance determined by GTT, and body weight gain (Figures 2(c)–2(e)).

3.3. Inhibition of UBA1 Attenuated Diet-Induced Atherosclerosis in Apoe-/- Mice. We then explored the atherosclerosis development in the *Apoe-/-* mice with or without UBA1 inhibition by PYR-41, after 8 weeks on the atherogenic diet feeding. We found that PYR-41 treatment significantly reduced the atherosclerosis burden in the entire inner surface of the aortas and the aortic root, respectively (Figures 3(a) and 3(b)). Besides atherosclerosis burden, PYR-41 also changed the plaque composition, decreasing macrophage infiltration and plaque necrosis while not altering smooth muscle cell accumulation in the plaques (Figures 3(c)–3(e)). These data suggested that inhibition of UBA1 attenuated diet-induced atherosclerosis probably through inhibiting macrophage infiltration and plaque necrosis in *Apoe-/-* mice.

Table 1: Primer sequences used in the quantitative real-time PCR.

Name	Type	Sequence (5′-3′)
Mcp-1	Forward	TAAAAACCTGGATCGGAACCAAA
	Reverse	GCATTAGCTTCAGATTTACGGGT
Vcam-1	Forward	GTTCCAGCGAGGGTCTACC
	Reverse	AACTCTTGGCAAACATTAGGTGT
Icam-1	Forward	GCCTTGGTAGAGGTGACTGAG
	Reverse	GACCGGAGCTGAAAAGTTGTA
Il-1β	Forward	CTTCCCCAGGGCATGTTAAG
	Reverse	ACCCTGAGCGACCTGTCTTG
Il-6	Forward	TTCCATCCAGTTGCCTTCTTG
	Reverse	TTGGGAGTGGTATCCTCTGTGA
Tnfα	Forward	ATGGCCTCCCTCTCATCAGT
	Reverse	CTTGGTGGTTTGCTACGACG
Il-4	Forward	GGTCTCAACCCCCAGCTAGT
	Reverse	GCCGATGATCTCTCTCAAGTGAT
Il-10	Forward	GCTCTTACTGACTGGCATGAG
	Reverse	CGCAGCTCTAGGAGCATGTG
Nox1	Forward	CCCATCCAGTCTCCAAACATGAC
	Reverse	ACCAAAGCTACAGTGGCAATCAC
Nox2	Forward	CTTCTTGGGTCAGCACTGGC
	Reverse	GCAGCAAGATCAGCATGCAG
Nox4	Forward	CTTGGTGAATGCCCTCAACT
	Reverse	TTCTGGGATCCTCATTCTGG
Gapdh	Forward	AGGTCGGTGTGAACGGATTTG
	Reverse	GGGGTCGTTGATGGCAACA

3.4. Inhibition of UBA1 Reduced Proinflammatory Cytokine Levels in Diet-Induced Atherosclerosis in Apoe-/- Mice. We then explored whether UBA1 inhibition reduced circulating macrophages in diet-treated *Apoe-/-* mice. As shown in Figure 4(a), flow cytometry analysis revealed that PYR-41 treatment did not alter circulating monocytes, neutrophils, or T cells in the *Apoe-/-* mice received 2 weeks of atherogenic diet feeding. In the meantime, we observed that PYR-41 reduced the aortic expression of *Mcp-1*, *Vcam-1*, and *Icam-1*, key players in the monocyte recruitment, determined by real-time PCR analysis (Figure 4(b)). Furthermore, PYR-41 also inhibited the aortic expression of proinflammatory cytokines *Il-1β* and *Il-6* but did not alter the expression of anti-inflammatory *Il-4* or *Il-10* significantly (Figure 4(c)).

3.5. Inhibition of UBA1 Decreased Oxidative Stress in Diet-Induced Atherosclerosis in Apoe-/- Mice. Previous studies have suggested that PYR-41 inhibited the NADPH oxidase (*Nox1*, *Nox2*, and *Nox4*) expression, leading to reduced

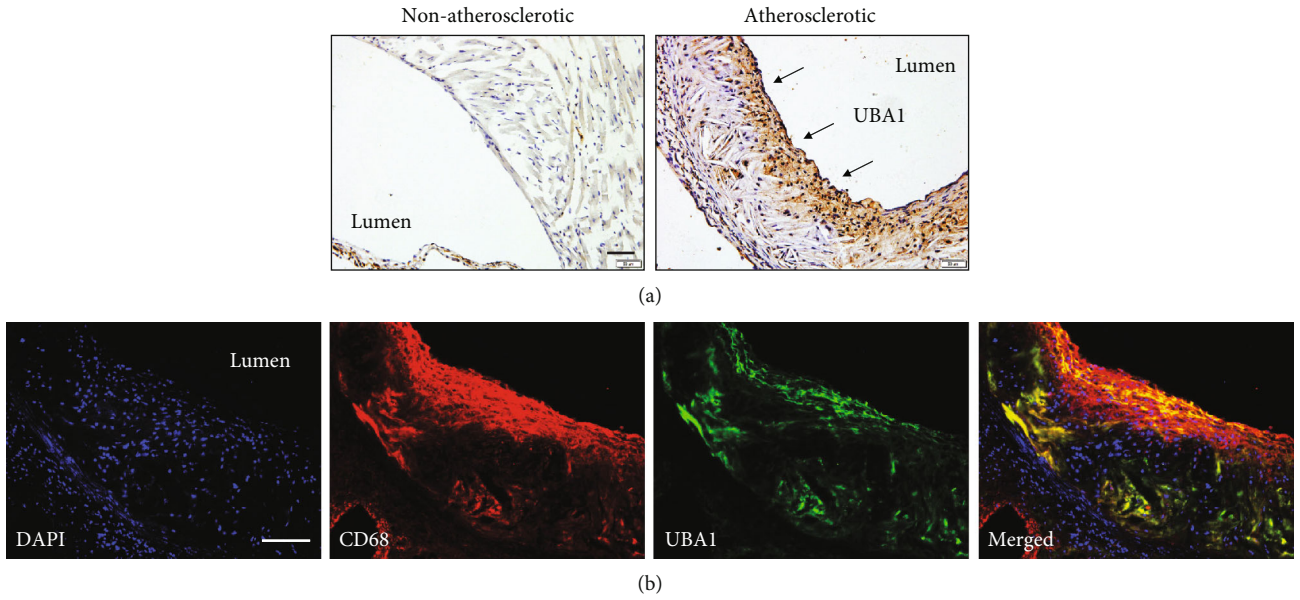

Figure 1: UBA1 expression was upregulated and mainly derived from macrophages in the atherosclerotic plaques of *Apoe*-/- mice. (a) Expression of UBA1 in the vessels with (right) or without atherosclerotic plaques (left). (b) Colocalization of UBA1 with the macrophage marker CD68 in the atherosclerotic plaques.

cellular reactive oxygen species (ROS) generation and oxidative stress that could directly induce cell death [15]. Here, we confirmed that PYR-41 treatment decreased the aortic expression of *Nox1*, *Nox2*, and *Nox4* in the *Apoe*-/- mice fed on atherogenic diet for 2 weeks (Figure 5(a)). The reduced activity of *Noxs* further led to decreased ROS generation and oxidative stress in the atherosclerotic plaques, as shown by DHE staining, which might subsequently contribute to plaque necrosis (Figure 5(b)).

3.6. Inhibition of UBA1 Blunted Ox-LDL-Induced Lipid Accumulation and Expression of Proinflammatory Cytokines and NADPH Oxidases in Cultured Macrophages. Finally, we explored whether PYR-41 could directly inhibit macrophage proinflammatory response and oxidative stress induced by oxidized low-density lipoprotein (ox-LDL) in a murine macrophage cell line, RAW264.7 cells. As shown in Figure 6(a), PYR-41 pretreatment significantly attenuated ox-LDL-induced lipid deposition in the RAW264.7 cells, shown by Oil-red O staining. Using real-time PCR analysis, we further showed that PYR-41 inhibited the expression of proinflammatory *Il-1β* and *Il-6* but did not alter the anti-inflammatory *Il-4* or *Il-10* expression (Figure 6(b)). PYR-41 also reduced the expression of *Nox1*, *Nox2*, and *Nox4* in ox-LDL-treated RAW264.7 cells (Figure 6(c)).

4. Discussion

In this study, we showed that UBA1 played an important role in the development of atherosclerosis in the *Apoe*-/- mice. The main findings of this study included (1) UBA1 expression was upregulated and mainly derived from macrophages in the diet-induced atherosclerotic plaques, (2) inhibition of UBA1 did not alter main metabolic parameters after atherogenic diet feeding, and (3) inhibition of UBA1 decreased atherosclerosis development by reducing macrophage inflammatory responses and oxidative stress. These results suggested that UBA1 inhibitor PYR-41 might represent a potential therapeutic agent for the treatment of atherosclerosis.

Atherosclerosis is primarily driven by the combination of arterial lipid deposition and inflammatory responses mediated by immune cells including monocyte-macrophages, neutrophils, and T cells [2]. Monocyte-derived macrophages play a crucial role in atherosclerosis. Upon recruitment by chemoattractant molecule *Mcp-1* and adhesion molecules *Vcam-1* and *Icam-1*, monocytes infiltrate the arterial walls and differentiate into macrophages, the latter uptake modified lipoproteins, in particular oxidized low-density lipoproteins, to form lipid-laden macrophages known as foam cells [18]. These foam cells can be typically classified as M1 cells toward proinflammatory cascade and plaque progression by secreting proinflammatory cytokines, such as *Il-1β*, *Il-6*, and *Tnfα*, and M2 cells toward inflammation and plaque regression by secreting anti-inflammatory cytokines, such as *Il-4* and *Il-10* [18, 19]. Besides cytokine secretion, foam cells also produce ROS, which are mainly mediated by NADPH oxidases (*Nox1*, *Nox2*, and *Nox4*), and therefore might cause oxidative stress that is capable of inducing cell death and necrotic core formation [20]. In this study, we observed that UBA1 expression was significantly increased and mainly derived from lesional macrophages in the atherosclerotic plaques. Further, using a small molecule inhibitor PYR-41, we demonstrated that UBA1 inactivation reduced macrophage proinflammatory responses, promoting macrophage phenotype turnover toward M1 cells. We also demonstrated that UBA1 inactivation suppressed oxidative stress by Nox-mediated ROS generation and therefore might be

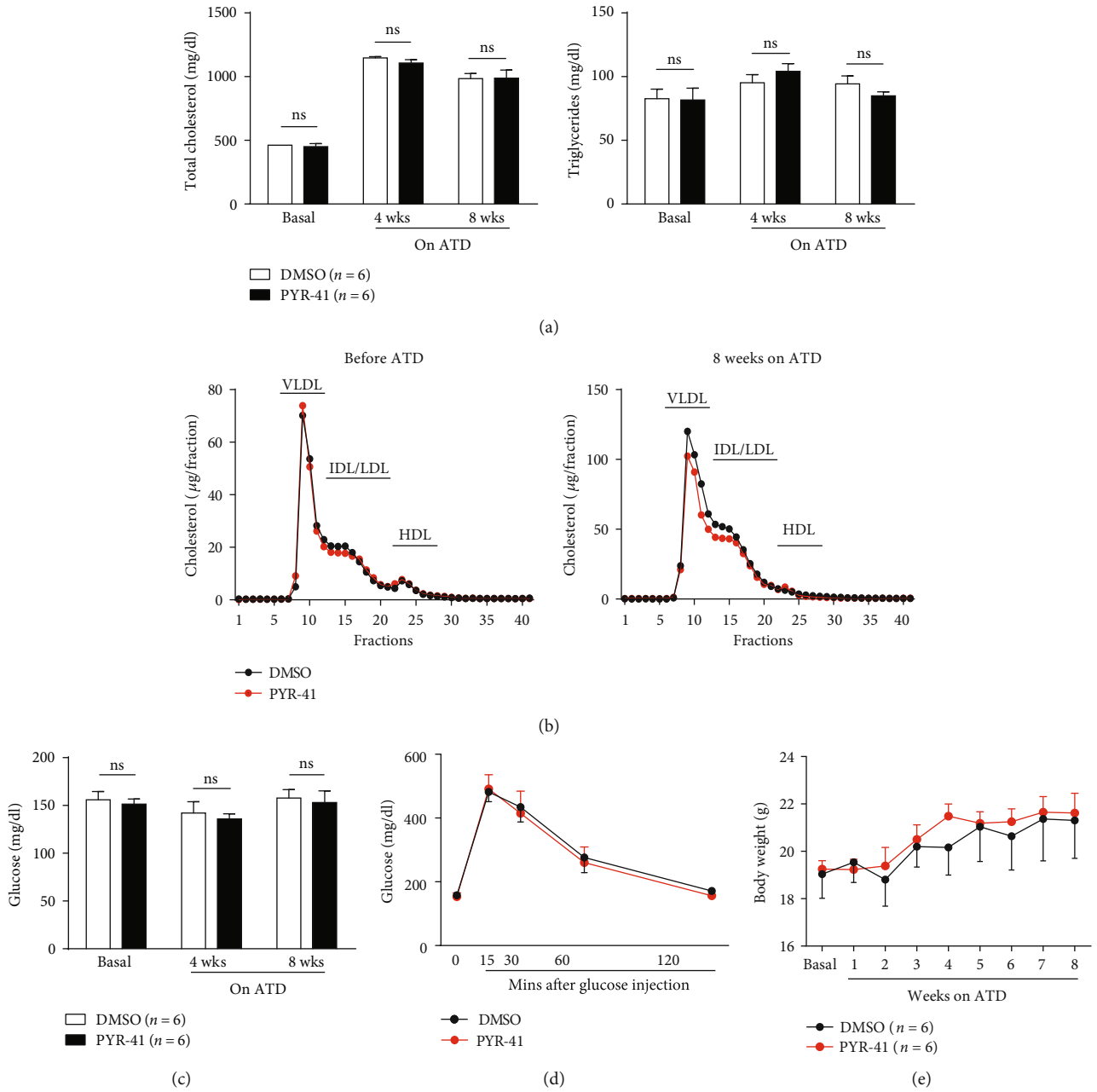

Figure 2: Inhibition of UBA1 did not alter the main metabolic parameters during diet-induced atherogenesis in *Apoe*-/- mice. (a) Plasma total cholesterol and triglyceride levels before and after the atherogenic diet feeding. (b) Plasma lipoprotein profiles fractioned by FPLC before (left) and after (right) the atherogenic diet feeding. (c) Plasma glucose levels before and after the atherogenic diet feeding. (d) Insulin resistance detected by the glucose tolerance test after 8 weeks on the atherogenic diet. (e) Body weight gain during the atherogenic diet feeding. $n = 6$ per group; ns: not significant; ATD: atherogenic diet.

correlated with less macrophage death and necrotic core formation. Thus, our data for the first time identify a possible link between E1 activating enzyme and macrophage behaviors in atherosclerosis.

Currently, only a few E1/UBA1 inhibitors have been reported. PYR-41, whose full name is 4[4-(5-nitro-furan-2-ylmethylene)-3,5-dioxo-pyrazolidin-1-yl]-benzoic acid ethyl ester, is the first cell-permeable E1/UBA1 inhibitor, although the molecular basis is unknown [21]. Previous studies from our group have showed that PYR-41 is able to prevent the degradation of a wide range of target proteins, such as IκBα and MKP-1 [15, 22]. Among them, IκBα is an inhibitory protein for NF-κB signaling pathway, which is known to play a critical role in regulating inflammatory cytokine and NADPH oxidase expression during cardiac remodeling and atherosclerosis [15, 23]. Interestingly, our recent data indicate that PYR-41 might suppress inflammation and oxidative stress possibly through stabilization of IκBα and inhibition of

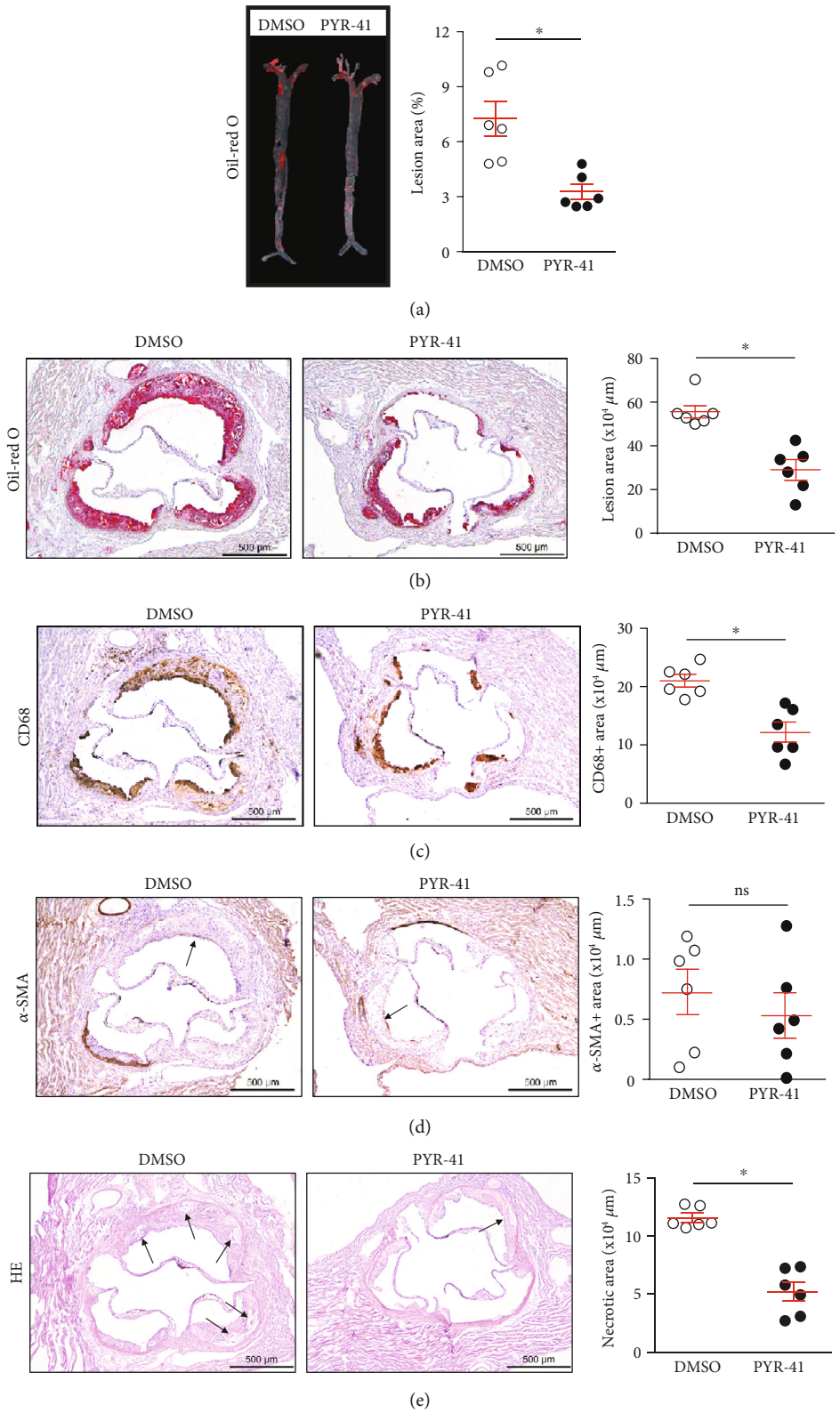

Figure 3: Inhibition of UBA1 attenuated diet-induced atherosclerosis in *Apoe*-/- mice. (a, b) Oil red O staining and quantitation of the atherosclerotic burden in the *en face* aorta (a) and the aortic root (b). (c) CD68 immunochemical staining and quantitation of the lesional macrophages in the aortic root. (d) *α*-SMA immunochemical staining and quantitation of the lesional smooth muscle cells in the aortic root. (e) HE staining and quantitation of the lesional necrotic areas in the aortic root. $n = 6$ per group; ∗: <0.05; ns: not significant.

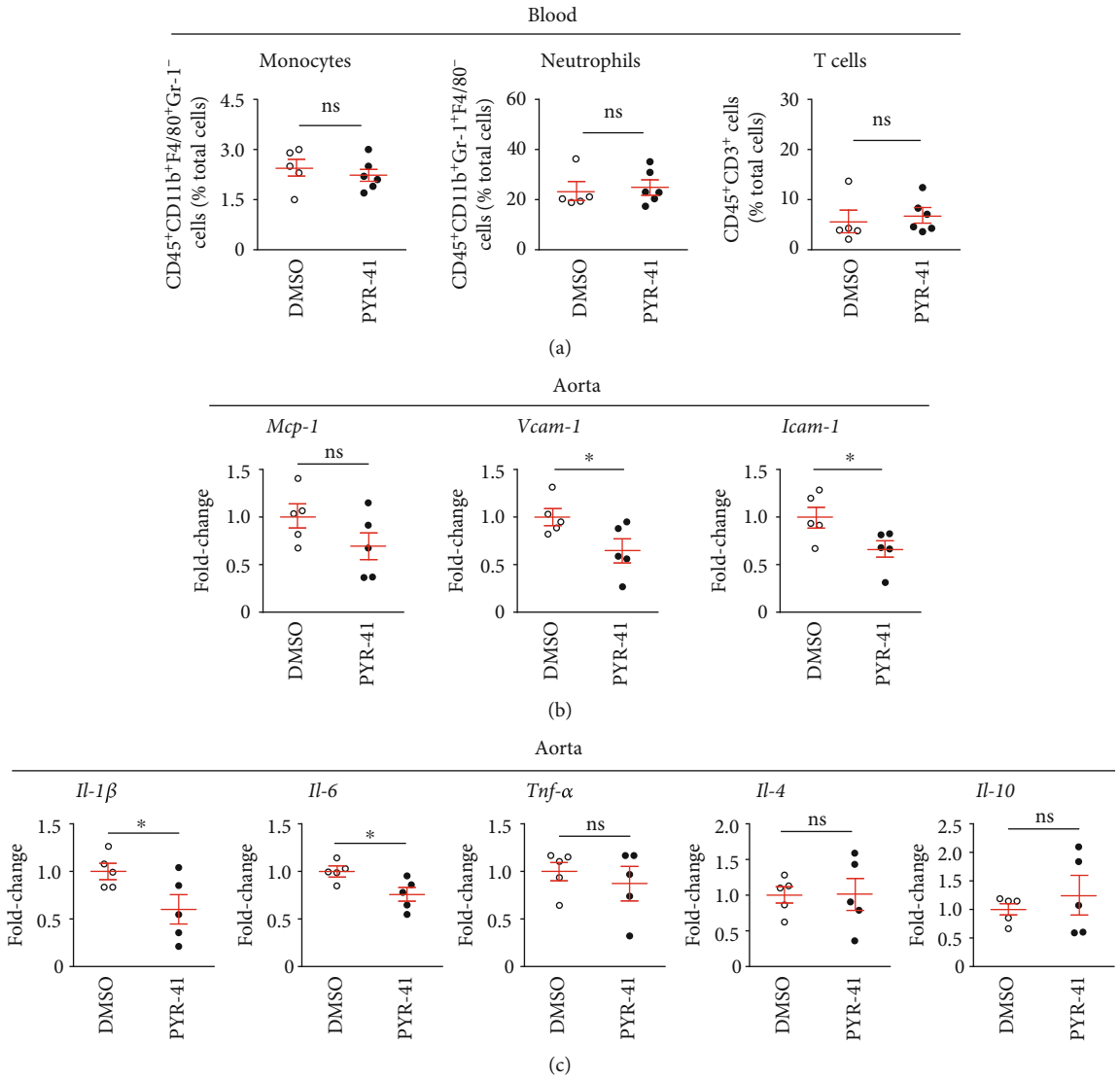

Figure 4: Inhibition of UBA1 decreased proinflammatory cytokine levels in diet-induced atherosclerosis in *Apoe*-/- mice. (a) Flow cytometry analysis of circulating monocytes, neutrophils, and T cells. (b) Quantitative real-time PCR analysis of aortic expression of cytokines associated with monocyte recruitment (*Mcp-1*, *Vcam-1*, and *Icam-1*). (c) Quantitative real-time PCR analysis of aortic expression of macrophage-derived proinflammatory (*Il-1β*, *Il-6*, and *Tnfα*) and anti-inflammatory (*Il-4* and *Il-10*) cytokines. $n = 5$-6 per group; ∗: <0.05; ns: not significant.

NF-κB activation in several cell and disease models [15, 22]. However, whether this is the case in atherosclerosis needs further exploration. In addition to inhibit NF-κB signaling, PYR-41 also reduces p53 degradation and activates the transcriptional activity of this tumor suppressor, therefore might induce p53-expressing cell death [21]. Other E1/UBA1 inhibitors include chemical inhibitor NSC624206 [24] and some natural compounds such as panepophenanthrin, himeic acid A, largazole, and hyrtioreticulins A and B [25–28]. Studies of these inhibitors supported that UBA1 might be an attractive target for drug discovery to fight against cancer, neurodegenerative disorders, and infectious diseases [29, 30]. Our data for the first time identified an inhibitory effect of UBA1 inhibitor PYR-41 in atherosclerosis, therefore might expand the therapeutic potent of UBA1 as a potential pharmaceutical target against atherosclerosis.

5. Main Text

(1) UBA1 expression was significantly increased and mainly derived from lesional macrophages in the diet-induced atherosclerotic plaques

(2) Inhibition of UBA1 did not alter main metabolic parameters after atherogenic diet feeding

(3) Inhibition of UBA1 suppressed atherosclerosis development by reducing macrophage proinflammatory responses and oxidative stress

6. Conclusions

In conclusion, we demonstrated that UBA1 expression was upregulated and mainly derived from macrophages in the

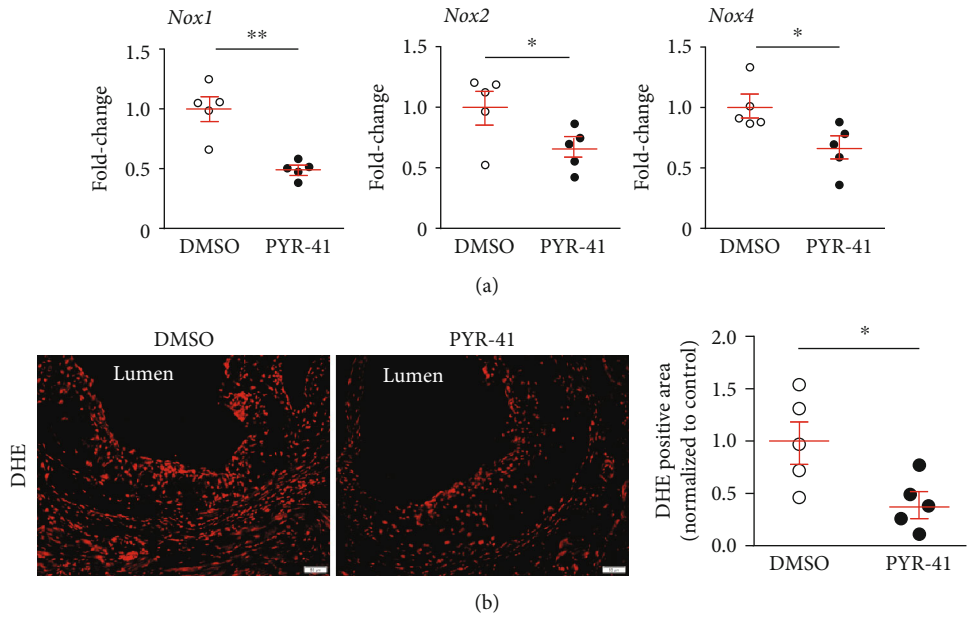

Figure 5: Inhibition of UBA1 decreased cellular oxidative stress in diet-induced atherosclerosis in *Apoe-/-* mice. (a) Quantitative real-time PCR analysis of aortic expression of NADPH oxidases (*Nox1*, *Nox2*, and *Nox4*). (b) DHE staining and quantitation of the lesional oxidative stress level in the aortic root. $n = 5$ per group; ∗: <0.05.

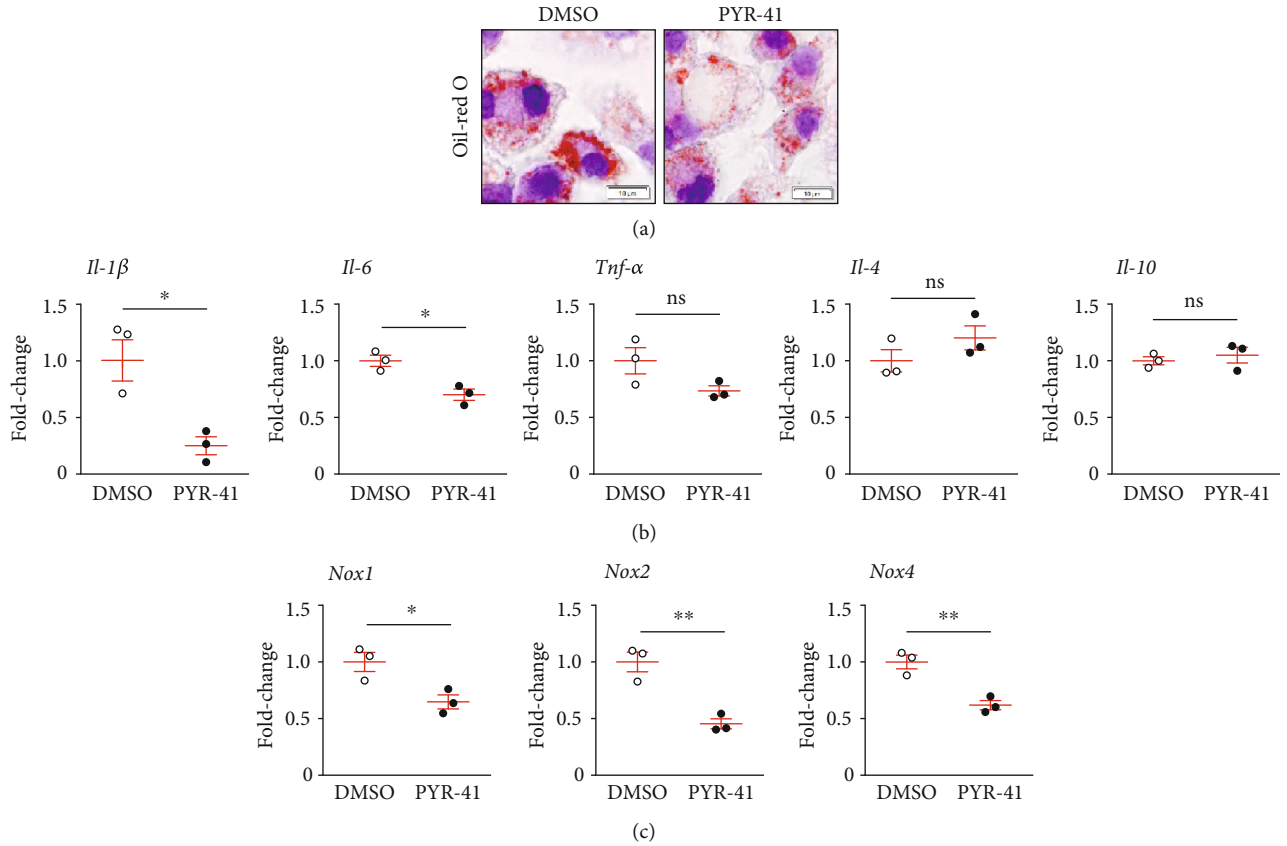

Figure 6: Inhibition of UBA1 blunted ox-LDL-induced lipid accumulation and expression of proinflammatory cytokines and NADPH oxidases in cultured macrophages. (a) Oil red O staining of ox-LDL-treated RAW264.7 cells. (b) Quantitative real-time PCR analysis of proinflammatory (*Il-1β*, *Il-6*, and *Tnfα*) and anti-inflammatory (*Il-4* and *Il-10*) cytokine expression in ox-LDL-treated RAW264.7 cells. (c) Quantitative real-time PCR analysis of NADPH oxidase (*Nox1*, *Nox2*, and *Nox4*) expression in ox-LDL-treated RAW264.7 cells. $n = 3$ per group; ∗: <0.05; ∗∗: <0.01; ns: not significant.

atherosclerotic plaques of *Apoe*-/- mice. Inhibition of UBA1 decreased diet-induced atherosclerosis by reducing macrophage infiltration and plaque necrosis. Macrophage UBA1 might be explored as a potential pharmaceutical target against atherosclerosis.

Abbreviations

Apoe: Apolipoprotein E
α-SMA: α-Smooth muscle actin
ATD: Atherogenic diet
FPLC: Fast protein liquid chromatography
GTT: Glucose tolerance test
Icam-1: Intercellular adhesion molecule-1
IκB: Inhibitor of nuclear factor-κB
Il: Interleukin
Mcp-1: Monocyte chemoattractant protein-1
NF-κB: Nuclear factor-κB
Nox: NADPH oxidase
PYR-41: 4[4-(5-Nitro-furan-2-ylmethylene)-3,5-dioxo-pyrazolidin-1-yl]-benzoic acid ethyl ester
ROS: Reactive oxygen species
UBA1: Ubiquitin-like modifier activating enzyme 1
UPS: Ubiquitin-proteasome system
Vcam-1: Vascular cell adhesion molecule-1.

Data Availability

The data used to support the findings of this study are included within the article.

Conflicts of Interest

The authors declare that there is no conflict of interest regarding the publication of this article.

Acknowledgments

This study was supported by the Youth Science Fund Program of National Natural Science Foundation of China (81600335 to Jiawei Liao) and the National Natural Science Foundation of China (81570313 to Yunlong Xia; 81630009 and 81330003 to Hui-Hua Li).

References

[1] "Cardiovascular diseases (CVDs)," https://www.who.int/news-room/fact-sheets/detail/cardiovascular-diseases-(cvds).

[2] R. Ross, "Atherosclerosis–an inflammatory disease," *The New England Journal of Medicine*, vol. 340, no. 2, pp. 115–126, 1999.

[3] N. Wilck and A. Ludwig, "Targeting the ubiquitin-proteasome system in atherosclerosis: status quo, challenges, and perspectives," *Antioxidants & Redox Signaling*, vol. 21, no. 17, pp. 2344–2363, 2014.

[4] M. Hochstrasser, "Ubiquitin, proteasomes, and the regulation of intracellular protein degradation," *Current Opinion in Cell Biology*, vol. 7, no. 2, pp. 215–223, 1995.

[5] A. Ciechanover and A. L. Schwartz, "The ubiquitin-proteasome pathway: the complexity and myriad functions of proteins death," *Proceedings of the National Academy of Sciences*, vol. 95, no. 6, pp. 2727–2730, 1998.

[6] F. Wang, A. Lerman, and J. Herrmann, "Dysfunction of the ubiquitin-proteasome system in atherosclerotic cardiovascular disease," *American Journal of Cardiovascular Disease*, vol. 5, no. 1, pp. 83–100, 2015.

[7] S. R. Powell, J. Herrmann, A. Lerman, C. Patterson, and X. Wang, "The ubiquitin-proteasome system and cardiovascular disease," *Progress in Molecular Biology and Translational Science*, vol. 109, pp. 295–346, 2012.

[8] J. Herrmann, W. D. Edwards, D. R. Holmes Jr. et al., "Increased ubiquitin immunoreactivity in unstable atherosclerotic plaques associated with acute coronary syndromes," *Journal of the American College of Cardiology*, vol. 40, no. 11, pp. 1919–1927, 2002.

[9] R. Marfella, M. D'Amico, C. Di Filippo et al., "Increased activity of the ubiquitin-proteasome system in patients with symptomatic carotid disease is associated with enhanced inflammation and may destabilize the atherosclerotic plaque: effects of rosiglitazone treatment," *Journal of the American College of Cardiology*, vol. 47, no. 12, pp. 2444–2455, 2006.

[10] D. Versari, J. Herrmann, M. Gossl et al., "Dysregulation of the ubiquitin-proteasome system in human carotid atherosclerosis," *Arteriosclerosis, Thrombosis, and Vascular Biology*, vol. 26, no. 9, pp. 2132–2139, 2006.

[11] J. P. McGrath, S. Jentsch, and A. Varshavsky, "UBA 1: an essential yeast gene encoding ubiquitin-activating enzyme," *The EMBO Journal*, vol. 10, no. 1, pp. 227–236, 1991.

[12] J. Jin, X. Li, S. P. Gygi, and J. W. Harper, "Dual E1 activation systems for ubiquitin differentially regulate E2 enzyme charging," *Nature*, vol. 447, no. 7148, pp. 1135–1138, 2007.

[13] E. J. Groen and T. H. Gillingwater, "UBA1: at the crossroads of ubiquitin homeostasis and neurodegeneration," *Trends in Molecular Medicine*, vol. 21, no. 10, pp. 622–632, 2015.

[14] Z. Qin, B. Cui, J. Jin et al., "The ubiquitin-activating enzyme E1 as a novel therapeutic target for the treatment of restenosis," *Atherosclerosis*, vol. 247, pp. 142–153, 2016.

[15] Q. Shu, S. Lai, X. M. Wang et al., "Administration of ubiquitin-activating enzyme UBA1 inhibitor PYR-41 attenuates angiotensin II-induced cardiac remodeling in mice," *Biochemical and Biophysical Research Communications*, vol. 505, no. 1, pp. 317–324, 2018.

[16] J. Liao, X. Liu, M. Gao et al., "Dyslipidemia, steatohepatitis and atherogenesis in lipodystrophic apoE deficient mice with Seipin deletion," *Gene*, vol. 648, pp. 82–88, 2018.

[17] Y. Zhang, X. An, Q. Lin, J. Bai, F. Wang, and J. Liao, "Splenectomy had no significant impact on lipid metabolism and atherogenesis in Apoe deficient mice fed on a severe atherogenic diet," *Cardiovascular Pathology*, vol. 36, pp. 35–41, 2018.

[18] K. J. Moore and I. Tabas, "Macrophages in the pathogenesis of atherosclerosis," *Cell*, vol. 145, no. 3, pp. 341–355, 2011.

[19] N. Leitinger and I. G. Schulman, "Phenotypic polarization of macrophages in atherosclerosis," *Arteriosclerosis, Thrombosis, and Vascular Biology*, vol. 33, no. 6, pp. 1120–1126, 2013.

[20] S. Tavakoli and R. Asmis, "Reactive oxygen species and thiol redox signaling in the macrophage biology of atherosclerosis," *Antioxidants & Redox Signaling*, vol. 17, no. 12, pp. 1785–1795, 2012.

[21] Y. Yang, J. Kitagaki, R. M. Dai et al., "Inhibitors of ubiquitin-activating enzyme (E1), a new class of potential cancer therapeutics," *Cancer Research*, vol. 67, no. 19, pp. 9472–9481, 2007.

[22] C. Chen, Y. Meng, L. Wang et al., "Ubiquitin-activating enzyme E1 inhibitor PYR41 attenuates angiotensin II-induced activation of dendritic cells via the IκBa/NF-κB and MKP1/ERK/STAT1 pathways," *Immunology*, vol. 142, no. 2, pp. 307–319, 2014.

[23] J. Liao, Y. Xie, Q. Lin et al., "Immunoproteasome subunit beta5i regulates diet-induced atherosclerosis through altering MERTK-mediated efferocytosis in Apoe knockout mice," *The Journal of Pathology*, vol. 250, no. 3, pp. 275–287, 2020.

[24] D. Ungermannova, S. J. Parker, C. G. Nasveschuk et al., "Identification and mechanistic studies of a novel ubiquitin E1 inhibitor," *Journal of Biomolecular Screening*, vol. 17, no. 4, pp. 421–434, 2012.

[25] S. Tsukamoto, H. Hirota, M. Imachi et al., "Himeic acid A: a new ubiquitin-activating enzyme inhibitor isolated from a marine-derived fungus, *Aspergillus sp.*," *Bioorganic & Medicinal Chemistry Letters*, vol. 15, no. 1, pp. 191–194, 2005.

[26] D. Ungermannova, S. J. Parker, C. G. Nasveschuk et al., "Largazole and its derivatives selectively inhibit ubiquitin activating enzyme (e1)," *PLoS One*, vol. 7, no. 1, article e29208, 2012.

[27] R. Yamanokuchi, K. Imada, M. Miyazaki et al., "Hyrtioreticulins A-E, indole alkaloids inhibiting the ubiquitin-activating enzyme, from the marine sponge _Hyrtios reticulatus_," *Bioorganic & Medicinal Chemistry*, vol. 20, no. 14, pp. 4437–4442, 2012.

[28] R. Sekizawa, S. Ikeno, H. Nakamura et al., "Panepophenanthrin, from a mushroom strain, a novel inhibitor of the ubiquitin-activating enzyme," *Journal of Natural Products*, vol. 65, no. 10, pp. 1491–1493, 2002.

[29] W. Xu, J. L. Lukkarila, S. R. da Silva, S. L. Paiva, P. T. Gunning, and A. D. Schimmer, "Targeting the ubiquitin E1 as a novel anti-cancer strategy," *Current Pharmaceutical Design*, vol. 19, no. 18, pp. 3201–3209, 2013.

[30] M. J. Edelmann, B. Nicholson, and B. M. Kessler, "Pharmacological targets in the ubiquitin system offer new ways of treating cancer, neurodegenerative disorders and infectious diseases," *Expert Reviews in Molecular Medicine*, vol. 13, article e35, 2011.

Hindawi
Journal of Immunology Research
Volume 2020, Article ID 1704631, 9 pages
https://doi.org/10.1155/2020/1704631

Review Article

Involvement of lncRNAs and Macrophages: Potential Regulatory Link to Angiogenesis

Yang Jia[1] **and Yedi Zhou**[2,3]

[1]*Department of Pediatrics, The Second Xiangya Hospital, Central South University, Changsha, Hunan 410011, China*
[2]*Department of Ophthalmology, The Second Xiangya Hospital, Central South University, Changsha, Hunan 410011, China*
[3]*Hunan Clinical Research Center of Ophthalmic Disease, Changsha, Hunan 410011, China*

Correspondence should be addressed to Yedi Zhou; zhouyedi@csu.edu.cn

Received 1 November 2019; Revised 29 January 2020; Accepted 4 February 2020; Published 29 February 2020

Guest Editor: Mohammad A. Khan

Macrophages are involved in angiogenesis, an essential process for organ growth and tissue repair, and could contribute to the pathogenesis of angiogenesis-related diseases such as malignant tumors and diabetic retinopathy. Recently, long noncoding RNAs (lncRNAs) have been proved to be important in cell differentiation, organismal development, and various diseases of pathological angiogenesis. Moreover, it has been indicated that numerous lncRNAs exhibit different functions in macrophage infiltration and polarization and regulate the secretion of inflammatory cytokines released by macrophages. Therefore, the focus of macrophage-related lncRNAs could be considered to be a potential method in therapeutic targeting angiogenesis-related diseases. This review mainly summarizes the roles played by lncRNAs which associated with macrophages in angiogenesis. The possible mechanisms of the regulatory link between lncRNAs and macrophages in various angiogenesis-related diseases were also discussed.

1. Introduction

Angiogenesis is the growth process of blood vessels and plays important roles in the physiological functions for organ growth and tissue repair [1], as well as a large number of angiogenesis-related diseases such as tumors, arthritis, diabetic retinopathy, and age-related macular degeneration [2]. Targeting angiogenesis is an effective therapeutic method for anticancer treatment and has been applied in many kinds of cancer (e.g., lung cancer [3, 4] and gastric cancer [5]). The treatment of antivascular endothelial growth factor (VEGF) has been applied in inhibiting angiogenesis, especially in cancer [6] and ocular diseases [7]. However, beyond VEGF, there are also a variety of other molecules that play important roles in the mechanisms of angiogenesis [8, 9].

Long noncoding RNAs (lncRNAs) are those which demonstrate no apparent protein-coding capacity and longer than 200 nucleotides [10]. Recent studies indicated a variety of regulatory functions of lncRNAs in a wide range of cellular and developmental processes as well as pathogenesis [11–15]. In particular, lncRNAs control cell differentiation and self-renewal through neural, skin, and muscle stem cells [16]. LncRNAs are also involved in diseases of pathological angiogenesis, such as diabetic retinopathy [17, 18].

Macrophages are important angiogenic effector cells and act as key modulators in both tumor growth and angiogenesis [19]. Many studies suggested that under various stimuli, macrophages could be polarized to two phenotypes: classically activated M1 phenotype and alternatively activated M2 phenotype [20–22]. Those M1 macrophages can destroy foreign organisms and inhibit tumor growth, while M2 phenotype functions in wound healing, chronic infections, tumor growth, and angiogenesis [23–29]. We previously revealed that M2 macrophages, rather than M1 phenotype, infiltrated in the inner layer of the retinas of oxygen-induced retinopathy and enhanced retinal neovascularization *in vivo* [30]. In a choroidal neovascularization mouse model, we recognized that M1 and M2 macrophages have different distributions, thus might have diverse potential biological functions in angiogenesis [31]. A recent study

reported that lncRNA MM2P regulated tumorigenesis and angiogenesis via modulating M2-like macrophage polarization [32], indicating that lncRNAs and macrophages might be involved and have a potential regulatory link to angiogenesis.

In the present review, we summarize the roles of lncRNAs associated with macrophages in angiogenesis and discuss the possible mechanisms of the regulatory link between lncRNAs and macrophages in various angiogenesis-related diseases.

2. LncRNAs Regulate Macrophage Infiltration, Polarization, and Functions

Monocytes are considered as the precursors of macrophages, originated from hematopoietic stem cells, and monocyte/-macrophage differentiation plays a critical role in response to the immune system and pathological diseases [33–35]. It has been indicated that lncRNA lnc-MC was involved in monocyte/macrophage differentiation, positively regulated by PU.1, a hematopoiesis-specific transcription factor, and negatively interacted with miR-199a to promote differentiation process [36]. Besides monocyte/macrophage differentiation, lncRNAs seemed to be involved in macrophage infiltration. For example, downregulation of LRNA9884 significantly suppressed macrophage infiltration by reducing the level of monocyte chemoattractant protein-1 (MCP-1) in a type 2 diabetic nephropathy mice model [37]. Moreover, lncRNA CASC2c could inhibit macrophage migration and M2 polarization by negatively regulating the expression of coagulation factor X, which was reported to promote the infiltration of macrophages to the glioblastoma multiforme tumor cells, and polarize macrophages to M2 phenotype [38]. In contrast, activated lncRNA UCA1 promoted macrophage infiltration, resulting in carcinogenesis and progression of breast cancer [39].

LncRNAs could also induce macrophage polarization and lead to regulatory effects on their functions. Lipopolysaccharide (LPS) and interleukin- (IL-) 4 induction was commonly applied for M1/M2 macrophage polarization, respectively [32]. Ye et al. observed that lncRNA Cox-2 is expressed higher in LPS-induced M1 macrophages than IL-4-induced M2 macrophages, and silencing lncRNA Cox-2 expression markedly altered the macrophage polarization from M1 to M2 phenotype [40]. In addition, lncRNA Cox-2 siRNA significantly enhanced the ability of macrophages in tumor proliferation, invasion, and migration by mediating M1/M2 polarization [40]. Moreover, using the gain-of-function and loss-of-function strategies, lncRNA TUC339 was recognized to be required for macrophage polarization to regulate the release of pro- or anti-inflammatory cytokines and thereby affect tumor growth [41]. Overexpression of TUC339 in hepatocellular carcinoma (HCC) cells suppressed the expression of proinflammatory factors, such as IL-1β and TNF-α, and knockdown of TUC339 obtained an opposite effect [41]. It has been reported that LPS could strengthen the lncRNA CCL2 levels to mediate the expressions of inflammatory factors in macrophages, and this enhancement could be suppressed by SIRT1 in sepsis [42]. Knockdown of lncRNA CCL2 resulted in a reduction of IL-1β, IL-6, and TNF-α [42]. In response to LPS, lncRNA Nfkb2 and lncRNA Rel, located near proinflammatory transcription genes, were increased and closely related to the inflammatory response in mouse macrophages [43].

Some lncRNAs could target related molecules or signaling pathways to regulate macrophage polarization. For example, lncRNA GAS5 was significantly reduced in M2-polarized microglia, and overexpression of GAS5 suppressed microglial M2 polarization via inhibition of transcription of IRF4, which is an important regulatory molecule of M2 polarization [44]. As we discussed, lncRNA MM2P was higher expressed in M2 macrophages rather than in M1 macrophages, and blockade of lncRNA MM2P could weaken the IL-4/STAT6 signaling pathway, resulting in a reduction of both cytokine-regulated M2 polarization and M2-induced angiogenesis [32]. NF-κB, which is a downstream signaling pathway of toll-like receptors (TLRs) after specific microbial and pathogen recognition, could induce transcription of proinflammatory genes and is strongly involved in the regulation of macrophage polarization [45]. After LPS stimulation, the expression of lncRNA Mirt2 was induced in macrophages and suppressed the proinflammatory factors (such as TNF, IL-1β, IL-6, and IL-12) by inhibiting the activation of NF-κB and MAPK pathways [46]. In contrast to LPS, Mirt2 also could promote the polarization of M2 macrophages induced by IL-4, but the mechanism might be independent from STAT6 and PPARγ pathways [46]. Under LPS-mediated inflammatory conditions, lncRNA Tnfaip3 exerts a coregulatory role with NF-κB in modulating inflammatory gene transcription in macrophages [47]. Another NF-κB-mediated lncRNA FIRRE exhibited posttranscriptional elevation of inflammatory genes in macrophages and epithelial cells by interacting with heterogeneous nuclear ribonucleoproteins U after LPS stimulating [48]. Overall, these studies showed that the expression profiles of lncRNAs can be clearly distinguished between M1 and M2 macrophages, indicating that lncRNAs could be involved in regulating macrophage polarization. Dysregulation of lncRNAs may affect macrophage polarization by targeting both downstream signaling pathways and the release of inflammation cytokines.

According to competing endogenous RNA (ceRNA) networks, lncRNAs could act as sponges to regulate the functions of miRNAs [49]. Studies had demonstrated that lncRNA NIFK-AS1 and lncRNA CCAT1 could inhibit the polarization of M2 macrophages by targeting miR146a and miR-148a, respectively [50, 51]. Moreover, lncRNA XIST and lncRNA GNAS-AS1 exhibited the promotion of M2 polarization, such functions were associated with T-cell-specific transcription factor 4 (TCF-4) and miR-4319, respectively [52, 53].

MALAT1 is an important lncRNA that has been widely investigated [18, 54–57]. Recent studies had reported that the MALAT1 regulates the production of inflammatory cytokines [56] and was increased in a LPS-induced acute lung injury model to regulate the release of IL-1β, IL-6, and TNF-α [58]. Silencing of MALAT1 inhibited the proinflammatory responses by enhancing miR-146a levels in macrophages and epithelial cells [58]. In LPS-induced septic cardiomyocytes, expression of MALAT1 was induced by

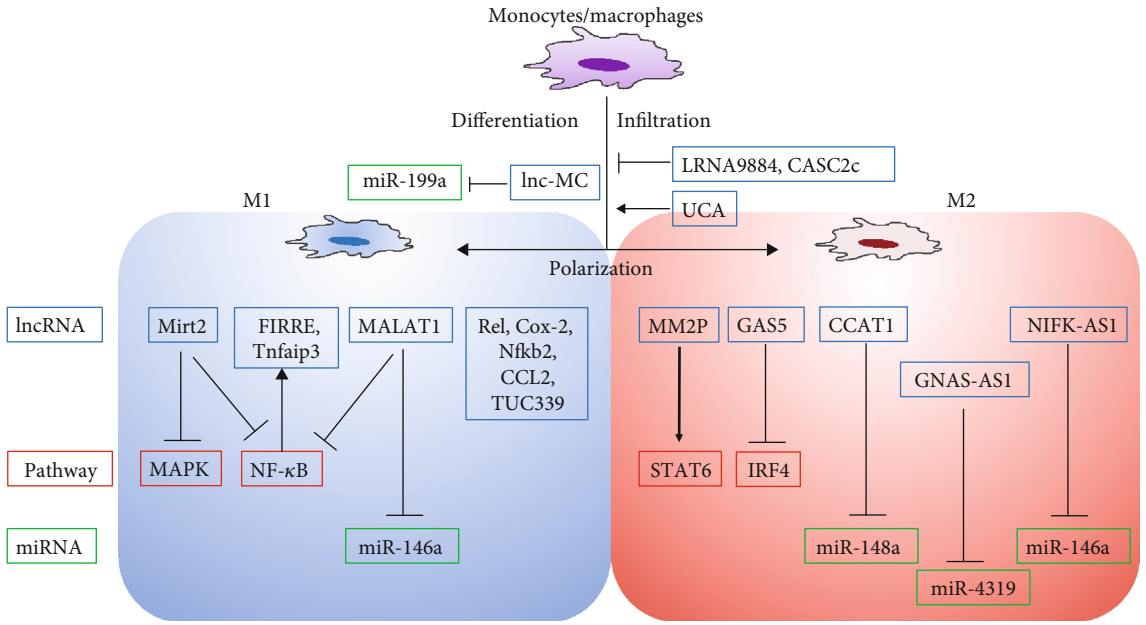

Figure 1: The mechanisms of lncRNAs regulate macrophage infiltration, polarization, and functions.

IL-6 and elevated the production of TNF-α partially through serum amyloid antigen 3 (SAA3) [59]. By targeting SAA3, MALAT1 also could modulate the expression of IL-6 and TNF-α in the endothelial cells under high-glucose conditions [60]. Although the proinflammatory activities of MALAT1 in macrophages were reported, Zhao et al. presented an opposite effect of MALAT1, which functions as an anti-inflammatory regulation *in vitro* [61]. In this study, scientists had demonstrated that MALAT1 was upregulated by LPS to suppress the production of proinflammatory TNF-α and IL-6 by interacting with the NF-κB pathway in macrophages. The knockdown of MALAT1 achieved enhancement of TNF-α and IL-6 [61]. It is known that tumor-associated macrophages (TAMs) exhibit similar functions to M2 macrophages [62] and MALAT1 was upregulated in TAMs compared to nonpolarized macrophages and promoted angiogenesis through secretion of fibroblast growth factor-2 (FGF2) protein [63]. Moreover, in macrophages, MALAT1 regulates lysosomal-associated membrane protein 1 (lamp1) expression by sponging miR-23-3p [64]. For the above contradictory effect of MALAT1 in inflammatory responses, further investigations are required to reveal the essential mechanisms of MALAT1 to macrophage functions in angiogenesis.

Together, the above studies suggest that lncRNAs could regulate macrophage infiltration, polarization, inflammation, and secretion by targeting various pathways to change the pro- and/or anti-inflammatory response mechanisms (Figure 1). Further studies on the mechanism of lncRNAs in macrophages can lead to enhance the understanding on how lncRNAs might be involved in inflammation and thereby affect the regulation of immune response of angiogenesis.

3. Link between Macrophages and Angiogenesis

It is widely considered that M1 macrophages present a proinflammatory effect and M2 macrophages present an anti-inflammatory effect. Besides, M2 macrophages also induce proangiogenic functions, and the induction of M2 macrophages enhances cancer invasion and metastasis, as well as the development of neovascular diseases through VEGF [65–67]. By now, although the activation of the downstream pathway during angiogenesis is still not completely clear, activated macrophages could influence the angiogenic process through the production of angiogenic factors such as IL-1, IL-6, IL-8, TNF-α, TGF-α, TGF-β, GM-CSF, bFGF, and VEGF [68]. Moreover, activation of NF-κB and STAT3 is involved in the upstream pathway of macrophage-induced angiogenesis [69, 70]. Thus, macrophages and angiogenesis are very closely linked with complicated mechanisms.

4. Involvement of lncRNAs in the Pathogenesis of Angiogenesis-Related Diseases

4.1. Tumor Angiogenesis. Many studies revealed the involvement of lncRNAs in the recruitment of macrophages to tumor cells and M1/M2 polarization of macrophages to change the tumor microenvironment.

As we discussed before, MALAT1 not only acted as a potential cancer biomarker [54] but also regulated angiogenesis in diabetic retinopathy [71], tumor [63, 72–74], hindlimb ischemia [75], and brain vascular endothelium [76]. In particular, as we described, Huang et al. reported that MALAT1 enhanced thyroid cancer angiogenesis by regulating FGF2 secretion of TAMs [63]. In HCC cells, MALAT1 could promote angiogenesis and regulate polarization of macrophages through sponging miR-140 [74]. These suggested that macrophages might be an important modulator of angiogenesis in the mechanisms of MALAT1.

As mentioned above, MM2P could contribute to promoting M2 polarization of macrophages and inducing angiogenesis, resulting in tumor deterioration [32]. As we described, lncRNA UCA1 was demonstrated to be involved in macrophage recruitment to promote breast cancer invasion in a previous study [39]. In cervical cancer cells, UCA1 was upexpressed and negatively associated with miR-206, and knockdown of UCA1 directly decreased VEGF through miR-206 upregulation, and thereby suppressed tumor growth, viability, migration, and invasion [77]. Another lncRNA TUC339 was significantly increased in cancer stem cell-derived exosomes, and VEGF was enhanced in exosomes derived from cancer stem cells correspondingly [78]. The knockdown of TUC339 reduced HCC cell growth and spread [79]. The mechanism has been uncovered that TUC339 could regulate the macrophage polarization, functioning as promotion of anti-inflammatory cytokines and angiogenesis, thereby accelerating tumor proliferation [41]. Sang et al. showed that lncRNA CamK-A was involved in macrophage infiltration and angiogenesis by triggering the transcription of the NF-κB signaling pathway in tumor cells [80]. By promoting NF-κB downstream cytokines (e.g., VEGF, IL-6, and TNF-α), Camk-A could remodel tumor microenvironment to recruit macrophages to tumors and contribute to angiogenesis [80]. LncRNA LNMAT1 upregulated CCL2 and recruited M2 macrophages to the tumor, and promoted lymphatic metastasis via excretion of VEGF-C [81]. These studies indicated that lncRNAs could regulate the recruitment of macrophages to the tumor, macrophage polarization, secretion of VEGF, and thereby the induction of pathological angiogenesis and tumor growth and spread.

It has been demonstrated that lncRNA PVT1 is involved in the high microvessel density in gastric cancer as well as the promotion of tumor growth through activation of the STAT3 signaling pathway as well as secretion of VEGFA [82]. The knockdown of lncRNA ROR was reported to reduce angiogenesis through inhibition of NF-κB and JAK1/STAT3 pathways [83]. Moreover, overexpression of miR-26 could rescue the negative effects of ROR silencing, demonstrating that ROR functions as a molecular sponge for miR-26 in these activations [83]. LncRNA LIMT was suppressed by epidermal growth factor (EGF) and downregulated in breast cancer and ovarian cancer, and the EGF secreted from TAMs suppressed the levels of LIMT through activation of the EGF-ERK pathway [84, 85]. Although the direct links between these lncRNAs and macrophages were poorly indicated, it is possible that lncRNAs could interact with macrophage-related signaling pathways to regulate the tumor angiogenesis.

4.2. Angiogenesis in Other Diseases. Many major causes for blindness, such as age-related macular degeneration, retinopathy of prematurity, diabetic retinopathy, and retinal vein occlusions, are due to the pathological angiogenesis [86]. In particular, diabetic retinopathy, a complication of diabetes mellitus, is a major cause of blindness worldwide in which pathological processes are characterized by the formation of abnormal blood vessels within the eye [87]. LncRNAs could target macrophage-related signaling pathways to regulate the pathological angiogenesis. With the high-glucose treatment in human retinal endothelial cells, the expression of lncRNA ANRIL was increased and regulated VEGF expression through polycomb repressive complex 2 (PRC2) complex [88]. By binding to the NF-κB signaling pathway, ANRIL could induce pathologic damage of retinopathy in the diabetic rat model [89]. Moreover, ANRIL could also promote angiogenesis by activating the NF-κB pathway in diabetes combined with cerebral infraction in a rat model [90]. Similarly, the expression of lncRNA MIAT was also elevated on high glucose stress through impacting the VEGF signaling pathway, while knockdown of MIAT attenuated retinal vessel dysfunction [91]. Clinical investigations in diabetes patients had shown that increased expression of MIAT was markedly associated with diabetic retinopathy process, and the increased MIAT decreased the viability of ARPE-19 cells in vitro via targeting the TGF-β1 pathway [92]. The high-glucose conditions suppress the expression of lncRNA MEG3, whereas the rescue of MEG3 could delay diabetic retinopathy by inhibiting TGF-1 and VEGF levels [93]. In addition, MEG3 could also be regulated by activation of the PI3k/Akt pathway in diabetes mellitus-related microvascular dysfunction [94].

LncRNA NEAT1 was reported to be involved in M2 macrophage polarization [95] and could promote inflammation in macrophages [96, 97]. NEAT1 could accelerate angiogenesis by enhancing VEGF, SIRT1, and BCL-XL in brain microvascular endothelial cells [98]. Indeed, loss of NEAT1 expression exhibits downregulation of VEGF and upregulation of miR-377 resulting in antiangiogenesis and proapoptosis [98], while the mechanisms of macrophage polarization and functions lack investigation. In contrast, lncRNA MEG3 negatively regulated angiogenesis after ischemic stroke via suppressing the Notch pathway [99], and the silencing of MEG3 resulted in a proangiogenesis effect in vascular endothelial cells [100]. Yan et al. found MEG3 could be activated and participated in apoptosis of macrophages under oxidized low-density lipoprotein stimulation, indicating a novel role of MEG3/miR-204/CDKN2A pathway in macrophages [101]. Therefore, these two lncRNAs were reported to be related to both angiogenesis and macrophages in each study, and it is highly hypothesized that lncRNAs might alter macrophage functions to regulate pathological angiogenesis. On the other hand, we demonstrated that M2 macrophages, rather than M1, have essential functions in promoting retinal pathological neovasculization, while more experimental evidence is needed to support this hypothesis [30]. In our previous study, 198 upregulated and 175 downregulated lncRNAs were identified by microarray analysis in an oxygen-induced retinopathy mouse model [102]. Among them, we highlighted four validated lncRNAs that could be potentially involved in cell adhesion molecules and thereby affect the progress of pathological retinal angiogenesis [102]. In a mouse model of choroidal neovascularization induced by laser photocoagulation, we identified 716 altered lncRNAs, and the altered target genes of 7 validated lncRNAs were enriched in the immune system process and the chemokine signaling pathway [103]. Therefore, macrophages might also be involved in the immunological regulation associated with those altered lncRNAs.

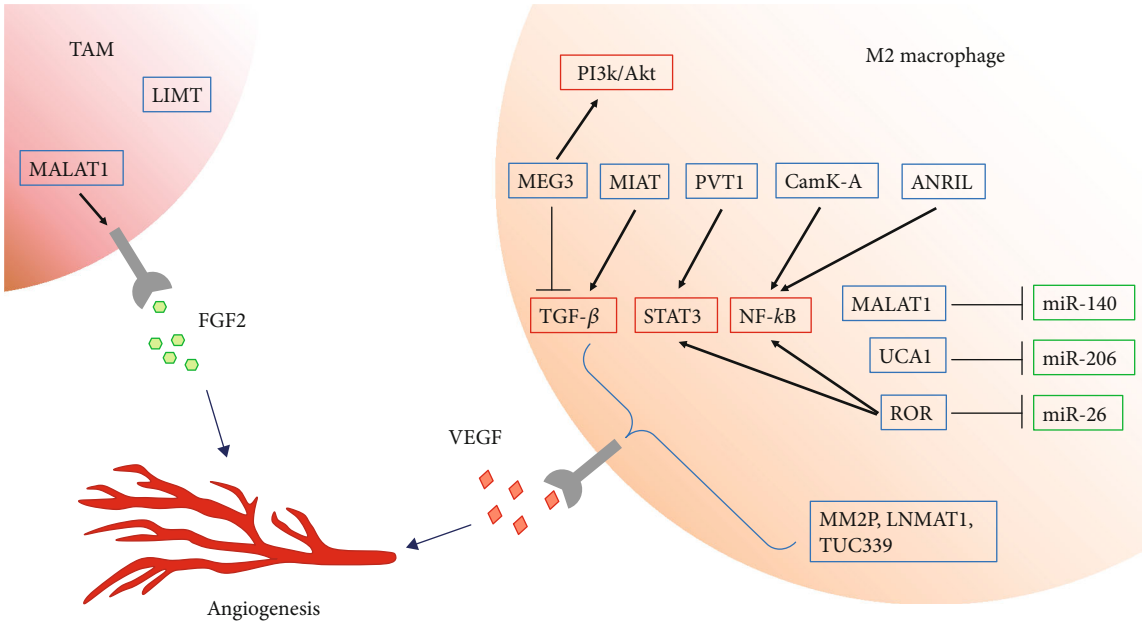

Figure 2: lncRNAs target macrophage-related pathways or miRNAs in macrophages to induce angiogenesis via elevating expression of VEGF or FGF2 in angiogenesis-related diseases.

Moreover, lncRNA could be involved in monocyte/-macrophage differentiation to regulate the pathogenesis. For example, lncRNA NTT was reported to be elevated in rheumatoid arthritis and its activation contributes to monocyte/macrophage differentiation, resulting in the pathological process of rheumatoid arthritis [104].

Thus, lncRNAs are involved in various diseases associated with angiogenesis (Figure 2) and partially via the regulation of the functions of macrophages.

5. Summary

In sum, lncRNAs have been proved to play essential roles in angiogenesis in a variety of diseases. As shown in Figure 2, the mechanisms of direct effect to endothelial cells include regulating the secretion of growth factors or cytokines, such as VEGF or FGF2, and through a diverse range of pathways. On the other hand, some lncRNAs may also be associated with macrophage infiltration, differentiation, and polarization, and both lncRNAs and macrophages were involved in and have potential links to angiogenesis. Though some progress has been achieved in characterizing the functional lncRNAs in regulation of macrophage polarization, the mechanisms remain unclear, and further investigations are needed to understand the exact roles of lncRNAs which link to macrophages and angiogenesis. Therefore, targeting lncRNAs and the links with macrophages could be considered a novel therapeutic method in treating angiogenesis in different diseases.

Conflicts of Interest

The authors report no conflicts of interest.

Acknowledgments

This work was supported by the National Natural Science Foundation of China (No. 81800855), Hunan Province Natural Science Foundation (No. 2018JJ3765), Changsha Science and Technology Project (kq1907075), and Hunan Department of Science and Technology (No. 2015TP2007).

References

[1] P. Carmeliet, "Angiogenesis in life, disease and medicine," *Nature*, vol. 438, no. 7070, pp. 932–936, 2005.

[2] A. Fallah, A. Sadeghinia, H. Kahroba et al., "Therapeutic targeting of angiogenesis molecular pathways in angiogenesis- dependent diseases," *Biomedicine & Pharmacotherapy*, vol. 110, pp. 775–785, 2019.

[3] S. M. Lee, P. Baas, and H. Wakelee, "Anti-angiogenesis drugs in lung cancer," *Respirology*, vol. 15, no. 3, pp. 387–392, 2010.

[4] A. Onn, J. Bar, and R. S. Herbst, "Angiogenesis inhibition and lung-cancer therapy," *The Lancet Oncology*, vol. 15, no. 2, pp. 124-125, 2014.

[5] M. Zang, L. Hu, B. Zhang et al., "Luteolin suppresses angiogenesis and vasculogenic mimicry formation through inhibiting Notch1-VEGF signaling in gastric cancer," *Biochemical and Biophysical Research Communications*, vol. 490, no. 3, pp. 913–919, 2017.

[6] N. Ferrara, K. J. Hillan, H. P. Gerber, and W. Novotny, "Discovery and development of bevacizumab, an anti-VEGF antibody for treating cancer," *Nature Reviews Drug Discovery*, vol. 3, no. 5, pp. 391–400, 2004.

[7] P. Osaadon, X. J. Fagan, T. Lifshitz, and J. Levy, "A review of anti-VEGF agents for proliferative diabetic retinopathy," *Eye*, vol. 28, no. 5, pp. 510–520, 2014.

[8] T. Nakama, S. Yoshida, K. Ishikawa et al., "Inhibition of choroidal fibrovascular membrane formation by new class of

RNA interference therapeutic agent targeting periostin," *Gene Therapy*, vol. 22, no. 2, pp. 127–137, 2015.

[9] Y. Kobayashi, S. Yoshida, Y. Zhou et al., "Tenascin-C secreted by transdifferentiated retinal pigment epithelial cells promotes choroidal neovascularization via integrin alphaV," *Laboratory Investigation*, vol. 96, no. 11, pp. 1178–1188, 2016.

[10] G. Bohmdorfer and A. T. Wierzbicki, "Control of chromatin structure by long noncoding RNA," *Trends in Cell Biology*, vol. 25, no. 10, pp. 623–632, 2015.

[11] N. A. Rapicavoli, K. Qu, J. Zhang, M. Mikhail, R. M. Laberge, and H. Y. Chang, "A mammalian pseudogene lncRNA at the interface of inflammation and anti-inflammatory therapeutics," *eLife*, vol. 2, article e00762, 2013.

[12] L. Yang, C. Lin, C. Jin et al., "lncRNA-dependent mechanisms of androgen-receptor-regulated gene activation programs," *Nature*, vol. 500, no. 7464, pp. 598–602, 2013.

[13] X. Sun, Y. Yuan, Y. Xiao et al., "Long non-coding RNA, *Bmcob*, regulates osteoblastic differentiation of bone marrow mesenchymal stem cells," *Biochemical and Biophysical Research Communications*, vol. 506, no. 3, pp. 536–542, 2018.

[14] K. Liu, H. Yao, Y. Wen et al., "Functional role of a long noncoding RNA LIFR-AS1/miR-29a/TNFAIP3 axis in colorectal cancer resistance to pohotodynamic therapy," *Biochimica et Biophysica Acta (BBA) - Molecular Basis of Disease*, vol. 1864, no. 9, pp. 2871–2880, 2018.

[15] J. Jia, M. Zhang, Q. Li, Q. Zhou, and Y. Jiang, "Long noncoding ribonucleic acid NKILA induces the endoplasmic reticulum stress/autophagy pathway and inhibits the nuclear factor-k-gene binding pathway in rats after intracerebral hemorrhage," *Journal of Cellular Physiology*, vol. 233, no. 11, pp. 8839–8849, 2018.

[16] R. A. Flynn and H. Y. Chang, "Long noncoding RNAs in cell-fate programming and reprogramming," *Cell Stem Cell*, vol. 14, no. 6, pp. 752–761, 2014.

[17] B. Yan, Z. F. Tao, X. M. Li, H. Zhang, J. Yao, and Q. Jiang, "Aberrant expression of long noncoding RNAs in early diabetic retinopathy," *Investigative Ophthalmology & Visual Science*, vol. 55, no. 2, pp. 941–951, 2014.

[18] S. Biswas, A. A. Thomas, S. Chen et al., "MALAT1: an epigenetic regulator of inflammation in diabetic retinopathy," *Scientific Reports*, vol. 8, no. 1, p. 6526, 2018.

[19] C. Lamagna, M. Aurrand-Lions, and B. A. Imhof, "Dual role of macrophages in tumor growth and angiogenesis," *Journal of Leukocyte Biology*, vol. 80, no. 4, pp. 705–713, 2006.

[20] M. Hesketh, K. B. Sahin, Z. E. West, and R. Z. Murray, "Macrophage phenotypes regulate scar formation and chronic wound healing," *International Journal of Molecular Sciences*, vol. 18, no. 7, article 1545, 2017.

[21] A. Mantovani, A. Sica, S. Sozzani, P. Allavena, A. Vecchi, and M. Locati, "The chemokine system in diverse forms of macrophage activation and polarization," *Trends in Immunology*, vol. 25, no. 12, pp. 677–686, 2004.

[22] M. Locati, A. Mantovani, and A. Sica, "Macrophage activation and polarization as an adaptive component of innate immunity," *Development and Function of Myeloid Subsets*, vol. 120, pp. 163–184, 2013.

[23] S. Gordon and F. O. Martinez, "Alternative activation of macrophages: mechanism and functions," *Immunity*, vol. 32, no. 5, pp. 593–604, 2010.

[24] S. Nakao, K. Noda, S. Zandi et al., "VAP-1-mediated M2 macrophage infiltration underlies IL-1β- but not VEGF-A-induced lymph- and angiogenesis," *The American Journal of Pathology*, vol. 178, no. 4, pp. 1913–1921, 2011.

[25] S. Zandi, S. Nakao, K. H. Chun et al., "ROCK-isoform-specific polarization of macrophages associated with age-related macular degeneration," *Cell Reports*, vol. 10, no. 7, pp. 1173–1186, 2015.

[26] B. M. Delavary, W. M. van der Veer, M. van Egmond, F. B. Niessen, and R. H. J. Beelen, "Macrophages in skin injury and repair," *Immunobiology*, vol. 216, no. 7, pp. 753–762, 2011.

[27] A. Mantovani, T. Schioppa, C. Porta, P. Allavena, and A. Sica, "Role of tumor-associated macrophages in tumor progression and invasion," *Cancer Metastasis Reviews*, vol. 25, no. 3, pp. 315–322, 2006.

[28] V. W. H. Ho and L. M. Sly, "Derivation and characterization of murine alternatively activated (M2) macrophages," *Methods in Molecular Biology*, vol. 531, pp. 173–185, 2009.

[29] N. Jetten, S. Verbruggen, M. J. Gijbels, M. J. Post, M. P. J. de Winther, and M. M. P. C. Donners, "Anti-inflammatory M2, but not pro-inflammatory M1 macrophages promote angiogenesis in vivo," *Angiogenesis*, vol. 17, no. 1, pp. 109–118, 2014.

[30] Y. Zhou, S. Yoshida, S. Nakao et al., "M2 macrophages enhance pathological neovascularization in the mouse model of oxygen-induced retinopathy," *Investigative Ophthalmology & Visual Science*, vol. 56, no. 8, pp. 4767–4777, 2015.

[31] Y. Zhou, S. Yoshida, Y. Kubo et al., "Different distributions of M1 and M2 macrophages in a mouse model of laser-induced choroidal neovascularization," *Molecular Medicine Reports*, vol. 15, no. 6, pp. 3949–3956, 2017.

[32] J. Cao, R. Dong, L. Jiang et al., "LncRNA-MM2P identified as a modulator of macrophage M2 polarization," *Cancer Immunology Research*, vol. 7, no. 2, pp. 292–305, 2019.

[33] F. Geissmann, "Development of monocytes, macrophages, and dendritic cells (vol 327, pg 656, 2010)," *Science*, vol. 330, no. 6009, pp. 1318–1318, 2010.

[34] C. Shi and E. G. Pamer, "Monocyte recruitment during infection and inflammation," *Nature Reviews Immunology*, vol. 11, no. 11, pp. 762–774, 2011.

[35] C. Auffray, M. H. Sieweke, and F. Geissmann, "Blood monocytes: development, heterogeneity, and relationship with dendritic cells," *Annual Review of Immunology*, vol. 27, pp. 669–692, 2009.

[36] M. T. Chen, H. S. Lin, C. Shen et al., "PU.1-regulated long noncoding RNA lnc-MC controls human monocyte/-macrophage differentiation through interaction with MicroRNA 199a-5p," *Molecular and Cellular Biology*, vol. 35, no. 18, pp. 3212–3224, 2015.

[37] Y. Y. Zhang, P. M. K. Tang, P. C. T. Tang et al., "LRNA9884, a novel Smad3-dependent long noncoding RNA, promotes diabetic kidney injury indb/dbMice via enhancing MCP-1-dependent renal inflammation," *Diabetes*, vol. 68, no. 7, pp. 1485–1498, 2019.

[38] Y. Zhang, J. Feng, H. Fu et al., "Coagulation factor X regulated by CASC2c recruited macrophages and induced M2 polarization in glioblastoma multiforme," *Frontiers in Immunology*, vol. 9, 2018.

[39] S. Chen, C. Shao, M. Xu et al., "Macrophage infiltration promotes invasiveness of breast cancer cells via activating long

non-coding RNA UCA1," *International Journal of Clinical and Experimental Pathology*, vol. 8, no. 8, pp. 9052–9061, 2015.

[40] Y. Ye, Y. Xu, Y. Lai et al., "Long non-coding RNA cox-2 prevents immune evasion and metastasis of hepatocellular carcinoma by altering M1/M2 macrophage polarization," *Journal of Cellular Biochemistry*, vol. 119, no. 3, pp. 2951–2963, 2018.

[41] X. Li, Y. Lei, M. Wu, and N. Li, "Regulation of macrophage activation and polarization by HCC-derived exosomal lncRNA TUC339," *International Journal of Molecular Sciences*, vol. 19, no. 10, article 2958, 2018.

[42] Y. Jia, Z. Li, W. Cai et al., "SIRT1 regulates inflammation response of macrophages in sepsis mediated by long noncoding RNA," *Biochimica et Biophysica Acta-Molecular Basis of Disease*, vol. 1864, no. 3, pp. 784–792, 2018.

[43] A.-P. Mao, J. Shen, and Z. Zuo, "Expression and regulation of long noncoding RNAs in TLR4 signaling in mouse macrophages," *BMC Genomics*, vol. 16, no. 1, article 1270, 2015.

[44] D. Sun, Z. Yu, X. Fang et al., "LncRNA GAS5 inhibits microglial M2 polarization and exacerbates demyelination," *EMBO Reports*, vol. 18, no. 10, pp. 1801–1816, 2017.

[45] N. Wang, H. Liang, and K. Zen, "Molecular mechanisms that influence the macrophage M1–M2 polarization balance," *Frontiers in Immunology*, vol. 5, p. 9, 2014.

[46] M. Du, L. Yuan, X. Tan et al., "The LPS-inducible lncRNA Mirt2 is a negative regulator of inflammation," *Nature Communications*, vol. 8, no. 1, p. 2049, 2017.

[47] S. Ma, Z. Ming, A. Y. Gong et al., "A long noncoding RNA, lincRNA-Tnfaip3, acts as a coregulator of NF-κB to modulate inflammatory gene transcription in mouse macrophages," *The FASEB Journal*, vol. 31, no. 3, pp. 1215–1225, 2017.

[48] Y. Lu, X. Liu, M. Xie et al., "The NF-κB–Responsive long noncoding RNA FIRRE regulates posttranscriptional regulation of inflammatory gene expression through interacting with hnRNPU," *Journal of Immunology*, vol. 199, no. 10, pp. 3571–3582, 2017.

[49] L. Salmena, L. Poliseno, Y. Tay, L. Kats, and P. P. Pandolfi, "A ceRNA hypothesis: the Rosetta Stone of a hidden RNA language?," *Cell*, vol. 146, no. 3, pp. 353–358, 2011.

[50] Y. X. Zhou, W. Zhao, L. W. Mao et al., "Long non-coding RNA NIFK-AS1 inhibits M2 polarization of macrophages in endometrial cancer through targeting miR-146a," *International Journal of Biochemistry & Cell Biology*, vol. 104, pp. 25–33, 2018.

[51] J. Liu, D. Ding, Z. Jiang, T. du, J. Liu, and Z. Kong, "Long noncoding RNA CCAT1/miR-148a/PKC zeta prevents cell migration of prostate cancer by altering macrophage polarization," *Prostate*, vol. 79, no. 1, pp. 105–112, 2019.

[52] Y. Sun and J. Xu, "TCF-4 regulated lncRNA-XIST promotes M2 polarization of macrophages and is associated with lung cancer," *Oncotargets and Therapy*, vol. 12, pp. 8055–8062, 2019.

[53] Z. Li, C. Feng, J. Guo, X. Hu, and D. Xie, "GNAS-AS1/miR-4319/NECAB3 axis promotes migration and invasion of non-small cell lung cancer cells by altering macrophage polarization," *Functional & Integrative Genomics*, vol. 20, no. 1, pp. 17–28, 2020.

[54] Z. X. Li, Q. N. Zhu, H. B. Zhang, Y. Hu, G. Wang, and Y. S. Zhu, "MALAT1: a potential biomarker in cancer," *Cancer Management and Research*, vol. 10, pp. 6757–6768, 2018.

[55] M. Zhao, S. Wang, Q. Li, Q. Ji, P. Guo, and X. Liu, "MALAT1: a long non-coding RNA highly associated with human cancers (Review)," *Oncology Letters*, vol. 16, no. 1, pp. 19–26, 2018.

[56] L. E. Abdulle, J. L. Hao, O. P. Pant et al., "MALAT1 as a diagnostic and therapeutic target in diabetes-related complications: a promising long-noncoding RNA," *International Journal of Medical Sciences*, vol. 16, no. 4, pp. 548–555, 2019.

[57] T. Gutschner, M. Hammerle, and S. Diederichs, "MALAT1- a paradigm for long noncoding RNA function in cancer," *Journal of Molecular Medicine*, vol. 91, no. 7, pp. 791–801, 2013.

[58] L. Dai, G. Zhang, Z. Cheng et al., "Knockdown of LncRNA MALAT1 contributes to the suppression of inflammatory responses by up-regulating miR-146a in LPS-induced acute lung injury," *Connective Tissue Research*, vol. 59, no. 6, pp. 581–592, 2018.

[59] Y. T. Zhuang, D. Y. Xu, G. Y. Wang, J. L. Sun, Y. Huang, and S. Z. Wang, "IL-6 induced lncRNA MALAT1 enhances TNF-α expression in LPS-induced septic cardiomyocytes via activation of SAA3," *European Review for Medical and Pharmacological Sciences*, vol. 21, no. 2, pp. 302–309, 2017.

[60] P. Puthanveetil, S. Chen, B. Feng, A. Gautam, and S. Chakrabarti, "Long non-coding RNA MALAT1 regulates hyperglycaemia induced inflammatory process in the endothelial cells," *Journal of Cellular and Molecular Medicine*, vol. 19, no. 6, pp. 1418–1425, 2015.

[61] G. Zhao, Z. Su, D. Song, Y. Mao, and X. Mao, "The long noncoding RNA MALAT1 regulates the lipopolysaccharide-induced inflammatory response through its interaction with NF-κB," *FEBS Letters*, vol. 590, no. 17, pp. 2884–2895, 2016.

[62] S. Ramanathan and N. Jagannathan, "Tumor associated macrophage: a review on the phenotypes, traits and functions," *Iranian Journal of Cancer Prevention*, vol. 7, no. 1, pp. 1–8, 2014.

[63] J. K. Huang, L. Ma, W. H. Song et al., "LncRNA-MALAT1 promotes angiogenesis of thyroid cancer by modulating tumor-associated macrophage FGF2 protein secretion," *Journal of Cellular Biochemistry*, vol. 118, no. 12, pp. 4821–4830, 2017.

[64] Z. Ma, J. Zhang, X. Xu et al., "LncRNA expression profile during autophagy and Malat1 function in macrophages," *PLoS One*, vol. 14, no. 8, article e0221104, 2019.

[65] D. Hanahan and R. A. Weinberg, "Hallmarks of cancer: the next generation," *Cell*, vol. 144, no. 5, pp. 646–674, 2011.

[66] A. Sica, P. Larghi, A. Mancino et al., "Macrophage polarization in tumour progression," *Seminars in Cancer Biology*, vol. 18, no. 5, pp. 349–355, 2008.

[67] M. Du, K. M. Roy, L. Zhong, Z. Shen, H. E. Meyers, and R. C. Nichols, "VEGF gene expression is regulated post-transcriptionally in macrophages," *FEBS Journal*, vol. 273, no. 4, pp. 732–745, 2006.

[68] C. Sunderkötter, K. Steinbrink, M. Goebeler, R. Bhardwaj, and C. Sorg, "Macrophages and angiogenesis," *Journal of Leukocyte Biology*, vol. 55, no. 3, pp. 410–422, 1994.

[69] K. H. Seo, H. M. Ko, J. H. Choi et al., "Essential role for platelet-activating factor-induced NF-κB activation in macrophage-derived angiogenesis," *European Journal of Immunology*, vol. 34, no. 8, pp. 2129–2137, 2004.

[70] M. Ramirez-Pedraza and M. Fernandez, "Interplay between macrophages and angiogenesis: a double-edged sword in liver disease," *Frontiers in Immunology*, vol. 10, 2019.

[71] P. Liu, S. B. Jia, J. M. Shi et al., "LncRNA-MALAT1 promotes neovascularization in diabetic retinopathy through regulating miR-125b/VE-cadherin axis," *Bioscience Reports*, vol. 39, no. 5, 2019.

[72] A. E. Tee, B. Liu, R. Song et al., "The long noncoding RNA MALAT1 promotes tumor-driven angiogenesis by up-regulating pro-angiogenic gene expression," *Oncotarget*, vol. 7, no. 8, pp. 8663–8675, 2016.

[73] X. J. Huang, Y. Xia, G. F. He et al., "MALAT1 promotes angiogenesis of breast cancer," *Oncology Reports*, vol. 40, no. 5, pp. 2683–2689, 2018.

[74] Z.-H. Hou, X. W. Xu, X. Y. Fu, L. D. Zhou, S. P. Liu, and D. M. Tan, "Long non-coding RNA MALAT1 promotes angiogenesis and immunosuppressive properties of HCC cells by sponging miR-140," *American Journal of Physiology-Cell Physiology*, 2019.

[75] X. Zhang, X. Tang, M. Hamblin, and K. J. Yin, "Long non-coding RNA Malat1 regulates angiogenesis in hindlimb ischemia," *International Journal of Molecular Sciences*, vol. 19, no. 6, p. 1723, 2018.

[76] L. Ren, C. Wei, K. Li, and Z. Lu, "LncRNA MALAT1 up-regulates VEGF-A and ANGPT2 to promote angiogenesis in brain microvascular endothelial cells against oxygen-glucose deprivation via targetting miR-145," *Bioscience Reports*, vol. 39, no. 3, 2019.

[77] Q. Yan, Y. Tian, and F. Hao, "Downregulation of lncRNA UCA1 inhibits proliferation and invasion of cervical cancer cells through miR-206 expression," *Oncology Research*, 2018.

[78] F. A. Alzahrani, M. A. el-Magd, A. Abdelfattah-Hassan et al., "Potential effect of exosomes derived from cancer stem cells and MSCs on progression of DEN-induced HCC in rats," *Stem Cells International*, vol. 2018, Article ID 8058979, 17 pages, 2018.

[79] T. Kogure, I. K. Yan, W. L. Lin, and T. Patel, "Extracellular vesicle-mediated transfer of a novel long noncoding RNA TUC339: a mechanism of intercellular signaling in human hepatocellular cancer," *Genes & Cancer*, vol. 4, no. 7-8, pp. 261–272, 2013.

[80] L. Sang, H. Q. Ju, G. P. Liu et al., "LncRNA *CamK-A* regulates Ca^{2+}-signaling-mediated tumor microenvironment remodeling," *Molecular Cell*, vol. 72, no. 1, pp. 71–83.e7, 2018.

[81] C. Chen, W. He, J. Huang et al., "*LNMAT1* promotes lymphatic metastasis of bladder cancer via CCL2 dependent macrophage recruitment," *Nature Communications*, vol. 9, no. 1, article 3826, 2018.

[82] J. Zhao, P. du, P. Cui et al., "LncRNA PVT1 promotes angiogenesis via activating the STAT3/VEGFA axis in gastric cancer," *Oncogene*, vol. 37, no. 30, pp. 4094–4109, 2018.

[83] W. W. Qin, Z. L. Xin, H. Q. Wang, K. P. Wang, X. Y. Li, and X. Wang, "Inhibiting lncRNA ROR suppresses growth, migration and angiogenesis in microvascular endothelial cells by up-regulating miR-26," *European Review for Medical and Pharmacological Sciences*, vol. 22, no. 22, pp. 7985–7993, 2018.

[84] A. Sas-Chen, M. R. Aure, L. Leibovich et al., "LIMT is a novel metastasis inhibiting lncRNA suppressed by EGF and down-regulated in aggressive breast cancer," *EMBO Molecular Medicine*, vol. 8, no. 9, pp. 1052–1064, 2016.

[85] X. Y. Zeng, H. Xie, J. Yuan et al., "M2-like tumor-associated macrophages-secreted EGF promotes epithelial ovarian cancer metastasis via activating EGFR-ERK signaling and suppressing lncRNA LIMT expression," *Cancer Biology & Therapy*, vol. 20, no. 7, pp. 956–966, 2019.

[86] A. Yoshida, S. Yoshida, T. Ishibashi, and H. Inomata, "Intraocular neovascularization," *Histology and Histopathology*, vol. 14, no. 4, pp. 1287–1294, 1999.

[87] N. Cheung, P. Mitchell, and T. Y. Wong, "Diabetic retinopathy," *The Lancet*, vol. 376, no. 9735, pp. 124–136, 2010.

[88] A. A. Thomas, B. Feng, and S. Chakrabarti, "ANRIL: a regulator of VEGF in diabetic retinopathy," *Investigative Ophthalmology & Visual Science*, vol. 58, no. 1, pp. 470–480, 2017.

[89] J. C. Wei, Y. L. Shi, and Q. Wang, "LncRNA ANRIL knockdown ameliorates retinopathy in diabetic rats by inhibiting the NF-κB pathway," *European Review for Medical and Pharmacological Sciences*, vol. 23, no. 18, pp. 7732–7739, 2019.

[90] B. Zhang, D. Wang, T. F. Ji, L. Shi, and J. L. Yu, "Overexpression of lncRNA ANRIL up-regulates VEGF expression and promotes angiogenesis of diabetes mellitus combined with cerebral infarction by activating NF-κB signaling pathway in a rat model," *Oncotarget*, vol. 8, no. 10, pp. 17347–17359, 2017.

[91] B. Yan, J. Yao, J. Y. Liu et al., "lncRNA-MIAT regulates microvascular dysfunction by functioning as a competing endogenous RNA," *Circulation Research*, vol. 116, no. 7, pp. 1143–1156, 2015.

[92] Q. Li, L. Pang, W. Yang, X. Liu, G. Su, and Y. Dong, "Long non-coding RNA of myocardial infarction associated transcript (LncRNA-MIAT) promotes diabetic retinopathy by upregulating transforming growth factor-β1 (TGF-β1) signaling," *Medical Science Monitor*, vol. 24, pp. 9497–9503, 2018.

[93] D. Zhang, H. Qin, Y. Leng et al., "LncRNA MEG3 overexpression inhibits the development of diabetic retinopathy by regulating TGF-β1 and VEGF," *Experimental and Therapeutic Medicine*, vol. 16, no. 3, pp. 2337–2342, 2018.

[94] G.-Z. Qiu, W. Tian, H. T. Fu, C. P. Li, and B. Liu, "Long non-coding RNA-MEG3 is involved in diabetes mellitus-related microvascular dysfunction," *Biochemical and Biophysical Research Communications*, vol. 471, no. 1, pp. 135–141, 2016.

[95] Y. Gao, P. Fang, W. J. Li et al., "LncRNA NEAT1 sponges miR-214 to regulate M2 macrophage polarization by regulation of B7-H3 in multiple myeloma," *Molecular Immunology*, vol. 117, pp. 20–28, 2020.

[96] P. Zhang, L. Cao, R. Zhou, X. Yang, and M. Wu, "The lncRNA *Neat1* promotes activation of inflammasomes in macrophages," *Nature Communications*, vol. 10, no. 1, article 1495, 2019.

[97] D. D. Chen, L. L. Hui, X. C. Zhang, and Q. Chang, "NEAT1 contributes to ox-LDL-induced inflammation and oxidative stress in macrophages through inhibiting miR-128," *Journal of Cellular Biochemistry*, vol. 120, no. 2, pp. 2493–2501, 2019.

[98] Z. W. Zhou, L. J. Zheng, X. Ren, A. P. Li, and W. S. Zhou, "LncRNA NEAT1 facilitates survival and angiogenesis in oxygen-glucose deprivation (OGD)-induced brain microvascular endothelial cells (BMECs) via targeting miR-377 and upregulating SIRT1, VEGFA, and BCL-XL," *Brain Research*, vol. 1707, pp. 90–98, 2019.

[99] J. Liu, Q. Li, K. S. Zhang et al., "Downregulation of the long non-coding RNA Meg3 promotes angiogenesis after ischemic brain injury by activating notch signaling," *Molecular Neurobiology*, vol. 54, no. 10, pp. 8179–8190, 2017.

[100] C. He, W. Yang, J. Yang et al., "Long noncoding RNA MEG3 negatively regulates proliferation and angiogenesis in vascular endothelial cells," *DNA and Cell Biology*, vol. 36, no. 6, pp. 475–481, 2017.

[101] L. Yan, Z. Liu, H. Yin, Z. Guo, and Q. Luo, "Silencing of MEG3 inhibited ox-LDL-induced inflammation and apoptosis in macrophages via modulation of the MEG3/miR-204/CDKN2A regulatory axis," *Cell Biology International*, vol. 43, no. 4, pp. 409–420, 2019.

[102] L. Zhang, X. Fu, H. Zeng et al., "Microarray analysis of long non-coding RNAs and messenger RNAs in a mouse model of oxygen-induced retinopathy," *International Journal of Medical Sciences*, vol. 16, no. 4, pp. 537–547, 2019.

[103] L. Zhang, H. Zeng, J. H. Wang et al., "Altered long non-coding RNAs involved in immunological regulation and associated with choroidal neovascularization in mice," *International Journal of Medical Sciences*, vol. 17, no. 3, pp. 292–301, 2020.

[104] C. A. Yang, J. P. Li, J. C. Yen et al., "lncRNA NTT/PBOV1 axis promotes monocyte differentiation and is elevated in rheumatoid arthritis," *International Journal of Molecular Sciences*, vol. 19, no. 9, article 2806, 2018.

Hindawi
Journal of Immunology Research
Volume 2020, Article ID 1906204, 10 pages
https://doi.org/10.1155/2020/1906204

Research Article

Nε-Carboxymethyl-Lysine Negatively Regulates Foam Cell Migration via the Vav1/Rac1 Pathway

Zhengyang Bao,[1,2] Lili Zhang,[1] Lihua Li,[3] Jinchuan Yan,[1] Qiwen Pang,[1] Zhen Sun,[1] Yue Geng,[1] Lele Jing,[1] Chen Shao,[1] and Zhongqun Wang[1]

[1]*Department of Cardiology, Affiliated Hospital of Jiangsu University, Zhenjiang 212001, China*
[2]*Department of Internal Medicine, Affiliated Wuxi Maternity and Child Health Care Hospital of Nanjing Medical University, Wuxi 214000, China*
[3]*Department of Pathology, Affiliated Hospital of Jiangsu University, Zhenjiang 212001, China*

Correspondence should be addressed to Zhongqun Wang; wangtsmc@126.com

Received 27 October 2019; Accepted 22 January 2020; Published 28 February 2020

Guest Editor: Mohammad A. Khan

Background. Macrophage-derived foam cells play a central role in atherosclerosis, and their ultimate fate includes apoptosis, promotion of vascular inflammation, or migration to other tissues. Nε-Carboxymethyl-lysine (CML), the key active component of advanced glycation end products, induced foam cell formation and apoptosis. Previous studies have shown that the Vav1/Rac1 pathway affects the macrophage cytoskeleton and cell migration, but its role in the pathogenesis of diabetic atherosclerosis is unknown. *Methods and Results*. In this study, we used anterior tibiofibular vascular samples from diabetic foot amputation patients and accident amputation patients, and histological and cytological tests were performed using a diabetic $ApoE^{-/-}$ mouse model and primary peritoneal macrophages, respectively. The results showed that the atherosclerotic plaques of diabetic foot amputation patients and diabetic $ApoE^{-/-}$ mice were larger than those of the control group. Inhibition of the Vav1/Rac1 pathway reduced vascular plaques and promoted the migration of macrophages to lymph nodes. Transwell and wound healing assays showed that the migratory ability of macrophage-derived foam cells was inhibited by CML. Cytoskeletal staining showed that advanced glycation end products inhibited the formation of lamellipodia in foam cells, and inhibition of the Vav1/Rac1 pathway restored the formation of lamellipodia. *Conclusion*. CML inhibits the migration of foam cells from blood vessels via the Vav1/Rac1 pathway, and this process affects the formation of lamellipodia.

1. Introduction

The recruitment of macrophages to the intima and phagocytosis of lipids to form foam cells is an essential step in the progression of atherosclerosis [1, 2]. Regarding the fate of foam cells in plaques, the traditional belief is that apoptosis of macrophages further increases plaque inflammation and promotes the progression of atherosclerosis [3]. However, with a deeper understanding of the pathogenesis of atherosclerosis, researchers have gradually realized that the migration of foam cells from arterial wall lesions and the migration of monocytes and macrophages are dynamic processes. The obstruction of foam cell migration is another important factor in the accumulation of foam cells in plaques [4].

Nε-Carboxymethyl-lysine (CML) is a major active ingredient in advanced glycation end products. Studies have shown that Nε-carboxymethyl-lysine can promote foam cell formation, inhibit foam cell migration, and accelerate the progression of atherosclerosis, but the specific mechanism is not yet clear [5, 6]. Vav1 protein, as a member of the guanine exchange factors (GEFs), affects the activity of the Rho GTPase family through phosphorylation of its specific site [7]. Rahaman et al. and Chen et al. found that the degree of Vav1 phosphorylation was increased in atherosclerotic plaques, while knocking out Vav1 reduced plaque area [8, 9]; in vitro experiments showed that the loss of the Vav1 gene recovered the migratory ability of oxLDL-induced foam cells [10], but

whether the migration of foam cells is affected by Vav1 gene expression and phosphorylation in diabetes is not clear.

Members of the Rho GTPase family play an important role in intracellular signaling pathways. Previous studies have shown that the Rho GTPase family can participate in intercellular function changes, including cell adhesion, contraction, proliferation, and migration, by regulating the polymerization state of the cytoskeleton [11]. During cell signal transduction, Rho protein exists in the GTP-binding form (active state) and GDP-binding state (inactive state) and initiates or terminates the cell signal cascade activation reaction through the transition between the two binding states [12]. Studies have shown that Rho protein regulates cell migration by regulating the phosphorylation level of myosin light chain (MLC), but it is not clear whether Rho protein affects foam cell migration during diabetic atherosclerosis [13]. Ras-related C3 botulinum toxin substrate 1 (Rac1), as a member of Rho GTPase super family, plays a central role in cytoskeleton polymerization and migration. This study used in vitro and in vivo experiments to demonstrate that Vav1/Rac1 signaling promotes the progression of atherosclerosis by affecting the migratory ability of foam cells in atherosclerotic plaques.

2. Materials and Methods

2.1. Human Studies. Anterior tibial arteries from human diabetic amputees ($n = 4$) and from normal amputees ($n = 4$) were obtained from the Affiliated Hospital of Jiangsu University (Zhenjiang, China) from February 2015 to June 2017. This study was approved by the Chinese Clinical Trial Registry and conducted in agreement with the institutional guidelines. Written informed consent was obtained from all patients. Ethical review number is ChiECRCT20190206.

2.2. Animal Studies. The experimental protocols were approved by the Institutional Animal Care and Use Committee of Jiangsu University (Jiangsu, China) and performed in accordance with the Guidelines for Animal Experimentation of the National Institutes of Health. Male $ApoE^{-\backslash-}$ mice with a C57BL/6J background were obtained from the Jackson Laboratory (USA). The diabetic $ApoE^{-\backslash-}$ model was established as described previously. In brief, at 6 weeks of age, the mice were rendered diabetic through intraperitoneal injection for five consecutive days of 40 mg/kg STZ dissolved in 100 mM citrate buffer (pH 4.5). Mice with blood glucose levels of ≥300 mg/dL after 2 weeks of STZ administration were considered diabetic.

2.3. Cell Culture. Peritoneal macrophages (PMφ) were harvested from C57BL/6 mice 4 days after thioglycollate injection by peritoneal lavage as described. Isolated PMφ were plated on glass coverslips. After 1 hour of incubation at 37°C, nonadherent cells were removed by gentle washing, and the remaining cells were cultured overnight in DMEM containing 10% FBS before use in the phagocytosis assay.

The Raw 264.7 macrophage cell line was purchased from the American Type Culture Collection and cultured in DMEM medium supplemented with 10% FBS, 2 mM L-glutamine, 100 U/mL penicillin, and 100 μg/mL streptomycin at 37°C in a humidified atmosphere with 5% CO_2. A foam cell model was established by using Raw 264.7 macrophages loaded with 40 μg/mL oxLDL.

2.4. Oil Red O Staining. Atherosclerotic lesions in the aorta or para-aortic lymph nodes of $ApoE^{-\backslash-}$ mice were subsequently stained with freshly filtered Oil Red O working solution for 30 min at room temperature, and then, the staining was evaluated under an inverted microscope (Olympus, IX51).

2.5. In Vivo Studies of Macrophage Migration from the Peritoneum. The mice ($n = 4$/group) were injected intraperitoneally with 3% thioglycollate to trigger sterile peritonitis. After 4 days, peritoneal macrophages were labeled by injection of 1 μm Fluoresbrite green fluorescent plain microspheres (Polysciences). On the next day, the mice were injected with an inflammatory stimulus (400 ng LPS) to induce efflux of macrophages from the peritoneum to the draining lymph nodes. Following LPS injection (3 hours), the percentage of macrophages in the lavage fluid was quantified by flow cytometry using the PE/Cy7-conjugated anti-mouse F4/80 antibodies (BioLegend).

2.6. Transwell Migration Assay. PM cells suspended in DMEM containing 1% FBS were placed in a 24-well Transwell migration chamber and treated with oxLDL and CML. DMEM containing 10% FBS was added into the lower chambers. Afterwards, the medium from the upper chamber was carefully aspirated. The membrane was fixed with 4% PFA for 30 min and stained with 0.1% crystal violet for 20 min. Migration of Raw 264.7 cells was evaluated by viewing under high-power magnification and counting the migrated cells in six randomly selected fields/well viewed.

2.7. Wound Healing Assay. PM cells were seeded in a 6-well culture plate and grown to 80–85% confluence; subsequently, a scratch was made through the cell layer by using a sterile micropipette tip. The wounded areas were photographed under a light microscope. Cell migration was assessed by measuring the size of the scratch area.

2.8. Immunofluorescence Staining. Isolated aortas and para-aortic lymph nodes were placed in 10% neutral buffered formalin overnight, embedded in paraffin, and sliced into 4 μm thick sections. Atherosclerotic lesions in the aorta or the para-aortic lymph nodes were shown by Oil Red O staining. The distribution and expression levels of CD68 were estimated by immunofluorescence staining. The mean fluorescence density of positive cells was determined as the optical density/area by ImageJ. Semiquantitative analysis of immunofluorescence staining of CD68 was determined as the mean fluorescence density of CD68/DAPI.

2.9. Western Blot Assay. Raw 264.7 cells, isolated aortas, or para-aortic lymph nodes were washed with cold PBS and incubated in lysis buffer (RIPA) containing 1 mmol/L PMSF protease inhibitor (Sigma, St. Louis, MO, USA) and phosphatase inhibitors (Invitrogen, Carlsbad, CA, USA) on ice

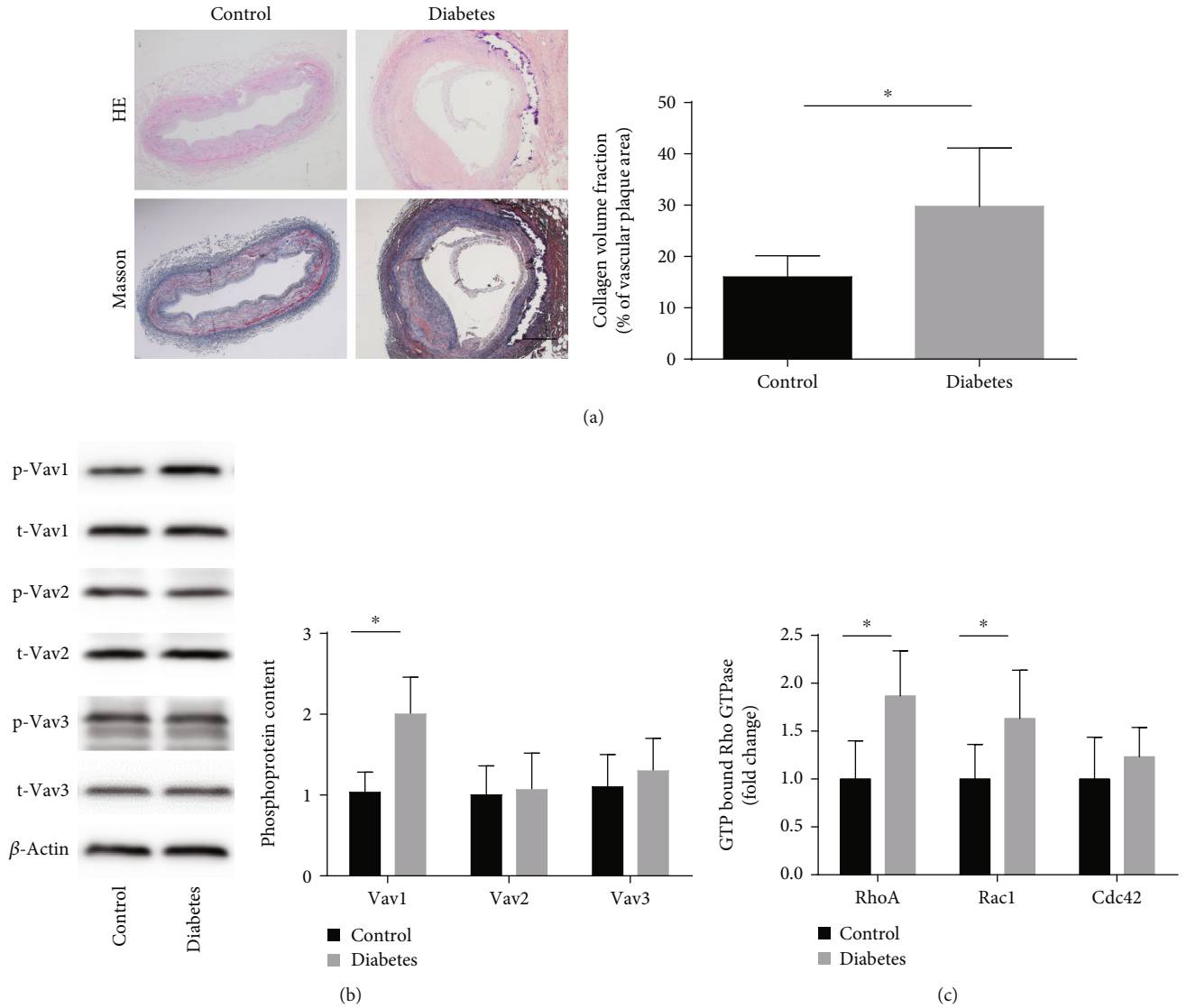

Figure 1: Phosphoprotein of Vav1 and activity of RhoA and Rac1 increase in diabetes amputees. (a) Representative images of anterior tibial artery sections stained with Masson/hematoxylin from accident amputees and diabetic amputees; scale bars, 50 μm. (b) The phosphoprotein content of Vav was detected by Western blot. (c) The activity of GTP-bound GTPase was detected by G-Lisa; values are presented as the mean ± SD from three independent experiments. $^*P < 0.05$.

and then centrifuged at 12,000 g and 4°C for 15 min. Protein concentrations were determined using a micro BCA protein assay kit (Thermo Fisher Scientific, Rockford, USA). Protein samples were loaded onto a polyacrylamide gel and transferred onto PVDF membranes by using a semidry method. The membranes were blocked in 5% milk in TBST, followed by overnight incubation with primary antibodies. The membranes were subsequently washed with TBST and then incubated with HRP-conjugated secondary antibodies. Immunoreactive bands were visualized by chemiluminescence (ECL Amersham Pharmacia). Protein expression levels were quantified by densitometric analysis by using LANE 1D software.

2.10. Statistical Analysis. Data are presented as the mean ± S.D., and SPSS 17.0 software was used to analyze the data. Comparisons between two variables were analyzed using the unpaired Student's t-test. Comparisons among multiple treatment groups were assessed by one-way ANOVA, followed by a post hoc LSD test. $P < 0.05$ was considered statistically significant.

3. Results

3.1. Vav1 Expression Is Elevated in the Vasculature of Diabetic Foot Amputation Patients, while Vav2 and Vav3 Expressions Are Not Elevated. Anterior tibial arteries from diabetic and control amputees (accident amputation) were obtained from the Affiliated Hospital of Jiangsu University. Masson's staining revealed that the fiber cap of atherosclerosis lesion in diabetic amputees was thinner than that in control amputees (Figure 1(a)). We performed Western blot

analysis to evaluate the degree of phosphorylation of Vav family members in the lower extremity anterior tibial arteries of patients with diabetic foot amputation and of patients with car accident amputation. The results showed that the degree of Vav1 phosphorylation was significantly increased in patients with diabetic amputation, while there was no significant difference in the degree of phosphorylation of Vav2 and Vav3 compared with that of the control group (Figure 1(b)).

3.2. The Activity of Rac1 and RhoA Increased in the Vasculature of Diabetic Foot Amputation Patients. The Vav family acts as important guanine exchange factors (GEFs) that regulate the activity of small GTPases. By regulating the binding and dissociation of small GTPases and GTP in atherosclerosis, we detected intravascular small GTPase activity in patients with diabetic foot amputation and accident amputation. The results showed that enzymatic activity of the small GTPase family members Rac1 and RhoA (with GTP-binding state) increased, but the expression of another small GTPase, Cdc42, did not change significantly (Figure 1(c)).

3.3. Interfering with the Expression of the Vav1 Reduces the Accumulation of Foam Cells in the Plate and Promotes Foam Cell Migration to Paravascular Lymph Nodes. We established a diabetic $ApoE^{-/-}$ mouse model based on previous methods in our group and administered Vav1 antibody to $ApoE^{-/-}$ mice. Oil Red O staining and CD68 immunogold staining showed increased lipid accumulation in the plaques of high-fat diet-fed $ApoE^{-/-}$ mice, increased foam cells in plaques, vascular plaque area in diabetic $ApoE^{-/-}$ mice, and lipid accumulation in foam cells. The $ApoE^{-/-}$ mice fed with a high-fat diet had further elevation of these factors, and the antibody interfered with the expression of Vav1 (Figure 2(a)). The paravascular lymph nodes of each group were harvested and stained with CD68 and Oil Red O. The high-fat diet-fed $ApoE^{-/-}$ mice showed increased CD68-positive macrophages in the paravascular lymph nodes, and Oil Red O staining showed increased lipid accumulation in the lymph nodes. In the para-aortic lymph nodes of diabetic $ApoE^{-/-}$ mice, the number of CD68-positive macrophages and lipid accumulation increased than that in the high-fat diet-fed $ApoE^{-/-}$ mice, while macrophage and lipid accumulation were significantly higher in the lymph nodes of diabetic mice treated with the anti-Vav1 antibody than those of the mice that were not administered with the Vav1 antibody (Figures 3(a) and 3(b)). Combined with the above results, we believe that lipid accumulation in plaques of diabetic $ApoE^{-/-}$ mice is associated with decreased foam cell migration, and inhibition of Vav1 expression inhibits plaque progression and lipid accumulation. Lymph node staining results suggest that it may be related to inhibition of foam cell migration.

3.4. Vav1 Affects the Effect of Advanced Glycation End Products on Foam Cell Migration but Does Not Affect Intracellular Lipid Accumulation. Advanced glycation end products are the end products of diabetic metabolic disorders, and they promote the progression of atherosclerosis by binding to intracellular and extracellular receptors. Western blot analysis revealed that the degree of phosphorylation of Vav1 was significantly increased (Figure 4(a)), and G-Lisa analysis showed that CML increase the activity of RhoA and Rac1 and Vav1 siRNA interference decreased the activity of Rac1 but have no change on RhoA (Figure 4(c)). Transwell migration assays, wound healing assays, and peritoneal macrophage migration assays showed that advanced glycation end products reduced foam cell migration in vivo and in vitro (Figures 5(a)–5(c)). Using Vav1 siRNA to interfere with Vav1 expression, we found that there was no significant change in intracellular lipid accumulation, but foam cell migratory ability was restored in vivo after inhibition of Vav1 expression.

3.5. The Vav1/Rac1 Pathway Affects Foam Cell Migration by Regulating Cytoskeletal Separation and Polymerization. We detected the activity of RhoA and Rac1 in foam cells after CML stimulation by G-Lisa assay. The results showed that CML promoted an increase in RhoA and Rac1 activity in foam cells. Inhibition of Vav1 expression by siRNA reduced Rac1 activity, but the change in RhoA activity was not statistically significant. We used 6-thio-GTP, an inhibitor of the Vav1/Rac1 pathway, to pretreat the macrophages, and the results showed that the effect of CML on the migration of foam cells was blocked. Then, we focused on the effect of Vav1/Rac1 on the cell cytoskeleton. Phalloidin staining showed that CML stimulation promoted cytoskeletal spreading and reduced the formation of lamellipodia. After the addition of Vav1 siRNA or 6-thio-GTP, the lamellipodia production was restored (Figure 5(d)), suggesting that the Vav1/Rac1 pathway affects the foam cell cytoskeleton, thereby inhibiting foam cell migration.

4. Discussion

Macrovascular complications are the most important lethal and disabling complications in diabetes and are mainly caused by increased oxidative stress, insulin resistance, increased advanced glycation end products, and disorders of glycolipid metabolism [14, 15]. AGEs are involved in microvascular and macrovascular complications through the formation of crosslinks between molecules in the basement membrane of the extracellular matrix and by engaging the receptors for advanced glycation [16, 17]. This study showed that advanced glycation end products inhibited foam cell migration out of the blood vessels by activating the Vav1/Rac1 pathway and reducing the production of lamellipodia.

Excessive accumulation of free cholesterol in macrophages leads to activation of downstream cascades, including the NLRP3 inflammasome, Toll-like receptor signaling, and the endoplasmic reticulum stress response [18]. These inflammatory signals exacerbate not only the oxidative stress in the plaque but also the migration of other inflammatory cells (including monocytes) to the intima [19]. However, reversing atherosclerosis requires the migration of macrophages to plaques and reduction of inflammation. However, during the progression of atherosclerosis, the

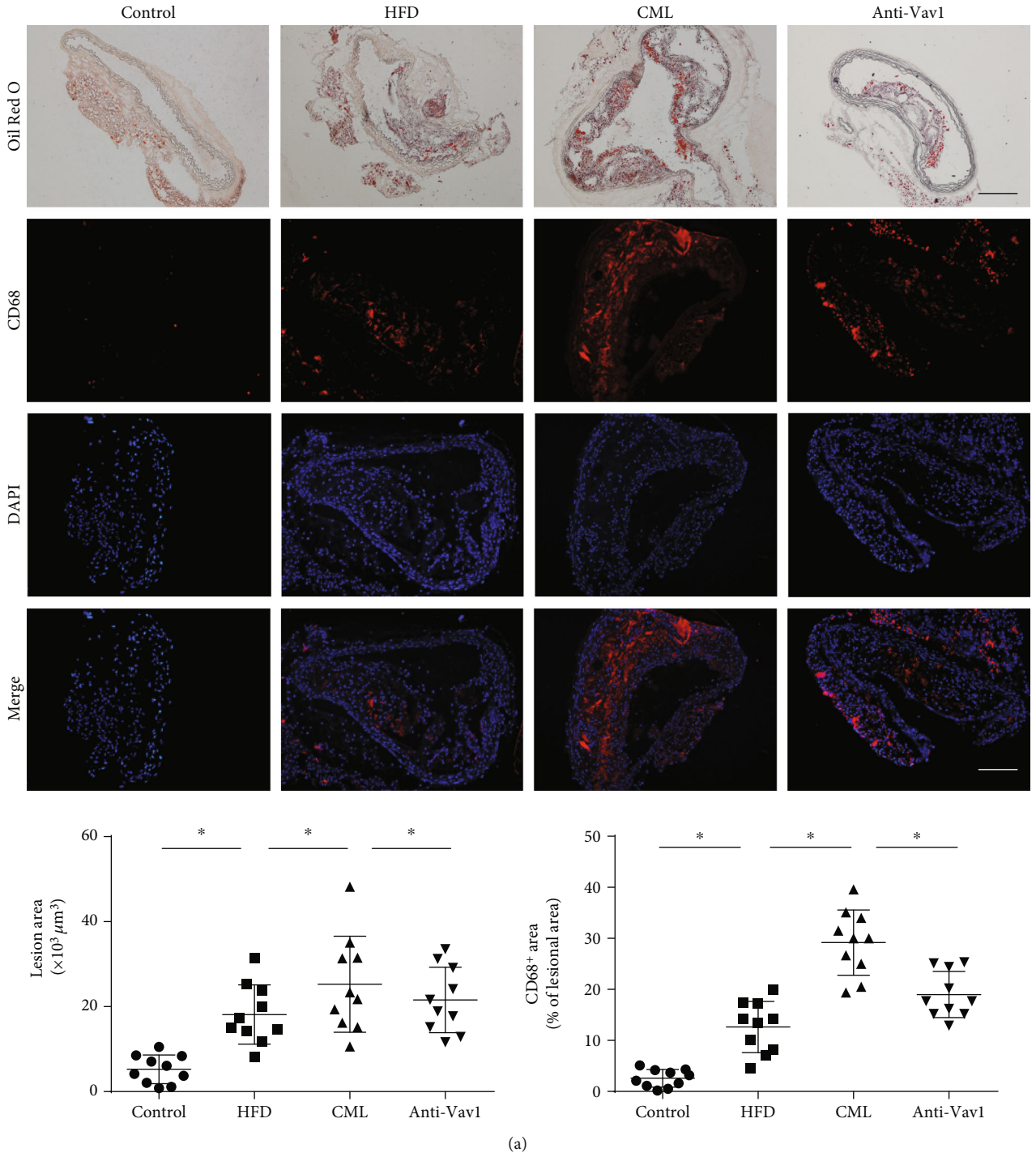

(a)

Figure 2: Continued.

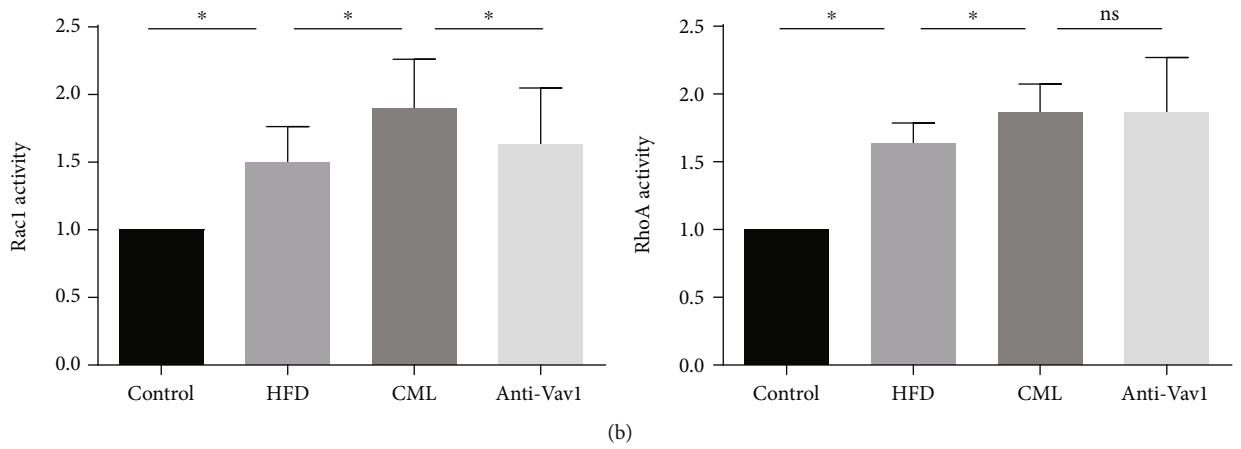

Figure 2: Inhibition of Vav1 expression antagonizes the effect of CML on lipid accumulation in diabetic ApoE$^{-/-}$ mice. (a) ApoE$^{-/-}$ mice were fed with an HF diet and treated with CML and/or anti-Vav1 for 12 weeks. Representative images of aortic root stained with Oil Red O and immunofluorescence. Scale bars, 20 μm. (b) The activity of GTP-bound GTPase was detected by G-Lisa; values are presented as the mean ± SD from three independent experiments. $^*P < 0.05$.

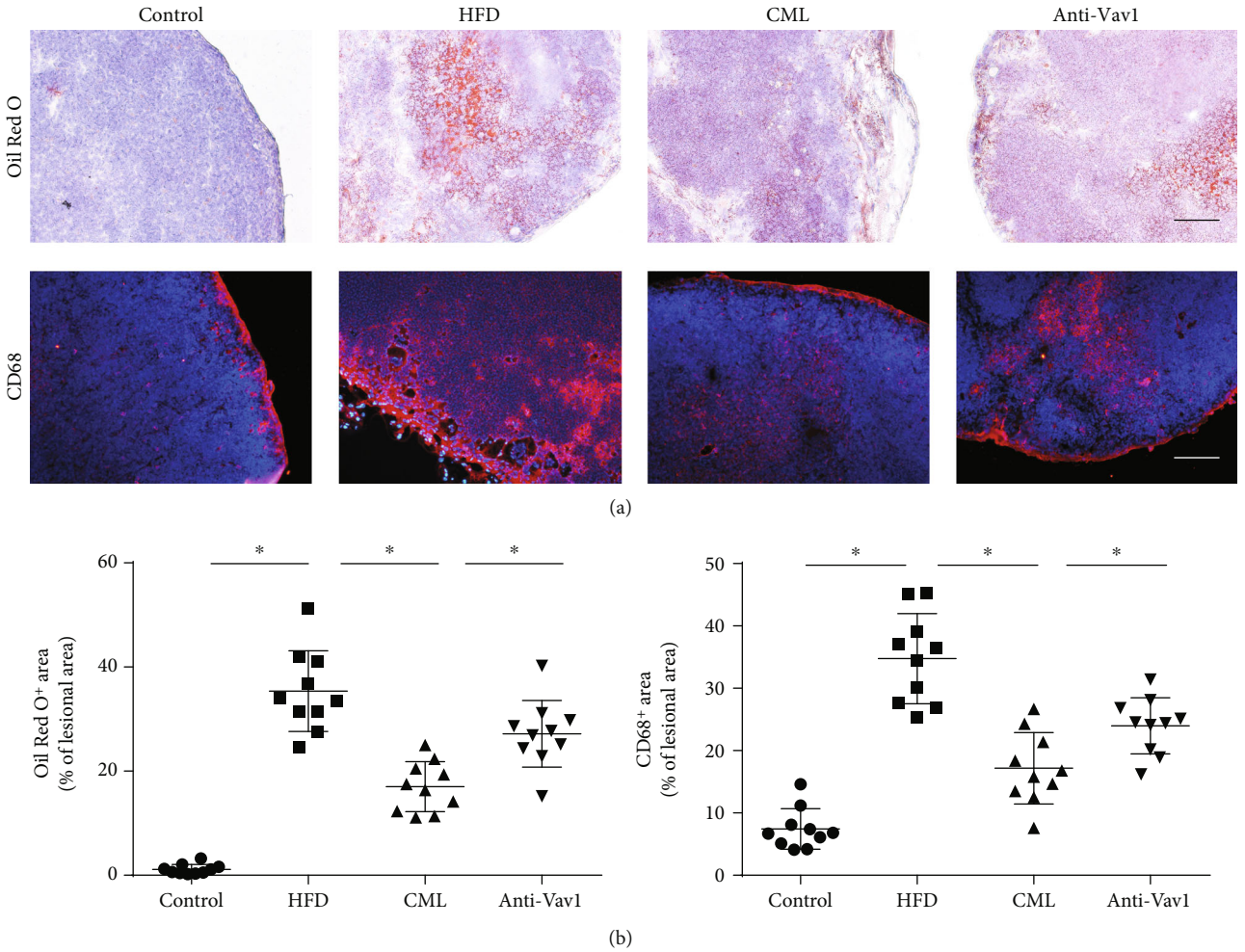

Figure 3: CML inhibits foam cells migrating to the para-aortic lymph node, inhibiting Vav1 reverse macrophage migration ability. (a) Oil Red O staining and immunofluorescence staining for CD68 in the para-aortic lymph node. Scale bars, 20 μm. (b) The extent of Oil Red O-positive area and CD68-positive area in the para-aortic lymph node; values are presented as the mean ± SD from three independent experiments. $^*P < 0.05$.

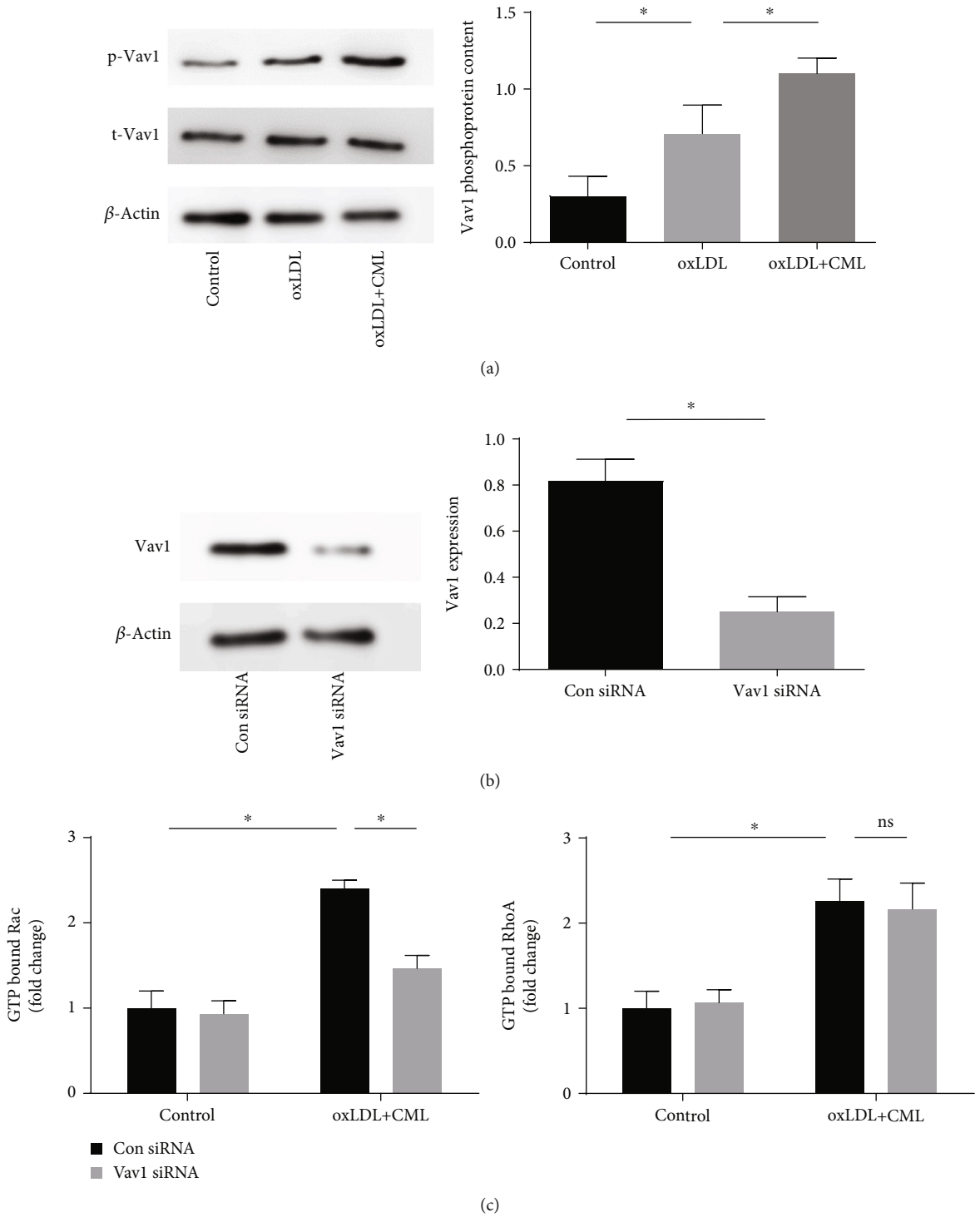

Figure 4: CML increase the phosphorylation of Vav1 in macrophage-derived foam cells, inhibiting Vav1 expression which reduces the activity of Rac1 but has no change on RhoA activity. (a) Phosphorylation of Vav1 was investigated by Western blot. (b) Vav1 siRNA were used to interrupt the expression of Vav1; the effect of Vav1 siRNA was investigated by Western blot. (c) The activity of GTP-bound GTPase was detected by G-Lisa; values are presented as the mean ± SD from three independent experiments. $^*P < 0.05$.

expression of retention factors prevents macrophages from escaping from the arterial wall [20]. Existing studies have shown that sAGEs can activate monocytes and AGEs deposited on bone marrow macrophages inhibit monocyte migration, inducing a process called "apoptaxis" [21]. In this study, we found that advanced glycation end products inhibit foam cell migration in vascular plaques and promote the progression of atherosclerosis, which illustrates the role of advanced glycation end products in diabetic atherosclerosis.

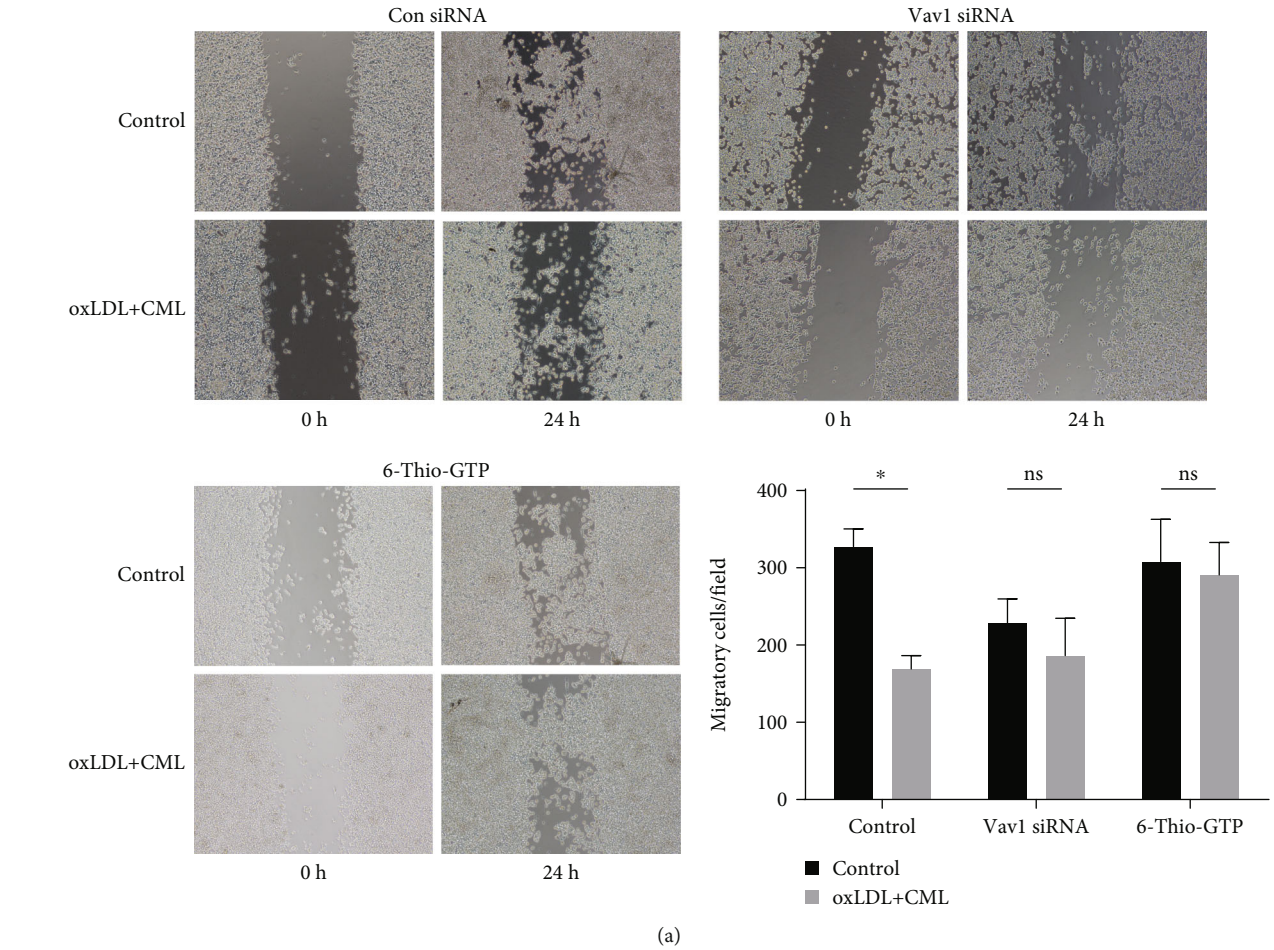

(a)

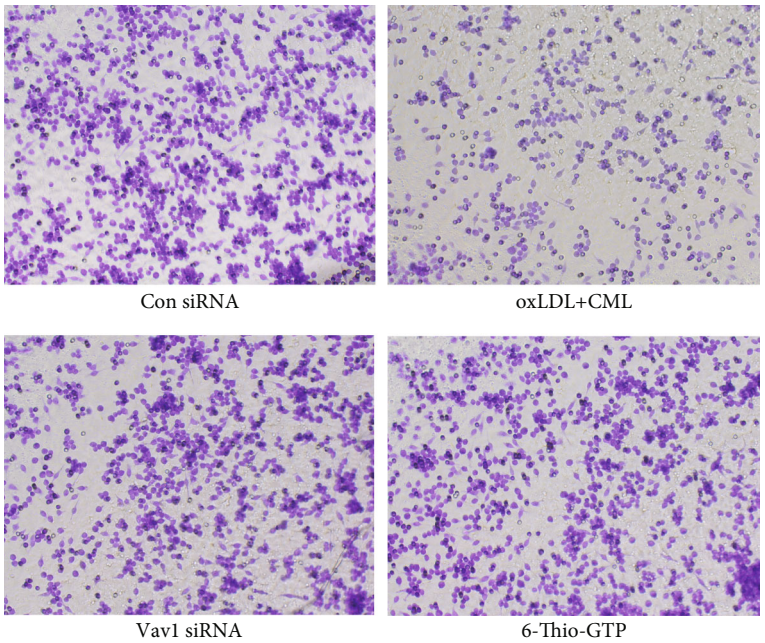

(b)

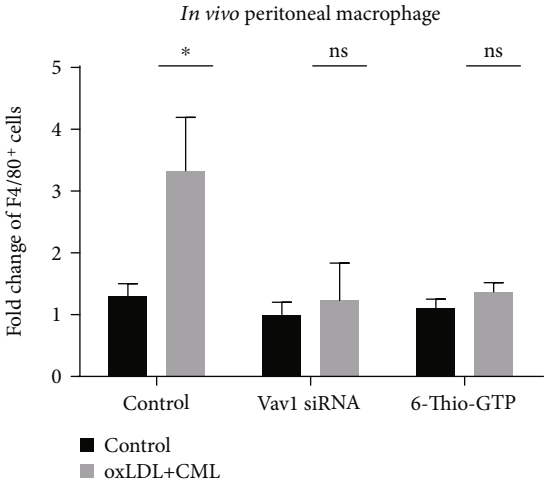

(c)

Figure 5: Continued.

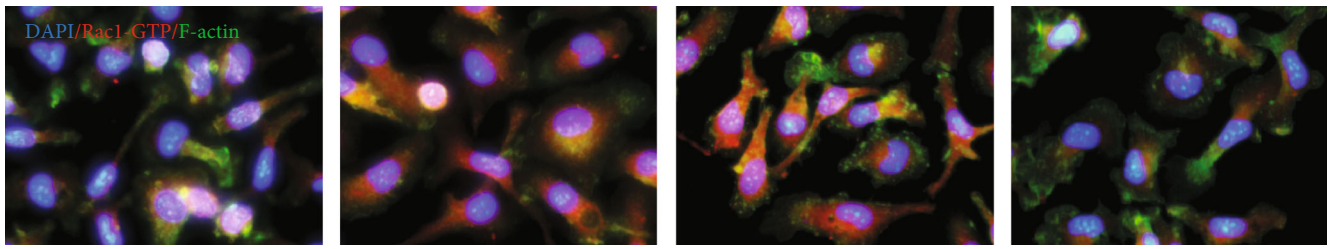

Figure 5: CML inhibit lamellipodia formation and foam cell migration in vivo and in vitro via Vav1/Rac1 pathway. Wound healing assay (a) and Transwell migration assay (b) were used to evaluate the cell migration capacity in vitro (200x magnification). (c) In vivo migration assay: wild type, Vav1 siRNA, and 6-thio-GTP pretreated peritoneal macrophage were treated with oxLDL+CML for 24 h before injected into mice peritoneally, three hours after LPS injection peritoneal cells were collected and the percentage of macrophages in the lavage was quantified by flow cytometry; $^*P < 0.05$. (d) Peritoneal macrophages were exposed to CML+oxLDL in the presence or absence of Vav1 siRNA, and 6-thio-GTP, CD68, Rac1-GTP, and DAPI were stained. Values are presented as the mean ± SD from three independent experiments. Scale bars, 10 μm.

Cell migration begins with the establishment of a protruding force for membrane extension and traction for contraction [22]. The Rho GTPase superfamily, including Rho, Rac1, and Cdc42, are known to act as molecular switches with their GTP- or GDP-binding forms and are involved in cell migration processes [23, 24]. Recent studies have shown that the guanylate exchange factor Vav family regulates macrophage morphology by regulating Rac1 and RhoA activities [10]. In addition, in atherosclerosis, signals transmitted by oxLDL and CD36 in platelets or macrophages regulate downstream signaling molecules such as MLCK, which affects the cytoskeleton [25]. Our study showed that the phosphorylation of Vav1 is significantly elevated in the process of diabetic atherosclerosis. In vitro experiments showed that hyperphosphorylation of Vav1 inhibits foam cell migration, mainly by regulating the activation of Rac1 but not RhoA. Although recent studies have shown that Vav/Cdc42 regulates actin polymerization to promote low-density lipoprotein uptake and metabolism [26], there is no evidence that Vav/Cdc42 regulates macrophage migration, which may require further research to explore.

The cell migration process involves the formation of lamellipodia, the dissociation of cells from the extracellular matrix, and contraction of the cytoskeletal tail. During this process, Rac promotes the formation of PDGF-stimulated lamellipodia, while RhoA stimulates contractile myogenesis downstream of LPA signaling. Protein fibers (i.e., stress fibers) are formed. CDC42 was later shown to promote and activate Rac, and there is considerable evidence that the activity of Rac maintains the directional front end of protruding lamellipodia [27]. In contrast, Rho is more active at the flank and posterior regions of the cell, antagonizing the function of Rac1 [28]. Staining of F-actin by phalloidin showed that advanced glycation end products inhibited the production of lamellipodia, and lamellipodia production was restored when Vav1/Rac1 was blocked by Vav1 siRNA and 6-thio-GTP. In subsequent experiments, we will use a real-time visualization tool to further investigate the role of the Vav1/Rac1 pathway in the cytoskeleton.

Our data provide additional research support for the final fate and specific matrix of foam cells in diabetes atherosclerosis and validate the role of peritoneal macrophage efflux experiments in foam cell migration studies in diabetic mice, while the role of Vav1/Rac1 in advanced glycation end products inhibiting foam cells needs to be further elucidated. The Vav1/Rac1 pathway inhibits foam cell migration by inhibiting the formation of lamellipodia in macrophages, and blocking each loop of this pathway inhibits the effect of advanced glycation end products. These findings provide further understanding of new ways to promote the regression of atherosclerotic plaques.

Data Availability

The data used to support the findings of this study are available from the corresponding author upon request.

Ethical Approval

This study was approved by the Chinese Clinical Trial Registry and conducted in agreement with the institutional guidelines. Ethical review number is ChiECRCT20190206.

Consent

Written informed consent was obtained from all patients.

Conflicts of Interest

The authors declare that they have no competing interests.

Authors' Contributions

Zhengyang Bao performed the experiments. Zhengyang Bao and Zhongqun Wang carried out the data analysis. Zhongqun Wang designed the study. Zhongqun Wang, Zhengyang Bao, Lihua Li, Yue Geng, Jinchuan Yan, Chen Shao, Zhen Sun, Lele Jing, Qiwen Pang, and Lili Zhang supervised the study. Zhengyang Bao wrote the manuscript with input from all authors.

Acknowledgments

This work was supported by the following foundations: the National Natural Science Foundation of China (Grant Nos. 81770450, 81370408, and 81670405), the Natural Science Foundation of Jiangsu Province (BK20131246), and the related foundation of Jiangsu Province (QNRC 2016836, WSN-044, and LGY2018092), and was project funded by the Priority Academic Program Development of Jiangsu Higher Education Institutions (Zhenjiang Cardiovascular Clinical Research Center Project, SS2018008).

References

[1] J. A. Beckman and M. A. Creager, "Vascular complications of diabetes," *Circulation Research*, vol. 118, no. 11, pp. 1771–1785, 2016.

[2] M. S. Gibson, N. Domingues, and O. V. Vieira, "Lipid and non-lipid factors affecting macrophage dysfunction and inflammation in atherosclerosis," *Frontiers in Physiology*, vol. 9, p. 654, 2018.

[3] L. Zhao, Z. Varghese, J. F. Moorhead, Y. Chen, and X. Z. Ruan, "CD36 and lipid metabolism in the evolution of atherosclerosis," *British Medical Bulletin*, vol. 126, no. 1, pp. 101–112, 2018.

[4] A. Shapouri-Moghaddam, S. Mohammadian, H. Vazini et al., "Macrophage plasticity, polarization, and function in health and disease," *Journal of Cellular Physiology*, vol. 233, no. 9, pp. 6425–6440, 2018.

[5] S. Xu, L. Li, J. Yan et al., "CML/CD36 accelerates atherosclerotic progression via inhibiting foam cell migration," *Biomedicine & Pharmacotherapy*, vol. 97, pp. 1020–1031, 2018.

[6] Z. Wang, Z. Bao, Y. Ding et al., "Nϵ-carboxymethyl-lysine-induced PI3K/Akt signaling inhibition promotes foam cell apoptosis and atherosclerosis progression," *Biomedicine & Pharmacotherapy*, vol. 115, article 108880, 2019.

[7] X. R. Bustelo, "Vav family exchange factors: an integrated regulatory and functional view," *Small GTPases*, vol. 5, no. 2, p. e973757, 2014.

[8] S. O. Rahaman, W. Li, and R. L. Silverstein, "Vav guanine nucleotide exchange factors regulate atherosclerotic lesion development in mice," *Arteriosclerosis, Thrombosis, and Vascular Biology*, vol. 33, no. 9, pp. 2053–2057, 2013.

[9] K. Chen, W. Li, J. Major, S. O. Rahaman, M. Febbraio, and R. L. Silverstein, "Vav guanine nucleotide exchange factors link hyperlipidemia and a prothrombotic state," *Blood*, vol. 117, no. 21, pp. 5744–5750, 2011.

[10] Y. M. Park, J. A. Drazba, A. Vasanji, T. Egelhoff, M. Febbraio, and R. L. Silverstein, "Oxidized LDL/CD36 interaction induces loss of cell polarity and inhibits macrophage locomotion," *Molecular Biology of the Cell*, vol. 23, no. 16, pp. 3057–3068, 2012.

[11] S. Narumiya and D. Thumkeo, "Rho signaling research: history, current status and future directions," *FEBS Letters*, vol. 592, no. 11, pp. 1763–1776, 2018.

[12] A. Sadok and C. J. Marshall, "Rho GTPases," *Small GTPases*, vol. 5, no. 4, article e29710, 2014.

[13] A. Hall, "Rho family GTPases," *Biochemical Society Transactions*, vol. 40, no. 6, pp. 1378–1382, 2012.

[14] J.-B. Chang, N.-F. Chu, J.-T. Syu, A.-T. Hsieh, and Y.-R. Hung, "Advanced glycation end products (AGEs) in relation to atherosclerotic lipid profiles in middle-aged and elderly diabetic patients," *Lipids in Health and Disease*, vol. 10, no. 1, p. 228, 2011.

[15] M. G. Zeadin, C. I. Petlura, and G. H. Werstuck, "Molecular mechanisms linking diabetes to the accelerated development of atherosclerosis," *Canadian Journal of Diabetes*, vol. 37, no. 5, pp. 345–350, 2013.

[16] A. Goldin, J. A. Beckman, A. M. Schmidt, and M. A. Creager, "Advanced glycation end products: sparking the development of diabetic vascular injury," *Circulation*, vol. 114, no. 6, pp. 597–605, 2006.

[17] K. Prasad and S. Tiwari, "Therapeutic interventions for advanced glycation-end products and its receptor- mediated cardiovascular disease," *Current Pharmaceutical Design*, vol. 23, no. 6, pp. 937–943, 2017.

[18] D. A. Chistiakov, A. A. Melnichenko, V. A. Myasoedova, A. V. Grechko, and A. N. Orekhov, "Mechanisms of foam cell formation in atherosclerosis," *Journal of Molecular Medicine*, vol. 95, no. 11, pp. 1153–1165, 2017.

[19] D. A. Chistiakov, Y. V. Bobryshev, and A. N. Orekhov, "Macrophage-mediated cholesterol handling in atherosclerosis," *Journal of Cellular and Molecular Medicine*, vol. 20, no. 1, pp. 17–28, 2016.

[20] L. K. Curtiss, "Reversing atherosclerosis?," *The New England Journal of Medicine*, vol. 360, no. 11, pp. 1144–1146, 2009.

[21] Y. Iwashima, M. Eto, A. Hata et al., "Advanced glycation end products-induced gene expression of scavenger receptors in cultured human monocyte-derived macrophages," *Biochemical and Biophysical Research Communications*, vol. 277, no. 2, pp. 368–380, 2000.

[22] A. Cipres, D. P. O'Malley, K. Li, D. Finlay, P. S. Baran, and K. Vuori, "Sceptrin, a marine natural compound, inhibits cell motility in a variety of cancer cell lines," *ACS Chemical Biology*, vol. 5, no. 2, pp. 195–202, 2010.

[23] C. D. Nobes and A. Hall, "Rho GTPases control polarity, protrusion, and adhesion during cell movement," *The Journal of Cell Biology*, vol. 144, no. 6, pp. 1235–1244, 1999.

[24] T. Wittmann and C. M. Waterman-Storer, "Cell motility: can Rho GTPases and microtubules point the way?," *Journal of Cell Science*, vol. 114, Part 21, pp. 3795–3803, 2001.

[25] B. Choromańska, P. Myśliwiec, K. Choromańska, J. Dadan, and A. Chabowski, "The role of CD36 receptor in the pathogenesis of atherosclerosis," *Advances in Clinical and Experimental Medicine*, vol. 26, no. 4, pp. 717–722, 2017.

[26] R. K. Singh, A. S. Haka, P. Bhardwaj, X. Zha, and F. R. Maxfield, "Dynamic actin reorganization and Vav/Cdc42-dependent actin polymerization promote macrophage aggregated LDL (low-density lipoprotein) uptake and catabolism," *Arteriosclerosis, Thrombosis, and Vascular Biology*, vol. 39, no. 2, pp. 137–149, 2019.

[27] V. S. Kraynov, C. Chamberlain, G. M. Bokoch, M. A. Schwartz, S. Slabaugh, and K. M. Hahn, "Localized Rac activation dynamics visualized in living cells," *Science*, vol. 290, no. 5490, pp. 333–337, 2000.

[28] H. L. Wong, R. Pinontoan, K. Hayashi et al., "Regulation of rice NADPH oxidase by binding of Rac GTPase to its N-terminal extension," *Plant Cell*, vol. 19, no. 12, pp. 4022–4034, 2007.

Hindawi
Journal of Immunology Research
Volume 2020, Article ID 5284728, 11 pages
https://doi.org/10.1155/2020/5284728

Review Article

Galectin-3 Is a Potential Mediator for Atherosclerosis

Ziyu Gao,[1,2] Zhongni Liu,[2] Rui Wang,[3] Yinghong Zheng,[2] Hong Li,[2] and Liming Yang[1,2]

[1]*State Key Laboratory of Cardiovascular Disease, Fuwai Hospital, National Center for Cardiovascular Diseases, Beijing 100037, China*
[2]*Department of Pathophysiology, Key Laboratory of Cardiovascular Pathophysiology, Harbin Medical University, Harbin 150081, China*
[3]*Yangpu Hospital, Tongji University, Shanghai 200090, China*

Correspondence should be addressed to Liming Yang; limingyanghmu@163.com

Received 31 October 2019; Revised 13 January 2020; Accepted 4 February 2020; Published 14 February 2020

Guest Editor: Nivin Sharawy

Atherosclerosis is a multifactorial chronic inflammatory arterial disease forming the pathological basis of many cardiovascular diseases such as coronary heart disease, heart failure, and stroke. Numerous studies have implicated inflammation as a key player in the initiation and progression of atherosclerosis. Galectin-3 (Gal-3) is a 30 kDa β-galactose, highly conserved and widely distributed intracellularly and extracellularly. Gal-3 has been demonstrated in recent years to be a novel inflammatory factor participating in the process of intravascular inflammation, lipid endocytosis, macrophage activation, cellular proliferation, monocyte chemotaxis, and cell adhesion. This review focuses on the role of Gal-3 in atherosclerosis and the mechanism involved and several classical Gal-3 agonists and antagonists in the current studies.

1. Introduction

Atherosclerosis has become the prelude and the major manifestation of ischemic coronary-cerebrovascular disease such as ischemic heart disease and stroke. In the cohort of patients with ischemic stroke, the prevalence of atherosclerosis is increasing worldwide especially in Asian populations [1]. Atherosclerosis is a chronic inflammatory disease characterized by excessive accumulation of lipoprotein in macrophage, monocyte chemoattraction in vascular lesion, and the infiltration of vascular smooth muscle cells (VSMC) into the subendothelial space. Accumulating studies have indicated that inflammation plays an important role in the initiation and progression of atherosclerosis [2, 3].

Galectin-3 (Gal-3) is currently regarded as a potential cardiovascular inflammatory biomarker. It is a 29-35 kDa highly conserved β-galactoside-binding lectin and has received widespread interest in cardiovascular disease in recent decades. Gal-3 has been identified as a proinflammatory molecule that functions to drive the inflammatory response and oxidative stress. In addition, Gal-3 has an impact on the progress of atherosclerosis including endothelial dysfunction, lipid endocytosis, and VSMC migration. The role of Gal-3 in the cardiovascular area has been summarized by several review articles. However, previous reviews mainly focused on the association between Gal-3 and heart failure [4–6], and the influence of Gal-3 on atherosclerosis has not been carefully summarized. Up to now, extensive research has been carried out in the basic and epidemiological areas investigating the influence of Gal-3 on atherosclerosis. This review therefore summarizes the available research evidence on the effect of Gal-3 on atherosclerosis and the application of Gal-3 agonists and antagonists, with the aim of providing a better overview of Gal-3 as a new biomarker and contributor for atherosclerosis.

2. Galectin-3

2.1. Galectin-3 and Its Biochemical Activities. Among the galectin members, Gal-3 is the only member of vertebrate chimera-type galectin that contains a C-terminal carbohydrate recognition domain (CRD) and an N-terminal peptide [7]. The N-terminal peptide contains the first 12 amino acids

and an internal repeating domain. The CRD contains approximately 130 amino acids and specifically recognizes and binds to glycoprotein oligosaccharides expressed on the cell surface, within cells or in the extracellular matrix. Gal-3 proteins usually exist as monomers but can also form pentamers via N-terminal domain association when the concentration of Gal-3 monomers is high [8–10]. Gal-3 is coded by LGALS3 in the human genome and synthesized in the cytoplasm, then transported to the nucleus, other organelles, or secreted into the extracellular space. As Gal-3 lacks a signal sequence for insertion into the endoplasmic reticulum, Gal-3 can be secreted into the extracellular space via a nonclassical pathway [11, 12]. Gal-3 can be detected in a wide range of tissues and cells including skin, brain, intestinal tract, liver, and various cancer cells [13]. In addition, several studies have suggested that activated macrophage, monocyte, neutrophil, and mast cell also express Gal-3 [12, 14]. With its expression significantly and rapidly induced under diseased conditions, Gal-3 has received great interest over other galectins for its role in a variety of diseases including cancer, diabetes, and heart disease. As an important inflammatory biomarker, Gal-3 can promote the secretion of other proinflammatory factors like tumor necrosis factor-α (TNF-α) and interleukin-6 (IL-6) through activation of macrophages in a dose-dependent manner [15]. Gal-3 also participates in the progression of lipid endocytosis, cell apoptosis, cell differentiation, cell adhesion, and tumor metastasis [16–18].

2.2. Gal-3 and Inflammation. Gal-3 is a central regulator of critical processes under the setting of acute and chronic inflammation. Gal-3 is involved in the process of acute inflammatory response including chemoattraction of monocytes/-macrophages [19], neutrophil clearance [20], opsonization of apoptotic neutrophils [21], and mast cell degranulation [22]. Through interacting with nucleotide oligomerization domain-like receptor protein 3 (NLRP3), intracellular Gal-3 enhanced the effects of H5N1 infection by promoting host inflammatory responses and regulating interleukin-1 beta (IL-1β) production by macrophages. Compared to infected WT mice, infected Gal-3 knockout mice exhibited less inflammation in the lungs and reduced IL-1β levels in bronchoalveolar lavage fluid [23]. Chronic inflammation usually accompanied with fibrosis, loss of tissue structure, and subsequent organ failure is a heavy healthcare burden worldwide. Fibroblasts that represent key cells in the initiation and perpetuation of tissue fibrogenesis can promote inflammation by secreting inflammatory factors such as TNF-α, IL-6, and chemokines including C-X-C motif chemokine 8 (CXCL8), C-C chemokine ligand 2 (CCL2), C-C chemokine ligand 3 (CCL3), and C-C chemokine ligand 5 (CCL5) upon the activation of Gal-3 [24]. The expression of CCL2, CCL5, and CXCL8 stimulated by Gal-3 can attract monocyte and macrophage to the vascular lesion and plaque, especially in the core of lipid accumulation [15]. Gal-3 can bind with integrin in the cell surface to promote the adhesion between neutrophil and vascular endothelial cell through modifying cell-cell interaction [25]. Gal-3 has been identified as a critical molecule that mediates immunological functions in multiple immune cells, such as dendritic cells (DCs), B cells, and macrophages. Gal-3 inhibition downregulated expression of IL-6, IL-1β, and IL-23 p19, while it upregulated IL-10 and IL-12 p35 in toll-like receptor/NOD-like receptor- (TLR/NLR-) stimulated human monocyte-derived DCs, which inhibited subsequent Th17 and Th2 development. This finding indicated that intracellular Gal-3 acted as a cytokine hub of human DCs in responding to innate immunity signals [26]. Moreover, B cells with restrained endogenous Gal-3 expression skewed the balance toward plasma cell differentiation, which resulted in increased immunoglobulin production and parasite clearance during T. cruzi infection, providing evidence of a novel role for Gal-3 as an intracellular mediator of B cell survival and differentiation [27]. Disruption of the Gal-3 expression restrained IL-4/IL-13-induced alternative macrophage activation in recruited peritoneal macrophages *in vivo* without affecting IFN-γ/LPS-induced classical activation or IL-10-induced deactivation [28].

2.3. Gal-3 and Oxidative Stress. The relationship between Gal-3 and oxidative stress has been demonstrated *in vitro*, such that the treatment of monocytes with phorbol myristate acetate, a nicotinamide adenine dinucleotide phosphate (NADPH) oxidase-dependent inducer of reactive oxygen species, produced an increase in Gal-3 mRNA and protein expression [29]. Gal-3 stimulated the hyperoxide secretion from neutrophils through activation of NADPH II [30]. Excess hyperoxide led to an increased expression of cell surface glycoprotein and enhanced the oxidative stress induced by ischemia or reperfusion damage to further exacerbate vascular lesion [31]. Gal-3 was shown to induce oxidative stress through the release of O_2^- in cultured mast cells, an effect that was blocked by the antioxidant enzyme superoxide dismutase [32]. A study revealed that plasma Gal-3 concentration was increased in peripheral artery disease patients and correlated with F2-isoprostanes, the serologic marker of oxidative stress [33].

3. Gal-3 and Atherosclerosis

3.1. Gal-3 Level Increased in Atherosclerotic Vessels. Atherosclerosis is considered to be a complex inflammatory process that involves various inflammatory markers. In recent years, the relationship between Gal-3 and atherosclerosis has been investigated by substantial experimental studies. The level of Gal-3 was demonstrated to develop in human atherosclerosis plaque and some animal models, especially hypercholesterolemic rabbits and Apolipoprotein-E knockout ($ApoE^{-/-}$) mice with vascular stenosis. A study compared the Gal-3 level of aortic tissue between $ApoE^{-/-}$ mice on a high-fat diet and wild-type control and found that Gal-3 mRNA and protein levels in $ApoE^{-/-}$ mice were elevated 16.3 and 12.2 times than those of wild type, respectively. Moreover, the expression of Gal-3 increased in unstable plaque compared with stable regions from the same patient at both mRNA and protein levels, and Gal-3-treated human macrophages induced an 11-fold increase in human monocyte chemotaxis [15]. Endothelial cells, macrophages, and VSMC are the most important types of cells involved in the

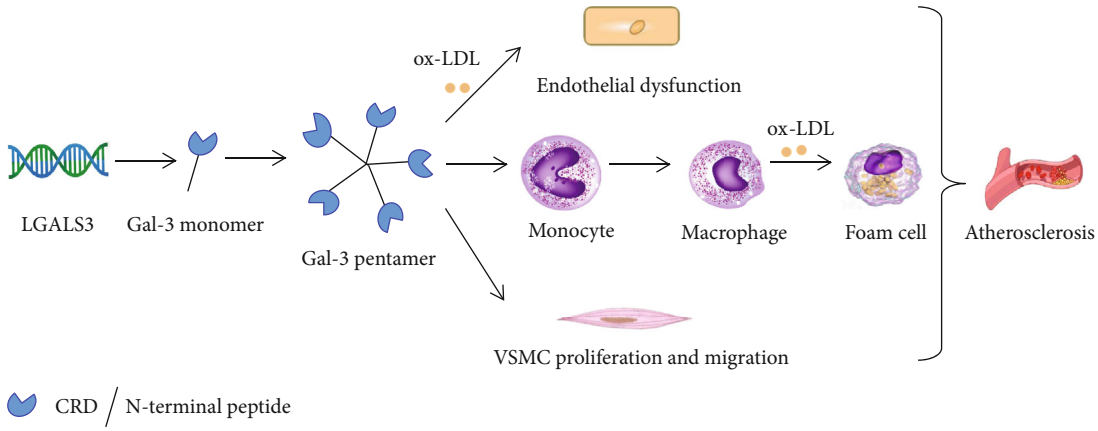

Figure 1: Gal-3 and its effect on different types of cells related to atherosclerosis. Gal-3: galectin-3; ox-LDL: oxidized low-density lipoprotein; VSMC: vascular smooth muscle cells; CRD: C-terminal carbohydrate recognition domain.

development of atherosclerosis, and Gal-3 can affect all these kinds of cells (Figure 1).

3.2. Gal-3 and Endothelial Dysfunction. Endothelial cells (ECs) play a crucial role in maintaining vascular homeostasis in response to various stimuli. Under conditions of chronic inflammation, sustained activation of ECs by inflammatory stimuli causes alterations in normal endothelial function, resulting in endothelial dysfunction which has been considered to be the basis and initial step of atherosclerosis, the most common cause of cardiovascular diseases [34, 35]. Several studies have shown that oxidized low-density lipoprotein (ox-LDL) induced endothelial cell injury by changing proinflammatory gene expression [36, 37]. Accumulating evidence has demonstrated that Gal-3 aggravated ox-LDL-mediated endothelial injury by inducing inflammation [38, 39]. Inhibition of Gal-3 abrogated cigarette smoke extract- (CSE-) induced autophagy and dysfunction of endothelial progenitor cells (EPCs) which have the potential to repair damaged blood vessels and promote angiogenesis [40]. And it was indicated that further progression of endothelial dysfunction increased the atherosclerotic plaque burden and Gal-3 staining in NADPH oxidase 4/low-density lipoprotein receptor knockout ($Nox4^{-/-}/Ldlr^{-/-}$) mice compared with $Ldlr^{-/-}$ mice [41]. However, Gal-3 deficiency led to exacerbated metabolic derangement and endothelial dysfunction in diabetic mice. And coagulation activity was enhanced suggesting a protective role for Gal-3 against thrombosis [42].

3.3. Gal-3 in Macrophage Differentiation and Foam Cell Formation. Ox-LDL induces endothelial dysfunction with focal inflammation which in turn causes increased expression of atherogenic signaling molecules that promote the adhesion of monocytes to the arterial endothelium and their penetration into the intima. Some studies have indicated that the synthesis and expression of Gal-3 are associated with differentiation and activation of macrophage. Liu et al. indicated that Gal-3 can be expressed on the surface of normal human peripheral blood monocytes. This finding indicated that Gal-3 levels increased significantly as monocytes differentiated into macrophages *in vitro*, and the secretion of Gal-3 by monocytes was regulated by lipopolysaccharide or interferon-γ [43]. Meanwhile, it has been demonstrated that human macrophage was the main origin of Gal-3 in both mRNA and protein levels [15]. Kim et al. indicated that Gal-3 expression in macrophage was signaled by Ras/MAP kinase pathway and that it can be upregulated by modified lipoprotein [44]. Thus, the elevated Gal-3 in atherosclerosis is associated with macrophage. One study demonstrated that Gal-3 is mainly distributed in macrophages and foam cells which are major components of atherosclerosis plaques, but not in VSMC, and Gal-3 expression increased with the plaque severity [45]. Similarly, another study found that the intraplaque Gal-3 expression levels were proportionally elevated as the degree of plaque extent and inflammation increased [46]. This finding showed that Gal-3 was heavily and exclusively accumulated in intimal plaques and that Gal-3 distribution was colocalized with plaque macrophages' distribution. The process of differentiated macrophages absorbing ox-LDL and transforming into foam cells has a profound association with Gal-3. Zhu et al. demonstrated that Gal-3 promoted lipoprotein uptake of foam cells to exacerbate atherosclerosis [47]. Moreover, the effect of Gal-3 on cardiac metabolic disturbance associated with obesity has been investigated. Marín-Royo et al. found that Gal-3 inhibition attenuated the consequences of cardiac lipotoxicity induced by high-fat diet *in vivo* [16]. Therefore, Gal-3 might exacerbate atherosclerosis plaque through promoting endocytosis of lipoprotein and disturbing lipid metabolism.

3.4. Gal-3 Stimulates VSMC Proliferation and Migration. Proliferation and migration of VSMC are important processes of atherosclerosis. Although VSMC are not the major origin of Gal-3 in circulating blood, the influence of Gal-3 on VSMC stimulates atherosclerosis. Tian et al. reported that Gal-3 expression increased in the phenotypic transformed VSMC treated with ox-LDL. Small interfering RNA silencing or knockdown of Gal-3 inhibited the phenotypic transformation and migration of VSMC [48], and another study of Tian et al. particularly indicated that exogenous Gal-3 promoted human VSMC proliferation and migration through the activation of canonical Wnt/β-catenin signaling pathway [49].

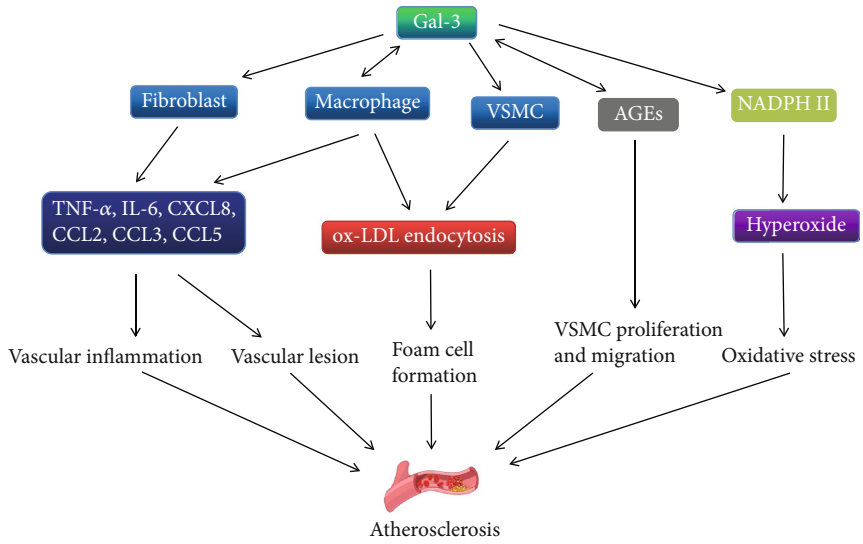

Figure 2: Diagram depicting the mechanisms by which Gal-3 promotes formation of atherosclerosis. Gal-3: galectin-3; TNF-α: tumor necrosis factor-α; IL-6: interleukin-6; CXCL8: C-X-C motif chemokine 8; CCL2: C-C chemokine ligand 2; CCL3: C-C chemokine ligand 3; CCL5: C-C chemokine ligand 5; ox-LDL: oxidized low-density lipoprotein; VSMC: vascular smooth muscle cells; AGEs: advanced glycation end products; NADPH II: nicotinamide-adenine dinucleotide phosphate II.

Menini et al. demonstrated that the effect of Gal-3 on VSMC within atherosclerotic plaque was related to the receptor for advanced glycation end products (RAGE) [50]. Gal-3 has been identified as an advanced glycation end product (AGE) receptor. Extracellular AGEs and its modified protein can bind with Gal-3 on the cell surface to form a protein complex and then attenuate the adhesion between VSMC and matrix glycoprotein. This attenuation of adhesion stimulates the proliferation and migration of VSMC for atherosclerosis exacerbation [47, 51]. These studies provide future directions for research on the treatment of atherosclerosis targeting on VSMC. Thus, as illustrated in Figure 2, Gal-3 can lead to atherosclerosis through inflammatory activation, vascular lesion, lipid endocytosis, VSMC migration, and oxidative stress.

4. Genetic Studies of Gal-3 in Atherosclerosis

Previous genetic studies of Gal-3 and atherosclerosis mainly focused on the comparison between Apolipoprotein-E/Gal-3 double knockout ($ApoE^{-/-}$/$gal\text{-}3^{-/-}$) mice and $ApoE^{-/-}$ mice. Mackinnon et al. indicated that the atherosclerosis plaque area of $ApoE^{-/-}$/$gal\text{-}3^{-/-}$ mice with a high-cholesterol diet was significantly smaller than that of $ApoE^{-/-}$ mice. Compared with $ApoE^{-/-}$ mice, the aortic plaque bulk of $ApoE^{-/-}$/$gal\text{-}3^{-/-}$ mice with a 12-week and 20-week high-cholesterol diet reduced by 35% and 40%, respectively [52]. Nachtigal et al. compared the severity of periaortic vascular adventitia inflammation between $ApoE^{-/-}$/$gal\text{-}3^{-/-}$ mice and $ApoE^{-/-}$ mice and found that aortic atherosclerosis plaques increased and vascular adventitia inflammation was aggravated in $ApoE^{-/-}$ mice as the age increased, but this phenomenon did not appear in $ApoE^{-/-}$/$gal\text{-}3^{-/-}$ mice [53]. Hsu et al. also demonstrated that lymphocyte amounts and macrophage infiltration ability decreased significantly in Gal-3 knockout mice compared to wild-type mice stimulated by inflammation [54]. These studies indicated that Gal-3 may exacerbate atherosclerosis through the activation of inflammation. In addition, phagocytosis of erythrocytes by macrophages has been regarded as a major pathological change in the progression of atherosclerosis. Sano et al. have investigated that the Gal-3-deficient macrophages reduced phagocytosis of erythrocytes and apoptotic thymocytes *in vitro* and *in vivo*, so Gal-3 may promote the phagocytosis of erythrocytes to aggravate atherosclerosis [55]. Arar et al. have demonstrated that the expression of LGALS3 was inactivated in quiescent vascular smooth muscle cells, but activated significantly in the aortas of hypercholesterolemic rabbits, balloon-injured rats, and cultured smooth muscle cells [56].

In recent years, some research has concentrated on atherosclerosis associated with heart failure and the mechanism that involves Gal-3. Yu et al. indicated that collagen production, processing, cleavage, cross-linking, and deposition were downregulated in Gal-3 knockout mice compared to those in wild-type mice. Moreover, cardiac remodeling, cardiac fibrosis, left ventricular dysfunction, and heart failure development were also found to be attenuated in Gal-3 knockout mice [57]. In the study by Watson et al., concomitant inhibition of renin-angiotensin system (RAS) and RAGE attenuated the development of atherosclerosis significantly. $RAGE^{-/-}$/$ApoE^{-/-}$ mice had less plaque area and attenuated macrophage infiltration than $ApoE^{-/-}$ mice [58]. Gal-3 is regarded as a type of RAGE, so the concomitant inhibition of RAS and Gal-3 may be a potential strategy for the treatment of atherosclerosis.

However, there are a few studies that demonstrate that Gal-3 is protective for atherosclerosis. Iacobini et al. indicated that the atherosclerosis plaque area of Gal-3 knockout mice was higher than that of wild-type mice, and increased accumulation of oxidized low-density lipoprotein was observed

in Gal-3 knockout mice [59]. A study also found that the macrophage infiltration and markers of systemic inflammation increased in LGALS3$^{-/-}$ mice compared with wild type [60]. Gal-3 may not only have negative effects but also have some positive effects on atherosclerosis. Hence, the effect of Gal-3 in atherosclerosis deserves further examination.

5. Epidemiological Studies of Gal-3 in Atherosclerosis

5.1. Gal-3 and Atherosclerosis. As a new biomarker of cardiovascular disease, the role of Gal-3 has been investigated by substantial epidemiological research. Several studies [61, 62] have suggested that the measurement of plasma Gal-3 concentration may be a good biomarker of diseases related to atherosclerosis. Nevertheless, the epidemiological studies associated with Gal-3 and atherosclerosis have primarily concentrated on heart failure and coronary artery disease in the last several years. Gal-3 was an independent risk factor for cardiovascular disease. A 10-year cohort study of 7968 participants indicated that the population with high Gal-3 levels was prone to suffer from cardiovascular disease [63]. Elderly individuals (mean age 69 years) with low Gal-3 had remarkably low cardiovascular risk over the follow-up period of 2.7 years [64]. Madrigal-Matute et al. indicated that Gal-3 plasma level was positively associated with carotid intima-media thickness and Gal-3 level increased in patients with carotid atherosclerosis compared with healthy controls [29]. Pusuroglu et al. and Ozturk et al. found that Gal-3 increased as carotid atherosclerosis became heavier in specific populations including obstructive sleep apnea syndrome and type 2 diabetes mellitus patients [65, 66]. Anyfanti et al. recently declared that in a cohort of relatively well-controlled rheumatoid arthritis (RA) patients with long-standing disease and low levels of systemic inflammation, serum Gal-3 levels were positively associated in the univariate analysis with carotid intima-media thickness, the marker of subclinical atherosclerosis, suggesting the potential utility of Gal-3 as a biomarker for subclinical cardiovascular disease in patients with RA [67]. Gal-3 is also shown to be a significant and independent predictor for coronary atherosclerosis [68]. In addition, Pei et al. investigated the effect of berberine on ox-LDL-induced macrophage activation and Gal-3 expression in neoatherosclerosis patients after percutaneous coronary intervention. They indicated that berberine suppressed Gal-3 upregulation and ox-LDL endocytosis through the NF-κB and AMPK signaling pathways [69]. These studies showed a potential property of Gal-3 as a biomarker for atherosclerosis.

5.2. Gal-3 and Heart Failure. Chronic heart failure is a series of complex syndromes associated with disability of cardiac ventricular ejection caused by organic or functional heart disease [70–72]. Current clinical biomarkers of chronic heart failure are brain natriuretic peptide and N-terminal pro-brain natriuretic peptide that have some limitations including age, renal function, and obesity [73–75]. Thus, searching for a new effective biomarker for heart failure is needed urgently. In the DEAL-HF study, 232 chronic heart failure patients were examined and followed up for four years. The baseline Gal-3 level was significantly associated with the prognosis and mortality of patients [76]. A study from de Boer et al., including 592 chronic heart failure patients whose left ventricular ejection fraction was less than 35%, also showed a consistent result with the DEAL-HF study. They indicated that Gal-3 was an independent marker for the prognosis of heart failure patients [77]. The Gal-3 level in chronic heart failure patients was higher than that in healthy controls, and increased Gal-3 was associated with the severity of heart failure and its complication as discussed by Meijers et al. [78]. Moreover, a Chinese population study indicated that the sensitivity and specificity of Gal-3 for heart failure diagnosis were 94.3% and 65.1%, respectively, as Gal-3 concentration reached 17.8 ng/mL [79]. In the CORONA study, 1492 patients with heart failure caused by ischemic myocardiosis were randomly divided into a Rosuvastatin treatment group and a control group: the mortality of the statin group was lower than that of the control group and Gal-3 decreased significantly in the statin group [80]. Polat et al. found that Gal-3 played an important role in prevention, classification, and personal therapy of heart failure [81]. Aforementioned studies revealed the clinical significance of Gal-3 in atherosclerosis-associated heart failure, but the mechanism of Gal-3 leading to heart failure needs to be further detected.

5.3. Gal-3 and Coronary Heart Disease. Except for heart failure, a great number of studies found that Gal-3 could also be regarded as an effective biomarker for coronary heart disease. Falcone's study included 125 coronary artery disease patients which were categorized into two groups with unstable angina or stable angina. Gal-3 level was significantly higher in unstable angina than stable angina, and it was higher in patients with three pieces of coronary artery disease than with one-two pieces [82]. Higueras et al. also indicated that Gal-3 was a risk factor for unstable angina [83]. Another study indicated that elevated circulating level of Gal-3 could be regarded as an independent predictor of the combined 30-day major adverse clinical outcome in patients with ST-segment elevation myocardial infarction undergoing primary percutaneous coronary intervention [84]. In a community cohort of patients with incident myocardial infarction (MI), elevated Gal-3 remained associated with increased risk of mortality and heart failure after adjustment for age, sex, comorbidities, and troponin, suggesting a role for measuring Gal-3 levels as a risk evaluation post-MI [85]. Moreover, Szadkowska et al. indicated that Gal-3 was an independent risk factor for reinfarction in MI patients after interventional operation, as Gal-3 reached 18.1 ng/mL [86]. In a prospective study containing 782 patients with coronary heart disease, the prognosis of low-Gal-3 patients was better than that of high-Gal-3 patients [87]. Moreover, the combined detection of Gal-3 and carotid intima-media thickness has been verified to be a more effective prediction for coronary artery disease [88]. Grandin et al. found that the acute coronary syndrome patients with high Gal-3 levels were more prone to suffer heart failure than low-Gal-3 patients [89]. Here, we summarized genetic and epidemiological studies of Gal-3 associated with atherosclerosis over the past two decades (Table 1).

Table 1: Brief research development of Gal-3 associated with atherosclerosis.

Research type	Targets	Main findings
Genetic	ApoE$^{-/-}$/gal-3$^{-/-}$ mice [52]	Atherosclerosis plaques were significantly smaller.
	ApoE$^{-/-}$/gal-3$^{-/-}$ mice [53]	Aortic atherosclerosis plaques decreased and vascular adventitia inflammation reduced.
	Gal-3 knockout mice [54]	Lymphocyte amounts and macrophage infiltration decreased significantly.
	Gal-3-deficient macrophages [55]	Phagocytosis of erythrocytes reduced.
Epidemiological	Heart failure patients [76]	Gal-3 level was significantly associated with the prognosis and mortality.
	Coronary heart disease patients [82]	Gal-3 level increased significantly in the unstable angina group.
	Myocardial infarction patients [86]	Gal-3 was regarded as an independent risk factor for reinfarction.
	Carotid atherosclerosis patients [29]	Gal-3 level was positively associated with carotid intima-media thickness and the prevalence of carotid atherosclerosis.
	Heart failure patients [79]	The sensitivity and specificity of Gal-3 for heart failure diagnosis were 94.3% and 65.1%, respectively.
	Patients with coronary artery disease [68]	Gal-3 was a significant and independent predictor.
	Patients with myocardial infarction [85]	Elevated Gal-3 was associated with mortality and heart failure.

Table 2: Classical Gal-3 modulators in the present relative studies.

Modulator	Subtype	Function	Targets	Mechanism	Authors
MCP	—	Inhibition	Leukocytes and endothelial cells	Inhibition of the adhesion between leucocytes and endothelial cells	Lu et al. [90]
			ApoE$^{-/-}$ mice	—	MacKinnon et al. [52]
			Heart failure mice	Reducing myocardial inflammation and fibrogenesis	Vergaro et al. [91]
Statin	Pravastatin	Inhibition	Acute coronary syndrome patients	—	Cannon et al. [94]
	Rosuvastatin		Heart failure patients		Gullestad et al. [80]
	Atorvastatin		ApoE$^{-/-}$ mice		Lee et al. [46]
Quinapril	—	Inhibition	Diabetic RAGE$^{-/-}$/gal-3$^{-/-}$ mice	Reducing macrophage infiltration and vascular collagen deposition	Watson et al. [58]
MRAs	—	Inhibition	Myocardial infarction mice	Attenuation of cardiac fibrosis, left ventricular dysfunction, and heart failure	Lax et al. [95]
LacNac	—	Inhibition	Gal-3$^{-/-}$ mice		Yu et al. [57]
Aldosterone	—	Activation	Macrophages	—	Lin et al. [96]
Doxazosin	—	Activation	Cardiomyocytes	—	Qian et al. [97]

Abbreviations: Gal-3: galectin-3; MCP: modified citrus pectin; MRAs: mineralocorticoid receptor antagonists; LacNac: N-acetyllactosamine.

6. Gal-3 Modulation

Gal-3 inhibition might be beneficial for atherosclerosis treatment due to the important role of Gal-3 in atherosclerosis and atherosclerosis-associated heart failure. As Gal-3 recognizes and binds to glycoprotein oligosaccharides via its carbohydrate recognition region, pharmacological inhibition of Gal-3 has almost exclusively targeted the CRD for inhibiting activities of this protein. Modified citrus pectin (MCP), a natural polysaccharide extracted from citrus plants, has been applied in experimental studies as a classical Gal-3 inhibitor. Lu et al. found that MCP inhibited the adhesion of leucocytes to endothelial cells to relieve atherosclerotic lesions through Gal-3 inhibition [90]. MacKinnon et al. also indicated that administration of MCP reduced the atherosclerosis plaque volume in ApoE$^{-/-}$ mice [52]. Gal-3 inhibition induced by MCP could also reverse the isoproterenol-induced left ventricular dysfunction characterized by reducing myocardial inflammation and fibrogenesis in heart failure mice [91]. Thiodigalactoside (TDG) derivatives targeting CRD sites have been approved as antagonists of Gal-3. TD-139, a thiodigalactoside analogue, has been used as an inhaled powder for the treatment of idiopathic pulmonary fibrosis and is speculated to antagonize Gal-3 [92]. Multivalent attachment of a TDG derivative using the bovine serum albumin has been identified as one of the most potent Gal-3 inhibitors so far [93].

At present, the frequently used clinical drug associated with Gal-3 to treat cardiovascular disease is statin. Cannon et al. indicated that the acute coronary syndrome patients with statin drug treatment had a lower level of Gal-3 than patients with standardized treatment [94]. The CORONA

study showed that Gal-3 level and all-cause mortality of Rosuvastatin-treated heart failure patients decreased significantly compared to the control group [80]. In addition, Lee et al. found that Atorvastatin markedly reduced Gal-3 expression within atherosclerotic plaques [46]. Moreover, some new Gal-3 inhibitors have been discovered in recent years. Watson et al. indicated that Quinapril treatment decreased Gal-3 expression, macrophage infiltration, and vascular collagen deposition within atherosclerosis plaque [58]. Lax et al. [95] demonstrated that mineralocorticoid receptor antagonists (MRAs) could inhibit Gal-3 to attenuate cardiac fibrosis, left ventricular dysfunction, and subsequent heart failure. Similarly, N-acetyllactosamine (LacNac) had the same effect with MRAs [57].

Regarding Gal-3 agonists, experimental evidence from Lin et al. revealed that aldosterone increased Gal-3 secretion in macrophages [96]. Another study from Qian et al. indicated that doxazosin exacerbated Gal-3 expression in cardiomyocytes [97]. The application of the aldosterone antagonist decreased the Gal-3 level and inhibited left ventricular dysfunction in patients with hypertension [98]. These findings proved that Gal-3 agonist inactivation may be useful for the clinical treatment of atherosclerosis (shown in Table 2).

7. Perspectives and Conclusions

There is strong evidence that Gal-3 participates in the initiation and progression of atherosclerosis. Numerous studies have shown that Gal-3 contributes to macrophage differentiation, foam cell formation, endothelial dysfunction, and VSMC proliferation and migration in atherosclerosis. In this review, we summarized several mechanisms pivotal to the development of atherosclerosis that are stimulated by local or circulating Gal-3. Amplification of cardiovascular inflammation and lipid accumulation in macrophage by Gal-3 are the most important mechanisms. Up to now, studies on Gal-3 have been focused on genetics and epidemiology suggesting that Gal-3 is positively related to the occurrence of atherosclerosis. Thus, Gal-3 can be regarded as a new biomarker for the risk evaluation of atherosclerosis and a new treatment target for atherosclerosis therapy. On the other hand, the application of Gal-3 inhibitors may be a potential treatment for atherosclerosis in the future. Moreover, macrophage plays a vital role in atherosclerosis, and some studies have indicated that Gal-3 can activate M2 macrophage differentiation, which has an anti-inflammatory property, through the CD98/phosphoinositide 3-kinase (PI3K) pathway [28, 99]. Activation of M2 macrophage differentiation by Gal-3 may be beneficial to the treatment of atherosclerosis through suppression of inflammation. As a key protein in autophagy progression, PI3K can be upregulated by Gal-3. Therefore, the augmentation of macrophage autophagy in atherosclerotic plaque through the Gal-3/PI3K/Akt/mTOR pathway is probably an effective therapy for atherosclerosis. To some extent, the multiple functions of Gal-3 depend on its N-terminal domain modification by matrix metalloproteinase (MMP). MMP-7 has been demonstrated to be a Gal-3 activator to exacerbate inflammation [100]. Hence, MMP can be regarded as a new target for further research on the connection between Gal-3 and atherosclerosis.

Conflicts of Interest

The authors declare no conflicts of interest.

Authors' Contributions

Ziyu Gao collected the literature and wrote the review manuscript. Zhongni Liu and Rui Wang helped in figure compilation. Yinghong Zheng revised and edited the manuscript. Liming Yang gave the idea behind the manuscript compilation. Hong Li and Liming Yang reviewed the article before final submission. All authors read and approved the manuscript prior to submission. Ziyu Gao and Zhongni Liu contributed equally to this work.

Acknowledgments

This review was funded by the National Natural Science Foundation of China (81571833 and 91939104), National Key Laboratory Open Project of Cardiovascular Disease (2019 kf-02), Ministry of Education Key Laboratory Open Project of Myocardial Ischemia (KF201908).

References

[1] P. B. Gorelick, K. S. Wong, H. J. Bae, and D. K. Pandey, "Large artery intracranial occlusive disease: a large worldwide burden but a relatively neglected frontier," *Stroke*, vol. 39, no. 8, pp. 2396–2399, 2008.

[2] J. Viola and O. Soehnlein, "Atherosclerosis - a matter of unresolved inflammation," *Seminars in Immunology*, vol. 27, no. 3, pp. 184–193, 2015.

[3] S. Taleb, "Inflammation in atherosclerosis," *Archives of Cardiovascular Diseases*, vol. 109, no. 12, pp. 708–715, 2016.

[4] E. Coburn and W. Frishman, "Comprehensive review of the prognostic value of galectin-3 in heart failure," *Cardiology in Review*, vol. 22, no. 4, pp. 171–175, 2014.

[5] R. A. de Boer, A. A. Voors, P. Muntendam, W. H. van Gilst, and D. J. van Veldhuisen, "Galectin-3: a novel mediator of heart failure development and progression," *European Journal of Heart Failure*, vol. 11, no. 9, pp. 811–817, 2009.

[6] V. Srivatsan, M. George, and E. Shanmugam, "Utility of galectin-3 as a prognostic biomarker in heart failure: where do we stand?," *European Journal of Preventive Cardiology*, vol. 22, no. 9, pp. 1096–1110, 2015.

[7] S. H. Barondes, V. Castronovo, D. N. Cooper et al., "Galectins: a family of animal beta-galactoside-binding lectins," *Cell*, vol. 76, no. 4, pp. 597-598, 1994.

[8] D. N. Cooper, "Galectinomics: finding themes in complexity," *Biochimica et Biophysica Acta (BBA) - General Subjects*, vol. 1572, no. 2-3, pp. 209–231, 2002.

[9] G. A. Rabinovich and M. A. Toscano, "Turning 'sweet' on immunity: galectin-glycan interactions in immune tolerance and inflammation," *Nature Reviews Immunology*, vol. 9, no. 5, pp. 338–352, 2009.

[10] N. Suthahar, W. C. Meijers, H. H. W. Silljé, J. E. Ho, F.-T. Liu, and R. A. de Boer, "Galectin-3 activation and inhibition in

heart failure and cardiovascular disease: an update," *Theranostics*, vol. 8, no. 3, pp. 593–609, 2018.

[11] F. T. Liu, R. J. Patterson, and J. L. Wang, "Intracellular functions of galectins," *Biochimica et Biophysica Acta*, vol. 1572, no. 2-3, pp. 263–273, 2002.

[12] R. C. Hughes, "Secretion of the galectin family of mammalian carbohydrate-binding proteins," *Biochimica et Biophysica Acta*, vol. 1473, no. 1, pp. 172–185, 1999.

[13] S. H. Barondes, D. N. Cooper, M. A. Gitt, and H. Leffle, "Galectins. Structure and function of a large family of animal lectins," *Journal of Biological Chemistry*, vol. 269, pp. 20807–20810, 1994.

[14] P. Gao, J. L. Simpson, J. Zhang, and P. G. Gibson, "Galectin-3: its role in asthma and potential as an anti-inflammatory target," *Respiratory Research*, vol. 14, no. 1, p. 136, 2013.

[15] M. Papaspyridonos, E. McNeill, J. P. de Bono et al., "Galectin-3 is an amplifier of inflammation in atherosclerotic plaque progression through macrophage activation and monocyte chemoattraction," *Arteriosclerosis, Thrombosis, and Vascular Biology*, vol. 28, no. 3, pp. 433–440, 2008.

[16] G. Marín-Royo, I. Gallardo, E. Martínez-Martínez et al., "Inhibition of galectin-3 ameliorates the consequences of cardiac lipotoxicity in a rat model of diet-induced obesity," *Disease Models & Mechanisms*, vol. 11, no. 2, article dmm032086, 2018.

[17] J. Dumic, S. Dabelic, and M. Flogel, "Galectin-3: an open-ended story," *Biochimica et Biophysica Acta (BBA) - General Subjects*, vol. 1760, pp. 616–635, 2006.

[18] F. T. Liu and G. A. Rabinovich, "Galectins as modulators of tumour progression," *Nature Reviews Cancer*, vol. 5, no. 1, pp. 29–41, 2005.

[19] V. V. Subhash, S. S. M. Ling, and B. Ho, "Extracellular galectin-3 counteracts adhesion and exhibits chemoattraction in Helicobacter pylori-infected gastric cancer cells," *Microbiology*, vol. 162, no. 8, pp. 1360–1366, 2016.

[20] R. D. Wright, P. R. Souza, M. B. Flak, P. Thedchanamoorthy, L. V. Norling, and D. Cooper, "Galectin-3-null mice display defective neutrophil clearance during acute inflammation," *Journal of Leukocyte Biology*, vol. 101, no. 3, pp. 717–726, 2017.

[21] A. Karlsson, K. Christenson, M. Matlak et al., "Galectin-3 functions as an opsonin and enhances the macrophage clearance of apoptotic neutrophils," *Glycobiology*, vol. 19, no. 1, pp. 16–20, 2009.

[22] M. Bambouskova, I. Polakovicova, I. Halova et al., "New regulatory roles of galectin-3 in high-affinity IgE receptor signaling," *Molecular and Cellular Biology*, vol. 36, no. 9, pp. 1366–1382, 2016.

[23] Y. J. Chen, S. F. Wang, I. C. Weng et al., "Galectin-3 enhances avian H5N1 influenza a virus-induced pulmonary inflammation by promoting NLRP3 inflammasome activation," *The American Journal of Pathology*, vol. 188, no. 4, pp. 1031–1042, 2018.

[24] A. Filer, M. Bik, G. N. Parsonage et al., "Galectin 3 induces a distinctive pattern of cytokine and chemokine production in rheumatoid synovial fibroblasts via selective signaling pathways," *Arthritis & Rheumatism*, vol. 60, no. 6, pp. 1604–1614, 2009.

[25] S. Sato, N. Ouellet, I. Pelletier, M. Simard, A. Rancourt, and M. G. Bergeron, "Role of galectin-3 as an adhesion molecule for neutrophil extravasation during streptococcal pneumonia," *The Journal of Immunology*, vol. 168, no. 4, pp. 1813–1822, 2002.

[26] S. S. Chen, L. W. Sun, H. Brickner, and P. Q. Sun, "Downregulating galectin-3 inhibits proinflammatory cytokine production by human monocyte-derived dendritic cells via RNA interference," *Cellular Immunology*, vol. 294, no. 1, pp. 44–53, 2015.

[27] E. V. Acosta-Rodríguez, C. L. Montes, C. C. Motrán et al., "Galectin-3 mediates IL-4-induced survival and differentiation of B cells: functional cross-talk and implications during-Trypanosoma cruziInfection," *The Journal of Immunology*, vol. 172, no. 1, pp. 493–502, 2004.

[28] A. C. MacKinnon, S. L. Farnworth, P. S. Hodkinson et al., "Regulation of alternative macrophage activation by galectin-3," *The Journal of Immunology*, vol. 180, no. 4, pp. 2650–2658, 2008.

[29] J. Madrigal-Matute, J. S. Lindholt, C. E. Fernandez-Garcia et al., "Galectin-3, a biomarker linking oxidative stress and inflammation with the clinical outcomes of patients with atherothrombosis," *Journal of the American Heart Association*, vol. 3, article e000785, 2014.

[30] J. Almkvist, J. Faldt, C. Dahlgren, H. Leffler, and A. Karlsson, "Lipopolysaccharide-induced gelatinase granule mobilization primes neutrophils for activation by galectin-3 and formyl-methionyl-Leu-Phe," *Infection and Immunity*, vol. 69, no. 2, pp. 832–837, 2001.

[31] B. A. P. Fernandes, G. Campanhole, P. H. M. Wang et al., "A role for galectin-3 in renal tissue damage triggered by ischemia and reperfusion injury," *Transplant International*, vol. 21, no. 10, pp. 999–1007, 2008.

[32] Y. Suzuki, T. Inoue, T. Yoshimaru, and C. Ra, "Galectin-3 but not galectin-1 induces mast cell death by oxidative stress and mitochondrial permeability transition," *Biochimica et Biophysica Acta (BBA) - Molecular Cell Research*, vol. 1783, pp. 924–934, 2008.

[33] I. Fort-Gallifa, A. Hernández-Aguilera, A. García-Heredia et al., "Galectin-3 in peripheral artery disease. Relationships with markers of oxidative stress and inflammation," *International Journal of Molecular Sciences*, vol. 18, no. 5, article ijms18050973, p. 973, 2017.

[34] J. Davignon and P. Ganz, "Role of endothelial dysfunction in atherosclerosis," *Circulation*, vol. 109, no. 23, Supplement 1, pp. III27–III32, 2004.

[35] I. Tabas, G. García-Cardeña, and G. K. Owens, "Recent insights into the cellular biology of atherosclerosis," *Journal of Cell Biology*, vol. 209, no. 1, pp. 13–22, 2015.

[36] J. B. Li, H. Y. Wang, Y. Yao et al., "Overexpression of microRNA-138 alleviates human coronary artery endothelial cell injury and inflammatory response by inhibiting the PI3K/Akt/eNOS pathway," *Journal of Cellular and Molecular Medicine*, vol. 21, no. 8, pp. 1482–1491, 2017.

[37] S. Zhang, C. Guo, Z. Chen, P. Zhang, J. Li, and Y. Li, "Vitexin alleviates ox-LDL-mediated endothelial injury by inducing autophagy via AMPK signaling activation," *Molecular Immunology*, vol. 85, pp. 214–221, 2017.

[38] X. Chen, J. Lin, T. Hu et al., "Galectin-3 exacerbates ox-LDL-mediated endothelial injury by inducing inflammation via integrin β1-RhoA-JNK signaling activation," *Journal of Cellular Physiology*, vol. 234, no. 7, pp. 10990–11000, 2019.

[39] H. C. Ou, W. C. Chou, C. H. Hung et al., "Galectin-3 aggravates ox-LDL-induced endothelial dysfunction through

LOX-1 mediated signaling pathway," *Environmental Toxicology*, vol. 34, no. 7, pp. 825–835, 2019.

[40] C. Pei, X. Wang, Y. Lin, L. Fang, and S. Meng, "Inhibition of galectin-3 alleviates cigarette smoke extract-induced autophagy and dysfunction in endothelial progenitor cells," *Oxidative Medicine and Cellular Longevity*, vol. 2019, Article ID 7252943, 13 pages, 2019.

[41] H. Langbein, C. Brunssen, A. Hofmann et al., "NADPH oxidase 4 protects against development of endothelial dysfunction and atherosclerosis in LDL receptor deficient mice," *European Heart Journal*, vol. 37, no. 22, pp. 1753–1761, 2016.

[42] A. L. Darrow and R. V. Shohet, "Galectin-3 deficiency exacerbates hyperglycemia and the endothelial response to diabetes," *Cardiovascular Diabetology*, vol. 14, no. 1, p. 73, 2015.

[43] F. T. Liu, D. K. Hsu, R. I. Zuberi, I. Kuwabara, E. Y. Chi, and W. R. Henderson Jr., "Expression and function of galectin-3, a beta-galactoside-binding lectin, in human monocytes and macrophages," *The American Journal of Pathology*, vol. 147, no. 4, pp. 1016–1028, 1995.

[44] K. Kim, E. P. Mayer, and M. Nachtigal, "Galectin-3 expression in macrophages is signaled by *Ras*/MAP kinase pathway and up-regulated by modified lipoproteins," *Biochimica et Biophysica Acta (BBA) - Molecular Cell Research*, vol. 1641, pp. 13–23, 2003.

[45] M. Nachtigal, Z. Al-Assaad, E. P. Mayer, K. Kim, and M. Monsigny, "Galectin-3 expression in human atherosclerotic lesions," *The American Journal of Pathology*, vol. 152, no. 5, pp. 1199–1208, 1998.

[46] Y. J. Lee, Y. S. Koh, H. E. Park et al., "Spatial and temporal expression, and statin responsiveness of galectin-1 and galectin-3 in murine atherosclerosis," *Korean Circulation Journal*, vol. 43, no. 4, pp. 223–230, 2013.

[47] W. Zhu, H. Sano, R. Nagai, K. Fukuhara, A. Miyazaki, and S. Horiuchi, "The role of galectin-3 in endocytosis of advanced glycation end products and modified low density lipoproteins," *Biochemical and Biophysical Research Communications*, vol. 280, no. 4, pp. 1183–1188, 2001.

[48] L. Tian, K. Chen, J. Cao et al., "Galectin-3-induced oxidized low-density lipoprotein promotes the phenotypic transformation of vascular smooth muscle cells," *Molecular Medicine Reports*, vol. 12, no. 4, pp. 4995–5002, 2015.

[49] L. Tian, K. Chen, J. Cao et al., "Galectin-3 induces the phenotype transformation of human vascular smooth muscle cells via the canonical Wnt signaling," *Molecular Medicine Reports*, vol. 15, no. 6, pp. 3840–3846, 2017.

[50] S. Menini, C. Iacobini, C. Ricci et al., "The galectin-3/RAGE dyad modulates vascular osteogenesis in atherosclerosis," *Cardiovascular Research*, vol. 100, no. 3, pp. 472–480, 2013.

[51] N. Seki, N. Hashimoto, H. Sano et al., "Mechanisms involved in the stimulatory effect of advanced glycation end products on growth of rat aortic smooth muscle cells," *Metabolism*, vol. 52, no. 12, pp. 1558–1563, 2003.

[52] A. C. MacKinnon, X. Liu, P. W. Hadoke, M. R. Miller, D. E. Newby, and T. Sethi, "Inhibition of galectin-3 reduces atherosclerosis in apolipoprotein E-deficient mice," *Glycobiology*, vol. 23, no. 6, pp. 654–663, 2013.

[53] M. Nachtigal, A. Ghaffar, and E. P. Mayer, "Galectin-3 gene inactivation reduces atherosclerotic lesions and adventitial inflammation in ApoE-deficient mice," *The American Journal of Pathology*, vol. 172, no. 1, pp. 247–255, 2008.

[54] D. K. Hsu, R. Y. Yang, Z. Pan et al., "Targeted disruption of the galectin-3 gene results in attenuated peritoneal inflammatory responses," *The American Journal of Pathology*, vol. 156, no. 3, pp. 1073–1083, 2000.

[55] H. Sano, D. K. Hsu, J. R. Apgar et al., "Critical role of galectin-3 in phagocytosis by macrophages," *The Journal of Clinical Investigation*, vol. 112, no. 3, pp. 389–397, 2003.

[56] C. Arar, J. C. Gaudin, L. Capron, and A. Legrand, "Galectin-3 gene (LGALS3) expression in experimental atherosclerosis and cultured smooth muscle cells," *FEBS Letters*, vol. 430, no. 3, pp. 307–311, 1998.

[57] L. Yu, W. P. Ruifrok, M. Meissner et al., "Genetic and pharmacological inhibition of galectin-3 prevents cardiac remodeling by interfering with myocardial fibrogenesis," *Circulation Heart Failure*, vol. 6, no. 1, pp. 107–117, 2013.

[58] A. M. Watson, J. Li, D. Samijono et al., "Quinapril treatment abolishes diabetes-associated atherosclerosis in RAGE/apolipoprotein E double knockout mice," *Atherosclerosis*, vol. 235, no. 2, pp. 444–448, 2014.

[59] C. Iacobini, S. Menini, C. Ricci et al., "Accelerated lipid-induced atherogenesis in galectin-3-deficient Mice," *Arteriosclerosis, Thrombosis, and Vascular Biology*, vol. 29, no. 6, pp. 831–836, 2009.

[60] N. N. Pejnovic, J. M. Pantic, I. P. Jovanovic et al., "Galectin-3 deficiency accelerates high-fat diet-induced obesity and amplifies inflammation in adipose tissue and pancreatic islets," *Diabetes*, vol. 62, no. 6, pp. 1932–1944, 2013.

[61] G. L. Salvagno and C. Pavan, "Prognostic biomarkers in acute coronary syndrome," *Annals of Translational Medicine*, vol. 4, no. 13, p. 258, 2016.

[62] A. I. Casanegra, J. A. Stoner, A. J. Tafur, H. A. Pereira, S. W. Rathbun, and A. W. Gardner, "Differences in galectin-3, a biomarker of fibrosis, between participants with peripheral artery disease and participants with normal ankle-brachial index," *Vascular Medicine*, vol. 21, no. 5, pp. 437–444, 2016.

[63] R. A. de Boer, D. J. van Veldhuisen, R. T. Gansevoort et al., "The fibrosis marker galectin-3 and outcome in the general population," *Journal of Internal Medicine*, vol. 272, no. 1, pp. 55–64, 2012.

[64] M. B. Mortensen, V. Fuster, P. Muntendam et al., "Negative risk markers for cardiovascular events in the elderly," *Journal of the American College of Cardiology*, vol. 74, no. 1, pp. 1–11, 2019.

[65] H. Pusuroglu, U. Somuncu, I. Bolat et al., "Galectin-3 is associated with coronary plaque burden and obstructive sleep apnoea syndrome severity," *Kardiologia Polska*, vol. 75, no. 4, pp. 351–359, 2017.

[66] D. Ozturk, O. Celik, S. Satilmis et al., "Association between serum galectin-3 levels and coronary atherosclerosis and plaque burden/structure in patients with type 2 diabetes mellitus," *Coronary Artery Disease*, vol. 26, no. 5, pp. 396–401, 2015.

[67] P. Anyfanti, E. Gkaliagkousi, E. Gavriilaki et al., "Association of galectin-3 with markers of myocardial function, atherosclerosis, and vascular fibrosis in patients with rheumatoid arthritis," *Clinical Cardiology*, vol. 42, no. 1, pp. 62–68, 2019.

[68] G. Aksan, O. Gedikli, K. Keskin et al., "Is galectin-3 a biomarker, a player-or both-in the presence of coronary atherosclerosis," *Journal of Investigative Medicine*, vol. 64, no. 3, pp. 764–770, 2016.

[69] C. Pei, Y. Zhang, P. Wang et al., "Berberine alleviates oxidized low-density lipoprotein-induced macrophage activation by downregulating galectin-3 via the NF-κB and AMPK signaling pathways," *Phytotherapy Research*, vol. 33, no. 2, pp. 294–308, 2018.

[70] C. S. Lam, A. Lyass, E. Kraigher-Krainer et al., "Cardiac dysfunction and noncardiac dysfunction as precursors of heart failure with reduced and preserved ejection fraction in the community," *Circulation*, vol. 124, no. 1, pp. 24–30, 2011.

[71] G. C. Kane, B. L. Karon, D. W. Mahoney et al., "Progression of left ventricular diastolic dysfunction and risk of heart failure," *Journal of the American Medical Association*, vol. 306, no. 8, pp. 856–863, 2011.

[72] A. G. Obrezan and D. Z. Baranov, "Myocardial strain properties in patients with chronic heart failure," *Kardiologiia*, vol. 59, no. 8, pp. 88–96, 2019.

[73] N. Ibrahim and J. L. Januzzi, "The potential role of natriuretic peptides and other biomarkers in heart failure diagnosis, prognosis and management," *Expert Review of Cardiovascular Therapy*, vol. 13, no. 9, pp. 1017–1030, 2015.

[74] L. F. Buckley, J. M. Canada, M. G. Del Buono et al., "Low NT-proBNP levels in overweight and obese patients do not rule out a diagnosis of heart failure with preserved ejection fraction," *ESC Heart Failure*, vol. 5, no. 2, pp. 372–378, 2018.

[75] M. Parovic, N. C. Okwose, K. Bailey et al., "NT-proBNP is a weak indicator of cardiac function and haemodynamic response to exercise in chronic heart failure," *ESC Heart Failure*, vol. 6, no. 2, pp. 449–454, 2019.

[76] D. J. Lok, P. Van Der Meer, P. W. de la Porte et al., "Prognostic value of galectin-3, a novel marker of fibrosis, in patients with chronic heart failure: data from the DEAL-HF study," *Clinical Research in Cardiology*, vol. 99, no. 5, pp. 323–328, 2010.

[77] R. A. de Boer, D. J. Lok, T. Jaarsma et al., "Predictive value of plasma galectin-3 levels in heart failure with reduced and preserved ejection fraction," *Annals of Medicine*, vol. 43, no. 1, pp. 60–68, 2011.

[78] W. C. Meijers, A. R. van der Velde, and R. A. de Boer, "The ARCHITECT galectin-3 assay: comparison with other automated and manual assays for the measurement of circulating galectin-3 levels in heart failure," *Expert Review of Molecular Diagnostics*, vol. 14, no. 3, pp. 257–266, 2014.

[79] Q. S. Yin, B. Shi, L. Dong, and L. Bi, "Comparative study of galectin-3 and B-type natriuretic peptide as biomarkers for the diagnosis of heart failure," *Journal of Geriatric Cardiology*, vol. 11, no. 1, pp. 79–82, 2014.

[80] L. Gullestad, T. Ueland, J. Kjekshus et al., "Galectin-3 predicts response to statin therapy in the Controlled Rosuvastatin Multinational Trial in Heart Failure (CORONA)," *European Heart Journal*, vol. 33, no. 18, pp. 2290–2296, 2012.

[81] V. Polat, E. Bozcali, T. Uygun, S. Opan, and O. Karakaya, "Diagnostic significance of serum galectin-3 levels in heart failure with preserved ejection fraction," *Acta Cardiologica*, vol. 71, no. 2, pp. 191–197, 2016.

[82] C. Falcone, S. Lucibello, I. Mazzucchelli et al., "Galectin-3 plasma levels and coronary artery disease: a new possible biomarker of acute coronary syndrome," *International Journal of Immunopathology and Pharmacology*, vol. 24, no. 4, pp. 905–913, 2011.

[83] J. Higueras, J. L. Martin-Ventura, L. Blanco-Colio et al., "Impact of plasma pro-B-type natriuretic peptide amino-terminal and galectin-3 levels on the predictive capacity of the LIPID clinical risk Scale in stable coronary disease," *Clínica e Investigación en Arteriosclerosis*, vol. 27, no. 2, pp. 57–63, 2015.

[84] T. H. Tsai, P. H. Sung, L. T. Chang et al., "Value and level of galectin-3 in acute myocardial infarction patients undergoing primary percutaneous coronary intervention," *Journal of Atherosclerosis and Thrombosis*, vol. 19, no. 12, pp. 1073–1082, 2012.

[85] R. Asleh, M. Enriquez-Sarano, A. S. Jaffe et al., "Galectin-3 levels and outcomes after myocardial infarction: a population-based study," *Journal of the American College of Cardiology*, vol. 73, no. 18, pp. 2286–2295, 2019.

[86] I. Szadkowska, R. N. Wlazel, M. Migala et al., "The association between galectin-3 and occurrence of reinfarction early after first myocardial infarction treated invasively," *Biomarkers*, vol. 18, no. 8, pp. 655–659, 2013.

[87] G. Maiolino, G. Rossitto, L. Pedon et al., "Galectin-3 predicts long-term cardiovascular death in high-risk patients with coronary artery disease," *Arteriosclerosis, Thrombosis, and Vascular Biology*, vol. 35, no. 3, pp. 725–732, 2015.

[88] A. Lisowska, M. Knapp, A. Tycińska et al., "Predictive value of Galectin-3 for the occurrence of coronary artery disease and prognosis after myocardial infarction and its association with carotid IMT values in these patients: a mid-term prospective cohort study," *Atherosclerosis*, vol. 246, pp. 309–317, 2016.

[89] E. W. Grandin, P. Jarolim, S. A. Murphy et al., "Galectin-3 and the development of heart failure after acute coronary syndrome: pilot experience from PROVE IT-TIMI 22," *Clinical Chemistry*, vol. 58, no. 1, pp. 267–273, 2012.

[90] Y. Lu, M. Zhang, P. Zhao et al., "Modified citrus pectin inhibits galectin-3 function to reduce atherosclerotic lesions in apoE-deficient mice," *Molecular Medicine Reports*, vol. 16, no. 1, pp. 647–653, 2017.

[91] G. Vergaro, M. Prud'homme, L. Fazal et al., "Inhibition of galectin-3 pathway prevents isoproterenol-induced left ventricular dysfunction and fibrosis in mice," *Hypertension*, vol. 67, no. 3, pp. 606–612, 2016.

[92] T. J. Hsieh, H. Y. Lin, Z. Tu et al., "Dual thio-digalactoside-binding modes of human galectins as the structural basis for the design of potent and selective inhibitors," *Scientific Reports*, vol. 6, no. 1, article 29457, 2016.

[93] H. Zhang, D. Laaf, L. Elling, and R. J. Pieters, "Thiodigalactoside-bovine serum albumin conjugates as high-potency inhibitors of galectin-3: an outstanding example of multivalent presentation of small molecule inhibitors," *Bioconjugate Chemistry*, vol. 29, no. 4, pp. 1266–1275, 2018.

[94] C. P. Cannon, E. Braunwald, C. H. McCabe et al., "Intensive versus moderate lipid lowering with statins after acute coronary syndromes," *The New England Journal of Medicine*, vol. 350, no. 15, pp. 1495–1504, 2004.

[95] A. Lax, J. Sanchez-Mas, M. C. Asensio-Lopez et al., "Mineralocorticoid receptor antagonists modulate galectin-3 and interleukin-33/ST2 signaling in left ventricular systolic dysfunction after acute myocardial infarction," *JACC: Heart Failure*, vol. 3, no. 1, pp. 50–58, 2015.

[96] Y. H. Lin, C. H. Chou, X. M. Wu et al., "Aldosterone induced galectin-3 secretion in vitro and in vivo: from cells to humans," *PLoS One*, vol. 9, no. 9, article e95254, 2014.

[97] X. Qian, M. Li, M. B. Wagner, G. Chen, and X. Song, "Doxazosin stimulates galectin-3 expression and collagen synthesis in HL-1 cardiomyocytes independent of protein kinase C pathway," *Frontiers in Pharmacology*, vol. 7, p. 495, 2016.

[98] A. C. Pouleur, H. Uno, M. F. Prescott et al., "Suppression of aldosterone mediates regression of left ventricular hypertrophy in patients with hypertension," *Journal of the Renin-Angiotensin-Aldosterone System*, vol. 12, no. 4, pp. 483–490, 2011.

[99] N. C. Henderson, E. A. Collis, A. C. Mackinnon et al., "CD98hc (SLC3A2) interaction with beta 1 integrins is required for transformation," *The Journal of Biological Chemistry*, vol. 279, no. 52, pp. 54731–54741, 2004.

[100] M. Puthenedam, F. Wu, A. Shetye, A. Michaels, K. J. Rhee, and J. H. Kwon, "Matrilysin-1 (MMP7) cleaves galectin-3 and inhibits wound healing in intestinal epithelial cells," *Inflammatory Bowel Diseases*, vol. 17, no. 1, pp. 260–267, 2011.

Hindawi
Journal of Immunology Research
Volume 2020, Article ID 8131754, 11 pages
https://doi.org/10.1155/2020/8131754

Review Article

Macrophage-Based Therapies for Atherosclerosis Management

Renyi Peng,[1,2] Hao Ji,[1,2] Libo Jin,[1,2] Sue Lin,[1,2] Yijiang Huang,[3] Ke Xu,[1,2] Qinsi Yang,[4] Da Sun,[1,2] and Wei Wu[1,5]

[1]*Institute of Life Sciences, Wenzhou University, Wenzhou, Zhejiang 325035, China*
[2]*Biomedical Collaborative Innovation Center of Zhejiang Province & Engineering Laboratory of Zhejiang Province for Pharmaceutical Development of Growth Factors, Biomedical Collaborative Innovation Center of Wenzhou, Wenzhou, Zhejiang 325035, China*
[3]*Department of Orthopaedics, The Second Affiliated Hospital and Yuying Children's Hospital of Wenzhou Medical University, Wenzhou, Zhejiang 325027, China*
[4]*Wenzhou Institute, University of Chinese Academy of Sciences, Wenzhou, Zhejiang 325000, China*
[5]*Key Laboratory for Biorheological Science and Technology of Ministry of Education, State and Local Joint Engineering Laboratory for Vascular Implants, Bioengineering College of Chongqing University, Chongqing 400030, China*

Correspondence should be addressed to Da Sun; sunday@wzu.edu.cn and Wei Wu; david2015@cqu.edu.cn

Received 1 November 2019; Revised 21 December 2019; Accepted 8 January 2020; Published 29 January 2020

Guest Editor: Nivin Sharawy

Atherosclerosis (AS), a typical chronic inflammatory vascular disease, is the main pathological basis of ischemic cardio/cerebrovascular disease (CVD). Long-term administration was characterized with low efficacy and serious side effects, while the macrophages with attractive intrinsic homing target have great potential in the efficient and safe management of AS. In this review, we focused on the systematical summary of the macrophage-based therapies in AS management, including macrophage autophagy, polarization, targeted delivery, microenvironment-triggered drug release, and macrophage- or macrophage membrane-based drug carrier. In conclusion, macrophage-based therapies have great promise to effectively manage AS in future research and clinic translation.

1. Introduction

Cardio/cerebrovascular disease (CVD) is the leading cause of morbidity and mortality worldwide. Atherosclerosis (AS) is considered the main pathological basis of ischemic CVD, including cerebrovascular disease, coronary heart disease, and peripheral arterial disease. AS is a typical chronic inflammatory vascular disease due to the accumulation of a large amount of lipids in the arterial wall, especially in the branched and bended arteries [1, 2]. The representative macrophages play an important role in the pathological progression in lesions of AS (Figure 1) [3]. The migration, activation, infiltration, and proliferation of macrophages lead to inflammation-mediated atherosclerotic plaque formation [4]. Furthermore, macrophages secrete abundant proteases and tissue factors to promote inflammation, lipid deposition, and plaque rapture. Thus, macrophages are regarded as an attractive target for managing AS [5, 6]. Despite the wide clinical use of local anti-inflammatory drugs, the traditional therapies have low bioavailability and severe side effects, far from meeting the long-term dosing requirements for the significant AS management in safety and efficiency [7]. This review discussed recent research studies on the role of macrophages in the pathogenesis of AS, especially systematically highlighting the advanced strategies in macrophage-based therapies for AS management, such as macrophage autophagy, polarization, targeted delivery, microenvironment-triggered drug release, and macrophage- or macrophage membrane-based drug carrier.

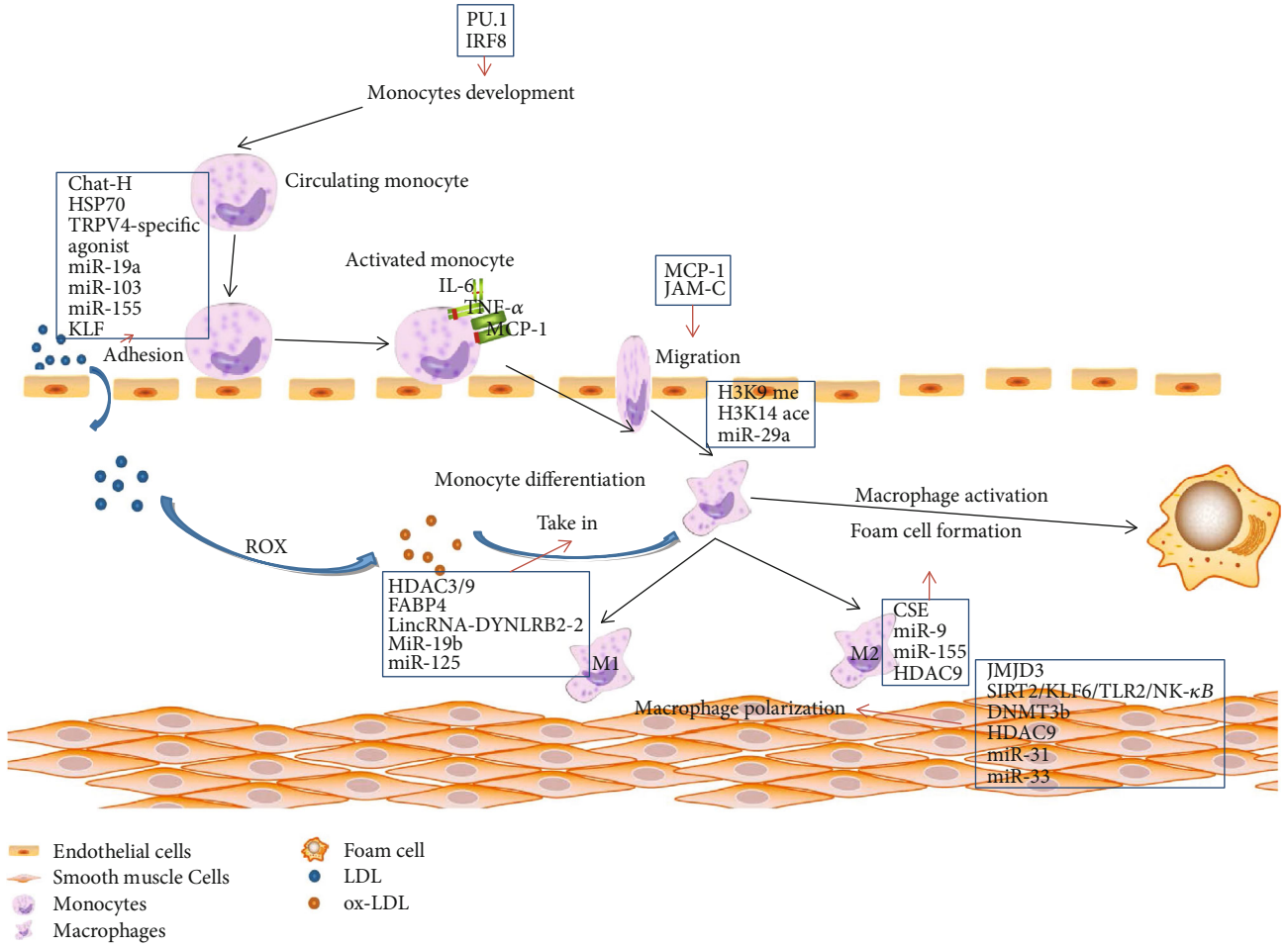

Figure 1: Illustration of monocyte and macrophage in AS. After recruited to endothelial cells, the active monocytes oversecrete IL-6, MCP-1, and TNF-α and subsequently differentiate into macrophages. Macrophages are polarized into two types: M1 and M2. Once macrophages uptake the ox-LDL and cholesterol, foam cells are formed and induced atherosclerotic progression. Reproduced with permission from [3], copyright 2017 Wiley.

2. Macrophages in AS

2.1. Macrophages in the Early Stage. In the early stage of AS, low-density lipoprotein (LDL) accumulates in the intima of blood vessels, activating the endothelium to express leukocyte adhesion molecules and chemokines and promoting the recruitment of monocytes and T cells [8, 9]. The macrophage colony-stimulating factor (M-CSF) and other differentiation factors accelerate differentiation of monocytes into macrophages, which upregulate pattern recognition receptors (PRRs), including toll-like receptors (TLRs) and scavenger receptors (SRs) [10]. The activation of the TLR pathway leads to an inflammatory response, while the SR pathway regulates the oxidized low-density lipoprotein (ox-LDL) resulting in foam cell formation. During the early stage of inflammation in the AS process, activated monocytes and lymphocytes absorb ox-LDL by SRs and promote foam cell transformation, and interaction with foam cell and accumulation of various factors contribute to the pathogenesis of atherosclerosis [11], while reduction in foam cell formation or ox-LDL uptake was verified to reduce the atherosclerotic plaque burden [12, 13]. ATP-binding cassette (ABC) transporters expressed by macrophages are involved in cholesterol reversal and reducing plasma cholesterol level [14]. ABCA1 and ABCG1 transporters reverse cholesterol transport and generate HDL, which affect the atherosclerotic progression. The genes encoding ABCA1 and ABCG1 are transcriptionally upregulated in response to the elevated cellular cholesterol levels [15], especially in the early stage. It had been shown that ABCA1 and ABCG1 gene knockout mice led to a large amount of lipid accumulation and foam cell formation in macrophages [16]. Furthermore, ABCA1 and ABCG1 are related to cell apoptosis and release of inflammatory factors. Studies showed that macrophages express high levels of ABCG1 and the multiple inflammatory genes in macrophages, which is consistent with the intracellular accumulation of multiple factors and promoted the progress of AS [16]. Deficiency of ABCA1 or ABCG1 in mice increased the apoptosis in macrophages and the inflammation in plaque, while apoptosis of macrophages in ABCA1- and ABCG1-deficient mice was increased, but the atherosclerotic progression was inhibited [17]. ABCA1 and ABCG1, as the cholesterol efflux transports, promote cholesterol efflux from cells by transporting phospholipids and

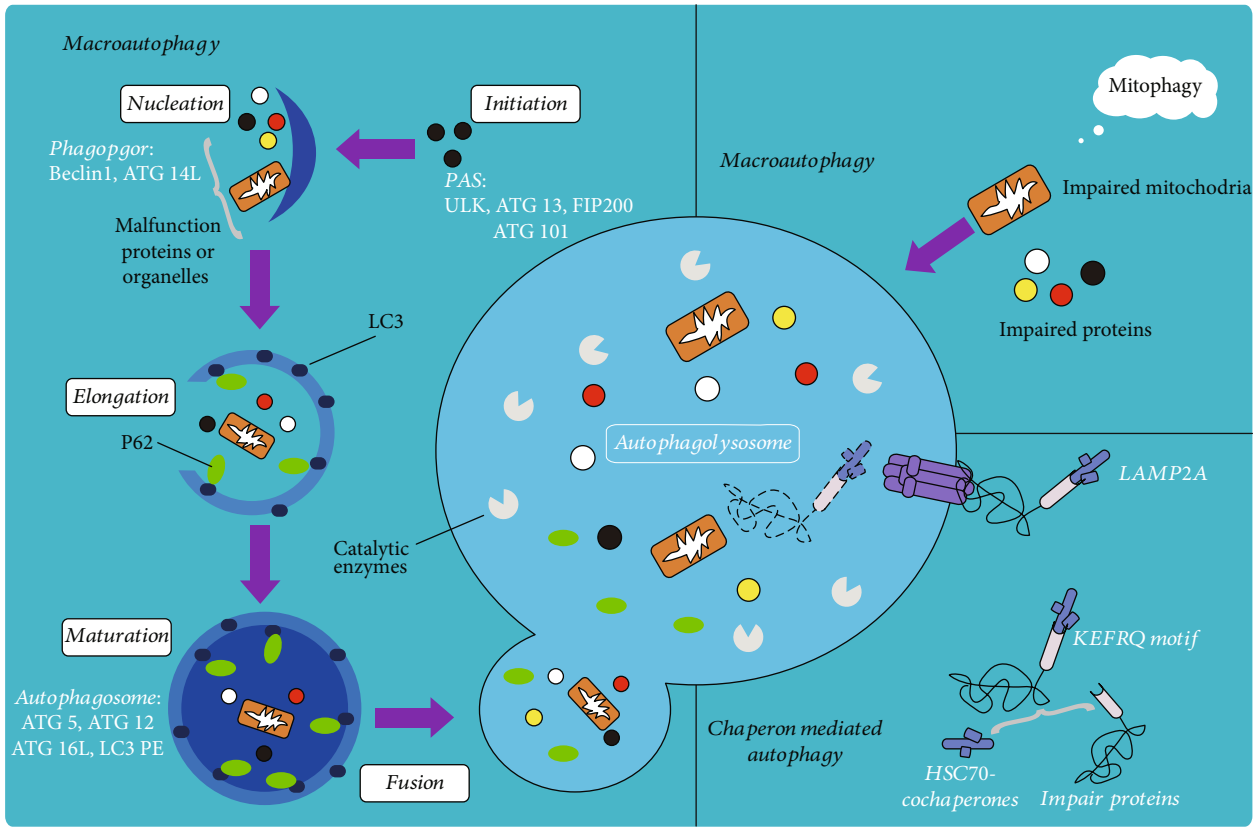

Figure 2: Illustration of macrophage autophagy in different routes. Reproduced with permission from [29], copyright 2019 Springer.

cholesterol to high-density lipoprotein or free apolipoprotein A-I [18]. Therefore, ABCA1 deficiency and ABCG1 deficiency will cause inflammatory activation of macrophages leading to AS pathological deterioration [19].

2.2. Macrophages in the Progression Stage. Macrophages play an important role in promoting plaque formation, diluting fibrous cap and necrotic core components, which leads to the increased inflammatory response and apoptotic signals of smooth muscle cells (SMCs) and leukocytes in atherosclerotic plaques [20, 21]. Moreover, macrophages reduce the amount of intimal fibroblast-like SMCs and degrade the collagen by oversecreting matrix metalloproteinase (MMP). In the site of vascular injury, macrophage apoptosis and phagocytic clearance of apoptotic cells resulted in increased necrotic core and decreased plaque stability [8, 22]. The rupture site of plaque is almost always located near the necrotic core of plaque, which is related to the diluent fiber cap. Thus, the strength of the fiber cap is an important indicator to determine the stability of plaque for the potential risk evaluation of plaque rupture [23]. Mhem, a nonfoam protective macrophage, stabilized plaque by reducing foam cell formation and enhancing anti-inflammation and tissue regeneration at the advanced stage of AS [24]. Mox, a macrophage induced by phospholipid oxide, also has a potential to be used for AS protection [7]. Mox macrophages, rich in advanced mouse lesions, play an atheroprotective role because the low-density lipoprotein receptor–deficient mice would emerge with accelerated atherogenesis which results from myeloid deficiency of Nrf2 [25]. Additionally, some inflammatory genes have upregulated expression in Mox macrophages in keeping with macrophages which respond to oxidized phospholipids by upregulation of inflammatory gene expression in wild-type mice [26].

3. Macrophage-Based Therapy Strategies

3.1. Inducing Macrophage Autophagy. Autophagy is a major catabolic process, which functions in the maintenance of the cellular homeostasis in eukaryotic cells (Figure 2). It is activated under stress conditions such as nutrient deprivation, hypoxia, oxidative stress, and DNA damage [27, 28]. Further, autophagy may lead to the occurrence and development of various diseases, including malignant tumors, neurodegenerative diseases, cardiovascular diseases, and immune system disorders; thus, autophagy may be served as a potential strategy for the treatment of AS [27, 28].

Autophagy is a catabolic cellular process that degrades misfolded and dysfunctional proteins, cytoplasmic components, and organelles [28]. The formation of atherosclerotic plaque is enhanced in the mice lacking the key autophagy-related gene5 (ATG5). The abundant increase of autophagy chaperone p62 is a nonautophagic protective response to AS, suggesting that the autophagy of macrophages and its related regulators play an important role in AS [30]. During the whole process of autophagy, many genes related to autophagy are involved in regulation [31, 32]. mTOR is a highly conserved serine/threonine protein kinase that acts

as a growth factor, a central sensor of cellular nutrition and energy state, and the core of autophagy regulation. mTOR exists in two different complexes, TORC1 and TORC2, which can integrate multiple signals from upstream pathways, inhibit ATG1(ULK1), and block the formation of autophagosomes [33]. mTORC1 inhibits autophagy by integrating upstream signals through the class I PI3K-PKB (also known as Akt) pathway when adequate nutrients are present. Under other stimuli, such as starvation and inflammatory oxidation, the activated class III PI3K-Beclin1 complex and the inactivated Beclin1/Bcl-2 complex are capable of inducing autophagy by promoting the assembly of ATG12-ATG5-ATG16L complex and ATG8/LC3. AMP-activated protein kinase (AMPK) inhibits mTORC1 activity and acts as a positive regulator of autophagy [32, 34]. Basal autophagy protects cells from environmental stimuli, while excessive autophagy leads to cell death and plaque instability, which is important for controlling the progression of AS. Inhibition of autophagy by silencing ATG5 or other autophagy mediators enhances the reductive coenzyme II oxidase-mediated oxidative stress and promotes the plaque necrosis and the deterioration of foam cells [35].

Nod-like receptor protein (NLRP3) inflammasome is closely related to the autophagy of AS and can be activated by the cholesterol crystals in plaques to promote the secretion of IL-1β, thus accelerating the development of AS [36]. Further, autophagy plays various roles in negatively regulating the activation of inflammasome, such as removing inflammasome-activating endogenous signals and isolating and degrading inflammasome components [37]. Autophagy removes the damaged mitochondria, reduces reactive oxygen species (ROS) production under stress, inhibits the activation of NLRP3, and even regulates NLRP3 activity by capturing and degrading the assembly of inflammasome complexes through the corresponding ubiquitination [38]. Furthermore, autophagy-induced mTOR inhibitors or AMPK activators reduce the inflammatory response to inhibit the development of AS plaques [39]. Shi et al. found that macrophage autophagy was enhanced and IL-1β secretion was reduced upon the starvation and mTOR inhibitor rapamycin treatment [40]. The PI3K/Akt/mTOR signaling pathway was blocked, while autophagy in macrophages was activated upon the rapamycin and mTOR-siRNA treatment in the rabbit model, which significantly inhibited the inflammatory response and enhanced the stability of plaques [41].

Autophagy inducers have been identified as an efficient and promising treatment for AS. Everolimus, a derivative of rapamycin and an inhibitor of mTOR, showed a significant therapeutic effect on malignancies including breast cancer and renal cell carcinoma [42]. Hsu et al. reported that the mRNA levels of autophagy were significantly increased and secreted protein expression was decreased by everolimus [43]. The results suggested that everolimus has great potential to inhibit AS by diminishing viability of foam cells, decreasing matrix degradation, and reducing the secretion of proinflammatory cytokine [43]. Resveratrol, a plant-derived polyphenolic compound, induces autophagy by inhibiting mTOR [42], which plays an important role in anti-AS and vasodilation [44]. Liu et al. reported that resveratrol could promote its cellular burial effect on ox-LDL-induced apoptotic RAW264.7 cells by activating Sirt1-mediated autophagy [45].

MicroRNAs (miRNA) regulate the autophagy through posttranscriptional repression of autophagy-related gene or upstream effectors [46, 47]. Therefore, miRNA regulation using miRNA inhibitors might be a potential therapeutic strategy for AS. Ouimet et al. identified miR-33 as a key post-transcriptional regulator of genes involved in cholesterol and fatty acid homeostasis [46]. They found that miR-33 inhibited apoptotic cell clearance via an autophagy-dependent mechanism, and macrophages treated with anti-miR-33 increased the efferocytosis, lysosomal biogenesis, and degradation of apoptotic cells [46].

Catechins (EGCG) activate autophagy by activating macrophages PI3K III. The anti-AS effect of berberine may also involve the activation of the AMPK/mTOR signaling pathway to induce autophagy and inhibit macrophage inflammatory response [48]. Berberine-induced autophagy inhibits cell inflammation induced by ox-LDL. Simvastatin can enhance macrophage autophagy induced by ox-LDL and reduce lipid aggregation and AS formation [49]. Ursolic acid, as a natural pentacyclic triterpenoid carboxylic acid, has the anti-AS potential to effectively enhance autophagy of macrophages and promote the cholesterol outflow of macrophages [49]. The anti-inflammatory effect is also related to the inactivation of the Akt/mTOR pathway and the inhibition of the secretion of IL-1β induced by lipopolysaccharide. Therefore, induction of macrophage autophagy can be a potential therapeutic strategy for AS [50].

3.2. Inducing Macrophage Polarization. Macrophages after activation included two main phenotypes: M1 type and M2 type. Subtype differentiation and related dysfunction of macrophages are the key steps to determine plaque progression and stability. Although both the M1 and M2 subtypes appear at the sclerotic lesion site, they show an opposite effect [21, 51]. Previous studies demonstrated that miRNA-216a activates telomerase, induces M1-type differentiation and aging, and promotes macrophage lipid uptake capacity and foam cell formation, thus accelerating the progression of atherosclerotic plaques [52, 53]. M1 macrophages respond to TLR and interferon-γ signaling, which can be induced by pathogen-associated molecular complexes (PAMP), lipopolysaccharide (LPS), and lipoproteins [54]. This type of macrophage can secrete proinflammatory cytokines such as tumor necrosis factor (TNF-α), interleukin-1β (IL-1β), IL-12, and IL-23 and the chemokines CXCL9, CXCL10, and CXCL11. High levels of ROS and nitric oxide (NO) can also be induced by proinflammatory macrophages, which contribute to further development of inflammatory responses [55, 56]. M2 macrophages with anti-inflammatory properties respond to Th2 cytokines IL-4 and IL-13 and secrete anti-inflammatory factors (such as IL-1 and IL-10 receptor agonists) [57]. M1 macrophages are accumulated in progressive plaques, while M2 in degenerative plaques contributing to tissue repair and remodeling. M1- and M2-type macrophages, cells with

proinflammatory and anti-inflammatory functions during the development of AS, were mutually transformed to manage the progress of plaque stability [22].

A key feature of macrophages is the high plasticity in response to various microenvironmental stimuli. Macrophages are actively involved in the immune response for engulfing pathogens and cell debris and secreting proinflammatory factors [58]. However, some macrophages such as M1 type and Mhem play a role in eliminating inflammatory responses and promoting tissue remodeling [59]. The lesion site of AS provides a specific microenvironment, enriched with the activated cells, the modified lipoproteins, the proinflammatory factors, and the apoptotic cells [60]. A large number of proinflammatory M1-type macrophages were found in AS lesions. In addition, the atherosclerotic progression is positively correlated with the increased M1 macrophages; cells with a high expression of proinflammatory markers are preferentially located in the friable shoulder of plaque and the adventitia [61]. After activation of M1 macrophages, expression of inducible nitric oxide synthase (iNOS), CD86, and major histocompatibility complex II (MHC II) was upregulated, and multiple proinflammatory factors including tumor necrosis factor-α (TNF-α), interleukin-1 (IL-1), interleukin-12 (IL-12), and proinflammatory medium NO were secreted [4, 62]. These proinflammatory factors can lead to endothelial injury, promote oxidative stress, enhance apoptosis, and accelerate the calcification rate of necrotic nucleus [63].

Anti-inflammatory M2-type macrophages were identified in the stable plaque areas with small possibility to form foam cells. Therefore, the plaque progression can be reflected by proinflammatory and anti-inflammatory macrophage subtypes [26]. Transcriptome-based network analysis is a powerful modern tool for studying macrophage activation and function, providing a set of data on specific genes involved in different stages of macrophage activation [64]. Macrophage activation was analyzed by examining the changes in macrophage gene transcription induced by 28 different stimuli or combinations of stimuli. The study identified 49 groups of genes with similar transcriptional induction that respond to various stimuli and regulate specific transcription factors that promote macrophage activation [65]. In conclusion, the response of macrophages in different individuals to various stimuli is largely influenced by genetic variation, especially in genomic regulatory elements that coordinate macrophage induction and activation.

In the stage of lesion initiation and progression, macrophage accumulates within the subendothelium or neointima [18]. The presence of apoB lipoproteins and expression of endothelial adhesion molecules contribute to these early macrophages which accumulate in susceptible regions of arteries. In advanced necrotic lesions, macrophage apoptosis is increased and partly induced by lipoproteins or oxidized phospholipids. In the advanced lesion, macrophages could not clear these apoptotic cells, which results in increasing inflammation and plaque necrosis because of release of inflammatory mediators from the residual, postapoptotic necrotic cells. Macrophage autophagy contributes to protecting against lesion necrosis [66]. Lesion regression can be achieved in the hyperlipidemic mice by reducing the aggressive lipid, and that in diabetic mice by normalizing the blood glucose. The regression and resolution in these mice is characterized by altering relative gene expression and reducing lesion macrophage content. However, the operative mechanism in human subjects is as yet to explore [67].

There are some therapies that could be used for the regulation of macrophage phenotype. Anti-inflammatory cytokine secreted by macrophages plays an important role in the occurrence and development of AS. Also, its expression level is closely related to the process of AS [68, 69]. Studies have found that endothelial injury and increased aortic stiffness directly accelerate the process of AS, while anti-TNF-α therapy can reduce aortic stiffness, reduce inflammation, and slow down the process of AS [15]. CD40 and CD40L are expressed in macrophages, ECs, VSMCs, and other cells associated with AS lesions, and the CD40/CD40L system may be a biomarker for clinical evaluation of AS stability [70]. Regulation of miRNA has become a research hotspot in recent years; because of the important role of miRNA in cardiovascular and cerebrovascular diseases, it can be expected that miRNA may become a promising biomarker for clinical diagnosis or even a drug therapeutic target [71]. Therefore, studying the role of macrophages and related biological macromolecules in the development of atherosclerosis is of great significance for the in-depth understanding of the etiology and pathogenesis of atherosclerosis, as well as for its diagnosis, treatment, and drug development.

3.3. Macrophages for Targeted Delivery. In addition to the stability of cellular structure, the surface glycoproteins of macrophages play a crucial role in homing function to achieve targeted delivery to AS lesions. Studies have shown that about 45.8% known proteins on the surface of macrophages are membrane proteins annotated by the gene ontology with different functions, such as CD11b, CD14, CD18, CD40, CD86, CD44, and CD16 [21, 72, 73]. For example, the interaction between CD40 and soluble CD40 ligands regulates the expression of cytokines, chemokines, adhesion molecules, and growth factors and promotes the inflammation and immune response, inducing the atherosclerotic plaque development and vulnerability. In addition, C-reactive protein promotes the expression of VCAM-1, ICAM-1, e-selectin, and monocyte chemoattractant protein-1 and promotes inflammation, which is an important inflammatory marker in atherosclerotic progression [4, 6, 21, 74].

These membrane surface proteins can be used for the design of targeted drug delivery systems to macrophages. Yu et al. designed a pH-responsive polymeric micelle with further mannose modification to achieve CD206 (mannose receptor)-targeted siRNA delivery [75]. The mannosylated nanoparticles improve the delivery of siRNA into primary macrophages by 4-fold relative to the delivery of a nontargeted version of the same carrier [75]. Scavenger receptors (SRs) expressed in the activated macrophages are considered to be the most promising target biomarkers for targeted drug

delivery [76–78]. Lewis et al. reported that glycosylated micelles competitively block macrophages SRs of MSR1 and CD36 to reduce the assimilation and accumulation of ox-LDL [79]. Small-molecule folate-targeted conjugates were found to specifically bind to the folate receptor-expressing macrophages *in vitro* and selectively accumulate at sites of inflammation *in vivo* [80–82]. A PEG-coated, acetic anhydride-capped, folate-targeted poly(amidoamine) (PAMAM) dendrimer was designed to deliver more cargo than small-molecule conjugates [82].

High-density lipoprotein (HDL) is an important plasma lipoprotein in the lipid transport system, which possesses several antiatherogenic functions including reverse cholesterol transport (RCT) and anti-inflammatory, antioxidant, and vascular protective properties [83–85]. Zhao et al. designed an atorvastatin calcium- (AT-) loaded dextran sulfate- (DXS-) coated core-shell reconstituted HDL (rHDL) [86]. Through the high affinity between DXS and scavenge receptor class AI (SR-AI), it was developed for the targeted drug delivery to macrophages and displayed biofunction of inhibiting ox-LDL uptake and promoting cholesterol efflux [86].

3.4. Macrophages for Triggering Cargo Release. More than 20% of cells are composed of macrophages in the well-known atherosclerotic lesions. Excessive ROS released by the active macrophages leads to oxidative/antioxidative imbalance [87]. The ROS may affect the conversion of LDL into ox-LDL, promoting the SMC death and accelerating the AS process [9, 21, 87]. Therefore, the excessive ROS might be a desirable target for triggering theranostic release in AS. Kim et al. designed a macrophage-targeted theranostic nanoparticle by coupling a photosensitizer with chlorin e6 hyaluronic acid [88]. The obtained nanoparticle MacTNP can be activated and emit near-infrared fluorescence by ROS in macrophage cells, which has great potential in selective NIR fluorescence imaging [88].

3.5. Macrophage- or Macrophage Membrane-Based Carrier. Compared with freely drug administration, carrier-mediated targeted drug delivery has been successfully used for the systemic delivery of a variety of antiatherogenic drugs with an enhancement in therapeutic efficacy and a reduction in side effects. However, carrier clearance by the immune system before reaching the targeted lesion is one of the major obstacles to efficient drug delivery due to the rigorous delivery demands *in vivo* [89, 90]. Besides, the biocompatibility and safety of artificially synthesized nanoparticles are much lower than those of natural materials. Further, the intrinsic sophisticated biofunctions of natural substances are difficult to construct due to their exceptional complex structures. Cell membrane coating carriers or cells have emerged as a promising therapeutic platform to evade the undesirable clearance through the biomimetic camouflage [91, 92]. Thus, cell- or cell membrane-based drug carriers have unique advantages in target activity, which significantly improve the bioavailability and reduce the side effects [93, 94]. A variety of chemokines in AS can be specifically recognized by macrophage to realize targeted therapy, termed macrophage homing. Thus, the macrophage membrane has been used to build a biomimetic drug delivery system for targeting AS with a good potential for accurate treatment of lesions, which provides the possibility for the macrophage cell membrane-based drug carrier with AS homing functions [95, 96]. In order to combine the reconfigurability of nanoparticles with the natural functions of cells, a drug carrier has been creatively combined with macrophage or macrophage membrane to construct the hybrid biomimetic drug delivery system with the tailorable functions [93, 97, 98]. Besides, the biomimetic carrier has excellent biocompatibility and low immunogenicity.

In the macrophage drug carrier, the drug loads into macrophage mainly by *in vitro* incubation or *in vivo* direct injection. The *in vitro* incubation method is involved in adequately incubating macrophages with drugs *in vitro* and subsequently reinjecting the cargo-loaded macrophage carrier into the body for therapy. The *in vivo* direct injection method refers to a direct injection into the body using the modified specific ligands or drug delivery systems with appropriate particle size to harvest the phagocytic macrophages as therapeutic medicament [99, 100]. Development of the macrophage targeting can enhance the targeted cargo (diagnostic imaging and anti-inflammatory drugs) delivery to atherosclerotic lesions for diagnosis and therapy [101, 102]. Martinez et al. demonstrated the ability of rhodamine-labeled lipid films rehydrated with macrophage proteins targeting activated endothelia through CD11a and CD18, which both bind to ICAM-1 [103]. Due to the increased circulation time and homing capabilities, the platform may be loaded with therapeutics with diverse physical properties and hence show promise for use in magnetic resonance imaging applications. Nevertheless, the former method of directly loading drugs into macrophages has some deficiencies in preparation, such as low loading efficiency, premature drug release, and undesirable drug inactivation [61, 104, 105]. Therefore, the macrophage membrane-camouflaged drug carrier has been developed by using the macrophage membrane to further coat the drug carrier on the surface. Due to the surface modification of the macrophage membrane, the macrophage membrane carrier inherits the specific biological functions of the source cells, such as long circulation and AS-relevant homing. This design strategy lays the foundation for the development of the advanced cell membrane-based nanotherapeutics against AS. Based on the high affinity between $\alpha 4\beta 1$ integrin and VCAM-1 in the macrophage membrane, Cheng and Li constructed a biomimetic "core-shell" structured nanoparticle with PLGA "core" and macrophage membrane "shell" to target drug delivery in AS lesions [106]. The results indicated that macrophage membrane-coated PLGA nanoparticle had a strong affinity to the target receptor VCAM-1, which could effectively identify the target cells and target tissues *in vivo*. With the variety of small molecules, biological macromolecules and tracer probe loading, polymeric and inorganic nanoparticles, liposomes, and abundant other bioactive carriers can be coated using the macrophage membrane to enhance the advanced theranostic application in AS (Figure 3).

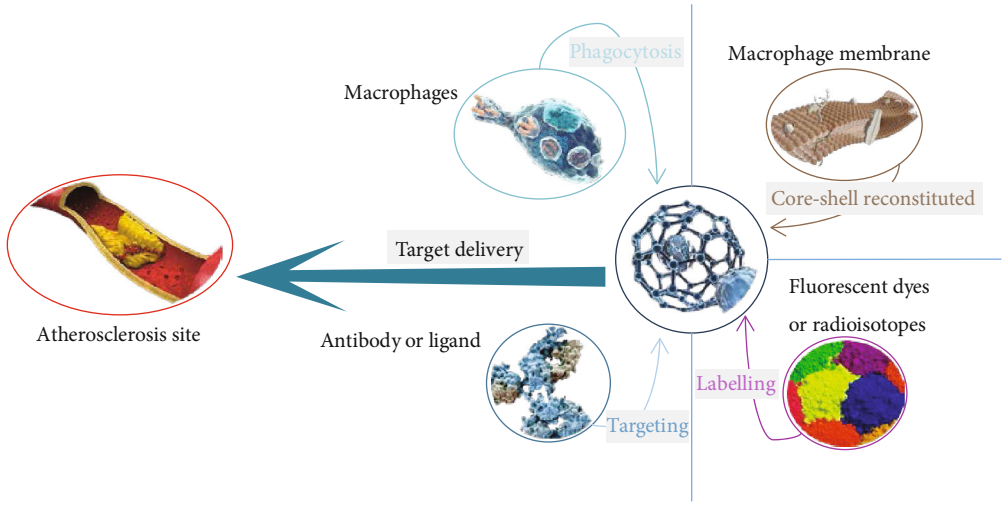

Figure 3: Illustration of functional modifications of the carrier.

4. Conclusion and Perspectives

Due to severe chronic inflammation, an extremely long-term administration has a high requirement for the efficacy and safety of AS treatment. The novel therapies based on the intrinsic cells are beneficial to reduce the undesirable clearance and immune responses. Macrophages play a critical role in the formation and progression of the atherosclerotic lesion. Artificially regulated or modified macrophages have been widely used, including regulating macrophage autophagy, inducing macrophage polarization, enhancing the active target delivery to macrophages, responding to the specific macrophage microenvironment for triggering drug release, and engineering the macrophage- or macrophage membrane-based drug carrier to efficiently manage AS lesion using the biomimetic therapy. In future studies, engineered macrophages with multifunctions will be further identified to self-adapt the atherosclerotic lesion for satisfying the advanced precision and personalized therapy. Therefore, macrophage-based therapy represents a novel platform with considerable potential for effective and safe AS management in future research and clinic translation applications.

Conflicts of Interest

The authors declare no conflict of interest.

Authors' Contributions

Renyi Peng, Hao Ji, and Libo Jin contributed equally to this work. Wei Wu and Da Sun are responsible for the conception and design of the study. Yijiang Huang, Ke Xu, Qinsi Yang, and Sue Lin are assigned to acquire the data and analysis. Wei Wu, Da Sun, Renyi Peng, Hao Ji, and Libo Jin wrote the manuscript. All authors read and approved the final manuscript.

Acknowledgments

This work was supported by the National Natural Science Foundation of China (51901160, 31971301, and 51603023), Natural Science Foundation of Zhejiang Province (LQ19E010004, LQ20C020003, and LQ20C200015), Wenzhou Science and Technology Project (N20170005), Chongqing Research Program of Basic Research and Frontier Technology (cstc2017jcyjAX0186), and Fundamental Research Funds for the Central Universities (2018CDHB1B08). We are grateful for the free usage of reproduced figures (Figure 1 from *Cardiovascular Therapeutics* of Wiley and Figure 2 from *Journal of Inflammation* of Springer).

References

[1] K. Medha, E. B. Kheireddine, D. C. Zhu et al., "Hyaluronic acid immobilized magnetic nanoparticles for active targeting and imaging of macrophages," *Bioconjugate Chemistry*, vol. 21, pp. 2128–2135, 2010.

[2] I. Sergin and B. Razani, "Self-eating in the plaque: what macrophage autophagy reveals about atherosclerosis," *Trends in Endocrinology & Metabolism*, vol. 25, no. 5, pp. 225–234, 2014.

[3] S. J. Jia, K. Q. Gao, and M. Zhao, "Epigenetic regulation in monocyte/macrophage: a key player during atherosclerosis," *Cardiovascular Therapeutics*, vol. 35, no. 3, article e12262, 2017.

[4] K. J. Moore and I. Tabas, "Macrophages in the pathogenesis of atherosclerosis," *Cell*, vol. 145, no. 3, pp. 341–355, 2011.

[5] A. Remmerie and C. L. Scott, "Macrophages and lipid metabolism," *Cellular Immunology*, vol. 330, pp. 27–42, 2018.

[6] A. J. Petty, A. Li, X. Wang et al., "Hedgehog signaling promotes tumor-associated macrophage polarization to suppress intratumoral $CD8^+$ T cell recruitment," *The Journal of Clinical Investigation*, vol. 129, no. 12, pp. 5151–5162, 2019.

[7] P. K. Shah, "Inflammation, infection and atherosclerosis," *Trends in Cardiovascular Medicine*, vol. 29, no. 8, pp. 468–472, 2019.

[8] X. F. Wei, X. X. Zhao, Q. Q. Wu et al., "Human amnion mesenchymal stem cells attenuate atherosclerosis by modulating macrophage function to reduce immune response," *International Journal of Molecular Medicine*, vol. 44, no. 4, pp. 1425–1435, 2019.

[9] A. R. Silva, P. Pacheco, A. Vieira-de-Abreu et al., "Lipid bodies in oxidized LDL-induced foam cells are leukotriene-synthesizing organelles: a MCP-1/CCL2 regulated phenomenon," *Biochimica et Biophysica Acta (BBA) - Molecular and Cell Biology of Lipids*, vol. 1791, no. 11, pp. 1066–1075, 2009.

[10] R. K. Singh, A. S. Haka, A. Asmal et al., "TLR4 (toll-like receptor 4)-dependent signaling drives extracellular catabolism of LDL (low-density lipoprotein) aggregates," *Arteriosclerosis, Thrombosis, and Vascular Biology*, vol. 40, no. 1, pp. 86–102, 2020.

[11] H. Kishikawa, S. Mine, C. Kawahara et al., "Glycated albumin and cross-linking of CD44 induce scavenger receptor expression and uptake of oxidized LDL in human monocytes," *Biochemical and Biophysical Research Communications*, vol. 339, no. 3, pp. 846–851, 2006.

[12] K. M. Patel, A. Strong, J. Tohyama et al., "Macrophage sortilin promotes LDL uptake, foam cell formation, and atherosclerosis," *Circulation Research*, vol. 116, no. 5, pp. 789–796, 2015.

[13] H. Cao, Q. Jia, L. Yan, C. Chen, S. Xing, and D. Shen, "Quercetin suppresses the progression of atherosclerosis by regulating MST1-mediated autophagy in ox-LDL-induced RAW264.7 macrophage foam cells," *International Journal of Molecular Sciences*, vol. 20, no. 23, article 6093, 2019.

[14] Y. Azuma, M. Takada, M. Maeda, N. Kioka, and K. Ueda, "The COP9 signalosome controls ubiquitinylation of ABCA1," *Biochemical and Biophysical Research Communications*, vol. 382, no. 1, pp. 145–148, 2009.

[15] K. J. Moore, F. J. Sheedy, and E. A. Fisher, "Macrophages in atherosclerosis: a dynamic balance," *Nature Reviews Immunology*, vol. 13, no. 10, pp. 709–721, 2013.

[16] M. Westerterp, K. Tsuchiya, I. W. Tattersall et al., "Deficiency of ATP-binding cassette transporters A1 and G1 in endothelial cells accelerates atherosclerosis in mice," *Arteriosclerosis, Thrombosis, and Vascular Biology*, vol. 36, no. 7, pp. 1328–1337, 2016.

[17] E. J. Tarling, D. D. Bojanic, R. K. Tangirala et al., "Impaired development of atherosclerosis in *Abcg1*$^{-/-}$ *Apoe*$^{-/-}$ mice: identification of specific oxysterols that both accumulate in *Abcg1*$^{-/-}$ *Apoe*$^{-/-}$ tissues and induce apoptosis," *Arteriosclerosis, Thrombosis, and Vascular Biology*, vol. 30, no. 6, pp. 1174–1180, 2010.

[18] I. Tabas and K. E. Bornfeldt, "Macrophage phenotype and function in different stages of atherosclerosis," *Circulation Research*, vol. 118, no. 4, pp. 653–667, 2016.

[19] M. Westerterp, A. J. Murphy, M. Wang et al., "Deficiency of ATP-binding cassette transporters A1 and G1 in macrophages increases inflammation and accelerates atherosclerosis in mice," *Circulation Research*, vol. 112, no. 11, pp. 1456–1465, 2013.

[20] H. Huang, H. Feng, and D. Zhuge, "M1 macrophage activated by notch signal pathway contributed to ventilator-induced lung injury in chronic obstructive pulmonary disease model," *The Journal of Surgical Research*, vol. 244, pp. 358–367, 2019.

[21] C. Kelly, C. Jefferies, and S.-A. Cryan, "Targeted liposomal drug delivery to monocytes and macrophages," *Journal of Drug Delivery*, vol. 2011, Article ID 727241, 11 pages, 2011.

[22] X. Li, P. Fang, W. Y. Yang, H. Wang, and X. Yang, "IL-35, as a newly proposed homeostasis-associated molecular pattern, plays three major functions including anti-inflammatory initiator, effector, and blocker in cardiovascular diseases," *Cytokine*, vol. 122, article 154076, 2019.

[23] A. Singhal and M. Subramanian, "Colony stimulating factors (CSFs): complex roles in atherosclerosis," *Cytokine*, vol. 122, article 154190, 2019.

[24] A. Paul, B. H. Chang, L. Li, V. K. Yechoor, and L. Chan, "Deficiency of adipose differentiation-related protein impairs foam cell formation and protects against atherosclerosis," *Circulation Research*, vol. 102, no. 12, pp. 1492–1501, 2008.

[25] H. Jinnouchi, L. Guo, A. Sakamoto et al., "Diversity of macrophage phenotypes and responses in atherosclerosis," *Cellular and Molecular Life Sciences*, vol. 76, no. 1, pp. 1–4, 2019.

[26] M. Kim, A. Sahu, Y. Hwang et al., "Targeted delivery of anti-inflammatory cytokine by nanocarrier reduces atherosclerosis in Apo E$^{-/-}$ mice," *Biomaterials*, vol. 226, article 119550, 2020.

[27] D. C. Rubinsztein, C. Patrice, and L. Beth, "Autophagy modulation as a potential therapeutic target for diverse diseases," *Nature Reviews Drug Discovery*, vol. 11, no. 9, pp. 709–730, 2012.

[28] B. Z. Shao, B. Z. Han, Y. X. Zeng, D. F. Su, and C. Liu, "The roles of macrophage autophagy in atherosclerosis," *Acta Pharmacologica Sinica*, vol. 37, no. 2, pp. 150–156, 2016.

[29] M. Hassanpour, R. Rahbarghazi, M. Nouri, N. Aghamohammadzadeh, N. Safaei, and M. Ahmadi, "Role of autophagy in atherosclerosis: foe or friend?," *Journal of Inflammation*, vol. 16, no. 1, p. 8, 2019.

[30] I. Sergin, S. Bhattacharya, R. Emanuel et al., "Inclusion bodies enriched for p62 and polyubiquitinated proteins in macrophages protect against atherosclerosis," *Science Signaling*, vol. 9, no. 409, article ra2, 2016.

[31] W. A. Boisvert, D. M. Rose, A. Boullier et al., "Leukocyte transglutaminase 2 expression limits atherosclerotic lesion size," *Arteriosclerosis, Thrombosis, and Vascular Biology*, vol. 26, no. 3, pp. 563–569, 2006.

[32] Y. Tang, H. Wu, B. Shao, Y. Wang, C. Liu, and M. Guo, "Celosins inhibit atherosclerosis in ApoE$^{-/-}$ mice and promote autophagy flow," *Journal of Ethnopharmacology*, vol. 215, pp. 74–82, 2018.

[33] H. Zheng, Y. Fu, Y. Huang, X. Zheng, W. Yu, and W. Wang, "mTOR signaling promotes foam cell formation and inhibits foam cell egress through suppressing the SIRT1 signaling pathway," *Molecular Medicine Reports*, vol. 16, no. 3, pp. 3315–3323, 2017.

[34] A. Kurdi, G. R. Y. De Meyer, and W. Martinet, "Potential therapeutic effects of mTOR inhibition in atherosclerosis," *British Journal of Clinical Pharmacology*, vol. 82, no. 5, pp. 1267–1279, 2016.

[35] B. Razani, C. Feng, T. Coleman et al., "Autophagy links inflammasomes to atherosclerotic progression," *Cell Metabolism*, vol. 15, no. 4, pp. 534–544, 2012.

[36] J. Harris, T. Lang, J. P. W. Thomas, M. B. Sukkar, N. R. Nabar, and J. H. Kehrl, "Autophagy and inflammasomes," *Molecular Immunology*, vol. 86, pp. 10–15, 2017.

[37] Y. S. Shim, J. W. Baek, M. J. Kang, Y. J. Oh, S. Yang, and I. T. Hwang, "Reference values for the triglyceride to high-density lipoprotein cholesterol ratio and non-high-density lipoprotein cholesterol in Korean children and adolescents: the Korean National Health and Nutrition Examination Surveys 2007-2013," *Journal and Atherosclerosis Thrombosis*, vol. 23, no. 12, pp. 1334–1344, 2016.

[38] T. Karasawa and M. Takahashi, "The crystal-induced activation of NLRP3 inflammasomes in atherosclerosis," *Inflammation and Regeneration*, vol. 37, no. 1, article 18, 2017.

[39] K. Drareni, J. F. Gautier, N. Venteclef, and F. Alzaid, "Transcriptional control of macrophage polarisation in type 2 diabetes," *Seminars in Immunopathology*, vol. 41, no. 4, pp. 515–529, 2019.

[40] C. S. Shi, K. Shenderov, N. N. Huang et al., "Activation of autophagy by inflammatory signals limits IL-1β production by targeting ubiquitinated inflammasomes for destruction," *Nature Immunology*, vol. 13, no. 3, pp. 255–263, 2012.

[41] J. Che, B. Liang, Y. Zhang, Y. Wang, J. Tang, and G. Shi, "Kaempferol alleviates ox-LDL-induced apoptosis by upregulation of autophagy via inhibiting PI3K/Akt/mTOR pathway in human endothelial cells," *Cardiovascular Pathology*, vol. 31, pp. 57–62, 2017.

[42] W. Martinet, H. De Loof, and G. R. Y. De Meyer, "mTOR inhibition: a promising strategy for stabilization of atherosclerotic plaques," *Atherosclerosis*, vol. 233, no. 2, pp. 601–607, 2014.

[43] S. Hsu, E. Koren, Y. Chan et al., "Effects of everolimus on macrophage-derived foam cell behavior," *Cardiovascular revascularization medicine: including molecular interventions*, vol. 15, no. 5, pp. 269–277, 2014.

[44] Y. Zhang, X. Cao, W. Zhu et al., "Resveratrol enhances autophagic flux and promotes ox-LDL degradation in huvecs via upregulation of SIRT1," *Oxidative Medicine and Cellular Longevity*, vol. 2016, Article ID 7589813, 13 pages, 2016.

[45] B. Liu, B. Zhang, R. Guo, S. Li, and Y. Xu, "Enhancement in efferocytosis of oxidized low-density lipoprotein-induced apoptotic RAW264.7 cells through Sirt1-mediated autophagy," *International Journal of Molecular Medicine*, vol. 33, no. 3, pp. 523–533, 2014.

[46] M. Ouimet, H. Ediriweera, M. S. Afonso et al., "microRNA-33 regulates macrophage autophagy in atherosclerosis," *Arteriosclerosis, Thrombosis, and Vascular Biology*, vol. 37, no. 6, pp. 1058–1067, 2017.

[47] S. K. Gupta and T. Thum, "Non-coding RNAs as orchestrators of autophagic processes," *Journal of Molecular and Cellular Cardiology*, vol. 95, pp. 26–30, 2016.

[48] Y. Hu, Y. Tao, and J. Hu, "Cannabinoid receptor 2 deletion deteriorates myocardial infarction through the downregulation of AMPK-mTOR-p70S6K signaling-mediated autophagy," *Bioscience Reports*, vol. 39, no. 4, 2019.

[49] B. Huang, M. Jin, H. Yan et al., "Simvastatin enhances oxidized-low density lipoprotein-induced macrophage autophagy and attenuates lipid aggregation," *Molecular Medicine Reports*, vol. 11, no. 2, pp. 1093–1098, 2015.

[50] S. Gao, L. Xu, Y. Zhang et al., "Salusin-α inhibits proliferation and migration of vascular smooth muscle cell via Akt/mTOR signaling," *Cellular Physiology Biochemistry*, vol. 50, no. 5, pp. 1740–1753, 2018.

[51] X. Jian, Y. Liu, Z. Zhao, L. Zhao, D. Wang, and Q. Liu, "The role of traditional Chinese medicine in the treatment of atherosclerosis through the regulation of macrophage activity," *Biomedicine & Pharmacotherapy*, vol. 118, article 109375, 2019.

[52] M. A. Hoeksema, J. L. Stoger, and M. P. de Winther, "Molecular pathways regulating macrophage polarization: implications for atherosclerosis," *Current Atherosclerosis Reports*, vol. 14, no. 3, pp. 254–263, 2012.

[53] X. Niu and G. S. Schulert, "Functional regulation of macrophage phenotypes by microRNAs in inflammatory arthritis," *Frontiers in Immunology*, vol. 10, p. 2217, 2019.

[54] K. Kapp, B. Volz, D. Oswald, B. Wittig, M. Baumann, and M. Schmidt, "Beneficial modulation of the tumor microenvironment and generation of anti-tumor responses by TLR9 agonist lefitolimod alone and in combination with checkpoint inhibitors," *Oncoimmunology*, vol. 8, no. 12, article e1659096, 2019.

[55] W. F. Eik, S. S. Marcon, T. Krupek et al., "Blood levels of pro-inflammatory and anti-inflammatory cytokines during an oral glucose tolerance test in patients with symptoms suggesting reactive hypoglycemia," *Brazilian Journal of Medical Biological Research*, vol. 49, no. 8, article e5195, 2016.

[56] H. L. Hongrui Guo, Z. Jian, H. Cui et al., "Nickel induces inflammatory activation via NF-κB, MAPKs, IRF3 and NLRP3 inflammasome signaling pathways in macrophages," *Aging*, vol. 11, no. 23, pp. 11659–11672, 2019.

[57] C. Porta, M. Rimoldi, G. Raes et al., "Tolerance and M2 (alternative) macrophage polarization are related processes orchestrated by p50 nuclear factor kappaB," *Proceedings of the National Academy of Sciences of the United States of America*, vol. 106, no. 35, pp. 14978–14983, 2009.

[58] G. Natoli and S. Monticelli, "Macrophage activation: glancing into diversity," *Immunity*, vol. 40, no. 2, pp. 175–177, 2014.

[59] M. Dall'Asta, E. Derlindati, D. Ardigo, I. Zavaroni, F. Brighenti, and D. Del Rio, "Macrophage polarization: the answer to the diet/inflammation conundrum?," *Nutrition Metabolism and Cardiovascular Diseases*, vol. 22, no. 5, pp. 387–392, 2012.

[60] D. Shiraishi, Y. Fujiwara, Y. Komohara, H. Mizuta, and M. Takeya, "Glucagon-like peptide-1 (GLP-1) induces M2 polarization of human macrophages via STAT3 activation," *Biochemical and Biophysical Research Communications*, vol. 425, no. 2, pp. 304–308, 2012.

[61] C. Cochain and A. Zernecke, "Macrophages and immune cells in atherosclerosis: recent advances and novel concepts," *Basic Research in Cardiology*, vol. 110, no. 4, p. 34, 2015.

[62] M. Kaplan, A. Shur, and Y. Tendler, "M1 macrophages but not M2 macrophages are characterized by upregulation of CRP expression via activation of NFκB: a possible role for ox-LDL in macrophage polarization," *Inflammation*, vol. 41, no. 4, pp. 1477–1487, 2018.

[63] M. O. J. Grootaert, M. Moulis, L. Roth et al., "Vascular smooth muscle cell death, autophagy and senescence in atherosclerosis," *Cardiovascular Research*, vol. 114, no. 4, pp. 622–634, 2018.

[64] S. McArdle, K. Buscher, Y. Ghosheh et al., "Migratory and dancing macrophage subsets in atherosclerotic lesions," *Circulation Research*, vol. 125, no. 12, pp. 1038–1051, 2019.

[65] R. Ostuni, V. Piccolo, I. Barozzi et al., "Latent enhancers activated by stimulation in differentiated cells," *Cell*, vol. 152, no. 1-2, pp. 157–171, 2013.

[66] K. S. Moulton, K. Vakili, D. Zurakowski et al., "Inhibition of plaque neovascularization reduces macrophage accumulation and progression of advanced atherosclerosis," *Proceedings of the National Academy of Sciences of the United States of America*, vol. 100, no. 8, pp. 4736–4741, 2003.

[67] P. R. Nagareddy, A. J. Murphy, R. A. Stirzaker et al., "Hyperglycemia promotes myelopoiesis and impairs the resolution of atherosclerosis," *Cell Metabolism*, vol. 17, no. 5, pp. 695–708, 2013.

[68] R. Laczko, A. Chang, L. Watanabe et al., "Anti-inflammatory activities of *Waltheria indica extracts* by modulating expression of IL-1B, TNF-α, TNFRII and NF-κB in human macrophages," *Inflammopharmacology*, vol. 27, no. 1, pp. 1–16, 2019.

[69] I. Tabas, "Macrophage death and defective inflammation resolution in atherosclerosis," *Nature Review Immunology*, vol. 10, no. 1, pp. 36–46, 2010.

[70] T. T. P. Seijkens, C. M. van Tiel, P. J. H. Kusters et al., "Targeting CD40-induced TRAF6 signaling in macrophages reduces atherosclerosis," *Journal of American College Cardiology*, vol. 71, no. 5, pp. 527–542, 2018.

[71] L. Zhang, J. Chen, Q. He, Z. Chao, X. Li, and M. Chen, "MicroRNA-217 is involved in the progression of atherosclerosis through regulating inflammatory responses by targeting sirtuin 1," *Molecular Medicine Reports*, vol. 20, no. 4, pp. 3182–3190, 2019.

[72] S. Colin, M. Fanchon, L. Belloy et al., "HDL does not influence the polarization of human monocytes toward an alternative phenotype," *International Journal of Cardiology*, vol. 172, no. 1, pp. 179–184, 2014.

[73] J. Zheng, H. Zhou, Y. Zhao, Q. Lun, B. Liu, and P. Tu, "Triterpenoid-enriched extract of *Ilex kudingcha* inhibits aggregated LDL- induced lipid deposition in macrophages by downregulating low density lipoprotein receptor-related protein 1 (LRP1)," *Journal of Functional Foods*, vol. 18, pp. 643–652, 2015.

[74] S. Kim, W. Kim, D. Woo et al., "TWEAK can induce pro-inflammatory cytokines and matrix metalloproteinase-9 in macrophages," *Circulation Journal*, vol. 68, pp. 396–405, 2004.

[75] S. S. Yu, C. M. Lau, W. J. Barham et al., "Macrophage-specific RNA interference targeting via "click", mannosylated polymeric micelles," *Molecular Pharmaceutics*, vol. 10, no. 3, pp. 975–987, 2013.

[76] T. Shimaoka, N. Kume, M. Minami et al., "Molecular cloning of a novel scavenger receptor for oxidized low density lipoprotein, sr-psox, on macrophages," *Journal of Biological Chemistry*, vol. 275, no. 52, pp. 40663–40666, 2000.

[77] P. Broz, S. M. Benito, C. Saw et al., "Cell targeting by a generic receptor-targeted polymer nanocontainer platform," *Journal of Controlled Release*, vol. 102, no. 2, pp. 475–488, 2005.

[78] B. G. Yi, O. K. Park, M. S. Jeong et al., "*In vitro* photodynamic effects of scavenger receptor targeted- photoactivatable nanoagents on activated macrophages," *International Journal of Biological Macromolecules*, vol. 97, pp. 181–189, 2017.

[79] D. R. Lewis, L. K. Petersen, A. W. York et al., "Sugar-based amphiphilic nanoparticles arrest atherosclerosis in vivo," *Proceedings of the National Academy of Sciences of the United States of America*, vol. 112, no. 9, pp. 2693–2698, 2015.

[80] F. Antohe, L. Radulescu, E. Puchianu, M. D. Kennedy, P. S. Low, and M. Simionescu, "Increased uptake of folate conjugates by activated macrophages in experimental hyperlipemia," *Cell and Tissue Research*, vol. 320, no. 2, pp. 277–285, 2005.

[81] W. Ayala-Lopez, W. Xia, B. Varghese, and P. S. Low, "Imaging of atherosclerosis in apoliprotein e knockout mice: targeting of a folate-conjugated radiopharmaceutical to activated macrophages," *Journal of Nuclear Medicine*, vol. 51, no. 5, pp. 768–774, 2010.

[82] S. Poh, K. S. Putt, and P. S. Low, "Folate-targeted dendrimers selectively accumulate at sites of inflammation in mouse models of ulcerative colitis and atherosclerosis," *Biomacromolecules*, vol. 18, no. 10, pp. 3082–3088, 2017.

[83] W. L. Zhang, Y. Xiao, J. P. Liu et al., "Structure and remodeling behavior of drug-loaded high density lipoproteins and their atherosclerotic plaque targeting mechanism in foam cell model," *International Journal of Pharmaceutics*, vol. 419, no. 1-2, pp. 314–321, 2011.

[84] T. Matoba, J. I. Koga, K. Nakano, K. Egashira, and H. Tsutsui, "Nanoparticle-mediated drug delivery system for atherosclerotic cardiovascular disease," *Journal of Cardiology*, vol. 70, no. 3, pp. 206–211, 2017.

[85] X. Gu, W. Zhang, J. Liu et al., "Preparation and characterization of a lovastatin-loaded protein-free nanostructured lipid carrier resembling high-density lipoprotein and evaluation of its targeting to foam cells," *AAPS PharmSciTech*, vol. 12, no. 4, pp. 1200–1208, 2011.

[86] Y. Zhao, C. Jiang, J. He et al., "Multifunctional dextran sulfate-coated reconstituted high density lipoproteins target macrophages and promote beneficial antiatherosclerotic mechanisms," *Bioconjugate Chemistry*, vol. 28, no. 2, pp. 438–448, 2017.

[87] P. Marchio, S. Guerra-Ojeda, J. M. Vila, M. Aldasoro, V. M. Victor, and M. D. Mauricio, "Targeting early atherosclerosis: a focus on oxidative stress and inflammation," *Oxidative Medicine and Cellular Longevity*, vol. 2019, Article ID 8563845, 32 pages, 2019.

[88] H. Kim, Y. Kim, I. H. Kim, K. Kim, and Y. Choi, "ROS-responsive activatable photosensitizing agent for imaging and photodynamic therapy of activated macrophages," *Theranostics*, vol. 4, no. 1, pp. 1–11, 2013.

[89] C. M. Hu, R. H. Fang, and L. Zhang, "Erythrocyte-inspired delivery systems," *Advanced Healthcare Materials*, vol. 1, no. 5, pp. 537–547, 2012.

[90] D. Peer, J. M. Karp, S. Hong, O. C. Farokhzad, R. Margalit, and R. Langer, "Nanocarriers as an emerging platform for cancer therapy," *Nature Nanotechnology*, vol. 2, no. 12, pp. 751–760, 2007.

[91] C. M. Hu, R. H. Fang, B. T. Luk, and L. Zhang, "Polymeric nanotherapeutics: clinical development and advances in stealth functionalization strategies," *Nanoscale*, vol. 6, no. 1, pp. 65–75, 2014.

[92] H. Cao, Z. Dan, X. He et al., "Liposomes coated with isolated macrophage membrane can target lung metastasis of breast cancer," *ACS Nano*, vol. 10, no. 8, pp. 7738–7748, 2016.

[93] W. Gao and L. Zhang, "Coating nanoparticles with cell membranes for targeted drug delivery," *Journal of Drug Targeting*, vol. 23, no. 7-8, pp. 619–626, 2015.

[94] B. T. Luk and L. Zhang, "Current advances in polymer-based nanotheranostics for cancer treatment and diagnosis," *Acs*

Applied Materials & Interfaces, vol. 6, no. 24, pp. 21859–21873, 2014.

[95] C. M. Hu, L. Zhang, S. Aryal, C. Cheung, R. H. Fang, and L. Zhang, "Erythrocyte membrane-camouflaged polymeric nanoparticles as a biomimetic delivery platform," *Proceedings of the National Academy of Sciences of the United States of America*, vol. 108, no. 27, pp. 10980–10985, 2011.

[96] J. G. Piao, L. Wang, F. Gao, Y. Z. You, Y. Xiong, and L. Yang, "Erythrocyte membrane is an alternative coating to polyethylene glycol for prolonging the circulation lifetime of gold nanocages for photothermal therapy," *ACS Nano*, vol. 8, no. 10, pp. 10414–10425, 2014.

[97] A. V. Kroll, R. H. Fang, and L. Zhang, "Biointerfacing and applications of cell membrane-coated nanoparticles," *Bioconjugate Chemistry*, vol. 28, no. 1, pp. 23–32, 2017.

[98] B. T. Luk and L. Zhang, "Cell membrane-camouflaged nanoparticles for drug delivery," *Journal of Controlled Release*, vol. 220, Part B, pp. 600–607, 2015.

[99] C. M. Hu, R. H. Fang, B. T. Luk et al., "'Marker-of-self' functionalization of nanoscale particles through a top-down cellular membrane coating approach," *Nanoscale*, vol. 5, no. 7, pp. 2664–2668, 2013.

[100] J. W. Yoo, D. J. Irvine, D. E. Discher, and S. Mitragotri, "Bio-inspired, bioengineered and biomimetic drug delivery carriers," *Nature Reviews Drug Discovery*, vol. 10, no. 7, pp. 521–535, 2011.

[101] R. Molinaro, C. Corbo, J. O. Martinez et al., "Biomimetic proteolipid vesicles for targeting inflamed tissues," *Nature Materials*, vol. 15, no. 9, pp. 1037–1046, 2016.

[102] E. V. Batrakova, H. E. Gendelman, and A. V. Kabanov, "Cell-mediated drug delivery," *Expert Opinion on Drug Delivery*, vol. 8, no. 4, pp. 415–433, 2011.

[103] J. O. Martinez, R. Molinaro, K. A. Hartman et al., "Biomimetic nanoparticles with enhanced affinity towards activated endothelium as versatile tools for theranostic drug delivery," *Theranostics*, vol. 8, no. 4, pp. 1131–1145, 2018.

[104] F. Moroni, E. Ammirati, G. D. Norata, M. Magnoni, and P. G. Camici, "The role of monocytes and macrophages in human atherosclerosis, plaque neoangiogenesis, and atherothrombosis," *Mediators of Inflammation*, vol. 2019, Article ID 7434376, 11 pages, 2019.

[105] J. Rojas, J. Salazar, M. S. Martinez et al., "Macrophage heterogeneity and plasticity: impact of macrophage biomarkers on atherosclerosis," *Scientifica*, vol. 2015, Article ID 851252, 17 pages, 2015.

[106] L. T. Cheng and C. Li, "A preliminary study on the biomimetic drug delivery system targeting atherosclerotic lesions," *Acta Pharmaceutica Sinica*, vol. 53, no. 2, pp. 297–303, 2018.

Hindawi
Journal of Immunology Research
Volume 2019, Article ID 4354786, 14 pages
https://doi.org/10.1155/2019/4354786

Review Article

Vascular Macrophages in Atherosclerosis

Hailin Xu,[1] Jingxin Jiang,[2] Wuzhen Chen,[2,3] Wenlu Li,[4] and Zhigang Chen[2,3]

[1]*Department of General Surgery, The First People's Hospital of Jiande, Hangzhou, China*
[2]*Department of Surgical Oncology, Second Affiliated Hospital, Zhejiang University School of Medicine, Hangzhou, China*
[3]*Key Laboratory of Tumor Microenvironment and Immune Therapy of Zhejiang Province, Hangzhou, China*
[4]*Neuroprotection Research Laboratory, Massachusetts General Hospital, Harvard Medical School, Charlestown, MA, USA*

Correspondence should be addressed to Wenlu Li; wli23@partners.org and Zhigang Chen; chenzhigang@zju.edu.cn

Received 18 April 2019; Revised 19 August 2019; Accepted 23 October 2019; Published 1 December 2019

Guest Editor: Heather Medbury

Atherosclerosis is the main pathological basis for the occurrence of most cardiovascular diseases, the leading global health threat, and a great burden for society. It has been well established that atherosclerosis is not only a metabolic disorder but also a chronic, sterile, and maladaptive inflammatory process encompassing both innate and adaptive immunity. Macrophages, the major immune cell population in atherosclerotic lesions, have been shown to play critical roles in all stages of atherosclerosis, including the initiation and progression of advanced atherosclerosis. Macrophages have emerged as a novel potential target for antiatherosclerosis therapy. In addition, the macrophage phenotype is greatly influenced by microenvironmental stimuli in the plaques and presents complex heterogeneity. This article reviews the functions of macrophages in different stages of atherosclerosis, as well as the phenotypes and functions of macrophage subsets. New treatment strategies based on macrophage-related inflammation are also discussed.

1. Introduction

Although much progress has been made in the diagnosis and treatment of cardiovascular disease (CVD) in recent years, CVD is still the leading cause of global morbidity and mortality [1]. The pathological cause of most CVD events, stroke, and peripheral arterial disease is atherosclerosis, thus motivating a number of researchers to study the pathophysiology of atherosclerosis over the past decades. Atherosclerosis is a focal vascular disease characterized by intimal thickening and plaque formation and mostly occurs at sites notably with endothelial cell injury and disturbed laminar flow [2]. Currently, it has been well established that atherosclerosis is both a component associated with metabolic disorder and a chronic inflammatory process in the arterial wall, which is induced initially by the subendothelial deposition of apolipoprotein B-containing lipoproteins (apoB-LPs) [3]. Macrophages, the major immune cell population in the arterial plaques, have been suggested to play a central role in the immune responses and progression of atherosclerosis (Figure 1) [2, 4]. Macrophages primarily originate from circulating monocytes and resident tissues. They are recruited to the lesion site by adhering to activated endothelial cells (ECs) and entering into the subendothelial cell space [5]. Then, macrophage proliferation becomes the predominant replenishment mechanism in advanced plaques [6]. Within the plaque, macrophages can take up lipid deposit particles and transform into foam cells, which is one of the hallmark events of the early atherosclerotic lesion [7]. These foam cells further induce a cascade of inflammatory responses that promote more lipoprotein retention, extracellular matrix (ECM) modification, and sustained chronic inflammation [8]. In addition, modified low-density lipoprotein (LDL), such as oxidized LDL (oxLDL), further induces the necrosis of foam cells, which can form a necrotic core, a typical feature of the instability of advanced plaques, leading to the rupture of plaques and further acute life-threatening clinical cardiovascular events [9]. Studies have concluded that increased lesional $CD68^+$ macrophages are associated with a higher risk of CVD and stroke events, while presenting a weak relationship with stenosis [10, 11]. Therefore, clarifying the macrophage-dependent inflammatory processes in

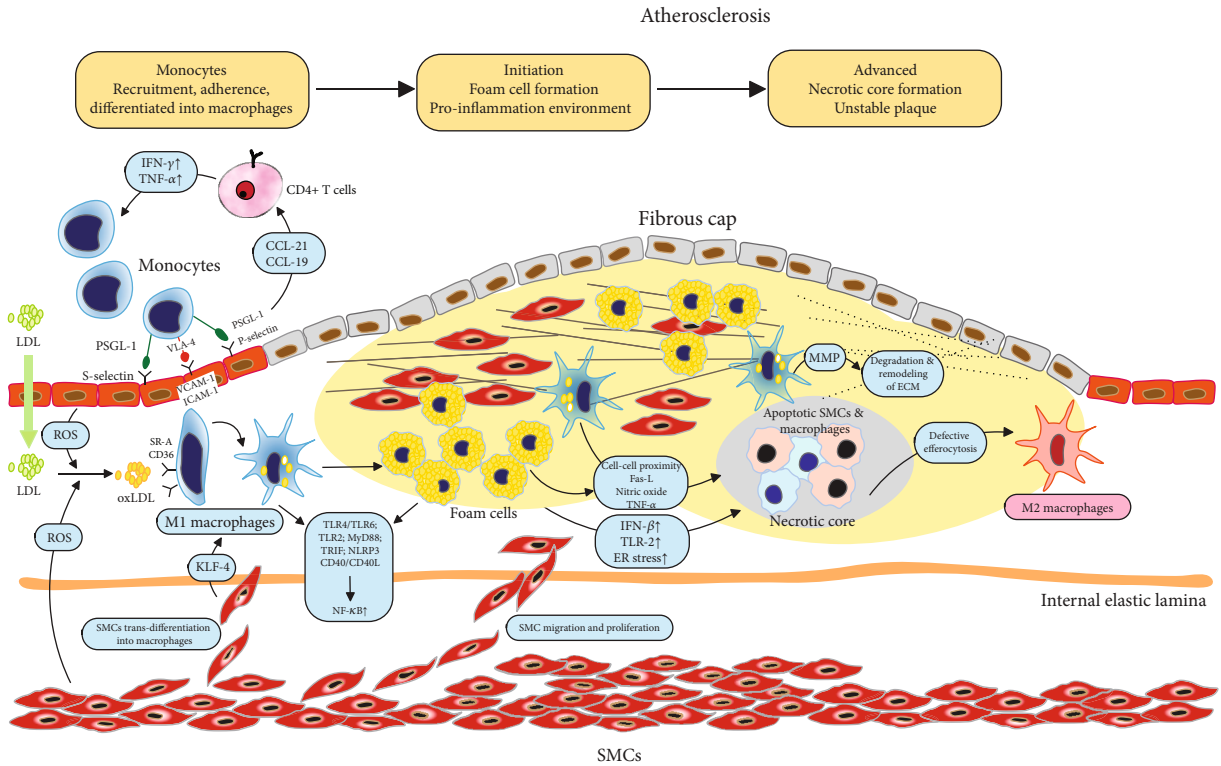

Figure 1: Roles of macrophages in different stages of atherosclerosis progression. Atherosclerosis is initiated by the subendothelial deposition of lipids. Circulating monocytes are recruited to the lesion site by adhering to activated endothelial cells (ECs) and entering the subendothelial cell space. Within the plaque, macrophages take up lipid deposit particles and transform into foam cells, forming early atherosclerotic lesions. Lesional macrophages further induce a cascade of inflammatory responses, promoting more lipoprotein retention, extracellular matrix (ECM) alteration, and sustained chronic inflammation. Oxidized LDL (oxLDL) further induces the necrosis of foam cells, which construct a necrotic core, leading to instability and rupture of advanced plaques. Abbreviations: CCL: chemokine ligand; ECM: extracellular matrix; ER: endoplasmic reticulum; Fas-L: Fas ligand; ICAM: intercellular adhesion molecule; IFN: interferon; IL: interleukin; KLF4: Kruppel-like factor 4; MMP: matrix metalloproteinase; NF-κB: nuclear factor of kappa B; NLRP3: leucine-rich repeat pyrin domain containing 3; oxLDL: oxidized low-density lipoprotein; PSGL-1: P-selectin glycoprotein ligand-1; ROS: reactive oxygen species; SMC: smooth muscle cells; SR-A: type A scavenger receptor; TLR: toll-like receptor; TNF: tumor necrosis factor; TRIF: toll-like receptor domain-containing adaptor; VCAM: vascular cell adhesion molecule; VLA-4: very-late antigen 4.

atherosclerosis progression and exploring macrophage-targeted strategies to reduce the residual risk of atherosclerotic CVD have become a hot research topic in recent years.

The macrophage phenotype is shaped greatly by microenvironment stimuli in the plaque, such as lipids, glucose, cytokines, and hemorrhage, and displays great plasticity [12]. Because complicated factors in the local milieu change with disease progression, macrophages are spatiotemporally heterogeneous. Traditionally, macrophages are classified into proinflammatory and anti-inflammatory phenotypes, which are well known as M1 and M2 phenotypes [13]. While in the plaque, this classification is reported to be an oversimplification of reality. In addition to M1 and M2, other macrophage subsets with distinct functions that do not resemble the M1/M2 transcriptomes and phenotypes have been reported [12, 14–17]. In addition, not only lesional macrophages but also circulating monocytes as well as their progenitor cells in the bone marrow are also stimulated by proatherogenic factors, such as cellular cholesterol content, and present great plasticity in genetic and epigenetic characteristics [18]. Owing to these functional complexities, although amply documented preclinical models are reported, few clinical trials have been developed to therapeutically target macrophages.

In this review, we will focus on the recent evidence on macrophage pathophysiology, presenting an overall view of the critical role of macrophages in different stages of atherosclerosis and their functional diversity. Moreover, we will review and discuss the major clinical strategies to modify macrophage-dependent chronic inflammation processes in plaques. Finally, we will highlight macrophages as a potential therapeutic target in atherosclerosis.

2. Origin of the Plaque Macrophage

Macrophages are considered to mainly originate from circulating monocytes, which are derived from the bone marrow [19] or spleen [20], which is widely known as the mononuclear phagocyte system (MPS). Monocytes in the circulation are recruited to the specific tissue site by various inducers such as tissue injury, pathogens, and proinflammatory cytokines and chemokines. Based on thymidine pulse-labeling animal models, van Furth et al. proposed that macrophage population replenishment was mainly dependent on

monocyte recruitment [21]. Recently, this conclusion was challenged by the results from genetic fate mapping studies (tracing cell lineages) of tissue-resident macrophages, such as Langerhans cells, lung alveolar macrophages, Kupffer cells, and microglia [22–25]. These tissue-resident macrophages are established during fetal development and mostly maintain and replenish themselves by proliferation [24].

Recently, lineage fate mapping studies of vascular smooth muscle cells (VSMCs) in murine models demonstrated that VSMC subsets with highly proliferative plasticity can also transdifferentiate into macrophage foam cells [26]. This is in accordance with the earlier findings that lesional foam cells coexpressed VSMC markers [27, 28] and activation of the transcription factor Kruppel-like factor 4 (KLF4) may be the critical mechanism [29]. However, *in vivo* studies found that these VSMC-derived macrophage-like cells are different in transcriptional profiles and functions compared to classical macrophage [29, 30], such as in phagocytosis or efferocytosis [31].

In addition to exogenous replenishment, the progression of advanced atherosclerotic lesions is mainly dependent on local cell proliferation, which is involved in focal intimal thickening of the human aorta and further contributes to the progression of atherosclerosis [6, 32].

3. Macrophages in the Initiation of Atherosclerosis

3.1. Monocyte-Endothelial Cell Adhesion. Monocyte-endothelial cell adhesion plays a key role in the initiation of atherosclerosis. Complicated signaling pathways are involved in this process, and among them, the most notable pathway is the interaction between P-selectin glycoprotein ligand-1 (PSGL-1) and selectins [33]. Activated lesional ECs express P- and E-selectin [34, 35]. Selectins bind to the properly glycosylated PSGL-1, their predominant ligand that is expressed on monocytes and leukocytes [34, 35]. Selectin-PSGL-1-mediated interactions promote the capture of both monocytes and leukocytes onto the endothelium, activate integrins, and induce monocyte activation [36, 37]. In addition to the adhesion functions, PSGL-1 interacts with chemokine ligand (CCL) 21 or CCL19 and efficiently attracts activated $CD4^+$ T cells to the vulnerable plaques [38, 39]. These $CD4^+$ T cells produce interferon- (IFN-) γ and tumor necrosis factor- (TNF-) α and contribute to the proinflammatory environment. In accordance with these findings, knockout of PSGL-1 in $ApoE^{-/-}$ mouse models showed less monocyte and leukocyte infiltration in atherosclerotic lesions and protection against atherosclerosis [40, 41]. Research based on double knockout mouse models including $P\text{-}selectin^{-/-}ApoE^{-/-}$ and $E\text{-}selectin^{-/-}ApoE^{-/-}$ mice also indicated decreased atherosclerosis formation [42, 43].

The binding of selectins to their ligands allows monocytes in circulation to be tethered and roll along the endothelium, and the subsequent ligation of monocyte integrins with vascular cell adhesion molecule 1 (VCAM1) or intercellular adhesion molecule 1 (ICAM1) on the ECs constructs a firm adhesion between monocytes or lymphocytes and ECs [33]. The most relevant integrin is very-late antigen 4 (VLA-4), also known as $\alpha 4\beta 1$ integrin [44], and is widely expressed on monocytes and lymphocytes and can bind with VCAM1, which is overexpressed on activated ECs [45]. When mouse models lacking one of the two VCAM1 ligand binding sites were double hit by LDL receptor knockout ($LDLR^{-/-}$), the mice developed reduced atherosclerotic lesions under a proatherogenic diet [46]. Utilizing *in vitro* studies, researchers found that after blockade of VLA-4 or VCAM1 by monoclonal antibodies, mononuclear cells rolled faster along the carotid arteries isolated from $ApoE^{-/-}$ mice than those in the control, and monocyte accumulation onto the endothelium was reduced by over 70% [47, 48]. Activated platelets on the inflamed endothelium also contribute to monocyte-endothelial interactions via augmentation of adhesion selection expression and secretion of proinflammatory chemokines such as CCL5 [49]. In addition, C-C chemokine receptor type (CCR) 2, CCR5, and CX3C chemokine receptor 1 (CX3CR1) signals are indicated to contribute to the migration of monocytes into arterial walls [50–52]. In the $ApoE^{-/-}$ mouse model, inhibition of three pathways, including CCL2, CX3CR1, and CCR5, almost abrogates macrophage accumulation and atherosclerosis (90% reduction), which is significantly more than the 28%, 36%, or 48% reduction in $ApoE^{-/-}\ CCL2^{-/-}$, $ApoE^{-/-}\ CX3CR1^{-/-}$, and $ApoE^{-/-}\ CCL2^{-/-}\ CX3CR1^{-/-}$ murine models, respectively [50]. Moreover, IFN-β signaling also enhances macrophage-endothelial cell adhesion and promotes immune cell infiltration to atherosclerosis-prone sites in mice, leading to the acceleration of lesion formation [53].

3.2. Macrophages and Foam Cells. After adhering to the ECs, monocytes penetrate through ECs into the subendothelial space and stay there because of their decreased migration ability, hindering the resolution of inflammation. Driven by prodifferentiation factors such as macrophage colony-stimulating factor (M-CSF), monocytes give rise to macrophage- or dendritic cell- (DC-) like phenotypes. These cells actively participate in scavenging lipoprotein particles and turn into foam cells, which present cytoplasmic and membrane-bound droplets, resulting in more accumulation of oxLDL in the subendothelial space [54, 55]. Several mechanisms have been proposed for this uptake process. Scavenger receptors expressed on the macrophages, especially the type A scavenger receptor (SR-A) and a member of the type B family, CD36, have been reported in early studies to be the main markers on lesional macrophages that transform into foam cells [8, 56]. Blocking SR-A inhibits the uptake of lipids and formation of foam cells, further prohibiting the local proliferation of macrophages in the lesion [6]. However, in triple knockout $Apoe^{-/-}\ CD36^{-/-}\ Msr1^{-/-}$ mouse models, no decrease was observed in the foam cell transformation compared with that of $Apoe^{-/-}$ mice, indicating that more mechanisms controlling this process remain to be clarified [57]. Recently, more novel scavenger receptors have been identified, such as LDL receptor-related protein 1 (LRP1) and lectin-like oxLDL receptor 1 (LOX1), which also contribute to lipid uptake [58, 59]. Blocking LRP1 in lesional macrophages has been proven to reduce the accumulation of cholesterol in macrophages [59]. In contrast, liver X receptor

(LXR), which is activated by oxLDL, promotes the outflow of cholesterol and reduces the expression of proinflammatory factors in macrophages, thus exerting a favorable effect on atherosclerosis [60]. In addition to oxLDL, Kruth et al. found that foam cell transformation could also take place via intake of native LDL independent of receptors [61]. This process is called fluid-phase endocytosis and relies on the activation of phorbol 12-myristate 13-acetate (PMA), the activator of protein kinase C (PKC).

3.3. Macrophages and Proinflammatory Cytokines. Foam cells secrete abundant proinflammatory cytokines and in turn promote the accumulation and proliferation of circulating monocytes. Toll-like receptors (TLRs) have been proven to play a critical role in inflammatory signaling cascades. TLRs are essential pattern recognition receptors that mediate innate immune responses during invading pathogen invasion, such as viral and bacterial infection [62]. Phospholipid-CD36 binding on the lesional macrophages induces TLR4/TLR6 heterodimer formation, followed by activating downstream molecules, including myeloid differentiation factor 88 (MyD88), interleukin (IL)-1, toll-like receptor domain-containing adaptor (TRIF), and nuclear factor of kappa B (NF-κB) [63]. In accordance with these reports, studies based on the mouse model have demonstrated that gene deletion of TLR2, TLR4, or MyD88 results in a reduction in atherosclerosis [64–66]. Endothelial-targeted blocking of NF-κB signals in the $Apoe^{-/-}$ mouse model resulted in a reduction in recruitment of macrophages to lesions [67]. Macrophage inflammasome signaling also plays a role in atherosclerosis. Crystalline cholesterol induces IL-1 family cytokines in macrophages by stimulating the caspase-1-activated nucleotide-binding domain and leucine-rich repeat pyrin domain containing 3 (NLRP3) inflammasome [68]. The NLRP3 inflammasome, as the most well-known inflammasome, is essential for necrotic core formation in advanced atherogenesis, and its silencing protects the stabilization of atherosclerotic plaques [69]. Except for B cells, ECs, SMCs, and platelets also express CD40 when induced by proinflammatory stimuli, such as IL-1, IL-3, IL-4, TNF-α, and IFN-γ [70]. Gene-targeting studies utilizing murine knockout models have established that CD40L participates in lesion progression and thrombosis [71]. *In vitro* studies indicate that ligation of CD40/CD40L stimulates proinflammatory cytokines and cell adhesion factors in vascular endothelial cells [72].

4. Macrophages in Advanced Atherosclerosis

4.1. Macrophages and Fibrous Caps. Stable plaques with intact fibrous caps rarely cause detrimental symptoms owing to the preservation of the arterial lumen, which relies on matrix metalloproteinase- (MMP-) mediated vascular remodeling [73, 74]. A plaque becomes unstable when the fibrous cap becomes thin and a necrotic core arises, followed by its breakdown from the endothelia and further acute, occlusive lumenal thrombosis, leading to thromboembolic events such as heart attack or stroke and high mortality [9].

Lesional macrophages promote the apoptosis of smooth muscle cells (SMCs) in the plaque in several ways, including cell-cell proximity [75] and activation of multiple cytotoxic signals including Fas-L, nitric oxide (NO), and TNF-α [76, 77], thus predisposing the plaque to rupture. Collagen synthesis by intimal SMCs is also reduced due to decreased macrophage-derived TGF-β [78, 79]. In addition, lesion macrophages promote extracellular matrix (ECM) remodeling by producing MMPs, especially MMP-2 and MMP-9, which can induce ECM protein degradation, thinning of the fibrous cap, and the formation of rupture-prone plaques [80]. Notably, different MMP members may play divergent roles during the atherosclerosis process, and MMPs present a dual role in this progression by promoting the migration and proliferation of vascular smooth muscle (VSMC) in the early stage while accelerating plaque instability by matrix destruction in advanced atherosclerosis [81]. For example, Gough et al. found that overexpression of an activated MMP-9 mutant (MMP-9 G100L) contributed to fibrous cap disruption, thrombus formation, plaque rupture, and mouse mortality in an $Apoe^{-/-}$ mouse model [82]. However, Johnson et al. observed a contradictory unfavorable effect on plaque size and stability when MMP-9 was knocked out in an $Apoe^{-/-}$ mouse model [83]. Therefore, more studies of MMP knockout or overexpression are needed to resolve the dispute that most likely results from differences in sites and stages of plaque development, assessment of plaque instability, dietary treatment, and mouse model strains. In addition, limitations such as utilization of indirect evidence as an endpoint for plaque rupture and a lack of acute lumenal thrombosis similar to that in human lesions in previous mouse model studies also restrain the application of these findings for clinical trials.

4.2. Macrophages and Necrotic Cores. The second feature of advanced plaques is the formation of necrotic cores. Generally, the necrotic core of a plaque is a hallmark of plaque vulnerability and contributes to nonresolving inflammation, thrombosis, fibrous cap breakdown, and plaque rupture [9]. The necrotic core is mainly composed of apoptotic lesional macrophages and defective phagocytic clearance [84]. A number of signals participate in necrotic core formation, including growth factor deprivation, oxidative stress, and death receptor activation by ligands [2]. In $Apoe^{-/-}$ mice, IFN-β not only induces the recruitment of macrophages to the lesion but also contributes to cell apoptosis and further necrotic core formation [53]. Similarly, oxLDL-CD36 complex-triggered TLR2-dependent signaling promotes the initial proinflammatory environment and further induces apoptosis of endoplasmic reticulum- (ER-) stressed macrophages [56].

ER stress, primarily the unfolded protein response (UPR), is a novel apoptotic mechanism discovered in recent years and has been proven to play critical roles in proatherosclerotic inflammation, necrotic core formation, and atherosclerosis plaque progression [85]. Factors associated with cardiovascular diseases are reported to be potent inducers of prolonged ER stress, including insulin resistance and obesity [86–88]. The expression of the UPR effector, C/EBP homologous protein (CHOP), shows a strong correlation

with the progression of human coronary artery lesions [89], and knockdown of CHOP expression *in vitro* decreases ER stress-dependent cell death [90, 91]. In addition, considerable studies have highlighted that ER stress is involved in the inflammation processes within the lesion through manipulating a variety of regulators, such as suppressing NF-κB signaling and activating activator protein-1 (AP-1), Jun amino-terminal kinases (JNK), spliced X-box binding protein 1 (XBP1), and reactive oxygen species (ROS) [92–95]. In addition, prolonged ER stress and abnormally activated UPR are also related to overactive autophagy, causing SMC and EC death and finally leading to a thinner fibrous cap [96]. *In vitro* studies indicated that nitric oxide (NO) donors, such as Molsidomine, spermine NONOate, or S-nitroso-N-acetylpenicillamine (SNAP), can preferentially eliminate macrophages in an ER stress-dependent manner and favor the stability of plaques [95].

In advanced lesions, macrophage apoptosis is followed by defective efferocytosis, which is the key driver for necrotic core formation [97]. Compared with the normal tonsil tissue in which each of the apoptotic cells was associated with a phagocyte, there were many free apoptotic cells in the advanced lesion [97]. Several mechanisms are proposed to contribute to this efferocytosis failure, including changes in the phenotypes of plaque cells that express markers such as CD47 and are poorly internalized by lesional efferocytes [98], reduced "eat me" signal calreticulin on the apoptotic cells [99], competition between the apoptotic cells and oxLDLs in binding to efferocytosis receptors [100], oxidative stress-induced efferocyte death [101], and the deficient expression and function of efferocytosis receptors as well as their bridging molecules such as MerTK-Gas6 [102]. Blocking CD47 and protecting MerTK on apoptotic macrophages to enhance efficient efferocytosis are potential strategies to ameliorate atherosclerosis in multiple mouse models [98]. Although the above studies give us some suggestions, the specific mechanisms of efferocytosis failures remain unknown and require careful assessment with *in vivo* and *in vitro* genetic causation testing in the future.

5. Macrophage Functional Diversity in Atherosclerosis

5.1. M1 and M2 Macrophages. As with the well-established T cell polarization system that is based on transcriptome, phenotype, and function, lesional macrophages are greatly influenced by the microenvironment signals and are polarized into different classes with diverse phenotypes and functions (Figure 2) [12]. Accurate research on macrophage differentiation and heterogeneity is limited by macrophage instability during the isolation process and phenotype differences between animal models and humans.

In the simplified dichotomy, immune-activated proinflammatory macrophages (M1) and immunomodulatory alternatively activated macrophages (M2) are the most classical classification, mirroring the two types of T helper cells (Th1 and Th2), and represent the extreme phenotypes of the complicated activation states [103]. M1 macrophages are typically polarized by Th1 cytokines, such as interferon (IFN-γ) and TNF and pathogen-associated molecular complexes (PAMPs), including lipopolysaccharides and lipoproteins [12]. Granulocyte macrophage colony-stimulating factor (GM-CSF) also promotes a proinflammatory M1 state through interferon regulatory factor 5 (IRF5) [104]. M1 macrophages produce high levels of proinflammatory cytokines, such as IL-6, IL-12, IL-23, TNF-α, and IL-1β, and Th1 recruitment-associated chemokines, such as CXCL-9, CXCL-10, and CXCL-11, and low levels of IL-10 [105, 106]. However, chronic M1 macrophage activation can also induce the NADPH oxidase system and subsequently generate ROS and NO, inducing chronic tissue damage and impairing wound healing [107]. At this point, M2 macrophages are necessary to counterbalance the proinflammatory response and function to modulate inflammation, scavenge apoptotic cells, accelerate angiogenesis and fibrosis, and promote tissue repair [108]. M2 macrophages are mainly induced in response to Th2-related cytokines, including IL-4, IL-33, and IL-13 [108]. Activated M2 macrophages are immunomodulatory and characterized by low levels of IL-12 and high levels of anti-inflammatory cytokines such as IL-10 and TGF-β and chemokines CCL17, CCL22, and CCL24 [14]. In fact, according to the differences in activation cues and gene expression profiles, M2 macrophages can be further divided into four subgroups, M2a, M2b, M2c, and M2d [14, 109]. M2a macrophages are induced by IL-4 and IL-13 and are characterized by high levels of CD206 and IL-1 receptor antagonist; M2b macrophages are an exception and are induced by immune complexes, IL-1β and PAMPs, and produce both proinflammatory cytokines IL-1, IL-6, and TNF-α and the anti-inflammatory cytokine IL-10; M2c macrophages are the most prominent anti-inflammatory subtype and are induced by IL-10, TGF-β, and glucocorticoids and produce IL-10, TGF-β and pentraxin 3 (PTX3); last, M2d macrophages are induced by TLR signals and characterized by angiogenic properties, playing a role both in plaque growth and tumor progression. Activation of the peroxisome proliferator-activated receptor γ (PPAR-γ) and signal transducer and activator of transcription 6 (STAT6) pathways is the main signal for M2 polarization [109, 110]. M1 and M2 macrophages present at different regions of the plaque: M1 macrophage marker staining is mostly confined to the shoulder of rupture-prone plaques, one of the most unstable areas within the plaque, while M2 macrophage markers are mainly present in the vascular adventitia or regions of stable plaques [111]. M1 macrophages are also more abundant in the lesions of infarction and CAD patients than M2 macrophages [112, 113].

5.2. Other Macrophage Phenotypes. Along with a deep understanding of the phenotypes and functions of lesional macrophages, it has been clearly proven that the M1-M2 dichotomy does not actually reflect the complicated subsets of macrophages in atherosclerosis (Figure 2) [4, 12, 111]. Stimuli vary spatiotemporally and drive malleable macrophages into a broad spectrum of activation states, rather than a stable analogous polarization, which might be the reason for the difficulty in keeping phenotypes of isolated macrophages

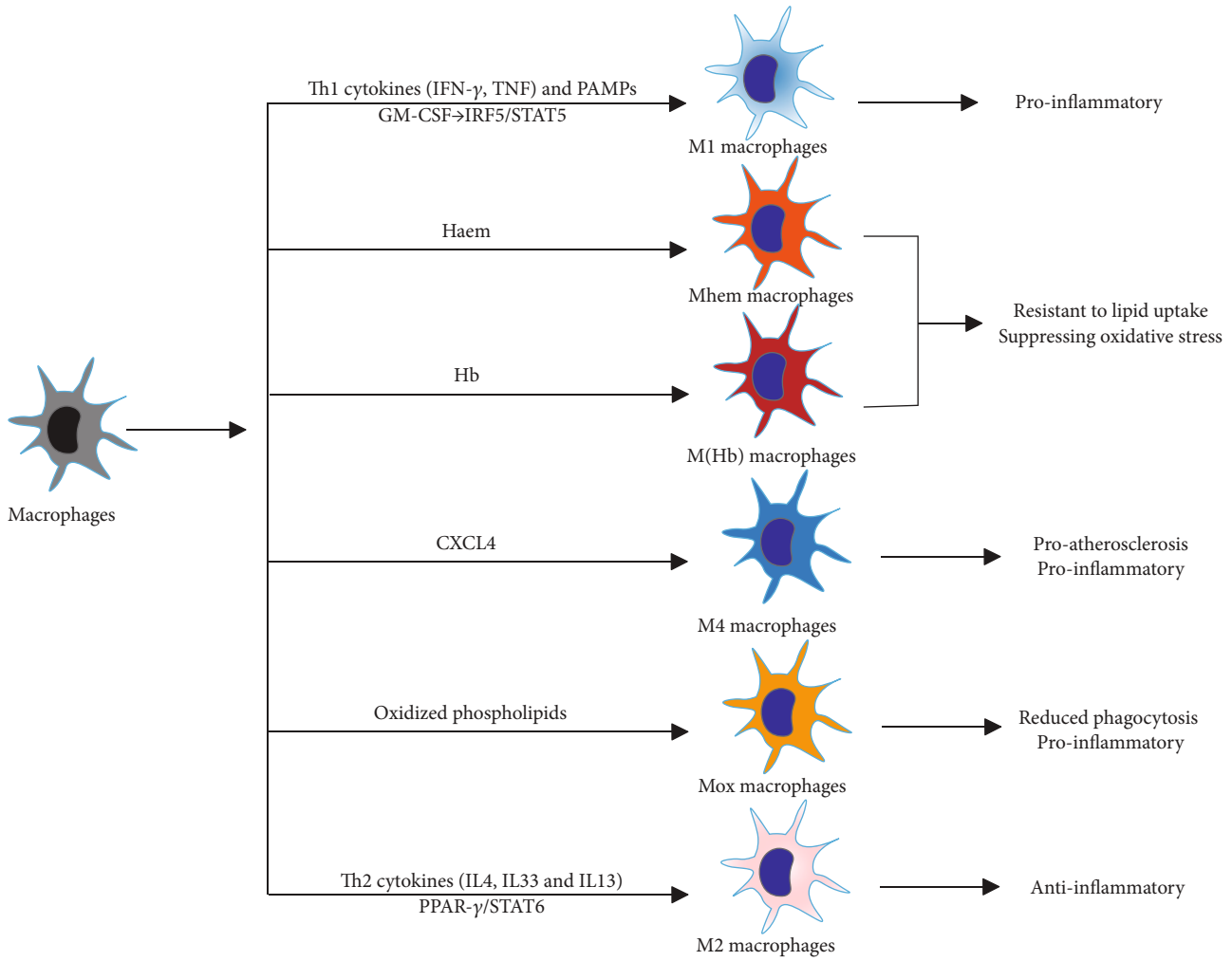

Figure 2: Macrophage subsets in the atherosclerotic lesion. M1 proinflammatory and M2 anti-inflammatory macrophages are polarized by Th1 and Th2 cytokines, respectively. Haem-induced phenotypes including M(Hb) and Mhem are M2-like and show anti-inflammatory effects such as resistant to lipid uptake and suppressing oxidative stress. Intermediate phenotypes Mox and M4 display reduced capacity for phagocytosis and are potentially proinflammatory by expressing proatherogenic markers. Abbreviations: CXCL4: C-X-C motif chemokine 4; GM-CSF: granulocyte macrophage colony-stimulating factor; IFN-γ: interferon-γ; IL: interleukin; IRF: interferon regulatory factor 5; PAMPs: pathogen-associated molecular complexes; STAT: signal transducer and activator of transcription; TNF: tumor necrosis factor.

stable. A novel way to classify macrophages is by stimulus: e.g., M(IFN-γ), M(IL-4), and M(IL-10). Recently, Piccolo et al. induced macrophages by dual stimulation with IFN-γ and IL-4, which are the inducers for M1 and M2 phenotype macrophages, respectively, and found that costimulation with two opposite stimuli drove macrophages to an intermediate state that we could call M(IFN-γ-IL-4) and displayed both M1- and M2-type specific gene transcriptome signatures [114]. In addition to M1-M2, oxidized phospholipids can induce macrophages to a Mox phenotype via activation of the transcription factor Nrf2 in mouse models [15]. Mox macrophages constitute approximately 30% of the total macrophages in advanced atherosclerotic lesions, and these cells express proinflammatory markers, such as IL-1β and cyclooxygenase 2, and display defective phagocytic and chemotactic capacities [15]. Rupture of microvessels within the lesion releases erythrocytes, which can be phagocytosed by macrophages and then induce them into M(Hb) and Mhem phenotypes [16, 17]. M(Hb) macrophages can be induced *in vitro* by hemoglobin-haptoglobin complexes and present a $CD206^+$ $CD163^+$ phenotype. M(Hb) macrophages have increased activity of LXR-α, which results in increased cholesterol efflux and reduced lipid accumulation, increased ferroportin expression, which leads to reduced intracellular iron accumulation, and increased secretion of anti-inflammatory factors such as IL-10. The Mhem phenotype is polarized by heme and is characterized by increased expression of cyclic AMP-dependent transcription factor- (ATF-) 1 and heme oxygenase 1 (HO-1) and suppressed oxidative stress or lipid accumulation, sharing similar properties with H(Hb) macrophages. Both M(Hb) and Mhem cells are hemorrhage-associated phenotypes that are generally resistant to transformation to foam cells, suppressing oxidative stress and potentially serving atheroprotective roles. C-X-C motif chemokine

4 (CXCL-4) chemokine induces M4 phenotype macrophages in human atherosclerotic plaques, which are $CD163^{-}$ and characterized by expression of MMP-7 and the calcium-binding protein S100A8 and presentation of proinflammatory and proatherogenic properties [115]. Interestingly, M1, M2, and hemorrhage-associated phenotypes can switch between one another, while the M4 macrophage phenotype seems to be irreversible [115].

6. Monocyte Phenotypes in Atherosclerosis

Similar to macrophages, their precursor cells, monocytes, are also induced into distinct phenotypes in the circulation before recruitment to the artery [18]. Three subsets are reported based on the expression of CD14 and CD16: classical, nonclassical, and intermediate monocytes. Classical monocytes are $CD14^{++}$ $CD16^{-}$ in humans and $Ly6C^{++}$ $CCR2^{+}$ $CX3CR1^{+}$ in mice [116]. Classical monocytes are the majority of total monocytes, have proinflammatory features, and differentiate into macrophages and DCs [117]. Nonclassical monocytes are $CD14^{+}$ $CD16^{++}$ in humans and $Ly6C^{-}$ $CCR2^{-}$ $CX3CR1^{++}$ in mice, circulate longer in the blood, present more M2-like properties, and may counterbalance the classical subsets [116]. Intermediate monocytes are the remaining $CD14^{++}$ $CD16^{+}$ subset and account for approximately 5% of the total monocyte population. Although the intermediate phenotype is the smallest subset population, most studies find positive relationships between this subtype and CVD events and plaque thinning [118]. This may be due to their CD11c integrin expression and stronger capacity to adhere to endothelium than the other two subsets [119]. Consistent with these results, a recent study utilized a novel experimental technique, time-of-flight mass cytometry, to analyze the phenotypes human monocyte subsets in CVD lesions and found that the percentage of intermediate and nonclassical monocytes was increased in the high CVD risk group [120]. It is reasonable to assume that different monocyte subsets might differentiate into distinct macrophages and further contribute to the formation of corresponding plaques with different vulnerabilities. However, thus far, no corresponding evidence is available to validate this hypothesis.

7. Therapeutic Strategies Targeting Macrophage-Dependent Inflammation

7.1. Antiatherosclerotic Biomarker Strategies. The traditional strategy to reduce CVD risk mostly focuses on the control of blood lipids, such as traditional drug statins, and antiplatelet therapy. Lowering blood lipids results in a decrease in both apoB-LP deposition and subsequent monocyte/macrophage infiltration [121, 122]. Recently, novel targeted drugs inhibiting proprotein convertase subtilisin-kexin type 9 (PCSK9), *Evolocumab* [123] and *Alirocumab* [124, 125], emerge as an add-on therapy for lowering LDL levels, both of which could prevent LDL receptor degradation, promote LDL clearance, and further reduce the risk of CAD events. Another cholesterol modulation agent, inhibition of the cholesteryl ester transfer protein (CETP), such as anacetrapib, reduces the risk of CAD in statin-treated patients [126] by raising high-density lipoprotein (HDL) and lowering LDL level [127].

With a deep understanding of the nature of atherosclerosis as chronic inflammation and the fact that macrophages are involved throughout the entire process of atherosclerosis, including lesion initiation, progression, advanced lesion necrosis, and plaque breakdown (Figure 1), strategies to modulate the proinflammatory environment in the lesion, macrophage-related responses in particular, have emerged as promising additive therapies. Notably, in addition to the LDL downregulating effect, PCSK9 inhibitors also show anti-inflammatory effects via both LDL receptor-dependent and independent pathways [128]. PCSK9 is normally expressed on atherosclerotic cells, including monocytes/macrophages, ECs, and VSMCs, and promotes the proinflammatory environment [129–131]. In PCSK9 knockout or overexpression mouse models, inflammatory cytokines such as TNF-α, IL-6, and monocyte chemoattractant protein-1 (MCP-1) are negatively correlated with PCSK9 expression [129, 130, 132].

Studies *in vitro* and in mice models have explored an abundance of plausible antibodies or inhibitory molecules targeted on proatherosclerotic biomarkers, such as adhesion molecules, scavenger receptors, efferocytosis-related receptors, ER stress signaling, oxidants, and macrophage inflammation. However, most strategies are far from being translated into therapeutic drugs. Several clinical trials have been undergoing targeting critical cytokines and chemokines involved in macrophage inflammation, such as CCR2, CX3CR1, TNF-α, IL-1β, and IL-6 [133]. CCR2 blockade MLN1202 [134], IL-6 receptor antagonist tocilizumab [135] (NCT02659150), IL-1β inhibitor Canakinumab (NCT01327846 [136]), and IL-1 blocker anakinra [137] are all demonstrated to lower blood C-reactive protein (hsCRP) levels, which is a reliable marker of proatherogenic inflammation. Canakinumab was indicated to reduce the CAD risk with a dose-dependent feature [136], and patients treated with Canakinumab who achieved hsCRP concentrations less than 2 mg/L benefited a 25% reduction of CVD risk [138]. Treatment with TNF-α blockers etanercept or infliximab and methotrexate is associated with nearly 30% lower CVD risk among patients with rheumatoid arthritis [139]. Antioxidant therapy such as febuxostat, an inhibitor of xanthine oxidase, also functions partly through effects on macrophages [140]. Antioxidant therapy could modify the process of atherogenesis by preventing oxidation of LDL, formation of ROS, and subsequent release of inflammatory cytokines in macrophages [141]. Clinical trials targeting other molecules, including CX3CR1, IL-12, LXR, IRF5, and PPAR-γ, are still on the way and have not reached any conclusion.

Notably, macrophage-related proatherosclerotic inflammatory responses are not easily distinguished from host defense, so therapeutic measures are likely to cause increased susceptibility to infections. The local target-based delivery systems would possibly lessen this problem by improving the drug efficacy. Anti-inflammatory biomarker drugs such as antibodies and siRNA carried by nanoparticles (NPs)

[142] or stents [143, 144] have been applied in animal models and *in vitro* studies to electively clear macrophage-related inflammation.

7.2. Strategies Targeting Macrophages. Antiatherosclerotic biomarkers or lipid modulation strategies are nonspecific measures that suppress the functions of macrophages and other cells in the plaque, such as SMCs and ECs. However, therapies directly and specifically targeting macrophages are scarce, and studies have thus far been preclinical work, possibly owing to the complicated phenotypical and functional heterogeneity of lesional macrophages.

Currently, novel drug delivery systems such as NPs, stents, liposomes, glucan shell microparticles, oligopeptide complexes, and monoclonal antibodies make it possible to selectively modify macrophages. Macrophage surface markers such as F4/80, CD11b, CD68, CD206, and scavenger receptors provide unique targets for all macrophages or different subsets [145]. Coupled with surface coating receptors or depending on their chemical properties, these systems could deliver drugs or RNAi to local atherosclerotic plaques or specific macrophage subsets and exert modifications with minimal off-target effects and toxicity [146]. Once in proximity to or inside of the macrophages, diverse approaches could be applied to modulate macrophages, including inducing cell apoptosis [147], inhibiting cell proliferation [148], and introducing anti-inflammatory agents [149]. Verheye et al. found that the rapamycin inhibitor everolimus delivered to plaques in a stent-based rabbit model led to autophagy in macrophages without affecting the number of SMCs [143]. In a high-fat diet mouse model, clodronate liposome injection effectively depleted visceral adipose tissue macrophages and blocked high-fat diet-induced weight gain and metabolic disorders [150]. Stoneman et al. explored the effect of total macrophage- and blood monocyte-targeted ablation by building a CD11b-diphtheria toxin (DT) receptor (DTR) transgenic mouse model via administration of DT [151]. Plaques were remarkedly reduced when DT was given at the initiation time of atherogenesis, while established plaques were not affected by DT, even though macrophages were reduced to a similar level, which suggests that the atherogenesis process is more sensitive to reduced monocytes/macrophages than stable plaques [50]. Unfortunately, although promising, all evidence has been developed *in vitro* or in animal models, and further studies are needed for more novel drugs and clinical translation.

In addition to the removal of macrophages, influencing macrophage polarization to an anti-inflammatory phenotype, M2 macrophages, rather than the M1 phenotype, is another option [152]. Any factor affecting M2 polarization signals might be a potential target. For example, inhibitors of dipeptidyl peptidase (DPP), such as gliptins and sitagliptin, are suggested to be able to promote M2 polarization *in vitro* via SDF-1/CXCR4 signaling [153]. Thiazolidinediones (TZDs), such as rosiglitazone and pioglitazone, activators of PPAR-γ, can promote monocytes to polarize to the M2 phenotype by modifying the expression of M2 markers, such as mannose receptor (MR) and CD163 [110].

8. Conclusions and Perspectives

Macrophages, the major immune cell population in arterial plaques, have been proven to play critical roles in the initiation and progression of atherosclerosis. Lesion-derived signals induce macrophages into complicated subsets with distinct gene expression profiles, phenotypes, and functions. Based on these results, several strategies are suggested, including blocking proinflammatory cytokines and chemokines, activating anti-inflammatory macrophages, depolarizing macrophages, and enhancing efferocytosis.

Although a number of studies have confirmed the critical functions of macrophages in atherosclerosis, many important problems remain unsolved. For example, the origins of macrophages from different organs or systems differ greatly, yet little is known about the proportions of proliferating resident macrophages or macrophages derived from circulating monocytes. This has important implications for the effectiveness of targeted drug therapy. In addition, the exact reason for the relation between intermediate monocytes and prognosis in CVD patients also needs to be clarified, as well as the functions of classical and nonclassical monocytes. In addition, more advanced techniques such as mass cytometry and single cell sequencing are needed to fully and more accurately characterize macrophage subsets and exploit novel therapeutic targets. Finally, much research is still needed before translating preclinical strategies directly targeting macrophages into clinical practice, including specific macrophage-targeted drugs and other targets, such as genetic modification.

Conflicts of Interest

The authors declare that they have no conflicts of interest.

Authors' Contributions

Hailin Xu and Jingxin Jiang contributed equally to this work.

Acknowledgments

This study is supported by the National Natural Science Foundation of China (Nos. 81502564, 81703498, and 81972598).

References

[1] B. Dahlof, "Cardiovascular disease risk factors: epidemiology and risk assessment," *The American Journal of Cardiology*, vol. 105, no. 1, pp. 3A–9A, 2010.

[2] K. J. Moore and I. Tabas, "Macrophages in the pathogenesis of atherosclerosis," *Cell*, vol. 145, no. 3, pp. 341–355, 2011.

[3] K. J. Moore, F. J. Sheedy, and E. A. Fisher, "Macrophages in atherosclerosis: a dynamic balance," *Nature Reviews Immunology*, vol. 13, no. 10, pp. 709–721, 2013.

[4] I. Park, C. Kassiteridi, and C. Monaco, "Functional diversity of macrophages in vascular biology and disease," *Vascular Pharmacology*, vol. 99, pp. 13–22, 2017.

[5] M. A. Gimbrone Jr. and G. Garcia-Cardena, "Endothelial cell dysfunction and the pathobiology of atherosclerosis," *Circulation Research*, vol. 118, no. 4, pp. 620–636, 2016.

[6] C. S. Robbins, I. Hilgendorf, G. F. Weber et al., "Local proliferation dominates lesional macrophage accumulation in atherosclerosis," *Nature Medicine*, vol. 19, no. 9, pp. 1166–1172, 2013.

[7] A. J. Lusis, "Atherosclerosis," *Nature*, vol. 407, no. 6801, pp. 233–241, 2000.

[8] P. Libby, M. Aikawa, and U. Schonbeck, "Cholesterol and atherosclerosis," *Biochimica et Biophysica Acta (BBA) - Molecular and Cell Biology of Lipids*, vol. 1529, no. 1-3, pp. 299–309, 2000.

[9] R. Virmani, A. P. Burke, F. D. Kolodgie, and A. Farb, "Vulnerable plaque: the pathology of unstable coronary lesions," *Journal of Interventional Cardiology*, vol. 15, no. 6, pp. 439–446, 2002.

[10] W. E. Hellings, F. L. Moll, J. P. de Vries et al., "Atherosclerotic plaque composition and occurrence of restenosis after carotid endarterectomy," *JAMA*, vol. 299, no. 5, pp. 547–554, 2008.

[11] S. Merckelbach, T. Leunissen, J. Vrijenhoek, F. Moll, G. Pasterkamp, and G. J. de Borst, "Clinical risk factors and plaque characteristics associated with new development of contralateral stenosis in patients undergoing carotid endarterectomy," *Cerebrovascular Diseases*, vol. 42, no. 1-2, pp. 122–130, 2016.

[12] G. Chinetti-Gbaguidi, S. Colin, and B. Staels, "Macrophage subsets in atherosclerosis," *Nature Reviews Cardiology*, vol. 12, no. 1, pp. 10–17, 2015.

[13] S. Goerdt, O. Politz, K. Schledzewski et al., "Alternative versus classical activation of macrophages," *Pathobiology*, vol. 67, no. 5-6, pp. 222–226, 2000.

[14] A. Mantovani, A. Sica, S. Sozzani, P. Allavena, A. Vecchi, and M. Locati, "The chemokine system in diverse forms of macrophage activation and polarization," *Trends in Immunology*, vol. 25, no. 12, pp. 677–686, 2004.

[15] A. Kadl, A. K. Meher, P. R. Sharma et al., "Identification of a novel macrophage phenotype that develops in response to atherogenic phospholipids via Nrf2," *Circulation Research*, vol. 107, no. 6, pp. 737–746, 2010.

[16] A. V. Finn, M. Nakano, R. Polavarapu et al., "Hemoglobin directs macrophage differentiation and prevents foam cell formation in human atherosclerotic plaques," *Journal of the American College of Cardiology*, vol. 59, no. 2, pp. 166–177, 2012.

[17] J. J. Boyle, M. Johns, T. Kampfer et al., "Activating transcription factor 1 directs Mhem atheroprotective macrophages through coordinated iron handling and foam cell protection," *Circulation Research*, vol. 110, no. 1, pp. 20–33, 2012.

[18] A. J. Murphy, M. Akhtari, S. Tolani et al., "ApoE regulates hematopoietic stem cell proliferation, monocytosis, and monocyte accumulation in atherosclerotic lesions in mice," *The Journal of Clinical Investigation*, vol. 121, no. 10, pp. 4138–4149, 2011.

[19] N. V. Serbina and E. G. Pamer, "Monocyte emigration from bone marrow during bacterial infection requires signals mediated by chemokine receptor CCR2," *Nature Immunology*, vol. 7, no. 3, pp. 311–317, 2006.

[20] C. S. Robbins, A. Chudnovskiy, P. J. Rauch et al., "Extramedullary hematopoiesis generates Ly-6C^{high} monocytes that infiltrate atherosclerotic lesions," *Circulation*, vol. 125, no. 2, pp. 364–374, 2012.

[21] R. van Furth and Z. A. Cohn, "The origin and kinetics of mononuclear phagocytes," *Journal of Experimental Medicine*, vol. 128, no. 3, pp. 415–435, 1968.

[22] F. Ginhoux, M. Greter, M. Leboeuf et al., "Fate mapping analysis reveals that adult microglia derive from primitive macrophages," *Science*, vol. 330, no. 6005, pp. 841–845, 2010.

[23] E. G. O'Koren, R. Mathew, and D. R. Saban, "Fate mapping reveals that microglia and recruited monocyte-derived macrophages are definitively distinguishable by phenotype in the retina," *Scientific Reports*, vol. 6, no. 1, article 20636, 2016.

[24] S. Epelman, K. J. Lavine, and G. J. Randolph, "Origin and functions of tissue macrophages," *Immunity*, vol. 41, no. 1, pp. 21–35, 2014.

[25] B. Ajami, J. L. Bennett, C. Krieger, W. Tetzlaff, and F. M. V. Rossi, "Local self-renewal can sustain CNS microglia maintenance and function throughout adult life," *Nature Neuroscience*, vol. 10, no. 12, pp. 1538–1543, 2007.

[26] J. Chappell, J. L. Harman, V. M. Narasimhan et al., "Extensive proliferation of a subset of differentiated, yet plastic, medial vascular smooth muscle cells contributes to neointimal formation in mouse injury and atherosclerosis models," *Circulation Research*, vol. 119, no. 12, pp. 1313–1323, 2016.

[27] E. R. Andreeva, I. M. Pugach, and A. N. Orekhov, "Subendothelial smooth muscle cells of human aorta express macrophage antigen in situ and in vitro," *Atherosclerosis*, vol. 135, no. 1, pp. 19–27, 1997.

[28] S. Allahverdian, A. C. Chehroudi, B. M. McManus, T. Abraham, and G. A. Francis, "Contribution of intimal smooth muscle cells to cholesterol accumulation and macrophage-like cells in human atherosclerosis," *Circulation*, vol. 129, no. 15, pp. 1551–1559, 2014.

[29] L. S. Shankman, D. Gomez, O. A. Cherepanova et al., "KLF4-dependent phenotypic modulation of smooth muscle cells has a key role in atherosclerotic plaque pathogenesis," *Nature Medicine*, vol. 21, no. 6, pp. 628–637, 2015.

[30] P. Zhu, L. Huang, X. Ge, F. Yan, R. Wu, and Q. Ao, "Transdifferentiation of pulmonary arteriolar endothelial cells into smooth muscle-like cells regulated by myocardin involved in hypoxia-induced pulmonary vascular remodelling," *International Journal of Experimental Pathology*, vol. 87, no. 6, pp. 463–474, 2006.

[31] Y. Vengrenyuk, H. Nishi, X. Long et al., "Cholesterol loading reprograms the microRNA-143/145–myocardin axis to convert aortic smooth muscle cells to a dysfunctional macrophage-like phenotype," *Arteriosclerosis, Thrombosis, and Vascular Biology*, vol. 35, no. 3, pp. 535–546, 2015.

[32] Š. Lhoták, G. Gyulay, J.-C. Cutz et al., "Characterization of proliferating lesion-resident cells during all stages of atherosclerotic growth," *Journal of the American Heart Association*, vol. 5, no. 8, 2016.

[33] J. Mestas and K. Ley, "Monocyte-endothelial cell interactions in the development of atherosclerosis," *Trends in Cardiovascular Medicine*, vol. 18, no. 6, pp. 228–232, 2008.

[34] R. P. McEver, K. L. Moore, and R. D. Cummings, "Leukocyte trafficking mediated by selectin-carbohydrate interactions," *Journal of Biological Chemistry*, vol. 270, no. 19, pp. 11025–11028, 1995.

[35] M. R. Elstad, T. R. La Pine, F. S. Cowley et al., "P-selectin regulates platelet-activating factor synthesis and phagocytosis by

monocytes," *The Journal of Immunology*, vol. 155, no. 4, pp. 2109–2122, 1995.

[36] A. S. Weyrich, T. M. McIntyre, R. P. McEver, S. M. Prescott, and G. A. Zimmerman, "Monocyte tethering by P-selectin regulates monocyte chemotactic protein-1 and tumor necrosis factor-alpha secretion. Signal integration and NF-kappa B translocation," *The Journal of Clinical Investigation*, vol. 95, no. 5, pp. 2297–2303, 1995.

[37] Y. Q. Ma, E. F. Plow, and J. G. Geng, "P-selectin binding to P-selectin glycoprotein ligand-1 induces an intermediate state of $\alpha M\beta 2$ activation and acts cooperatively with extracellular stimuli to support maximal adhesion of human neutrophils," *Blood*, vol. 104, no. 8, pp. 2549–2556, 2004.

[38] K. M. Veerman, D. A. Carlow, I. Shanina, J. J. Priatel, M. S. Horwitz, and H. J. Ziltener, "PSGL-1 regulates the migration and proliferation of $CD8^+$ T cells under homeostatic conditions," *The Journal of Immunology*, vol. 188, no. 4, pp. 1638–1646, 2012.

[39] C. Erbel, K. Sato, F. B. Meyer et al., "Functional profile of activated dendritic cells in unstable atherosclerotic plaque," *Basic Research in Cardiology*, vol. 102, no. 2, pp. 123–132, 2007.

[40] G. An, H. Wang, R. Tang et al., "P-selectin glycoprotein ligand-1 is highly expressed on Ly-$6C^{hi}$ monocytes and a major determinant for Ly-$6C^{hi}$ monocyte recruitment to sites of atherosclerosis in mice," *Circulation*, vol. 117, no. 25, pp. 3227–3237, 2008.

[41] W. Luo, H. Wang, M. K. Ohman et al., "P-selectin glycoprotein ligand-1 deficiency leads to cytokine resistance and protection against atherosclerosis in apolipoprotein E deficient mice," *Atherosclerosis*, vol. 220, no. 1, pp. 110–117, 2012.

[42] K. Ley and G. S. Kansas, "Selectins in T-cell recruitment to non-lymphoid tissues and sites of inflammation," *Nature Reviews Immunology*, vol. 4, no. 5, pp. 325–336, 2004.

[43] Z. M. Dong, S. M. Chapman, A. A. Brown, P. S. Frenette, R. O. Hynes, and D. D. Wagner, "The combined role of P- and E-selectins in atherosclerosis," *The Journal of Clinical Investigation*, vol. 102, no. 1, pp. 145–152, 1998.

[44] Y. Huo and K. Ley, "Adhesion molecules and atherogenesis," *Acta Physiologica Scandinavica*, vol. 173, no. 1, pp. 35–43, 2001.

[45] S. J. Shattil and M. H. Ginsberg, "Perspectives series: cell adhesion in vascular biology. Integrin signaling in vascular biology," *The Journal of Clinical Investigation*, vol. 100, no. 1, pp. 1–5, 1997.

[46] M. I. Cybulsky, K. Iiyama, H. Li et al., "A major role for VCAM-1, but not ICAM-1, in early atherosclerosis," *The Journal of Clinical Investigation*, vol. 107, no. 10, pp. 1255–1262, 2001.

[47] Y. Huo, A. Hafezi-Moghadam, and K. Ley, "Role of vascular cell adhesion molecule-1 and fibronectin connecting segment-1 in monocyte rolling and adhesion on early atherosclerotic lesions," *Circulation Research*, vol. 87, no. 2, pp. 153–159, 2000.

[48] C. L. Ramos, Y. Huo, U. Jung et al., "Direct demonstration of P-selectin– and VCAM-1–dependent mononuclear cell rolling in early atherosclerotic lesions of apolipoprotein E–deficient mice," *Circulation Research*, vol. 84, no. 11, pp. 1237–1244, 1999.

[49] R. R. Koenen, P. von Hundelshausen, I. V. Nesmelova et al., "Disrupting functional interactions between platelet chemokines inhibits atherosclerosis in hyperlipidemic mice," *Nature Medicine*, vol. 15, no. 1, pp. 97–103, 2009.

[50] C. Combadière, S. Potteaux, M. Rodero et al., "Combined inhibition of CCL2, CX3CR1, and CCR5 abrogates Ly$6C^{hi}$ and Ly$6C^{lo}$ Monocytosis and almost abolishes atherosclerosis in hypercholesterolemic mice," *Circulation*, vol. 117, no. 13, pp. 1649–1657, 2008.

[51] N. R. Veillard, S. Steffens, G. Pelli et al., "Differential influence of chemokine receptors CCR2 and CXCR3 in development of atherosclerosis in vivo," *Circulation*, vol. 112, no. 6, pp. 870–878, 2005.

[52] F. Tacke, D. Alvarez, T. J. Kaplan et al., "Monocyte subsets differentially employ CCR2, CCR5, and CX3CR1 to accumulate within atherosclerotic plaques," *The Journal of Clinical Investigation*, vol. 117, no. 1, pp. 185–194, 2007.

[53] P. Goossens, M. J. Gijbels, A. Zernecke et al., "Myeloid type I interferon signaling promotes atherosclerosis by stimulating macrophage recruitment to lesions," *Cell Metabolism*, vol. 12, no. 2, pp. 142–153, 2010.

[54] K. J. Williams and I. Tabas, "The response-to-retention hypothesis of early atherogenesis," *Arteriosclerosis, Thrombosis, and Vascular Biology*, vol. 15, no. 5, pp. 551–561, 1995.

[55] D. S. Leake, "Oxidised low density lipoproteins and atherogenesis," *Heart*, vol. 69, no. 6, pp. 476–478, 1993.

[56] V. V. Kunjathoor, M. Febbraio, E. A. Podrez et al., "Scavenger receptors class A-I/II and CD36 are the principal receptors responsible for the uptake of modified low density lipoprotein leading to lipid loading in macrophages," *Journal of Biological Chemistry*, vol. 277, no. 51, pp. 49982–49988, 2002.

[57] K. J. Moore, V. V. Kunjathoor, S. L. Koehn et al., "Loss of receptor-mediated lipid uptake via scavenger receptor A or CD36 pathways does not ameliorate atherosclerosis in hyperlipidemic mice," *The Journal of Clinical Investigation*, vol. 115, no. 8, pp. 2192–2201, 2005.

[58] M. Crucet, S. J. A. Wüst, P. Spielmann, T. F. Lüscher, R. H. Wenger, and C. M. Matter, "Hypoxia enhances lipid uptake in macrophages: role of the scavenger receptors Lox1, SRA, and CD36," *Atherosclerosis*, vol. 229, no. 1, pp. 110–117, 2013.

[59] A. P. Lillis, S. C. Muratoglu, D. T. Au et al., "LDL receptor-related protein-1 (LRP1) regulates cholesterol accumulation in macrophages," *PLoS One*, vol. 10, no. 6, article e0128903, 2015.

[60] N. J. Spann, L. X. Garmire, J. McDonald et al., "Regulated accumulation of desmosterol integrates macrophage lipid metabolism and inflammatory responses," *Cell*, vol. 151, no. 1, pp. 138–152, 2012.

[61] H. S. Kruth, N. L. Jones, W. Huang et al., "Macropinocytosis is the endocytic pathway that mediates macrophage foam cell formation with native low density lipoprotein," *Journal of Biological Chemistry*, vol. 280, no. 3, pp. 2352–2360, 2005.

[62] G. Zhu, Y. Xu, X. Cen, K. S. Nandakumar, S. Liu, and K. Cheng, "Targeting pattern-recognition receptors to discover new small molecule immune modulators," *European Journal of Medicinal Chemistry*, vol. 144, pp. 82–92, 2018.

[63] C. R. Stewart, L. M. Stuart, K. Wilkinson et al., "CD36 ligands promote sterile inflammation through assembly of a Toll-like receptor 4 and 6 heterodimer," *Nature Immunology*, vol. 11, no. 2, pp. 155–161, 2010.

[64] A. E. Mullick, P. S. Tobias, and L. K. Curtiss, "Modulation of atherosclerosis in mice by Toll-like receptor 2," *The Journal*

of Clinical Investigation, vol. 115, no. 11, pp. 3149–3156, 2005.

[65] H. Björkbacka, V. V. Kunjathoor, K. J. Moore et al., "Reduced atherosclerosis in MyD88-null mice links elevated serum cholesterol levels to activation of innate immunity signaling pathways," *Nature Medicine*, vol. 10, no. 4, pp. 416–421, 2004.

[66] K. S. Michelsen, M. H. Wong, P. K. Shah et al., "Lack of Toll-like receptor 4 or myeloid differentiation factor 88 reduces atherosclerosis and alters plaque phenotype in mice deficient in apolipoprotein E," *Proceedings of the National Academy of Sciences of the United States of America*, vol. 101, no. 29, pp. 10679–10684, 2004.

[67] R. Gareus, E. Kotsaki, S. Xanthoulea et al., "Endothelial Cell-Specific NF-κB Inhibition Protects Mice from Atherosclerosis," *Cell Metabolism*, vol. 8, no. 5, pp. 372–383, 2008.

[68] P. Duewell, H. Kono, K. J. Rayner et al., "NLRP3 inflammasomes are required for atherogenesis and activated by cholesterol crystals," *Nature*, vol. 464, no. 7293, pp. 1357–1361, 2010.

[69] F. Zheng, S. Xing, Z. Gong, W. Mu, and Q. Xing, "Silence of NLRP3 suppresses atherosclerosis and stabilizes plaques in apolipoprotein E-deficient mice," *Mediators of Inflammation*, vol. 2014, Article ID 507208, 8 pages, 2014.

[70] U. Schonbeck and P. Libby, "The CD40/CD154 receptor/ligand dyad," *Cellular and Molecular Life Sciences*, vol. 58, no. 1, pp. 4–43, 2001.

[71] S. X. Anand, J. F. Viles-Gonzalez, J. J. Badimon, E. Cavusoglu, and J. D. Marmur, "Membrane-associated CD40L and sCD40L in atherothrombotic disease," *Thrombosis and Haemostasis*, vol. 90, no. 3, pp. 377–384, 2003.

[72] Y. Chen, J. Chen, Y. Xiong et al., "Internalization of CD40 regulates its signal transduction in vascular endothelial cells," *Biochemical and Biophysical Research Communications*, vol. 345, no. 1, pp. 106–117, 2006.

[73] S. M. Lessner, D. E. Martinson, and Z. S. Galis, "Compensatory vascular remodeling during atherosclerotic lesion growth depends on matrix metalloproteinase-9 activity," *Arteriosclerosis, Thrombosis, and Vascular Biology*, vol. 24, no. 11, pp. 2123–2129, 2004.

[74] E. Ivan, J. J. Khatri, C. Johnson et al., "Expansive arterial remodeling is associated with increased neointimal macrophage foam cell content: the murine model of macrophage-rich carotid artery lesions," *Circulation*, vol. 105, no. 22, pp. 2686–2691, 2002.

[75] J. J. Boyle, P. L. Weissberg, and M. R. Bennett, "Human macrophage-induced vascular smooth muscle cell apoptosis requires NO enhancement of Fas/Fas-L interactions," *Arteriosclerosis, Thrombosis, and Vascular Biology*, vol. 22, no. 10, pp. 1624–1630, 2002.

[76] J. J. Boyle, D. E. Bowyer, P. L. Weissberg, and M. R. Bennett, "Human blood-derived macrophages induce apoptosis in human plaque-derived vascular smooth muscle cells by Fas-ligand/Fas interactions," *Arteriosclerosis, Thrombosis, and Vascular Biology*, vol. 21, no. 9, pp. 1402–1407, 2001.

[77] J. J. Boyle, P. L. Weissberg, and M. R. Bennett, "Tumor necrosis Factor-α promotes macrophage-induced vascular smooth muscle cell apoptosis by direct and autocrine mechanisms," *Arteriosclerosis, Thrombosis, and Vascular Biology*, vol. 23, no. 9, pp. 1553–1558, 2003.

[78] V. A. Fadok, D. L. Bratton, A. Konowal, P. W. Freed, J. Y. Westcott, and P. M. Henson, "Macrophages that have ingested apoptotic cells in vitro inhibit proinflammatory cytokine production through autocrine/paracrine mechanisms involving TGF-beta, PGE2, and PAF," *The Journal of Clinical Investigation*, vol. 101, no. 4, pp. 890–898, 1998.

[79] R. G. LeBaron, K. I. Bezverkov, M. P. Zimber, R. Pavelec, J. Skonier, and A. F. Purchio, "βIG-H3, a Novel Secretory Protein Inducible by Transforming Growth Factor-β, Is Present in Normal Skin and Promotes the Adhesion and Spreading of Dermal Fibroblasts In Vitro," *The Journal of Investigative Dermatology*, vol. 104, no. 5, pp. 844–849, 1995.

[80] D. A. Chistiakov, I. A. Sobenin, and A. N. Orekhov, "Vascular extracellular matrix in atherosclerosis," *Cardiology in Review*, vol. 21, no. 6, pp. 270–288, 2013.

[81] A. C. Newby, "Dual role of matrix metalloproteinases (matrixins) in intimal thickening and atherosclerotic plaque rupture," *Physiological Reviews*, vol. 85, no. 1, pp. 1–31, 2005.

[82] P. J. Gough, I. G. Gomez, P. T. Wille, and E. W. Raines, "Macrophage expression of active MMP-9 induces acute plaque disruption in apoE-deficient mice," *The Journal of Clinical Investigation*, vol. 116, no. 1, pp. 59–69, 2006.

[83] J. Johnson, S. George, A. Newby, and C. Jackson, "3HT03-3 matrix metalloproteinases-9 and -12 have opposite effects on atherosclerotic plaque stability," *Atherosclerosis Supplements*, vol. 4, no. 2, p. 196, 2003.

[84] I. Tabas, "Macrophage death and defective inflammation resolution in atherosclerosis," *Nature Reviews Immunology*, vol. 10, no. 1, pp. 36–46, 2010.

[85] C. Zhang, T. W. Syed, R. Liu, and J. Yu, "Role of endoplasmic reticulum stress, autophagy, and inflammation in cardiovascular disease," *Frontiers in Cardiovascular Medicine*, vol. 4, p. 29, 2017.

[86] T. Gotoh, M. Endo, and Y. Oike, "Endoplasmic reticulum stress-related inflammation and cardiovascular diseases," *International Journal of Inflammation*, vol. 2011, Article ID 259462, 8 pages, 2011.

[87] F. Bessone, M. V. Razori, and M. G. Roma, "Molecular pathways of nonalcoholic fatty liver disease development and progression," *Cellular and Molecular Life Sciences*, vol. 76, no. 1, pp. 99–128, 2019.

[88] I. Tabas, A. Tall, and D. Accili, "The impact of macrophage insulin resistance on advanced atherosclerotic plaque progression," *Circulation Research*, vol. 106, no. 1, pp. 58–67, 2010.

[89] M. Myoishi, H. Hao, T. Minamino et al., "Increased endoplasmic reticulum stress in atherosclerotic plaques associated with acute coronary syndrome," *Circulation*, vol. 116, no. 11, pp. 1226–1233, 2007.

[90] H. Tsukano, T. Gotoh, M. Endo et al., "The endoplasmic reticulum stress-C/EBP homologous protein pathway-mediated apoptosis in macrophages contributes to the instability of atherosclerotic plaques," *Arteriosclerosis, Thrombosis, and Vascular Biology*, vol. 30, no. 10, pp. 1925–1932, 2010.

[91] E. Thorp, G. Li, T. A. Seimon, G. Kuriakose, D. Ron, and I. Tabas, "Reduced apoptosis and plaque necrosis in advanced atherosclerotic lesions of Apoe−/− and Ldlr−/− mice lacking CHOP," *Cell Metabolism*, vol. 9, no. 5, pp. 474–481, 2009.

[92] J. Deng, P. D. Lu, Y. Zhang et al., "Translational repression mediates activation of nuclear factor kappa B by phosphorylated translation initiation factor 2," *Molecular and Cellular Biology*, vol. 24, no. 23, pp. 10161–10168, 2004.

[93] P. Hu, Z. Han, A. D. Couvillon, R. J. Kaufman, and J. H. Exton, "Autocrine tumor necrosis factor alpha links endoplasmic reticulum stress to the membrane death receptor pathway through IRE1α-mediated NF-κB activation and down-regulation of TRAF2 expression," *Molecular and Cellular Biology*, vol. 26, no. 8, pp. 3071–3084, 2006.

[94] S. B. Cullinan and J. A. Diehl, "Coordination of ER and oxidative stress signaling: the PERK/Nrf2 signaling pathway," *The International Journal of Biochemistry & Cell Biology*, vol. 38, no. 3, pp. 317–332, 2006.

[95] T. Gotoh and M. Mori, "Nitric oxide and endoplasmic reticulum stress," *Arteriosclerosis, Thrombosis, and Vascular Biology*, vol. 26, no. 7, pp. 1439–1446, 2006.

[96] J. Navarro-Yepes, M. Burns, A. Anandhan et al., "Oxidative stress, redox signaling, and autophagy: cell death versus survival," *Antioxidants & Redox Signaling*, vol. 21, no. 1, pp. 66–85, 2014.

[97] D. M. Schrijvers, G. R. Y. de Meyer, M. M. Kockx, A. G. Herman, and W. Martinet, "Phagocytosis of apoptotic cells by macrophages is impaired in atherosclerosis," *Arteriosclerosis, Thrombosis, and Vascular Biology*, vol. 25, no. 6, pp. 1256–1261, 2005.

[98] Y. Kojima, J. P. Volkmer, K. McKenna et al., "CD47-blocking antibodies restore phagocytosis and prevent atherosclerosis," *Nature*, vol. 536, no. 7614, pp. 86–90, 2016.

[99] Y. Kojima, K. Downing, R. Kundu et al., "Cyclin-dependent kinase inhibitor 2B regulates efferocytosis and atherosclerosis," *The Journal of Clinical Investigation*, vol. 124, no. 3, pp. 1083–1097, 2014.

[100] K. Gillotte-Taylor, A. Boullier, J. L. Witztum, D. Steinberg, and O. Quehenberger, "Scavenger receptor class B type I as a receptor for oxidized low density lipoprotein," *Journal of Lipid Research*, vol. 42, no. 9, pp. 1474–1482, 2001.

[101] L. Yvan-Charvet, T. A. Pagler, T. A. Seimon et al., "ABCA1 and ABCG1 protect against oxidative stress–induced macrophage apoptosis during efferocytosis," *Circulation Research*, vol. 106, no. 12, pp. 1861–1869, 2010.

[102] B. Cai, E. B. Thorp, A. C. Doran et al., "MerTK receptor cleavage promotes plaque necrosis and defective resolution in atherosclerosis," *The Journal of Clinical Investigation*, vol. 127, no. 2, pp. 564–568, 2017.

[103] C. D. Mills, K. Kincaid, J. M. Alt, M. J. Heilman, and A. M. Hill, "M-1/M-2 macrophages and the Th1/Th2 paradigm," *The Journal of Immunology*, vol. 164, no. 12, pp. 6166–6173, 2000.

[104] T. Krausgruber, K. Blazek, T. Smallie et al., "IRF5 promotes inflammatory macrophage polarization and T_H1-T_H17 responses," *Nature Immunology*, vol. 12, no. 3, pp. 231–238, 2011.

[105] F. A. W. Verreck, T. de Boer, D. M. L. Langenberg et al., "Human IL-23-producing type 1 macrophages promote but IL-10-producing type 2 macrophages subvert immunity to (myco)bacteria," *Proceedings of the National Academy of Sciences of the United States of America*, vol. 101, no. 13, pp. 4560–4565, 2004.

[106] D. M. Mosser, "The many faces of macrophage activation," *Journal of Leukocyte Biology*, vol. 73, no. 2, pp. 209–212, 2003.

[107] G. J. Kotwal and S. Chien, "Macrophage differentiation in normal and accelerated wound healing," *Results and Problems in Cell Differentiation*, vol. 62, pp. 353–364, 2017.

[108] S. Gordon and F. O. Martinez, "Alternative activation of macrophages: mechanism and functions," *Immunity*, vol. 32, no. 5, pp. 593–604, 2010.

[109] U. Juhas, M. Ryba-Stanislawowska, P. Szargiej, and J. Mysliwska, "Different pathways of macrophage activation and polarization," *Postępy Higieny i Medycyny Doświadczalnej*, vol. 69, pp. 496–502, 2015.

[110] M. A. Bouhlel, B. Derudas, E. Rigamonti et al., "PPARγ activation primes human monocytes into alternative M2 macrophages with anti-inflammatory properties," *Cell Metabolism*, vol. 6, no. 2, pp. 137–143, 2007.

[111] J. L. Stöger, M. J. J. Gijbels, S. van der Velden et al., "Distribution of macrophage polarization markers in human atherosclerosis," *Atherosclerosis*, vol. 225, no. 2, pp. 461–468, 2012.

[112] Y. Hirata, M. Tabata, H. Kurobe et al., "Coronary atherosclerosis is associated with macrophage polarization in epicardial adipose tissue," *Journal of the American College of Cardiology*, vol. 58, no. 3, pp. 248–255, 2011.

[113] M. de Gaetano, D. Crean, M. Barry, and O. Belton, "M1- and M2-type macrophage responses are predictive of adverse outcomes in human atherosclerosis," *Frontiers in Immunology*, vol. 7, p. 275, 2016.

[114] V. Piccolo, A. Curina, M. Genua et al., "Opposing macrophage polarization programs show extensive epigenomic and transcriptional cross-talk," *Nature Immunology*, vol. 18, no. 5, pp. 530–540, 2017.

[115] C. A. Gleissner, I. Shaked, K. M. Little, and K. Ley, "CXC chemokine ligand 4 induces a unique transcriptome in monocyte-derived macrophages," *The Journal of Immunology*, vol. 184, no. 9, pp. 4810–4818, 2010.

[116] F. Geissmann, S. Jung, and D. R. Littman, "Blood monocytes consist of two principal subsets with distinct migratory properties," *Immunity*, vol. 19, no. 1, pp. 71–82, 2003.

[117] A. Ghattas, H. R. Griffiths, A. Devitt, G. Y. Lip, and E. Shantsila, "Monocytes in coronary artery disease and atherosclerosis: where are we now?," *Journal of the American College of Cardiology*, vol. 62, no. 17, pp. 1541–1551, 2013.

[118] E. A. L. Biessen and K. Wouters, "Macrophage complexity in human atherosclerosis: opportunities for treatment?," *Current Opinion in Lipidology*, vol. 28, no. 5, pp. 419–426, 2017.

[119] G. A. Foster, R. M. Gower, K. L. Stanhope, P. J. Havel, S. I. Simon, and E. J. Armstrong, "On-chip phenotypic analysis of inflammatory monocytes in atherogenesis and myocardial infarction," *Proceedings of the National Academy of Sciences of the United States of America*, vol. 110, no. 34, pp. 13944–13949, 2013.

[120] A. Merino, P. Buendia, A. Martin-Malo, P. Aljama, R. Ramirez, and J. Carracedo, "Senescent $CD14^+CD16^+$ monocytes exhibit proinflammatory and proatherosclerotic activity," *The Journal of Immunology*, vol. 186, no. 3, pp. 1809–1815, 2011.

[121] S. Potteaux, E. L. Gautier, S. B. Hutchison et al., "Suppressed monocyte recruitment drives macrophage removal from atherosclerotic plaques of *Apoe*$^{-/-}$ mice during disease regression," *The Journal of Clinical Investigation*, vol. 121, no. 5, pp. 2025–2036, 2011.

[122] J. E. Feig, I. Pineda-Torra, M. Sanson et al., "LXR promotes the maximal egress of monocyte-derived cells from mouse

aortic plaques during atherosclerosis regression," *The Journal of Clinical Investigation*, vol. 120, no. 12, pp. 4415–4424, 2010.

[123] S. Hadjiphilippou and K. K. Ray, "Evolocumab and clinical outcomes in patients with cardiovascular disease," *The Journal of the Royal College of Physicians of Edinburgh*, vol. 47, no. 2, pp. 153–155, 2017.

[124] G. G. Schwartz, P. G. Steg, M. Szarek et al., "Alirocumab and cardiovascular outcomes after acute coronary syndrome," *The New England Journal of Medicine*, vol. 379, no. 22, pp. 2097–2107, 2018.

[125] K. K. Ray, H. M. Colhoun, M. Szarek et al., "Effects of alirocumab on cardiovascular and metabolic outcomes after acute coronary syndrome in patients with or without diabetes: a prespecified analysis of the ODYSSEY OUTCOMES randomised controlled trial," *The Lancet Diabetes and Endocrinology*, vol. 7, no. 8, pp. 618–628, 2019.

[126] The HPS3/TIMI55–REVEAL Collaborative Group, "Effects of anacetrapib in patients with atherosclerotic vascular disease," *The New England Journal of Medicine*, vol. 377, no. 13, pp. 1217–1227, 2017.

[127] A. Thompson, E. Di Angelantonio, N. Sarwar et al., "Association of cholesteryl ester transfer protein genotypes with CETP mass and activity, lipid levels, and coronary risk," *JAMA*, vol. 299, no. 23, pp. 2777–2788, 2008.

[128] Z. H. Tang, T. H. Li, J. Peng et al., "PCSK9: a novel inflammation modulator in atherosclerosis?," *Journal of Cellular Physiology*, vol. 234, no. 3, pp. 2345–2355, 2019.

[129] Z. Ding, S. Liu, X. Wang et al., "Hemodynamic shear stress via ROS modulates PCSK9 expression in human vascular endothelial and smooth muscle cells and along the mouse aorta," *Antioxidants & Redox Signaling*, vol. 22, no. 9, pp. 760–771, 2015.

[130] I. Giunzioni, H. Tavori, R. Covarrubias et al., "Local effects of human PCSK9 on the atherosclerotic lesion," *The Journal of Pathology*, vol. 238, no. 1, pp. 52–62, 2016.

[131] S. J. Bernelot Moens, A. E. Neele, J. Kroon et al., "PCSK9 monoclonal antibodies reverse the pro-inflammatory profile of monocytes in familial hypercholesterolaemia," *European Heart Journal*, vol. 38, no. 20, pp. 1584–1593, 2017.

[132] K. R. Walley, K. R. Thain, J. A. Russell et al., "PCSK9 is a critical regulator of the innate immune response and septic shock outcome," *Science Translational Medicine*, vol. 6, no. 258, article 258ra143, 2014.

[133] M. Back and G. K. Hansson, "Anti-inflammatory therapies for atherosclerosis," *Nature Reviews Cardiology*, vol. 12, no. 4, pp. 199–211, 2015.

[134] J. Gilbert, J. Lekstrom-Himes, D. Donaldson et al., "Effect of CC chemokine receptor 2 CCR2 blockade on serum C-reactive protein in individuals at atherosclerotic risk and with a single nucleotide polymorphism of the monocyte chemoattractant protein-1 promoter region," *The American Journal of Cardiology*, vol. 107, no. 6, pp. 906–911, 2011.

[135] O. Kleveland, G. Kunszt, M. Bratlie et al., "Effect of a single dose of the interleukin-6 receptor antagonist tocilizumab on inflammation and troponin T release in patients with non-ST-elevation myocardial infarction: a double-blind, randomized, placebo-controlled phase 2 trial," *European Heart Journal*, vol. 37, no. 30, pp. 2406–2413, 2016.

[136] P. M. Ridker, B. M. Everett, T. Thuren et al., "Antiinflammatory therapy with canakinumab for atherosclerotic disease," *The New England Journal of Medicine*, vol. 377, no. 12, pp. 1119–1131, 2017.

[137] A. Abbate, B. W. van Tassell, and G. G. L. Biondi-Zoccai, "Blocking interleukin-1 as a novel therapeutic strategy for secondary prevention of cardiovascular events," *BioDrugs*, vol. 26, no. 4, pp. 217–233, 2012.

[138] P. M. Ridker, J. MacFadyen, B. M. Everett et al., "Relationship of C-reactive protein reduction to cardiovascular event reduction following treatment with canakinumab: a secondary analysis from the CANTOS randomised controlled trial," *The Lancet*, vol. 391, no. 10118, pp. 319–328, 2018.

[139] C. Roubille, V. Richer, T. Starnino et al., "The effects of tumour necrosis factor inhibitors, methotrexate, non-steroidal anti-inflammatory drugs and corticosteroids on cardiovascular events in rheumatoid arthritis, psoriasis and psoriatic arthritis: a systematic review and meta-analysis," *Annals of the Rheumatic Diseases*, vol. 74, no. 3, pp. 480–489, 2015.

[140] J. Nomura, N. Busso, A. Ives et al., "Xanthine oxidase inhibition by febuxostat attenuates experimental atherosclerosis in mice," *Scientific Reports*, vol. 4, no. 1, 2014.

[141] P. Toledo-Ibelles and J. Mas-Oliva, "Antioxidants in the fight against atherosclerosis: is this a dead end?," *Current Atherosclerosis Reports*, vol. 20, no. 7, p. 36, 2018.

[142] W. J. Kelley, H. Safari, G. Lopez-Cazares, and O. Eniola-Adefeso, "Vascular-targeted nanocarriers: design considerations and strategies for successful treatment of atherosclerosis and other vascular diseases," *Wiley Interdisciplinary Reviews: Nanomedicine and Nanobiotechnology*, vol. 8, no. 6, pp. 909–926, 2016.

[143] S. Verheye, W. Martinet, M. M. Kockx et al., "Selective clearance of macrophages in atherosclerotic plaques by autophagy," *Journal of the American College of Cardiology*, vol. 49, no. 6, pp. 706–715, 2007.

[144] K. Nakano, K. Egashira, K. Ohtani et al., "Catheter-based adenovirus-mediated anti-monocyte chemoattractant gene therapy attenuates in-stent neointima formation in cynomolgus monkeys," *Atherosclerosis*, vol. 194, no. 2, pp. 309–316, 2007.

[145] S. Gordon, A. Pluddemann, and F. Martinez Estrada, "Macrophage heterogeneity in tissues: phenotypic diversity and functions," *Immunological Reviews*, vol. 262, no. 1, pp. 36–55, 2014.

[146] K. R. Peterson, M. A. Cottam, A. J. Kennedy, and A. H. Hasty, "Macrophage-targeted therapeutics for metabolic disease," *Trends in Pharmacological Sciences*, vol. 39, no. 6, pp. 536–546, 2018.

[147] J. Tang, M. E. Lobatto, L. Hassing et al., "Inhibiting macrophage proliferation suppresses atherosclerotic plaque inflammation," *Science Advances*, vol. 1, no. 3, article e1400223, 2015.

[148] N. van Rooijen and E. van Kesteren-Hendrikx, ""In Vivo" Depletion of Macrophages by Liposome-Mediated "Suicide"," *Methods in Enzymology*, vol. 373, pp. 3–16, 2003.

[149] C. A. Dinarello, "Anti-inflammatory agents: present and future," *Cell*, vol. 140, no. 6, pp. 935–950, 2010.

[150] L. Bu, M. Gao, S. Qu, and D. Liu, "Intraperitoneal injection of clodronate liposomes eliminates visceral adipose macrophages and blocks high-fat diet-induced weight gain and development of insulin resistance," *The AAPS Journal*, vol. 15, no. 4, pp. 1001–1011, 2013.

[151] V. Stoneman, D. Braganza, N. Figg et al., "Monocyte/macrophage suppression in CD11b diphtheria toxin receptor transgenic mice differentially affects atherogenesis and established plaques," *Circulation Research*, vol. 100, no. 6, pp. 884–893, 2007.

[152] Y. Bi, J. Chen, F. Hu, J. Liu, M. Li, and L. Zhao, "M2 macrophages as a potential target for antiatherosclerosis treatment," *Neural Plasticity*, vol. 2019, Article ID 6724903, 21 pages, 2019.

[153] C. Brenner, W. M. Franz, S. Kühlenthal et al., "DPP-4 inhibition ameliorates atherosclerosis by priming monocytes into M2 macrophages," *International Journal of Cardiology*, vol. 199, pp. 163–169, 2015.

Hindawi
Journal of Immunology Research
Volume 2019, Article ID 1278301, 15 pages
https://doi.org/10.1155/2019/1278301

Research Article

Distinct Redox Signalling following Macrophage Activation Influences Profibrotic Activity

Caitlin V. Lewis,[1] Antony Vinh,[1,2] Henry Diep,[1,2] Chrishan S. Samuel,[1] Grant R. Drummond,[1,2] and Barbara K. Kemp-Harper[1]

[1]*Cardiovascular Disease Program, Biomedicine Discovery Institute & Department of Pharmacology, Monash University, VIC 3800, Australia*
[2]*Department of Physiology, Anatomy & Microbiology, School of Life Sciences, La Trobe University, VIC 3086, Australia*

Correspondence should be addressed to Barbara K. Kemp-Harper; barbara.kemp@monash.edu

Received 19 April 2019; Accepted 13 September 2019; Published 11 November 2019

Guest Editor: Mohammad A. Khan

Aims. To date, the ROS-generating capacities of macrophages in different activation states have not been thoroughly compared. This study is aimed at determining the nature and levels of ROS generated following stimulation with common activators of M1 and M2 macrophages and investigating the potential for this to impact fibrosis. *Results*. Human primary and THP-1 macrophages were treated with IFN-γ+LPS or IL-4-activating stimuli, and mRNA expression of established M1 (CXCL11, CCR7, IL-1β) and M2 (MRC-1, CCL18, CCL22) markers was used to confirm activation. Superoxide generation was assessed by L-012-enhanced chemiluminescence and was increased in both M(IFN-γ+LPS) and M(IL-4) macrophages, as compared to unpolarised macrophages (MΦ). This signal was attenuated with NOX2 siRNA. Increased expression of the p47phox and p67phox subunits of the NOX2 oxidase complex was evident in M(IFN-γ+LPS) and M(IL-4) macrophages, respectively. Amplex Red and DCF fluorescence assays detected increased hydrogen peroxide generation following stimulation with IL-4, but not IFN-γ+LPS. Coculture with human aortic adventitial fibroblasts revealed that M(IL-4), but not M(IFN-γ+LPS), enhanced fibroblast collagen 1 protein expression. Macrophage pretreatment with the hydrogen peroxide scavenger, PEG-catalase, attenuated this effect. *Conclusion*. We show that superoxide generation is not only enhanced with stimuli associated with M1 macrophage activation but also with the M2 stimulus IL-4. Macrophages activated with IL-4 also exhibited enhanced hydrogen peroxide generation which in turn increased aortic fibroblast collagen production. Thus, M2 macrophage-derived ROS is identified as a potentially important contributor to aortic fibrosis.

1. Introduction

Macrophages are key cells of the innate immune system and their activation and function is important in tissue homeostasis, disease pathogenesis, and immune regulation [1]. Macrophages exist as a heterogeneous population, continually responding to local microenvironment cues [2]. Over recent years, research has explored the generally opposing roles of two broad populations of macrophage, the "classically activated" proinflammatory M1 macrophage and the "alternatively activated" M2 macrophage. Representing either ends of a spectrum of activation or "polarisation," M1 and M2 macrophages are thought to play predominant roles in inflammation and tissue repair, respectively, although this paradigm is now considered overly simplified [1–3]. It is now recognized that the precise stimuli for activation are important in determining the characteristics and expression profiles of activated macrophages, which can vary greatly across different *in vitro* and *in vivo* contexts [3]. Nonetheless, understanding how macrophages respond to different cytokines and factors in the microenvironment can inform on their contribution to various disease states and identify new therapeutic targets. To date, the reactive oxygen species (ROS)-generating capacities of macrophages in different activation states have not been thoroughly compared.

The initial infiltration of macrophages to a site of injury leads to the generation of proinflammatory cytokines and ROS. Whilst this defense mechanism contributes

to microbial killing, it also exacerbates inflammatory disease. M1 macrophages which are activated by these proinflammatory cytokines (e.g., IFN-γ) play a predominant role in this setting, and a contribution of ROS to these processes is evident [4]. Thus, M1 macrophage-derived superoxide, together with inducible nitric oxide synthase (iNOS)-derived nitric oxide (NO), can lead to the generation of the powerful oxidant, peroxynitrite. Whilst peroxynitrite is central to pathogen killing, it can also cause oxidation and nitration of proteins and lipids. Importantly, the ROS-generating capacity of M1 macrophages is reliant predominantly on the activity of the NOX2 isoform of the NADPH oxidase (NOX) family of enzymes which is highly expressed in macrophages. Inflammatory stimuli increase the expression and activity of NOX2 oxidase as an important mechanism of microbial killing [5–7]. Given their well-recognized ROS-generating capacity [8, 9], M1 macrophages have been shown to contribute to inflammation-associated organ damage [10], observed in diseases such as hypertension, diabetes, and kidney disease [11–13].

In the later phases of the disease process, macrophages release anti-inflammatory molecules and growth factors and promote healing and regeneration. Whilst initially beneficial, the healing process becomes pathological when it is continuous, leading to remodeling of the extracellular matrix. Macrophages recruited for these processes, termed "M2" or "alternatively activated" macrophages, are commonly activated by Th2 cytokines, anti-inflammatory cytokines, and growth factors [1]. This is of particular relevance in the setting of hypertension in which we have demonstrated the accumulation of M2 macrophages, as indicated by expression of the marker CD206 (also known as MRC-1), in the vessel wall associated with aortic stiffening and increased collagen deposition [14]. The profibrotic effects of M2 macrophages are generally attributed to their ability to generate transforming growth factor-β (TGF-β) and platelet-derived growth factor (PDGF) [1, 15], thereby promoting differentiation of fibroblasts to collagen-generating myofibroblasts [16, 17]. Of note, M2 macrophages also express NOX2 oxidase and have the capacity to generate ROS [18]. As such, it is possible that their generation of ROS, particularly hydrogen peroxide, may also contribute to this profibrotic response. Evidence in support of this concept comes from the observation that NOX-derived superoxide can be rapidly converted to hydrogen peroxide, which has been shown to directly stimulate collagen production and myofibroblast differentiation of fibroblasts *in vitro* [19]. Furthermore, the profibrotic effect of coculturing pulmonary fibroblasts with macrophages was shown to be reduced in the presence of the NOX inhibitor apocynin [20]. Thus, ROS may represent a novel mediator of the remodelling actions of M2 macrophages observed in fibrotic diseases, such as lung fibrosis, muscular dystrophy [21, 22] and the aortic stiffening associated with hypertension [14].

To date, it has been generally assumed that M1 macrophages have an enhanced oxidative capacity [2, 8, 9], contributing to their proinflammatory properties and tissue damaging effects. Hence, ROS generation is considered an "M1" function. However, no studies have directly compared the oxidative capacity, NOX2 activity, and the nature of the ROS generated by M1 and M2 macrophages. Whether the amount and type of ROS generated impacts on their functions in disease, particularly with regard to fibrosis, remains to be determined. Inconsistency in the terminology and definition of macrophage subsets and limitations in translation between *in vitro* and *in vivo* macrophages has recently been acknowledged [3]. This study is aimed at elucidating whether macrophages stimulated with commonly used Th1 (IFN-γ and LPS) versus Th2 (IL-4) stimuli exhibit a differential capacity to generate ROS. We also aim to compare the nature of the ROS generated and investigate whether this may, in turn, influence their profibrotic capacity. These macrophages will be referred to as M(IFN-γ+LPS) and M(IL-4) according to the recommendations from Murray et al. [3].

2. Materials and Methods

2.1. Primary Human Monocyte Isolation. Primary human monocytes were isolated from healthy blood donor buffy coats (Australian Red Cross Blood Service, Melbourne, Australia). Buffy coats were mixed with phosphate-buffered saline (PBS; without Ca^{2+}or Mg^{2+}; Sigma-Aldrich) supplemented with 0.5% fetal bovine serum (FBS; Sigma-Aldrich) and 2 mM ethylenediaminetetraacetic acid (EDTA; Sigma-Aldrich) and layered onto Ficoll-Paque PLUS (GE Healthcare no. 17-144) for density gradient centrifugation (400 g, 40 minutes, acceleration = 1, deceleration = 0). The peripheral blood mononuclear cell (PBMC) layer was collected and monocytes isolated using a human pan monocyte isolation kit (Miltenyi Biotec no. 130-096-537), according to the manufacturer's instructions. The purity of the monocyte population was confirmed to be at least 85% as determined by flow cytometry using $CD14^+/CD16^+$ expression.

2.2. Monocyte to Macrophage Differentiation and Macrophage Activation. The THP-1 human monocytic cell line was supplied by Dr. Meritxell Canals (Monash Institute of Pharmaceutical Sciences, Parkville, Australia). THP-1 cells were cultured in high-glucose RPMI 1640 medium (Gibco Life Technologies), supplemented with 10% heat-inactivated FBS and grown in T75 tissue culture flasks in a humidified incubator maintained at 37°C with 5% CO_2 (Sanyo MCO-18AIC CO_2 incubator, Quantum Scientific). THP-1 monocytes were passaged every 3-4 days and seeded on 6-well plates (1×10^6 cells/well) for RNA and protein extraction or 96-well plates (5×10^4 cells/well) for superoxide and hydrogen peroxide detection. THP-1 monocytes were differentiated to macrophages (MΦ) via the addition of 100 nM phorbol-12,13-dibutyrate (PDBu, Calbiochem) for 24 hours. THP-1 macrophages were subsequently left untreated (MΦ) or treated with either a combination of 5 ng/ml interferon-γ (IFN-γ; Sigma-Aldrich no. I3265) and 10 ng/ml lipopolysaccharide (LPS; Sigma-Aldrich no. L2630, E. coli 0111:B4 strain) or with 25 ng/ml interleukin-4 (IL-4; Sigma-Aldrich no. I4269), for 24, 48, or 72 hours for PCR, western blotting, and ROS detection. A subset of macrophages were treated in the presence of 100 nM NOX2 siRNA (Santa-Cruz no. sc-35503) or missense siRNA

(control siRNA-A; Santa-Cruz no. sc-37007). These cells were transfected using Lipofectamine RNAiMAX (Gibco Life Technologies) in opti-minimum essential medium (Opti-MEM, Gibco Life Technologies) for 6 hours prior to polarisation in complete RPMI 1640 culture medium.

Isolated donor blood-derived primary monocytes (1×10^6 cells/ml) were differentiated into macrophages by culturing for 7 days in RPMI 1640 GlutaMAX medium (Gibco Life Technologies), supplemented with 10% FBS, 1× antibiotic/antimyotic (Gibco Life Technologies, USA), 1 mM sodium pyruvate (Sigma-Aldrich), 1× nonessential amino acids (NEAA; Gibco Life Technologies), and 50 ng/ml macrophage colony-stimulating factor (M-CSF; Miltenyi Biotec no. 130-096-491). Following a 7-day macrophage differentiation, human primary macrophages were either left untreated (MΦ), treated with 100 ng/ml LPS and 20 ng/ml IFN-γ, or treated with 25 ng/ml IL-4 in the absence of M-CSF. Cells were treated for either 3, 6, or 24 hours for real-time PCR or for 24 hours for western blotting and L-012-enhanced chemiluminescence.

2.3. Aortic Fibroblast Coculture with M(IFN-γ+LPS) or M(IL-4) Macrophages. Primary human aortic adventitial fibroblasts (AoAF; Lonza no. CC-7014; Lonza) were grown in Stromal Cell Growth Medium (SCGM; Lonza no. CC-3205), containing 5% FBS and used from passages 2 to 8. Fibroblasts were maintained in T-75 flasks in a humidified incubator at 37°C with 5% CO_2. Once confluent, AoAFs were passaged in SCGM using Trypsin-EDTA solution (Lonza no. CC-5012) for cell detachment. For coculture experiments, THP-1 macrophages were first stimulated with IFN-γ/LPS or IL-4 for 72 hours in complete RPMI 1640 medium in 24-well cell culture inserts (0.4 μm pore, $<0.85 \times 10^8$ pores/cm^2, 5×10^4 cells/insert; Thermo Fisher Scientific). The THP-1 medium was replaced with serum-free RPMI 1640 medium, and the inserts were transferred to wells with AoAF (5×10^4 cells/well) in serum-free SCGM. THP-1 macrophages were stimulated with 10 μM PDBu in the presence or absence of 1000 U/ml PEG-catalase (Sigma-Aldrich no. C4963), and the cultures incubated for further 24 hours before lysates were harvested for western blotting.

2.4. RNA Extraction and Real-Time PCR. Total RNA was extracted from macrophages using the RNeasy Mini Kit (Qiagen) according to the manufacturer's instructions. RNase-free DNase (Qiagen) was used to remove any contaminating DNA. The amount of RNA in each sample was quantified using the NanoDrop 1000D spectrophotometer (Thermo Scientific), which measures absorbance at 260 nm and 280 nm. An $A_{260}:A_{280}$ ratio of 2 or more was considered sufficiently pure. 1 μg of RNA from each sample was reverse transcribed into cDNA using the High Capacity cDNA Reverse Transcription Kit (Applied Biosystems) with the reaction run in a thermal cycler (Bio-Rad MyCycler, Bio-Rad Laboratories). The resultant cDNA was used as a template for real-time PCR with TaqMan® primers and probes for IL-1β, CXCL11, CCR7, MRC-1, CCL22, CCL18, CYBA (p22phox), CYBB (NOX2), NCF1 (p47phox), NCF2 (p67phox), NCF4 (p40phox), NOX1, NOX4, NOX5, SOD1, SOD2, and SOD3 (Applied Biosystems). β-Actin and 18S were used as housekeeping genes. Real-time PCR was run in triplicate on the CFX96 Touch™ Real-Time PCR Detection Machine (Bio-Rad Laboratories). Gene expression was normalised to β-actin or 18S and quantified relative to the average MΦ value using the comparative cycle threshold (Ct) method with the formula: fold change = $2^{-\Delta\Delta Ct}$ [23].

2.5. Protein Extraction and Western Blotting. Total protein from macrophage and fibroblast cell lysates was collected in 1.5× Laemmli buffer (7.5% glycerol; 3.75% β-mercaptoethanol; 2.25% SDS; 75 mM Tris-HCl pH 6.8; 0.004% bromophenol blue) and 1× RIPA lysis and extraction buffer (Cell Signaling Technology, USA), respectively. Cell debris was cleared by centrifugation (13000 rpm, 10 min, 4°C) and supernatants collected. Protein concentrations were determined using either a modified Lowry protocol (RCDC colorimetric protein assay kit; Bio-Rad Laboratories) or bicinchoninic acid- (BCA-) based colorimetric quantification (Pierce™ BCA Protein Assay, Thermo Scientific). Equivalent volumes of protein in 1.5× Laemmli buffer were loaded into 7.5% or 10% polyacrylamide gels. Proteins were separated by SDS-PAGE and transferred onto low fluorescence polyvinylidene fluoride (LF PVDF) membranes using the Bio-Rad Trans Blot Turbo transfer system (Bio-Rad Laboratories). Membranes were blocked with 5% skim milk in Tris-buffered saline (TBS; 200 mM Tris, 150 mM NaCl, pH 7.5) with 0.1% Tween-20 for 1 hour and subsequently probed with primary antibodies against NOX2 (1 : 500; Santa-Cruz no. sc-130549 (CL5)), p47phox (1 : 1000; BD Transduction Laboratories no. 610354), p67phox (1 : 2000; EMD Millipore no. 07-002), SOD2 (1 : 1000; EMD Millipore no. 06-984), SOD3 (1 : 1000; EMD Millipore no. 07-704), αSMA (1 : 2500; Abcam no. ab5694) or collagen 1 (1 : 1000; Abcam no. ab34710), and the housekeeping protein GAPDH (1 : 20000; Abcam no. ab8245) overnight at 4°C. 1 hour incubation with horseradish peroxidase- (HRP-) conjugated anti-rabbit (1 : 10000; Dako) or anti-mouse (1 : 10000; Jackson ImmunoResearch Laboratories) secondary antibody was then performed and protein bands visualised using Clarity ECL substrate (Bio-Rad Laboratories) and the ChemiDoc MP system (Bio-Rad Laboratories). Densitometries of protein bands were quantified using Image Lab Software (Bio-Rad Laboratories) and normalised to the housekeeping protein, GAPDH.

2.6. Superoxide Detection via L-012-Enhanced Chemiluminescence. THP-1 or human primary macrophages were seeded and activated on white 96-well tissue culture plates (PerkinElmer) at 5×10^4 and 2×10^5 cells/well, respectively. Groups were set up in quintuplicate with a cell-free control group, comprising media alone, included to provide a background reference. On the day of experimentation, culture medium was removed and cells were washed and incubated in warmed Krebs-HEPES buffer (118 mM NaCl, 4.7 mM KCl, 1.2 mM KH_2PO_4, 1.2 mM $MgSO_4 \cdot 7H_2O$, 2.5 mM $CaCl_2$, 25 mM $NaHCO_3$, 11.7 mM glucose, 20 mM HEPES; pH 7.4) and background chemiluminescence

measured for 30 minutes. Chemiluminescence was measured using a Chameleon Luminescence Plate Reader (Hidex Ltd., Turku, Finland) and data acquired using the MicroWin (Mikrotek, Overath, Germany) data acquisition system. 100 μM L-012 (Wako Pure Chemical Industries) was then added to each well, and basal superoxide levels were monitored for 30 minutes. Finally, the protein kinase C (PKC) activator PDBu (10 μM) was added to each well and superoxide production was then measured for a further 30 minutes. PDBu-stimulated superoxide production was quantified as the average signal over 5 minutes at its peak. The basal signal from each signal was subtracted (average over final 5 minutes). In a subset of experiments, cells were treated with superoxide dismutase (SOD; 1000 U/ml; human recombinant, expressed in *E. coli*; Sigma-Aldrich S9076) just prior to the beginning of the assay, to confirm signal specificity for superoxide.

2.7. Hydrogen Peroxide Detection via Amplex Red. THP-1 macrophages were seeded and activated on black 96-well tissue culture plates (PerkinElmer) at 5×10^4 cells/well in quintuplicate. On the day of experimentation, the media was removed, cells rinsed with Krebs-HEPES solution, and Krebs-HEPES added to each well in the absence or presence of 1000 U/ml SOD or PEG-Catalase. Working Amplex Red solution (Invitrogen), comprising of Amplex Red (5 μM) and HRP (0.2 U/μl), was then added to sample wells and fluorescence detected over 90 minutes using a Hidex Chameleon Plate Reader at 37°C (520 nm excitation filter, 590 nm emission filter). Cells were either left unstimulated or stimulated with 10 μM PDBu immediately prior to reading. The final fluorescence measurement from each group was fitted to a hydrogen peroxide standard curve (0-5 μM). Fold changes in hydrogen peroxide concentration were calculated relative to the MΦ value recorded on the same day.

2.8. Intracellular ROS Detection via DCF. THP-1 macrophages were stimulated with IFN-γ/LPS or IL-4 for 72 hours in complete RPMI 1640 medium on 6-well plates at 1×10^6 cells/well. Adherent cells were washed with warmed PBS prior to incubation with a cell permeable ROS-sensitive dye, 5-(and-6)-chloromethyl-2′,7′-dichlorodihydrofluorescein diacetate, acetyl ester (CM-H_2DCFDA; DCF; 1 μM, Sigma-Aldrich no. D6883) for 30 minutes at 37°C. Cells were then left unstimulated or stimulated with 10 μM PDBu for a further 30 minutes. In a subset of experiments, macrophages were incubated with 1000 U/ml PEG-Catalase for 15 minutes prior to PDBu stimulation. Following stimulation, cells were detached with Accutase® solution (Sigma-Aldrich), centrifuged at 1500 rpm for 5 min and resuspended in PBS. Cells were then analysed on a LSR II flow cytometer (BD Biosciences). Fold changes in DCF fluorescence were calculated relative to the MΦ value recorded on the same day.

2.9. Statistical Analysis. All data are expressed as mean ± SEM. Comparisons of multiple treatment groups were made using an ordinary or repeated measures one-way analysis of variance (ANOVA) with a Dunnett's or Sidak's post hoc test, respectively. When comparing two groups, a Student's unpaired t-test was used. $P < 0.05$ was considered to be statistically significant, and data were graphed and analysed using GraphPad Prism 7.02 software.

3. Results

3.1. M(IFN-γ+LPS) and M(IL-4) Macrophages Express M1 and M2 Markers, Respectively, and Both Phenotypes Demonstrate Enhanced Superoxide Generation. Treatment of both PDBu-differentiated THP-1 macrophages and M-CSF-differentiated human primary monocyte-derived macrophages, with the combination of IFN-γ and LPS, leads to marked increases in the expression of M1 genes (CXCL11, CCR7, and IL-1β). In THP-1 cells, CXCL11 (Figure 1(a)) and CCR7 (Figure 1(b)) increased by up to 1000-fold, with the greatest change observed following 24 hours of treatment. IL-1β expression increased between 5- and 10-fold throughout the 72-hour treatment period (Figure 1(c)). The magnitude of increase in M1 genes was larger in primary macrophages, with increases of ~5000-fold for CXCL11 (Figure 1(d)), ~2000-fold for CCR7 (Figure 1(e)), and ~200-fold for IL-1β apparent at 6 hours (Figure 1(f)). Treatment with IL-4 resulted in an increase in the M2 marker MRC-1 (CD206) by approximately 5-fold throughout the treatment period in both THP-1 and primary macrophages (Figures 1(g) and 1(j)). A time-dependent increase in the M2 markers CCL18 and CCL22 was observed with CCL18 elevated 15- and 800-fold (Figures 1(h) and 1(k)) and CCL22 20- and 5-fold (Figures 1(i) and 1(l)), in THP-1 and primary macrophages, respectively.

Having demonstrated differential activation of macrophages, we next assessed basal and PDBu-stimulated superoxide generation in M(IFN-γ+LPS) and M(IL-4) after 72 hours and 24 hours, for THP-1 and human primary macrophages, respectively. In THP-1 cells, whilst basal superoxide levels did not differ significantly between macrophages in different activation states, PDBu-stimulated superoxide generation was increased by ~219% and ~115% in M(IFN-γ+LPS) and M(IL-4) macrophages, respectively, as compared to untreated macrophages (Figures 2(a) and 2(b)). Of note, both the basal and PDBu-stimulated superoxide signals were much larger in primary macrophages as compared to THP-1 (Figures 2(c) and 2(d)). Peak superoxide generation in response to PDBu in untreated primary macrophages (30560 ± 7162 counts/sec) was ~30-fold greater than that in untreated THP-1 macrophages (797 ± 112 counts/sec). Nonetheless, PDBu-stimulated superoxide generation was similar in primary M(IFN-γ+LPS) and M(IL-4) macrophages and up to 91% greater than that observed in MΦ (Figure 2(d)). The L-012 chemiluminescence signal was confirmed to be specific for superoxide via treatment with superoxide dismutase (Supplementary Figure 1a-d).

3.2. Differential Regulation of NOX2 Oxidase Subunit Expression following IFN-γ+LPS vs. IL-4 Stimulation. To examine the mechanisms contributing to increased superoxide generation in both M(IFN-γ+LPS) and M(IL-4) macrophages, NOX isoform and subunit expression were

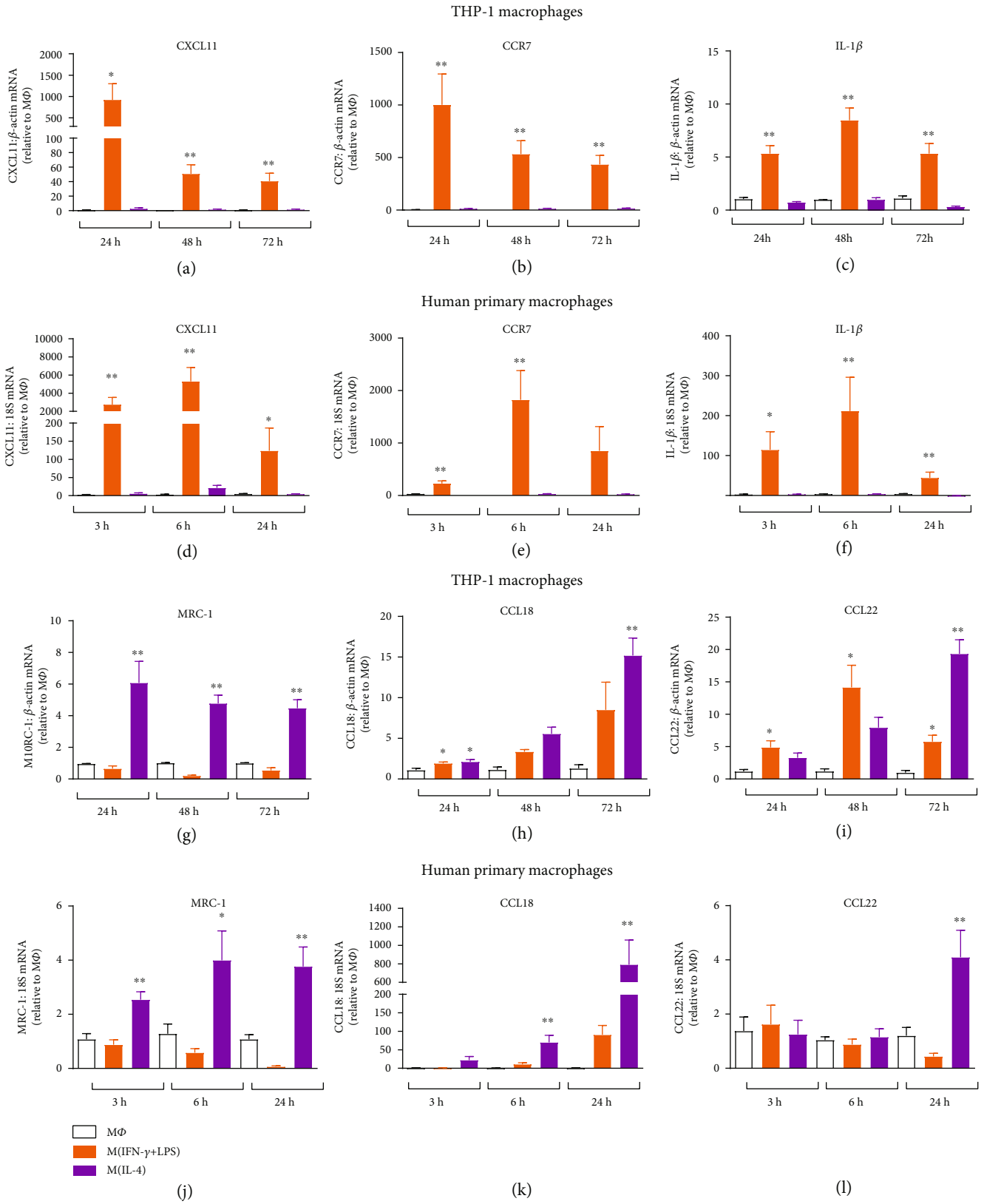

Figure 1: Time course of M1 and M2 marker mRNA expression in human macrophages. PDBu-differentiated THP-1 macrophages or M-CSF-differentiated human primary macrophages were left untreated (MΦ) or treated with IFN-γ and LPS (THP-1: 5/10 ng/ml; primary: 20/100 ng/ml; IFN-γ+LPS) or IL-4 (25 ng/ml) for 3-72 hours. mRNA expression of M1 (CXCL11 (a, d); CCR7 (b, e), and IL-1β (c, f)) and M2 (MRC-1 (g, j); CCL18 (h, k); CCL22 (i, l)) markers were determined by RT-qPCR and expressed relative to untreated macrophages (MΦ). Results presented as mean ± SEM, $n = 4$-8. $^{*}P < 0.05$, $^{**}P < 0.01$ vs. MΦ (1-way ANOVA followed by Dunnett's post hoc test).

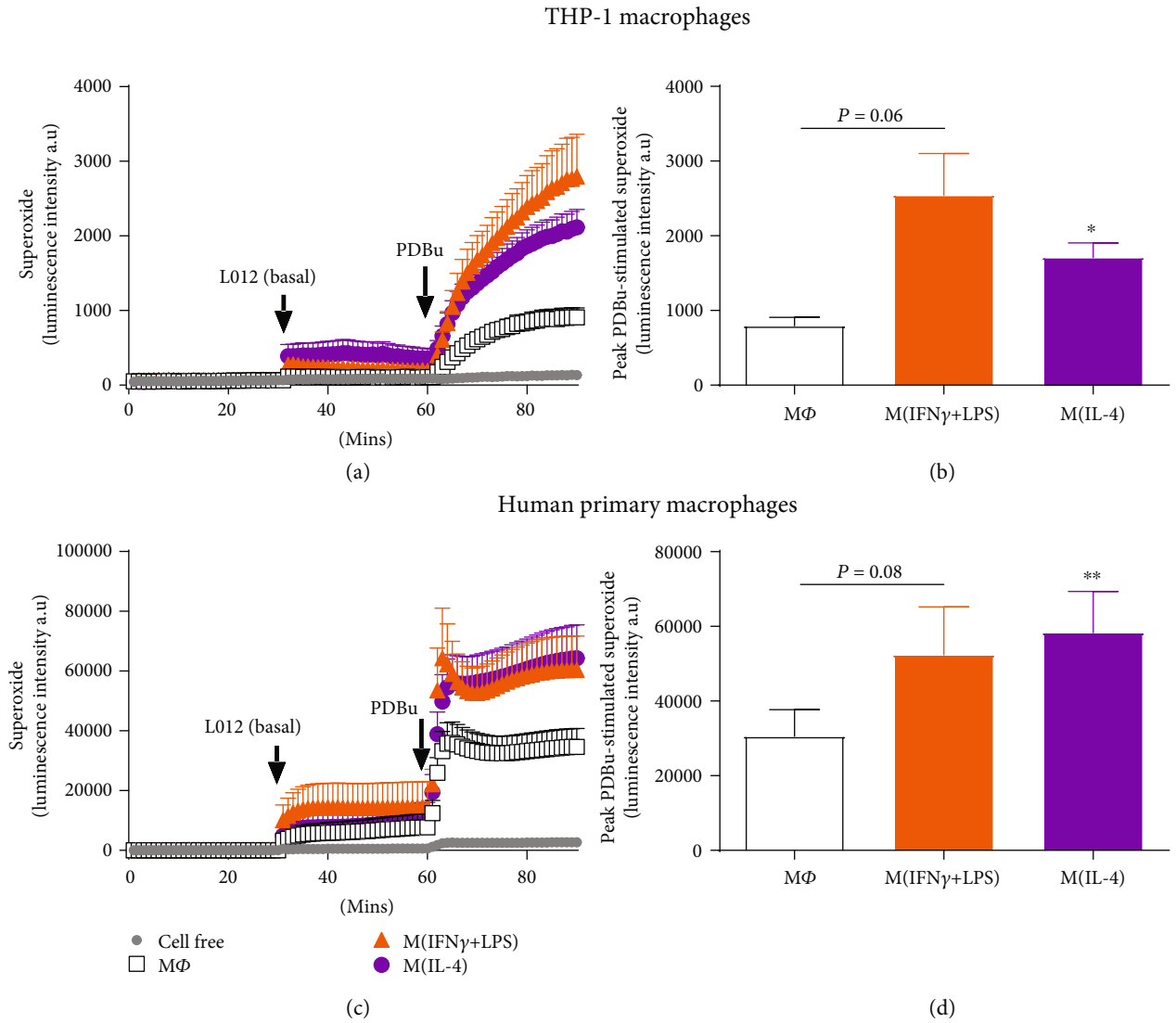

Figure 2: PDBu-stimulated superoxide generation in activated human macrophages. PDBu-differentiated THP-1 macrophages (a, b) or M-CSF-differentiated human primary macrophages (c, d) were left untreated (MΦ) or treated with IFN-γ+LPS (M1) or IL-4 (M2) for 24 (THP-1) or 72 hours (primary macrophages), and superoxide generation was detected via L-012-enhanced chemiluminescence. Left hand side (LHS): average recordings demonstrating initial background readings (1-30 min), basal superoxide as detected following the addition of L-012 (100 μM; 31-60 min) and PDBu (10 μM)-stimulated superoxide generation (61-90 min) measured as luminescence intensity in arbitrary units (a.u) in (a) THP-1 and (c) primary macrophages. Right hand side (RHS): peak PDBu-stimulated (basal signal subtracted) superoxide generation in (b) THP-1 and (d) primary macrophages. All results presented as mean ± SEM, $n = 7$. $^{*}P < 0.05$, $^{**}P < 0.01$ vs. MΦ (1-way repeated measures ANOVA followed by Dunnett's post hoc test).

assessed. Thus, NOX2 oxidase comprises the membrane-bound catalytic subunits, NOX2 and p22phox, together with the cytosolic regulatory subunits, p47phox, p67phox, and p40phox. In THP-1 macrophages, NOX2 mRNA was increased approximately 2-fold following IFN-γ+LPS activation, yet remained unchanged in macrophages activated with IL-4 (Figure 3(a)). Interestingly, mRNA expression of the p47phox subunit was upregulated in M(IFN-γ+LPS) macrophages (20-fold at 24 hours; 6-fold at 48 and 72 hours, Figure 3(b)), while the p67phox subunit was upregulated in M(IL-4) macrophages (up to 6-fold at 48 and 72 hours, Figure 3(c)). p22phox and p40phox subunits were unchanged (Supplementary Figure 2a and b). NOX2 protein expression did not appear to differ between macrophages in different activation states (Figure 3(d)); however, the observed changes in p47phox and p67phox mRNA were found to translate to increases in protein expression. p47phox protein was increased approximately 2.5-fold in M(IFN-γ+LPS) macrophages (Figure 3(e)) whilst p67phox protein was increased approximately 2-fold in M(IL-4) macrophages (Figure 3(f)). In contrast to THP-1 macrophages, IFN-γ+LPS stimulation of human primary macrophages was not associated with a change in NOX2 subunit mRNA expression. Although a decrease in NOX2 mRNA was observed in M(IL-4) macrophages at 24 hours (Figure 3(g)), NOX2 was unchanged at the level of

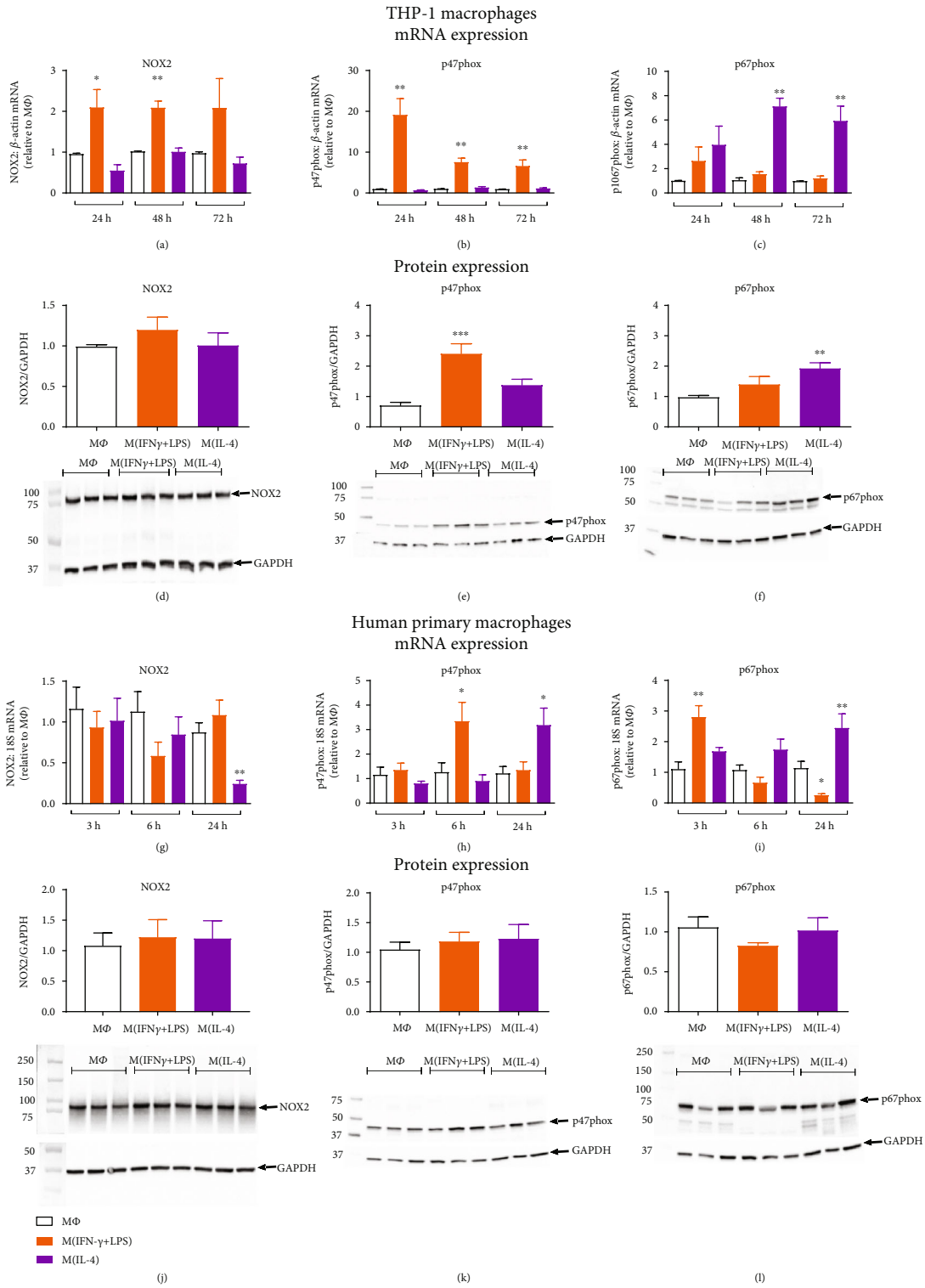

FIGURE 3: NOX2 oxidase subunit expression in activated human macrophages. PDBu-differentiated THP-1 macrophages or M-CSF-differentiated human primary macrophages were left untreated (MΦ) or treated with IFN-γ+LPS (M1) or IL-4 (M2) for 3 to 72 hours. Time course of NOX2 (a, g), p47phox (b, h), and p67phox (c, i) mRNA expression determined by RT-qPCR and expressed relative to the average MΦ (untreated) value. Protein expression of NOX2 (d, j), p47phox (e, k), and p67phox (f, l) after 24 (primary macrophages) or 72 hours (THP-1 macrophages), determined via western blotting. Representative blots, depicting $n = 3$, are shown below each graph with GAPDH used as a loading control. All results presented as mean ± SEM, $n = 5$-8. $^{*}P < 0.05$, $^{**}P < 0.01$, $^{***}P < 0.001$ vs. MΦ (1-way ANOVA followed by Dunnett's post hoc test).

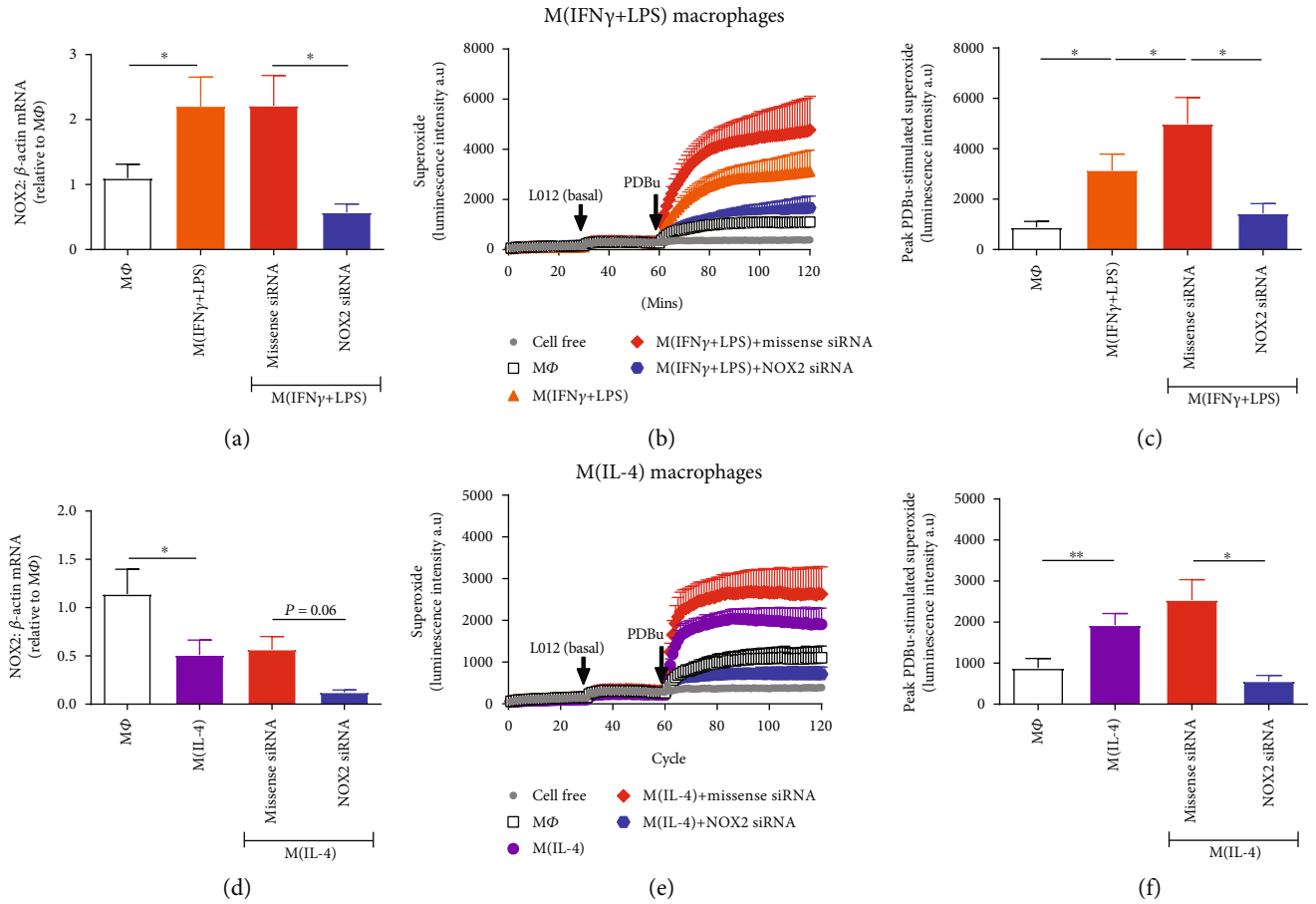

Figure 4: Effect of NOX2 siRNA on M1 and M2 macrophage-derived superoxide. Knockdown of NOX2 mRNA expression in THP-1 macrophages using NOX2 siRNA was confirmed in macrophages treated with both IFN-γ+LPS (a) and IL-4 (d) macrophages for 72 hours via RT-qPCR and expressed relative to the average MΦ (untreated) value. Effect of NOX2 siRNA and missense siRNA on the PDBu-stimulated superoxide signal in M(IFN-γ/LPS) and M(IL-4) macrophages detected via L-012-enhanced chemiluminescence. (b, e) Average recordings demonstrating initial background readings (1-30 min), basal superoxide as detected following the addition of L-012 (100 μM; 31-60 min), and PDBu (10 μM)-stimulated superoxide generation (61-120 min) measured as luminescence intensity in arbitrary units (a.u) in M(IFN-γ/LPS) (b) and M(IL-4) (e) macrophages. (c, f) Peak PDBu-stimulated (basal signal subtracted) superoxide generation in M(IFN-γ+LPS) (c) and M(IL-4) (f) macrophages. All results presented as mean ± SEM, $n = 5$-6. $^{*}P < 0.05$, $^{**}P < 0.01$ vs. MΦ (1-way repeated measures ANOVA followed by Dunnett's post hoc test).

the protein (Figure 3(j)). Whilst a time-dependent increase in p47phox mRNA (6 hours, Figure 3(h)) and p67phox mRNA (24 hours, Figure 3(i)) was also associated with M(IFN-γ+LPS) and M(IL-4) stimulation, respectively, in human primary macrophages, such changes were not observed at the level of the protein (Figures 3(k) and 3(l)). Furthermore, no significant differences were observed for p22phox mRNA expression. The p40phox subunit was decreased at the mRNA level in primary M(IFN-γ+LPS) macrophages (Supplementary Figure 2d and e), yet whether this translated to a reduction in p40phox protein was not confirmed. NOX1 and NOX4 mRNA could not be detected in either THP-1 or primary macrophages, in any of the activation states (Ct values > 40). NOX5 mRNA expression however was observed in both cell lines and was increased in THP-1 macrophages when activated with IL-4 (Supplementary Figure 2c and f).

To confirm that the superoxide signal in THP-1 macrophages was indeed NOX2 oxidase-derived, NOX2 siRNA was utilised to knock down its expression in all macrophage phenotypes. In M(IFN-γ+LPS) and M(IL-4) macrophages, NOX2 mRNA expression was reduced by 74% (Figure 4(a)) and 79% (Figure 4(d)), respectively, following NOX2 siRNA treatment as compared to macrophages treated with missense siRNA. In both phenotypes of macrophages, there was a trend for missense siRNA to increase the PDBu-stimulated superoxide signal to levels above the vehicle-treated cells (Figures 4(c) and 4(f)). Nonetheless, the marked reduction in NOX2 expression in M(IFN-γ+LPS) and M(IL-4) macrophages attenuated the superoxide signal to levels similar to those observed in untreated macrophages. Specifically, treatment with NOX2 siRNA reduced the peak PDBu-stimulated superoxide signal in M(IFN-γ+LPS) and M(IL-4) by 71% (Figure 4(c)) and 78% (Figure 4(f)), respectively.

3.3. M(IL-4) Macrophage Activation Is Associated with Increased Hydrogen Peroxide Generation. In addition to

superoxide, hydrogen peroxide generation was assessed in polarised THP-1 macrophages using two methods, Amplex Red for extracellular and H_2DCFDA (DCF) for intracellular detection. Of note, a robust basal hydrogen peroxide signal was detected, by both Amplex Red and DCF, in all macrophage phenotypes and was not further modulated by PDBu stimulation (Supplementary Figure 1e and f). Nevertheless, subsequent experiments comparing hydrogen peroxide generation between macrophages in different activation states incorporated PDBu. Amplex Red fluorescence, following PDBu stimulation for 90 minutes, showed a mean hydrogen peroxide concentration of approximately 2 μM for M(IL-4) macrophages, compared to 1 μM in both M(IFN-γ+LPS) and MΦ (Figure 5(b)). When calculated relative to the MΦ signal, there was a 1.5-fold increase in hydrogen peroxide generation following M(IL-4) activation with no change in M(IFN-γ+LPS) macrophages (Figure 5(c)). The hydrogen peroxide signal was abolished in the presence of the hydrogen peroxide scavenger, PEG-catalase, and amplified with superoxide dismutase, demonstrating that the assay was specific for hydrogen peroxide (Supplementary Figure 1g and h). To further demonstrate increased hydrogen peroxide production in M(IL-4) macrophages, the intracellular ROS indicator DCF was used and fluorescence detected via flow cytometry (Figures 5(d) and 5(e)). As with the Amplex Red assay, hydrogen peroxide levels were significantly greater in M(IL-4), as compared to M(IFN-γ+LPS) macrophages (Figure 5(e)). As shown in the representative histogram (Figure 5(d)), PEG-catalase reduced the signal in M(IL-4) macrophages, suggesting that it was primarily hydrogen peroxide being detected.

To elucidate the potential mechanisms underlying the increased hydrogen peroxide generation following IL-4 activation, we assessed the mRNA expression of different superoxide dismutase isoforms. While SOD1 (cytoplasmic) expression was not altered (Figure 5(f)), SOD2 (mitochondrial) mRNA expression was increased in IFN-γ+LPS-activated macrophages by 25-fold at 24 hours and 10-fold at 48 and 72 hours (Figure 5(g)). This change was reflected at the protein level, with a 3-fold increase in SOD2 expression in M(IFN-γ+LPS) macrophages at 72 hours (Figure 5(i)). SOD3 (extracellular) mRNA expression was unchanged in response to IFN-γ+LPS activation but increased by 4-fold in IL-4-activated macrophages at 72 hours (Figure 5(h)). However, no change in SOD3 protein expression was observed (Figure 5(j)).

3.4. Hydrogen Peroxide Generation Contributes to the Profibrotic Activity of M(IL-4) Macrophages. To investigate whether M(IL-4) macrophage-derived hydrogen peroxide may contribute to the profibrotic actions of M2 macrophages in the vessel wall, macrophages were cocultured with human aortic adventitial fibroblasts and markers of fibrosis (collagen 1, αSMA) measured. Coculture of aortic fibroblasts with M(IL-4) macrophages increased fibroblast collagen 1 expression, as compared to coculture with untreated (MΦ) macrophages (Figure 6(a)). PEG-catalase treatment significantly attenuated this effect (Figure 6(a)). Aortic fibroblast αSMA expression did not differ in response to coculture with macrophages in distinct activation states (Figure 6(b)), suggesting a lack of effect of macrophage-derived hydrogen peroxide on myofibroblast differentiation.

4. Discussion

M1 macrophage infiltration into tissues is a hallmark of inflammatory diseases, and NOX2 oxidase activity has long been associated with M1 function [2]. In this study, we challenge the idea that ROS generation is solely a function of M1 macrophages. Specifically, we demonstrate that activation of macrophages with IL-4 enhances superoxide generation to an equivalent degree as activation of macrophages with IFN-γ and LPS and increases hydrogen peroxide production. Of particular relevance to aortic stiffening, an important process involved in the development and clinical consequences of hypertension [24, 25], we reveal a potential role for M2 macrophage-derived hydrogen peroxide in promoting profibrotic responses in aortic adventitial fibroblasts.

Upregulation of NOX2 oxidase activity is observed in macrophages stimulated with the Th1 cytokine IFN-γ or bacterial component LPS as part of the response to microbial infection [5, 7]. This has been generally assumed to be a specific M1 macrophage function [15]. Although IL-4 has been shown to inhibit LPS-stimulated, but enhance IFN-γ-stimulated, ROS production in macrophages [26], we are the first to demonstrate that it can drive an increase in macrophage superoxide production alone. Importantly, the superoxide signal in both populations of activated macrophages was at least 2-fold higher than in untreated macrophages and was confirmed to be NOX2-derived using NOX2 siRNA. Our findings that stimulation of macrophages with the Th2 cytokine IL-4 results in increased NOX2-derived ROS further support a contribution of NOX2 to the activation of macrophages towards the M2 phenotype, as suggested in previous studies [27, 28]. It should be noted that our findings are not consistent with a study by Kraaij et al. (2013), who reported a reduction in ROS when macrophage differentiation occurred in the presence of IL-4. However, distinct methodological approaches may account for these apparent differences. Thus, Kraaij et al. (2013) treated human primary monocytes with IL-4 during the 7-day M-CSF differentiation period [18], rather than postdifferentiation, as is the more commonly accepted method of M2 macrophage activation [29–31]. As such, this previous study may be indicative of the effects of IL-4 on monocyte to macrophage differentiation rather than on macrophage ROS generation per se.

Although contrary to the generally accepted dogma that M1 macrophages are the major ROS-generating macrophage phenotype [2, 9], our observation that M(IL-4) macrophage function may also involve ROS is perhaps not unexpected. M2 macrophages phagocytose cell debris as part of their tissue repair function [32] and roles for ROS in phagocytosis are well documented [33]. Indeed, ROS have been shown to play a critical signalling role in the activation of macrophages towards the M2 phenotype in both humans and mice [27, 28] and M2 macrophage accumulation and wound healing responses *in vivo* are impaired in the absence of

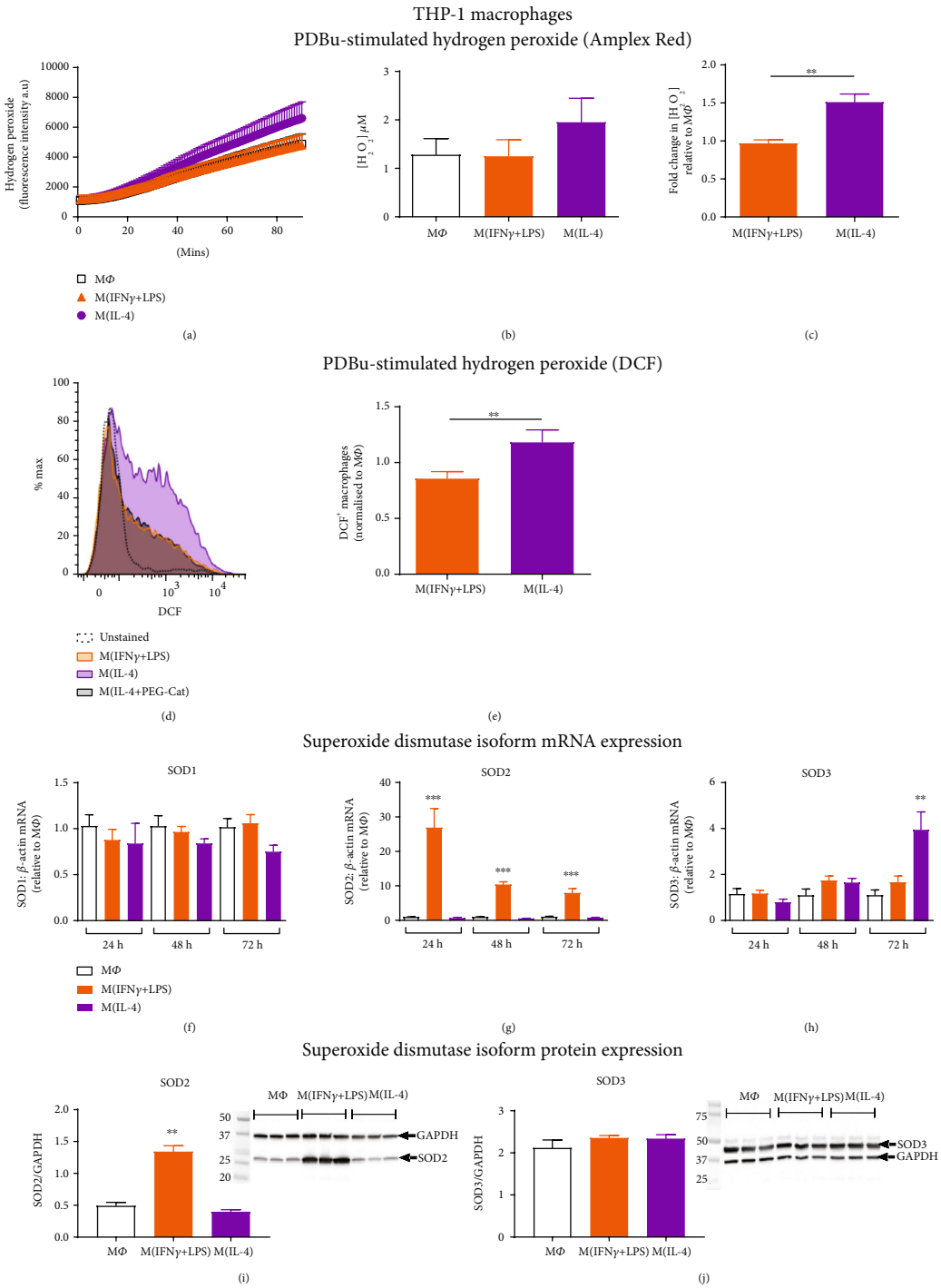

FIGURE 5: PDBu-stimulated hydrogen peroxide generation in activated human macrophages. PDBu-differentiated THP-1 macrophages were left untreated (MΦ) or activated with IFN-γ+LPS or IL-4 for 72 hours. (a) Average trace depicting the accumulation of PDBu (10 μM)-stimulated hydrogen peroxide in the culture media over 90 min detected via Amplex Red fluorescence. (b) Hydrogen peroxide concentration was calculated at 90 minutes and expressed as mean concentration ± SEM. (c) M(IFN-γ+LPS) and M(IL-4) hydrogen peroxide concentration expressed as a fold change relative to the untreated macrophage (MΦ) control, $n = 8$. (d) Representative histogram and gating strategy for DCF^+ macrophages, depicting M1 versus M2 polarisation and the effect of catalase-polyethylene glycol (PEG-Cat; 1000 U/ml) on the M2 signal. (e) Mean DCF^+ macrophages, normalised to the response in untreated macrophages (MΦ), $n = 7$. (f) SOD1, (g) SOD2, and (h) SOD3 mRNA expression in activated THP-1 macrophages at 24, 48, and 72 hours, determined by RT-qPCR and expressed relative to the average MΦ (untreated) value, $n = 5$-8. (i) SOD2 and (j) SOD3 protein expression in activated THP-1 macrophages at 72 hours, determined by western blotting, $n = 6$. Representative blots, depicting for $n = 3$, shown on RHS, with GAPDH used as a loading control. All results expressed as mean ± SEM, $^{**}P < 0.01$, $^{***}P < 0.001$ (1-way ANOVA followed by Dunnett's post hoc test (g, h, i) or Student's unpaired t-test (c, e)).

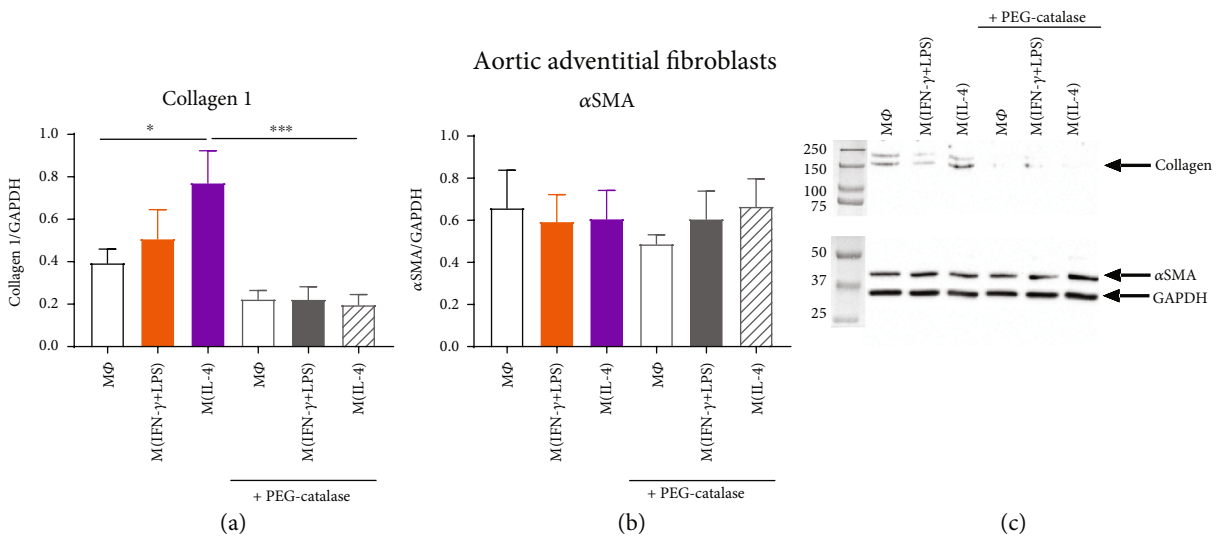

Figure 6: Effect of macrophage coculture on collagen and alpha-smooth muscle actin expression in human aortic adventitial fibroblasts. PDBu-differentiated THP-1 macrophages were left untreated (MΦ) or activated with IFN-γ+LPS or IL-4 for 72 hours in cell culture inserts. THP-1 macrophages were subsequently transferred to wells containing aortic adventitial fibroblasts, stimulated with 10 μM PDBu in the absence or presence of 1000 U/ml PEG-catalase, and incubated for 24 hours. (a) Collagen 1 and (b) αSMA protein were measured in aortic adventitial fibroblasts, $n = 10$-12. (c) Representative blot, depicting $n = 1$, is shown with GAPDH used as a loading control. Results presented as mean ± SEM, $^{*}P < 0.05$, $^{***}P < 0.001$ (1-way ANOVA followed by Sidak's post hoc test).

NOX1 and NOX2 in mice [27]. In addition to potential roles in wound healing, a contribution of NOX2-derived ROS to the resolution of inflammation has also emerged [34, 35] and M(IL-10) macrophage-derived ROS have been shown to induce the activation of T-regulatory cells [36]. Collectively, these previous studies support our findings for the involvement of NOX2 oxidase, not only in the function of proinflammatory M1 macrophages but also in other activation states, suggesting roles for NOX2 in immunoregulatory and profibrotic responses in addition to well-known roles in inflammation and microbial killing.

To further investigate the role of NOX2 oxidase in M(IL-4) macrophage ROS generation, we examined the expression of individual NOX2 oxidase subunits. Our findings with regard to NOX2 subunit expression suggest that the mechanism by which each macrophage phenotype increases superoxide differs. Upregulation of the p47phox and, to a lesser extent, the NOX2 catalytic subunit appeared to drive the increase in M(IFN-γ+LPS) macrophage superoxide generation. Roles for each of these subunits in promoting NOX2 activity have been shown previously [37, 38]. Furthermore, our results in THP-1 macrophages are consistent with a previous study of human monocytes (MonoMac1 cell line) in which the proinflammatory cytokine, TNFα, enhanced p47phox, p67phox, and NOX2 expression with the rank order of expression being p47phox (up to 20-fold) > p67phox (up to 5-fold) > NOX2 (up to 2.5-fold) [37]. NOX2 and p47phox expression are downstream of proinflammatory signalling pathways involving transcription factors associated with M1 macrophage activation such as nuclear factor light chain enhancer of activated B cells (NFκB) [39], signal transducer and activator of transcription (STAT) 1 [40], and interferon regulator factor- (IRF-) 1 [40, 41]. These increases in NOX2 subunit expression in M(IFN-γ+LPS) were hence expected. By contrast, IL-4 treatment was associated with upregulation of the p67phox subunit alone. Although yet to be investigated, this may be via the induction of STAT3 [42, 43] and p38 mitogen-activated protein kinase (MAPK) [44–46], signalling pathways utilised by IL-4. It should be acknowledged that a limitation of the current study was that our findings of enhanced p47phox and p67phox expression in M(IFN-γ+LPS) and M(IL-4) macrophages were not observed at the protein level in human primary macrophages. This may be due to the heterogeneity of donor blood monocytes as compared to the immortalised THP-1 line, but does question the relevance of these findings and highlights the importance of confirming observations in primary cells.

Collectively, our data support a predominant role of NOX2 oxidase in the generation of superoxide from activated macrophages. However, in agreement with recent reports [47, 48], we also observed NOX5 expression, at least at the mRNA level, in all macrophage phenotypes. Moreover, NOX5 mRNA expression was upregulated by IL-4 in THP-1 cells. Although NOX2 siRNA treatment revealed that the superoxide signal was predominantly NOX2-derived, a contribution of NOX5 to the signal cannot be excluded, particularly considering that it too can be activated via PKC (induced by PDBu stimulation) [49, 50]. Nonetheless, we show for the first time that the superoxide generating capacity of M(IFN-γ+LPS) and M(IL-4) macrophages is equivalent and driven predominantly via NOX2 oxidase.

Following generation, superoxide can interact with nitric oxide to form the powerful oxidant, peroxynitrite, or be dismutated to form hydrogen peroxide. Considering the proinflammatory and reparative properties of M1 and M2 macrophages, respectively, we suggest that whilst both phenotypes generate similar levels of superoxide, the final

oxidative end product may differ. Importantly, we demonstrated increases in both extracellular and intracellular hydrogen peroxide following activation towards the M2 phenotype with IL-4, an effect which was not evident with M1 activation with IFN-γ and LPS. In agreement with this finding for IL-4 stimulation, a previous study reported that augmented macrophage-derived hydrogen peroxide and Cu,Zn-SOD (SOD1) expression were associated with M2 polarisation in the setting of pulmonary fibrosis [51]. Whilst we did not detect a change in SOD1 mRNA, a modest increase in extracellular SOD (SOD3) mRNA was observed following IL-4 treatment, although this did not translate to enhanced SOD3 protein in the macrophage lysates. It should be acknowledged that our investigations of M2 macrophage hydrogen peroxide generation require further exploration to determine the precise mechanisms involved. It remains to be determined if the regulation of catalase or antioxidant enzymes such as glutathionine peroxidase (GPx) and thioredoxin reductase (TrxR) expression may also influence hydrogen peroxide levels in these cells. Furthermore, dismutation of NOX2-derived superoxide may not necessarily be the major source of the hydrogen peroxide signal observed. Given the lack of effect of PDBu stimulation per se on hydrogen peroxide generation, a constitutively active hydrogen peroxide-producing enzyme, such as NOX4, could be involved. Whilst we did not detect NOX4 mRNA in any of our macrophage samples, NOX4 mRNA and protein expressions have been observed in two recent studies of human primary macrophages [52, 53]. Further investigation of NOX4 protein expression and the use of NOX2 and NOX4 siRNA will aid in the identification of the source of M2 macrophage-derived hydrogen peroxide. Future studies should address these limitations in addition to *in vivo* experiments characterising M2 macrophage hydrogen peroxide production in tissues, such as within the vessel wall, during hypertension.

Somewhat surprisingly, M(IFN-γ+LPS) macrophages did not demonstrate increased hydrogen peroxide production, despite the increase in superoxide production observed and expression of SOD in these cells. Although not investigated in this study, iNOS is commonly used as a marker of M1 macrophages [2]. Potentially, the iNOS in these cells is outcompeting SOD, and thus, the superoxide generated is rapidly reacting with nitric oxide to produce peroxynitrite, rather than being dismutated to form hydrogen peroxide. This remains to be fully investigated. Interestingly, potential for increased mitochondrial hydrogen peroxide generation in M1 macrophages was observed in our study with robust upregulation of the mitochondrial SOD isoform, SOD2, following combined IFN-γ/LPS stimulation. This is consistent with findings following TLR receptor activation and LPS stimulation of macrophages [54, 55]. Although increased SOD2 expression was not associated with increased hydrogen peroxide generation in M(IFN-γ+LPS) macrophages in our study, we did not specifically investigate mitochondrial ROS, which would not be released from the cell. It remains likely that SOD2 upregulation may be a mechanism by which M1 macrophages are protected against oxidative stress during infection and could be linked with mitochondrial dysfunction, as M1 activation shifts cells from oxidative to glycolytic metabolism [56, 57], compared to M2 activation which is shown to increase mitochondrial content and oxidative phosphorylation [57]. Hence, macrophage phenotype may influence mitochondrial ROS production and mitochondrial dysfunction could contribute to the overall oxidative capacity of M1 macrophages. Intriguingly, increased macrophage thiol oxidative stress, associated with metabolic stress, has been shown to enhance chemotaxis leading to enhanced macrophage recruitment in the setting of atherosclerosis [58]. It would be interesting to investigate whether our activated macrophage cultures also demonstrate alterations in the glutathione (GSH)/glutathione disulphide (GSSG) ratio and chemotactic responses and whether this may also be linked to differences in the bioenergetics of these cells.

Although further investigation of the discussed mechanisms will be important, hydrogen peroxide generation appears to be a function of M(IL-4) macrophages and may be implicated in fibrotic diseases. ROS have been shown to contribute to a multitude of profibrotic and remodelling actions in the vessel wall [59–62]. Thus hydrogen peroxide enhances ROS production in vascular and cardiac cells *in vitro* [19, 63] and promotes remodelling in the intact vasculature [59]. We next sought to determine if M(IL-4) macrophage-derived hydrogen peroxide can promote vascular fibrosis. Indeed, coculture of IL-4-stimulated macrophages with aortic fibroblasts led to increased fibroblast collagen 1 expression, an effect which was negated by the hydrogen peroxide scavenger, PEG-catalase, and was not evident with M(IFN-γ+LPS) macrophage coculture. Of note, macrophage-derived hydrogen peroxide, whether it be generated from MΦ, M(IFN-γ+LPS), or M(IL-4) macrophages, did not appear to contribute to myofibroblast differentiation (detected by αSMA expression). Nonetheless, the greater capacity for M(IL-4) macrophages to generate hydrogen peroxide and promote collagen production could contribute to the aortic remodelling and stiffening response observed as a consequence of M2 macrophage accumulation in the vessel wall of hypertensive mice [14]. Future studies should investigate whether a profibrotic effect of M2-derived hydrogen peroxide is also observed in other cells involved in aortic stiffening such as vascular smooth muscle cells and validate the findings in mouse models of hypertension to shed further light on these mechanisms.

5. Conclusions

This study compared the ROS-generating capacities of M1 and M2 macrophages and revealed a previously unrecognised role of ROS in M2 macrophage function. Although previously considered a key mediator of M1 macrophage activity, we have shown that increased NOX2-derived superoxide generation also occurs following IL-4-stimulated M2 activation. Furthermore, we show that IL-4 increased macrophage hydrogen peroxide, which promoted enhanced aortic fibroblast collagen synthesis highlighting a potential role in aortic fibrosis. Given the role of M2 macrophages in the development of aortic stiffening during hypertension, our findings may be of particular importance in this setting and we reveal M2-derived ROS as a potential therapeutic target.

Data Availability

The RT-qPCR, western blot, and ROS detection data used to support the findings of this study are available from the corresponding author upon request.

Conflicts of Interest

The authors declare that there is no conflict of interest regarding the publication of this paper.

Acknowledgments

We acknowledge Dr. Meritxell Canals for providing us with the THP-1 cell line and the Australian Red Cross Blood Service for supplying donor buffy coat for PBMC isolation. Professor Grant Drummond was supported by a Senior Research Fellowship from the National Health and Medical Research Council of Australia (NHMRC) (GNT1006017), while Associate Professor Chrishan Samuel was supported by a NHMRC Senior Research Fellowship (GNT1041766). This work was supported by NHMRC Grant GNT1041326.

Supplementary Materials

Superoxide and hydrogen peroxide generation in M(IFN-γ+LPS) and M(IL-4) macrophages. Basal and PDBu-stimulated superoxide generation in M(IFN-γ+LPS) and M(IL-4) after 72 hours and 24 hours, for THP-1 and human primary macrophages, respectively, was assessed using L-012 chemiluminescence. The L-012 chemiluminescence signal was confirmed to be specific for superoxide via treatment with superoxide dismutase (Supplementary Figure 1a-d). In addition to superoxide, hydrogen peroxide generation was assessed in polarised THP-1 macrophages using two methods, Amplex Red for extracellular and H_2DCFDA (DCF) for intracellular detection. Of note, a robust basal hydrogen peroxide signal was detected, by both Amplex Red and DCF, in all macrophage phenotypes and was not further modulated by PDBu stimulation (Supplementary Figure 1e and f). The hydrogen peroxide signal was abolished in the presence of the hydrogen peroxide scavenger, PEG-catalase, and amplified with superoxide dismutase, demonstrating that the assay was specific for hydrogen peroxide (Supplementary Figure 1 g and h). *Differential regulation of NOX2 oxidase subunit expression following IFN-γ+LPS vs. IL-4 stimulation*. To examine the mechanisms contributing to increased superoxide generation in both M(IFN-γ+LPS) and M(IL-4) macrophages, NOX isoform and subunit expression were assessed. Thus, NOX2 oxidase comprises the membrane-bound catalytic subunits, NOX2 and p22phox, together with the cytosolic regulatory subunits, p47phox, p67phox, and p40phox. No significant differences were observed for p22phox mRNA expression in THP-1 and primary M(IFN-γ+LPS) and M(IL-4) macrophages (Supplementary Figure 2a and d). The p40phox subunit was decreased at the mRNA level in primary M(IFN-γ+LPS) macrophages (Supplementary Figure 2d and e), yet whether this translated to a reduction in p40phox protein was not confirmed. NOX1 and NOX4 mRNA could not be detected in either THP-1 or primary macrophages, in any of the activation states (Ct values > 40). NOX5 mRNA expression however was observed in both cell lines and was increased in THP-1 macrophages when activated with IL-4 (Supplementary Figure 2c and f). *(Supplementary Materials)*

References

[1] S. Gordon and F. O. Martinez, "Alternative activation of macrophages: mechanism and functions," *Immunity*, vol. 32, no. 5, pp. 593–604, 2010.

[2] A. Mantovani, A. Sica, S. Sozzani, P. Allavena, A. Vecchi, and M. Locati, "The chemokine system in diverse forms of macrophage activation and polarization," *Trends in immunology*, vol. 25, no. 12, pp. 677–686, 2004.

[3] P. J. Murray, J. E. Allen, S. K. Biswas et al., "Macrophage activation and polarization: nomenclature and experimental guidelines," *Immunity*, vol. 41, no. 1, pp. 14–20, 2014.

[4] B. Brüne, N. Dehne, N. Grossmann et al., "Redox control of inflammation in macrophages," *Antioxidants & Redox Signaling*, vol. 19, no. 6, pp. 595–637, 2013.

[5] P. E. Newburger, R. A. Ezekowitz, C. Whitney, J. Wright, and S. H. Orkin, "Induction of phagocyte cytochrome b heavy chain gene expression by interferon gamma," *Proceedings of the National Academy of Sciences*, vol. 85, no. 14, pp. 5215–5219, 1988.

[6] W. Han, H. Li, J. Cai et al., "NADPH oxidase limits lipopolysaccharide-induced lung inflammation and injury in mice through reduction-oxidation regulation of NF-κB activity," *The Journal of Immunology*, vol. 190, no. 9, pp. 4786–4794, 2013.

[7] P. E. Newburger, Q. Dai, and C. Whitney, "In vitro regulation of human phagocyte cytochrome b heavy and light chain gene expression by bacterial lipopolysaccharide and recombinant human cytokines," *Journal of Biological Chemistry*, vol. 266, no. 24, pp. 16171–16177, 1991.

[8] A. Sica and A. Mantovani, "Macrophage plasticity and polarization: in vivo veritas," *Journal of Clinical Investigation*, vol. 122, no. 3, pp. 787–795, 2012.

[9] N. Wang, H. Liang, and K. Zen, "Molecular mechanisms that influence the macrophage m1-m2 polarization balance," *Frontiers in Immunology*, vol. 5, 2014.

[10] S. Kossmann, H. Hu, S. Steven et al., "Inflammatory monocytes determine endothelial nitric-oxide synthase uncoupling and nitro-oxidative stress induced by angiotensin II," *Journal of Biological Chemistry*, vol. 289, no. 40, pp. 27540–27550, 2014.

[11] T.-D. Liao, X.-P. Yang, Y.-H. Liu et al., "Role of inflammation in the development of renal damage and dysfunction in angiotensin II-induced hypertension," *Hypertension*, vol. 52, no. 2, pp. 256–263, 2008.

[12] B. Calderon, A. Suri, and E. R. Unanue, "In CD4+ T-cell-induced diabetes, macrophages are the final effector cells that mediate islet β-cell killing," *The American Journal of Pathology*, vol. 169, no. 6, pp. 2137–2147, 2006.

[13] S. Lee, S. Huen, H. Nishio et al., "Distinct macrophage phenotypes contribute to kidney injury and repair," *Journal of the American Society of Nephrology*, vol. 22, no. 2, pp. 317–326, 2011.

[14] J. P. Moore, A. Vinh, K. L. Tuck et al., "M2 macrophage accumulation in the aortic wall during angiotensin II infusion in

mice is associated with fibrosis, elastin loss, and elevated blood pressure," *American Journal of Physiology-Heart and Circulatory Physiology*, vol. 309, no. 5, pp. H906–H917, 2015.

[15] D. M. Mosser and J. P. Edwards, "Exploring the full spectrum of macrophage activation," *Nature Reviews Immunology*, vol. 8, no. 12, pp. 958–969, 2008.

[16] J. E. Glim, F. B. Niessen, V. Everts, M. van Egmond, and R. H. Beelen, "Platelet derived growth factor-CC secreted by M2 macrophages induces alpha-smooth muscle actin expression by dermal and gingival fibroblasts," *Immunobiology*, vol. 218, no. 6, pp. 924–929, 2013.

[17] D. A. Guimarães, E. Rizzi, C. S. Ceron et al., "Atorvastatin and sildenafil decrease vascular TGF-β levels and MMP-2 activity and ameliorate arterial remodeling in a model of renovascular hypertension," *Redox Biology*, vol. 6, pp. 386–395, 2015.

[18] M. D. Kraaij, K. M. Koekkoek, S. W. van der Kooij, K. A. Gelderman, and C. van Kooten, "Subsets of human type 2 macrophages show differential capacity to produce reactive oxygen species," *Cellular Immunology*, vol. 284, no. 1-2, pp. 1–8, 2013.

[19] P. Wang, S. Zhou, L. Xu et al., "Hydrogen peroxide-mediated oxidative stress and collagen synthesis in cardiac fibroblasts: blockade by tanshinone IIA," *Journal of Ethnopharmacology*, vol. 145, no. 1, pp. 152–161, 2013.

[20] C. Chen, S. Yang, M. Zhang et al., "Triptolide mitigates radiation-induced pulmonary fibrosis via inhibition of axis of alveolar macrophages-NOXes-ROS-myofibroblasts," *Cancer Biology & Therapy*, vol. 17, no. 4, pp. 381–389, 2016.

[21] L. A. Murray, Q. Chen, M. S. Kramer et al., "TGF-beta driven lung fibrosis is macrophage dependent and blocked by serum amyloid P," *The International Journal of Biochemistry & Cell Biology*, vol. 43, no. 1, pp. 154–162, 2011.

[22] B. Vidal, A. L. Serrano, M. Tjwa et al., "Fibrinogen drives dystrophic muscle fibrosis via a TGFβ/alternative macrophage activation pathway," *Genes & Development*, vol. 22, no. 13, pp. 1747–1752, 2008.

[23] T. D. Schmittgen and K. J. Livak, "Analyzing real-time PCR data by the comparative C_T method," *Nature Protocols*, vol. 3, no. 6, pp. 1101–1108, 2008.

[24] B. M. Kaess, J. Rong, M. G. Larson et al., "Aortic stiffness, blood pressure progression, and incident hypertension," *JAMA*, vol. 308, no. 9, pp. 875–881, 2012.

[25] G. F. Mitchell, S.-J. Hwang, R. S. Vasan et al., "Arterial stiffness and cardiovascular events: the Framingham Heart Study," *Circulation*, vol. 121, no. 4, pp. 505–511, 2010.

[26] G. Bhaskaran, A. Nii, S. Sone, and T. Ogura, "Differential effects of interleukin-4 on superoxide anion production by human alveolar macrophages stimulated with lipopolysaccharide and interferon-γ," *Journal of Leukocyte Biology*, vol. 52, no. 2, pp. 218–223, 1992.

[27] Q. Xu, S. Choksi, J. Qu et al., "NADPH oxidases are essential for macrophage differentiation," *Journal of Biological Chemistry*, vol. 291, no. 38, pp. 20030–20041, 2016.

[28] Y. Zhang, S. Choksi, K. Chen, Y. Pobezinskaya, I. Linnoila, and Z. G. Liu, "ROS play a critical role in the differentiation of alternatively activated macrophages and the occurrence of tumor-associated macrophages," *Cell Research*, vol. 23, no. 7, pp. 898–914, 2013.

[29] F. O. Martinez, S. Gordon, M. Locati, and A. Mantovani, "Transcriptional profiling of the human monocyte-to-macrophage differentiation and polarization: new molecules and patterns of gene expression," *Journal of Immunology*, vol. 177, no. 10, pp. 7303–7311, 2006.

[30] B. Sudan, M. A. Wacker, M. E. Wilson, and J. W. Graff, "A systematic approach to identify markers of distinctly activated human macrophages," *Frontiers in Immunology*, vol. 6, 2015.

[31] D. Y. S. Vogel, J. E. Glim, A. W. D. Stavenuiter et al., "Human macrophage polarization in vitro: maturation and activation methods compared," *Immunobiology*, vol. 219, no. 9, pp. 695–703, 2014.

[32] T. A. Wynn and K. M. Vannella, "Macrophages in tissue repair, regeneration, and fibrosis," *Immunity*, vol. 44, no. 3, pp. 450–462, 2016.

[33] G. M. Rosen, S. Pou, C. L. Ramos, M. S. Cohen, and B. E. Britigan, "Free radicals and phagocytic cells," *The FASEB Journal*, vol. 9, no. 2, pp. 200–209, 1995.

[34] M. Hultqvist, P. Olofsson, F. K. Wallner, and R. Holmdahl, "Pharmacological potential of NOX2 agonists in inflammatory conditions," *Antioxidants & Redox Signaling*, vol. 23, no. 5, pp. 446–459, 2014.

[35] M. Hultqvist, L. M. Olsson, K. A. Gelderman, and R. Holmdahl, "The protective role of ROS in autoimmune disease," *Trends in Immunology*, vol. 30, no. 5, pp. 201–208, 2009.

[36] M. D. Kraaij, N. D. L. Savage, S. W. van der Kooij et al., "Induction of regulatory T cells by macrophages is dependent on production of reactive oxygen species," *Proceedings of the National Academy of Sciences*, vol. 107, no. 41, pp. 17686–17691, 2010.

[37] K. A. Gauss, L. K. Nelson-Overton, D. W. Siemsen, Y. Gao, F. R. DeLeo, and M. T. Quinn, "Role of NF-κB in transcriptional regulation of the phagocyte NADPH oxidase by tumor necrosis factor-α," *Journal of Leukocyte Biology*, vol. 82, no. 3, pp. 729–741, 2007.

[38] Y. L. Siow, K. K. W. Au-Yeung, C. W. H. Woo, and O. Karmin, "Homocysteine stimulates phosphorylation of NADPH oxidase p47phoxand p67phoxsubunits in monocytes via protein kinase Cβ activation," *Biochemical Journal*, vol. 398, no. 1, pp. 73–82, 2006.

[39] J. Anrather, G. Racchumi, and C. Iadecola, "NF-κB regulates phagocytic NADPH oxidase by inducing the expression of gp91^{phox}," *Journal of Biological Chemistry*, vol. 281, no. 9, pp. 5657–5667, 2006.

[40] A. Kumatori, D. Yang, S. Suzuki, and M. Nakamura, "Cooperation of STAT-1 and IRF-1 in interferon-γ-induced transcription of the gp91^{phox} gene," *Journal of Biological Chemistry*, vol. 277, no. 11, pp. 9103–9111, 2002.

[41] V. H. Olavarria, J. E. Figueroa, and V. Mulero, "Induction of genes encoding NADPH oxidase components and activation of IFN regulatory factor-1 by prolactin in fish macrophages," *Innate Immunity*, vol. 19, no. 6, pp. 644–654, 2013.

[42] A. Bhattacharjee, M. Shukla, V. P. Yakubenko, A. Mulya, S. Kundu, and M. K. Cathcart, "IL-4 and IL-13 employ discrete signaling pathways for target gene expression in alternatively activated monocytes/macrophages," *Free Radical Biology and Medicine*, vol. 54, pp. 1–16, 2013.

[43] A. Manea, L. I. Tanase, M. Raicu, and M. Simionescu, "Jak/STAT signaling pathway regulates nox1 and nox4-based NADPH oxidase in human aortic smooth muscle cells," *Arteriosclerosis, Thrombosis, and Vascular Biology*, vol. 30, no. 1, pp. 105–112, 2010.

[44] X. Fu, D. G. Beer, J. Behar, J. Wands, D. Lambeth, and W. Cao, "cAMP-response element-binding protein mediates acid-

induced NADPH oxidase NOX5-S expression in Barrett esophageal adenocarcinoma cells," *Journal of Biological Chemistry*, vol. 281, no. 29, pp. 20368–20382, 2006.

[45] V. Schenten, C. Melchior, N. Steinckwich, E. J. Tschirhart, and S. Brechard, "Sphingosine kinases regulate NOX2 activity via p38 MAPK-dependent translocation of S100A8/A9," *Journal of Leukocyte Biology*, vol. 89, no. 4, pp. 587–596, 2011.

[46] Y. S. Jang, H. A. Kim, S. R. Park, M. R. Lee, J. B. Park, and P. H. Kim, "IL-4 stimulates mouse macrophages to express APRIL through p38MAPK and two different downstream molecules, CREB and Stat6," *Cytokine*, vol. 47, no. 1, pp. 43–47, 2009.

[47] A. Manea, S.-A. Manea, A. M. Gan et al., "Human monocytes and macrophages express NADPH oxidase 5; a potential source of reactive oxygen species in atherosclerosis," *Biochemical and Biophysical Research Communications*, vol. 461, no. 1, pp. 172–179, 2015.

[48] V. Marzaioli, M. Hurtado-Nedelec, C. Pintard et al., "NOX5 and p22phox are 2 novel regulators of human monocytic differentiation into dendritic cells," *Blood*, vol. 130, no. 15, pp. 1734–1745, 2017.

[49] L. Serrander, V. Jaquet, K. Bedard et al., "NOX5 is expressed at the plasma membrane and generates superoxide in response to protein kinase C activation," *Biochimie*, vol. 89, no. 9, pp. 1159–1167, 2007.

[50] F. Chen, Y. Yu, S. Haigh et al., "Regulation of NADPH oxidase 5 by protein kinase C isoforms," *PLoS One*, vol. 9, no. 2, 2014.

[51] C. He, A. J. Ryan, S. Murthy, and A. B. Carter, "Accelerated development of pulmonary fibrosis via Cu,Zn-superoxide dismutase-induced alternative activation of macrophages," *Journal of Biological Chemistry*, vol. 288, no. 28, pp. 20745–20757, 2013.

[52] C. F. Lee, M. Qiao, K. Schroder, Q. Zhao, and R. Asmis, "Nox4 is a novel inducible source of reactive oxygen species in monocytes and macrophages and mediates oxidized low density lipoprotein–induced macrophage death," *Circulation Research*, vol. 106, no. 9, pp. 1489–1497, 2010.

[53] J.-S. Moon, K. Nakahira, K.-P. Chung et al., "NOX4-dependent fatty acid oxidation promotes NLRP3 inflammasome activation in macrophages," *Nature Medicine*, vol. 22, no. 9, pp. 1002–1012, 2016.

[54] E. M. Peterman, C. Sullivan, M. F. Goody, I. Rodriguez-Nunez, J. A. Yoder, and C. H. Kim, "Neutralization of mitochondrial superoxide by superoxide dismutase 2 promotes bacterial clearance and regulates phagocyte numbers in zebrafish," *Infection and Immunity*, vol. 83, no. 1, pp. 430–440, 2015.

[55] R. Rakkola, S. Matikainen, and T. A. Nyman, "Proteome analysis of human macrophages reveals the upregulation of manganese-containing superoxide dismutase after toll-like receptor activation," *Proteomics*, vol. 7, no. 3, pp. 378–384, 2007.

[56] K. C. El Kasmi and K. R. Stenmark, "Contribution of metabolic reprogramming to macrophage plasticity and function," *Seminars in Immunology*, vol. 27, no. 4, pp. 267–275, 2015.

[57] S. Tavakoli, D. Zamora, S. Ullevig, and R. Asmis, "Bioenergetic profiles diverge during macrophage polarization: implications for the interpretation of 18F-FDG PET imaging of atherosclerosis," *Journal of Nuclear Medicine*, vol. 54, no. 9, pp. 1661–1667, 2013.

[58] M. Qiao, Q. Zhao, C. F. Lee et al., "Thiol oxidative stress induced by metabolic disorders amplifies macrophage chemotactic responses and accelerates atherogenesis and kidney injury in LDL receptor-deficient mice," *Arteriosclerosis, Thrombosis, and Vascular Biology*, vol. 29, no. 11, pp. 1779–1786, 2009.

[59] S. A. Barman, F. Chen, Y. Su et al., "NADPH oxidase 4 is expressed in pulmonary artery adventitia and contributes to hypertensive vascular remodeling," *Arteriosclerosis, Thrombosis, and Vascular Biology*, vol. 34, no. 8, pp. 1704–1715, 2014.

[60] M. J. Haurani and P. J. Pagano, "Adventitial fibroblast reactive oxygen species as autacrine and paracrine mediators of remodeling: bellwether for vascular disease?," *Cardiovascular Research*, vol. 75, no. 4, pp. 679–689, 2007.

[61] D. I. Brown and K. K. Griendling, "Regulation of signal transduction by reactive oxygen species in the cardiovascular system," *Circulation Research*, vol. 116, no. 3, pp. 531–549, 2015.

[62] J. Liu, A. Ormsby, N. Oja-Tebbe, and P. J. Pagano, "Gene transfer of NAD(P)H oxidase inhibitor to the vascular adventitia attenuates medial smooth muscle hypertrophy," *Circulation Research*, vol. 95, no. 6, pp. 587–594, 2004.

[63] H. Cai, "NAD(P)H oxidase–dependent self-propagation of hydrogen peroxide and vascular disease," *Circulation Research*, vol. 96, no. 8, pp. 818–822, 2005.

Hindawi
Journal of Immunology Research
Volume 2019, Article ID 5063089, 11 pages
https://doi.org/10.1155/2019/5063089

Research Article

Urinary NGAL and RBP Are Biomarkers of Normoalbuminuric Renal Insufficiency in Type 2 Diabetes Mellitus

Aimei Li,[1] Bin Yi,[1] Yan Liu,[1] Jianwen Wang,[1] Qing Dai,[1] Yuxi Huang,[1] Yan Chun Li,[1,2] and Hao Zhang[1]

[1]*Department of Nephrology, The Third Xiangya Hospital, Central South University, Changsha, 410013 Hunan, China*
[2]*Department of Medicine, Division of Biological Sciences, The University of Chicago, Chicago, IL 60637, USA*

Correspondence should be addressed to Hao Zhang; zhanghaoliaoqing@163.com

Received 7 March 2019; Revised 24 July 2019; Accepted 21 August 2019; Published 15 September 2019

Guest Editor: Nivin Sharawy

Objectives. As a screening index of diabetic kidney disease (DKD), urinary albumin/creatine ratio (UACR) is commonly used. However, approximately 23.3%-56.6% of DKD patients with estimated glomerular filtration rate (eGFR) < 60 ml/min per 1.73 m^2 are normoalbuminuric. Thus, urinary biomarkers of nonalbuminuric renal insufficiency in type 2 diabetes mellitus (T2DM) patients are urgently needed. *Methods*. This cross-sectional study enrolled 209 T2DM patients with normoalbuminuria whose diabetes duration was more than 5 years. The patients were classified into two groups, NO-CKD (eGFR ≥ 60 ml/min per 1.73 m^2, $n = 165$) and NA-DKD (eGFR < 60 ml/min per 1.73 m^2, $n = 44$). Levels of urinary neutrophil gelatinase-associated lipocalin (NGAL), retinol-binding protein (RBP), plasminogen activator inhibitor-1 (PAI-1), vascular cell adhesion molecule-1 (VCAM-1), and E-cadherin were detected, and their correlations with eGFR, plasma TNF-α, IL-6, endothelin-1 (ET-1), and 8-hydroxydeoxyguanosine (8-OHdG) were assessed. *Results*. Among patients with renal insufficiency, 26.0% was normoalbuminuric. Compared to the NO-CKD group, the NA-DKD group was older with lower hemoglobin (HB) levels and higher systolic blood pressure (SBP), plasma TNF-α, IL-6, and 8-OHdG levels. Logistic regression analysis suggested that age, TNF-α, and 8-OHdG were independent risk factors for nonalbuminuric renal insufficiency. Compared to the NO-CKD group, the NA-DKD group exhibited significant increases in urinary NGAL and RBP levels but not PAI-1, VCAM-1, and E-cadherin. Urinary NGAL and RBP both correlated negatively with eGFR and positively with plasma IL-6 and 8-OHdG. Multiple linear regression indicated NGAL ($\beta = -0.287$, $p = 0.008$) and RBP ($\beta = -44.545$, $p < 0.001$) were independently correlated with eGFR. *Conclusion*. Age, plasma TNF-α, and 8-OHdG are independent risk factors for renal insufficiency in T2DM patients with normoalbuminuria. Urinary NGAL and RBP can serve as noninvasive biomarkers of normoalbuminuric renal insufficiency in T2DM.

1. Introduction

Renal insufficiency, one of the main microvascular complications of diabetes, is characterized by chronic inflammation and is associated with a substantially increased risk of mortality [1]. Due to the rising incidence of diabetes, diabetic kidney disease (DKD) has become the primary cause of chronic kidney disease (CKD) among the elderly population in China [2].

DKD is defined as albuminuria (urinary albumin/-creatine ratio (UACR) > 30 mg/g), an impaired glomerular filtration rate (GFR) (GFR ≤ 60 ml/min per 1.73 m^2), or both [3]. As the noninvasive of urine test, elevated urinary albumin level is considered an early index of DKD. However, approximately 23.3%-56.6% of patients with T2DM and kidney function decline have normal albuminuria [4–8]. It has been reported that among T2DM patients with renal insufficiency, all-cause mortality in the normoalbuminuric group is not significantly lower than that in the proteinuric group [9]. Moreover, normoalbuminuric renal insufficiency is a strong predictor of mortality in individuals with T2DM [10]. However, there is no sensitive urinary biomarker for normoalbuminuric renal insufficiency in T2DM.

Compared to T2DM patients with albuminuria, patients with a decreased GFR and normoalbuminuria are more likely to be older and have lower HbA1c and diabetic retinopathy prevalence and higher prevalence of coronary heart disease [6, 11, 12]. The classical pathological changes in diabetic nephropathy include thickening of the glomerular basement membrane, mesangial expansion, nodular sclerosis, global glomerular sclerosis, arteriolar hyalinosis, and interstitial fibrosis [13, 14]. However, a study conducted by Ekinci et al. [15] found that in T2DM patients with reduced eGFR, compared with 22 of 23 patients with albuminuria, only 3 of 8 patients with normoalbuminuria had typical glomerular changes. Nonetheless, compared with only 1 of 23 patients with albuminuria, 3 of 8 patients with normoalbuminuria had predominantly interstitial or vascular changes. Moreover, varying degrees of arteriosclerosis are observed in 7/8 subjects with normoalbuminuria. These findings suggest that tubulointerstitial damage and macroangiopathy may be involved in the development of normoalbuminuric renal insufficiency.

Numerous risk factors are known to contribute to the pathogenesis of DKD, including inflammation, endothelial dysfunction, oxidative stress, and epigenetic regulations [16–18], while the pathogenesis of normoalbuminuric renal insufficiency remains unclear. Studies have supported elevated TNF-α and IL-6 levels participated in kidney damage of DM [19, 20]. Expression of endothelin-1 (ET-1) was elevated in the kidney of STZ-treated rat diabetic model [21]. Meanwhile, high level of plasma 8-hydroxydeoxyguanosine (8-OHdG) was associated with increased risk of kidney disease in DM patients [19, 20, 22–24]. In the current study, we analyzed the relationship between plasma TNF-α, IL-6, ET-1, and 8-OHdG with eGFR in T2DM patients with normoalbuminuria and evaluated the role of indicators of tubulointerstitial damage (neutrophil gelatinase-associated lipocalin (NGAL), retinol-binding protein (RBP), plasminogen activator inhibitor-1 (PAI-1), vascular cell adhesion molecule-1 (VCAM-1), and E-cadherin) in the urine as potential biomarkers for normoalbuminuric renal insufficiency in T2DM.

2. Methods

2.1. Study Participants. We recruited 432 Chinese T2DM patients (diagnosed according to the 1999 World Health Organization (WHO) criteria), including 169 patients with declined kidney function (eGFR < 60 ml/min per 1.73 m^2), from the Department of Nephrology and Endocrinology of the Third Xiangya Hospital of Central South University between September 2016 and December 2018. All patients involved in this study fulfilled the following inclusion criteria: age > 18 years old; initial diagnosis of diabetes ≥ 5 years ago; no fever, infection, or trauma; not undergoing surgery or dialysis; no acute diabetic complications (such as diabetic ketoacidosis or nonketone hypertonic coma); and no severe cardiovascular or cerebrovascular diseases in the 3-6 months before recruitment. Patients with normoalbuminuria (UACR < 30 mg/g, $n = 209$) were divided into NO-CKD (eGFR > 60 ml/min per 1.73 m^2, $n = 165$) group and NA-DKD (eGFR < 60 ml/min per 1.73 m^2, $n = 44$) group. eGFR was calculated based on the CKD-EPI-combined creatinine-cystatin C equation which appears to be the optimal GFR estimate method [25]. Informed consent was obtained from all participants before they participated in the study. This study adhered to the Declaration of Helsinki and was approved by the Ethics Committee of the Third Xiangya Hospital of Central South University.

2.2. Laboratory Measurements. All urine and blood samples were obtained from the patients in the morning after 12 h of fasting on the first day of their hospitalization. Patient medical history and anthropometric measurements were recorded on the same day. The urine samples were stored at -80°C after being centrifuged for 15 min at 2000×g. The blood samples, which were collected in tubes with K_2EDTA, were used for hemoglobin A1c (HbA1c) analysis. The serum was separated, aliquoted, and used for routine chemical tests. Hemoglobin (HB) was measured using an automatic blood cell analyzer (Sysmex, Japan). Total cholesterol (TC), triglyceride (TG), high-density lipoprotein (HDL), low-density lipoprotein (LDL), serum albumin (ALB), fasting blood sugar (FBS), plasma creatinine (CR), blood urea nitrogen (BUN), uric acid (UA), cystatin C (CYSC), urinary creatinine, urinary microalbumin, and urinary RBP levels were measured by an automatic biochemistry analyzer (Hitachi, Japan). HbA1c levels were measured by an automatic glycosylated hemoglobin analyzer (Bio-Rad, USA). Urinary NGAL, PAI-1, and VCAM-1 levels were measured by magnetic Luminex assays using human premixed multianalyte kits (R&D Systems, USA), and urinary E-cadherin and plasma ET-1, TNF-α, IL-6, and 8-OHdG levels were measured by enzyme-linked immunosorbent assays (ELISAs) using commercially available standard kits (R&D Systems, Abcam, CUSABIO, USA).

2.3. Statistical Analyses. SPSS version 16.0 (Chicago, IL, USA) and RStudio (Boston, MA, USA) were used for statistical analyses. Data are expressed as the mean ± SD for normally distributed values or the median (25-75th percentiles) for nonparametric values, and categorical variables are expressed as ratios. PAI-1, E-cadherin, TNF-α, and 8-OHdG values were logarithmically transformed. All urinary biomarkers were normalized to urinary creatinine, and the square root was then calculated for analyses. UACR values were Napierian logarithmically transformed. Pearson's or Spearman's correlation coefficients were calculated to assess the associations between biomarkers and eGFR. Multiple linear regression was used to analyze relationships among clinical parameters, urinary biomarkers, and eGFR. Logistic regression analysis was performed to identify risk factors for eGFR. Differences between groups were analyzed by ANOVA, followed by LSD's test for normally distributed values, the Kruskal-Wallis test for nonparametric values, or the chi-square test for categorical variables. Receiver operating characteristic (ROC) curves were drawn to calculate the area under the ROC curve (AUC). A very good test would have an AUC > 0.9, a good test would have an AUC of 0.7-0.9, a sufficient test would have an AUC of 0.5-0.7, and a faulty

Table 1: Clinical characteristics of T2DM patients with normoalbuminuria.

	NO-CKD ($N = 165$)	NA-DKD ($N = 44$)	p value
Age (years)	57.4 ± 12.1	66.4 ± 11.7	<0.001
Gender (male/female)	107/58	28/16	0.861
Diabetes duration (years)	9.9 ± 5.4	10.9 ± 6.2	0.269
BMI (kg/m^2)	24.15 ± 3.76	23.25 ± 3.07	0.147
SBP (mmHg)	129.8 ± 17.7	136.8 ± 20.9	0.028
DBP (mmHg)	79.9 ± 11.3	82.2 ± 13.2	0.253
HB (g)	132.7 ± 21.3	121.2 ± 26.7	0.003
HbA1C (%)	8.20 (6.85-10.0)	8.00 (7.33-9.00)	0.834
FBS (mmol/l)	8.18 ± 3.12	7.98 ± 3.28	0.714
TC (mmol/l)	4.33 ± 1.35	4.10 ± 1.33	0.310
TG (mmol/l)	1.43 (0.92-2.47)	1.67 (0.98-2.50)	0.654
HDL (mmol/l)	1.10 ± 0.33	1.06 ± 0.32	0.389
LDL (mmol/l)	2.07 ± 0.77	2.04 ± 0.79	0.828
ALB (g/l)	38.1 ± 6.6	37.7 ± 6.3	0.717
BUN (mmol/l)	5.17 (4.39-6.64)	8.21 (6.72-10.61)	<0.001
CR (mmol/l)	72.0 (60.0-84.0)	121.0 (86.0-169.5)	<0.001
UA (μmol/l)	313.4 ± 103.6	393.1 ± 139.6	<0.001
CYSC (mg/l)	0.76 (0.61-0.92)	1.40 (1.26-1.67)	<0.001

test would have an AUC ≤ 0.5. All reported p values are two-tailed, a p value < 0.05 was considered statistically significant, and a p value < 0.01 was considered highly significant.

3. Results

3.1. Patients' Baseline Characteristics. Among the 432 T2DM patients, 209 patients were normoalbuminuric, and 223 were albuminuric. Their clinical characteristics are presented in Table S1. Compared with patients with normoalbuminuria, the levels of urinary NGAL, RBP, PAI-1, VCAM-1, and E-cadherin were increased in patients with albuminuria, and all correlated positively with UACR (Figure S1). Our results were consistent with previous studies [26–30]. Because nonalbuminuric renal insufficiency in T2DM patients may be ignored clinically and there is no sensitive urinary biomarker, we focused on T2DM patients with nonalbuminuria in this study.

Among the 209 T2DM patients with normoalbuminuria, there were 165 patients without renal insufficiency (eGFR > 60 ml/min per 1.73 m^2, NO-CKD group) and 44 patients with renal insufficiency (eGFR < 60 ml/min per 1.73 m^2, NA-DKD group). 26.0% (44/169) of patients with renal insufficiency was normoalbuminuric. Compared to the NO-CKD group, the NA-DKD group had higher age, SBP, BUN, CR, UA, and CYSC levels and lower HB level (Table 1).

3.2. Correlations between Plasma TNF-α, IL-6, 8-OHdG, and ET-1 with eGFR in T2DM Patients with Normoalbuminuria. Inflammation, endothelial dysfunction, and oxidative stress are known to contribute to the pathogenesis of DKD [16, 17]. To explore the roles of inflammation, endothelial dysfunction, and oxidative stress in normoalbuminuric renal insufficiency, we examined levels of plasma TNF-α, IL-6, ET-1, and 8-OHdG in 209 T2DM patients with normoalbuminuria. The plasma TNF-α, IL-6, and 8-OHdG levels were higher in the NA-DKD group than in the NO-CKD group, while the plasma ET-1 level was not different between these two groups (Figure 1(a)). Single linear regression analysis showed that plasma TNF-α, IL-6, and 8-OHdG levels were each negatively correlated with eGFR ($r = -0.150$, $p = 0.03$; $r = -0.317$, $p < 0.001$; and $r = -0.629$, $p < 0.001$, respectively) (Figure 1(b)). After adjusting for potential confounding factors (age, SBP, and HB), logistic regression analyses revealed that age (odds ratio (OR) = 1.041, 95% CI 1.000-1.084, $p < 0.001$), TNF-α (OR = 131.481, 95% CI 9.289-1,861, $p = 0.048$), and 8-OHdG (OR = 4.593, 95% CI 274.062-76,980, $p < 0.001$) were independent risk factors for renal insufficiency in T2DM patients with normoalbuminuria (Figure 1(c)).

3.3. Correlations between Urinary NGAL, RBP, PAI-1, VCAM-1, and E-Cadherin with eGFR in T2DM Patients with Normoalbuminuria. Compared to NO-CKD group, levels of urinary NGAL and RBP but not PAI-1, VCAM-1, or E-cadherin were significantly elevated in NA-DKD group (Figure 2(a)). Single linear regression analysis revealed that urinary NGAL and RBP had negative correlations with eGFR ($r = -0.291$, $p = 0.001$ and $r = -0.345$, $p < 0.001$, respectively) in the study patients (Figure 2(b)). Moreover, multiple linear regression analyses showed that after adjusting for potential confounding factors (age, SBP, and HB), either NGAL or RBP and age were independently associated with eGFR ($Y_{eGFR} = 175.544 - 0.287\,\text{NGAL} - 1.303\,\text{age}$; $Y_{eGFR} = 177.730 - 44.545\,\text{RBP} - 1.334\,\text{age}$) (Figure 2(c)).

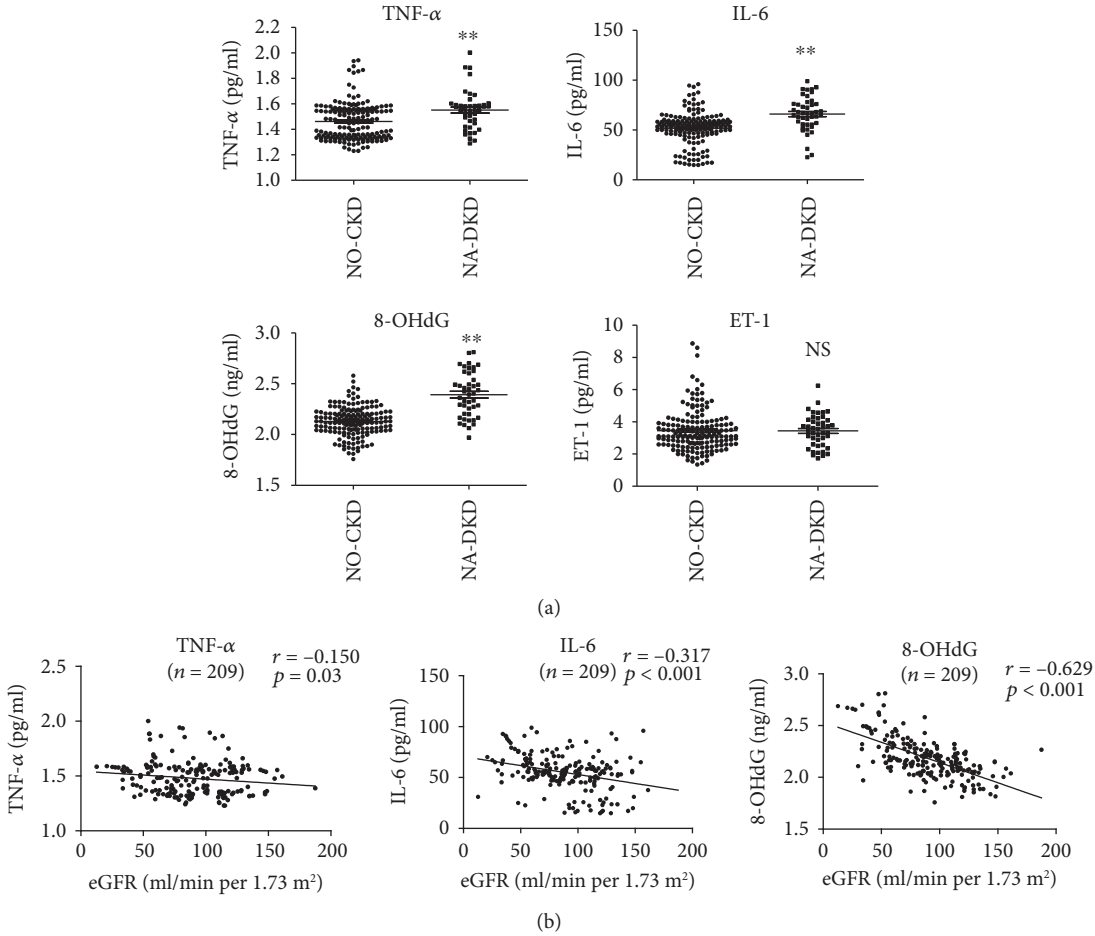

Risk factor	OR (95% CI)	p
Age	1.041 (1.000–1.084)	<0.05
TNF-α	131.481 (9.289–1,861)	<0.001
8-OHdG	4,593 (274.062–76,980)	<0.001

(c)

Figure 1: Correlations between plasma TNF-α, IL-6, 8-OHdG, and ET-1 with eGFR in T2DM patients with normoalbuminuria. (a) Differences in the plasma TNF-α, IL-6, 8-OHdG, and ET-1 levels in patients with normoalbuminuria with/without renal insufficiency. (b) Relationships of plasma TNF-α, IL-6, and 8-OHdG with the eGFR in T2DM patients with normoalbuminuria. (c) Logistic regression analyses between clinical parameters, plasma TNF-α, IL-6, and 8-OHdG and eGFR. 8-OHdG: 8-hydroxydeoxyguanosine; ET-1: endothelin-1; NO-CKD: normoalbuminuric T2DM patients without renal insufficiency; NA-DKD: normoalbuminuric T2DM patients with renal insufficiency; eGFR: estimated glomerular filtration rate. $^{**}p < 0.01$ vs. the NO-CKD group. NS: no significant.

3.4. Correlations between Plasma TNF-α, IL-6, ET-1, and 8-OHdG with Urinary NGAL and RBP. To identify the possible reason for the increase in NGAL and RBP levels in T2DM patients with normoalbuminuric renal insufficiency, we performed single linear regression analysis on the relationships between plasma TNF-α, IL-6, ET-1, and 8-OHdG with urinary NGAL and RBP in T2DM patients with normoalbuminuria. As shown in Figure 3(a), positive associations were found between NGAL and IL-6 ($r = 0.186$, $p = 0.007$) and NGAL and 8-OHdG ($r = 0.200$, $p = 0.004$). In addition, RBP was positively associated with IL-6 ($r = 0.157$, $p = 0.023$) and 8-OHdG ($r = 0.283$, $p < 0.001$) (Figure 3(b)), while there were no significant associations between NGAL or RBP and TNF-α or ET-1.

3.5. ROC Analyses of Urinary NGAL and RBP for Renal Insufficiency in T2DM Patients with Normoalbuminuria. Next, we analyzed the diagnostic accuracy of urinary NGAL and RBP for renal insufficiency in T2DM patients with normoalbuminuria via ROC curves. The results indicated that urinary NGAL had sufficient diagnostic accuracy (sensitivity = 0.773, specificity = 0.545, AUC = 0.674) and that RBP had good diagnostic accuracy (sensitivity = 0.591, specificity = 0.788, AUC = 0.723) for eGFR < 60 ml/min per 1.73 m^2 in T2DM patients, but the difference between urinary NGAL and RBP was not significant ($p = 0.32$) (Figure 4(a)). Next, we analyzed the diagnostic accuracy of combined detection of NGAL and RBP. The ROC curve showed that combined detection had good diagnostic

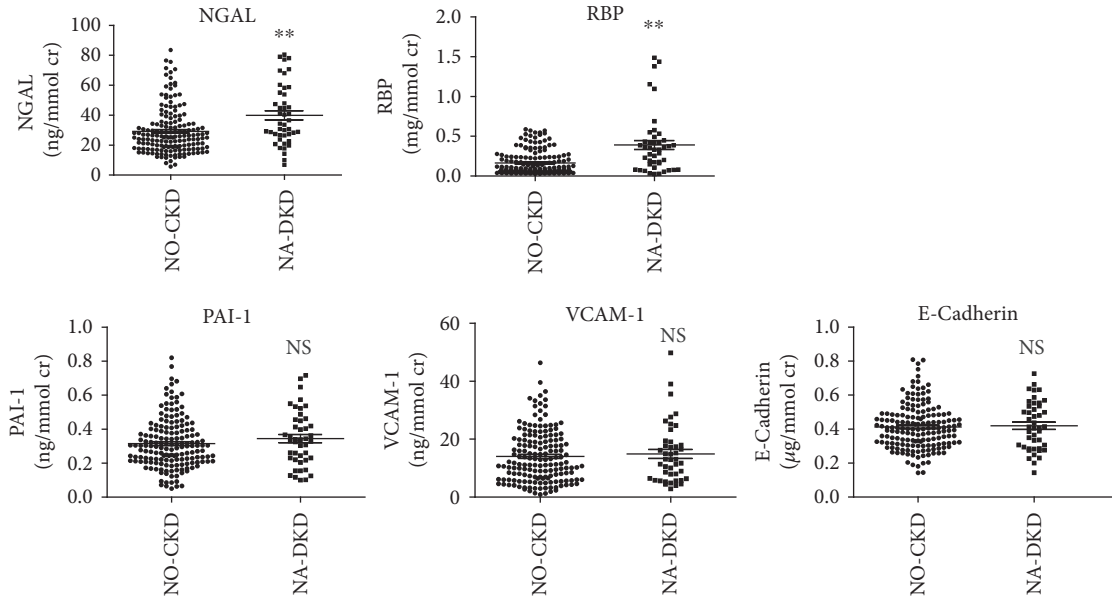

(a)

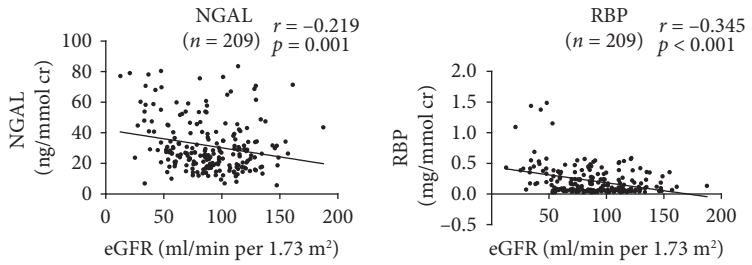

(b)

	B	Stand error	Standard regression coefficient	t	p
Constant	175.544	9.047	−	19.404	<0.001
NGAL	−0.287	0.107	−0.156	−2.684	0.008
Age	−1.303	0.145	−0.521	−8.969	<0.001

	B	Stand error	Standard regression coefficient	t	p
Constant	177.730	8.273	−	21.482	<0.001
RBP	−44.545	7.172	−0.334	−6.211	<0.001
Age	−1.334	0.135	−0.533	−9.901	<0.001

(c)

Figure 2: Correlations between urinary NGAL, RBP, PAI-1, VCAM-1, and E-cadherin with eGFR in T2DM patients with normoalbuminuria. (a) Levels of urinary NGAL, RBP, PAI-1, VCAM-1, and E-cadherin in patients with normoalbuminuria with/without renal insufficiency. (b) Single linear regression analysis of urinary NGAL, RBP, and eGFR in T2DM patients with normoalbuminuria. (c) Multiple linear regression analysis of urinary NGAL or RBP, clinical parameters, and eGFR. NGAL: neutrophil gelatinase-associated lipocalin; RBP: retinol-binding protein; PAI-1: plasminogen activator inhibitor-1; VCAM-1: vascular cell adhesion molecule-1. $^{**}p < 0.01$ vs. NO-CKD group. NS: no significant.

accuracy (sensitivity = 0.614, specificity = 0.752, AUC = 0.731) (Figure 4(b)), but there was no significant difference between combined detection and NGAL alone ($p = 0.13$) or RBP alone ($p = 0.66$).

3.6. Characteristics of Propensity Score-Matched Cohorts. Because age was independently associated with eGFR in T2DM patients with normoalbuminuric renal insufficiency, to better control for confounding factors, we used propensity score matching to compare urinary biomarkers between the NO-CKD and NA-DKD groups. Following the 2-to-1 matching by propensity score, 88 patients in the NO-CKD group were matched to 44 patients in the NA-DKD group. Among the matched patients, compared to the NO-CKD

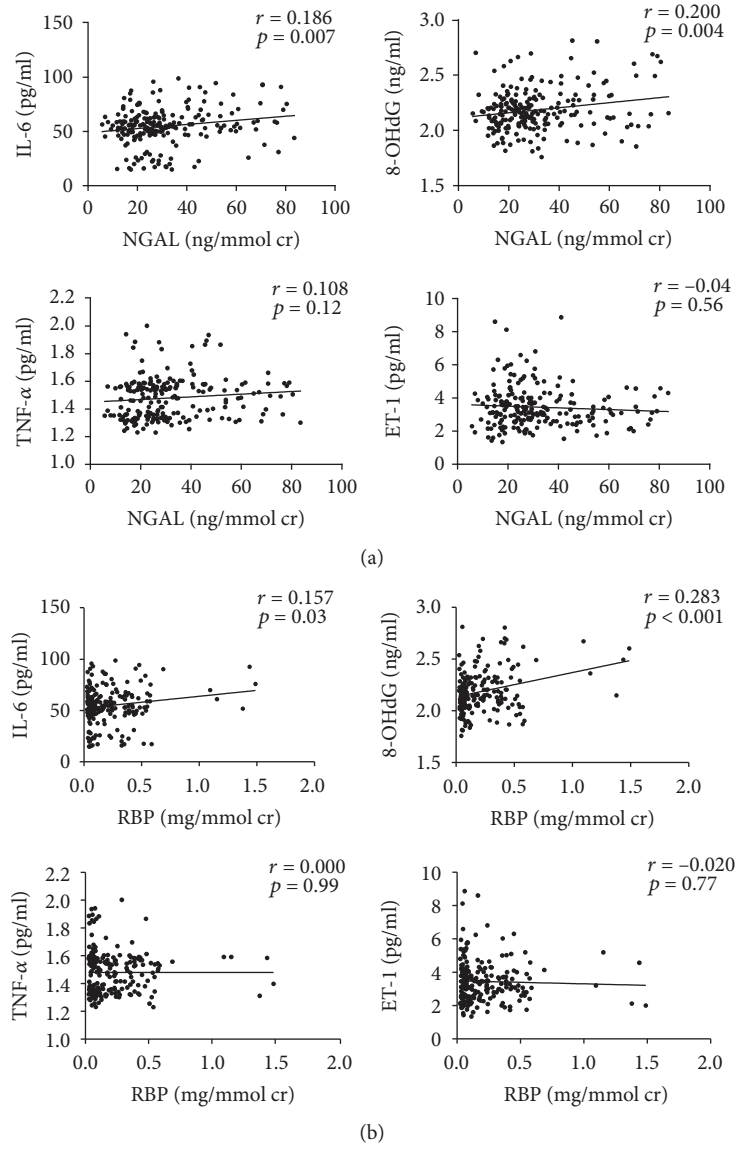

Figure 3: Correlations between plasma TNF-α, IL-6, ET-1, and 8-OHdG with urinary NGAL and RBP. (a) Single linear regression analysis of plasma TNF-α, IL-6, ET-1, and 8-OHdG and urinary NGAL. (b) Single linear regression analysis of plasma TNF-α, IL-6, ET-1, and 8-OHdG and urinary RBP.

group, the NA-DKD group had higher SBP, BUN, CR, UA, and CYSC, but no difference in age and HB (Table 2). Compared to the NO-CKD group, in age-matched patients, the levels of urinary NGAL and RBP but not PAI-1, VCAM-1, or E-cadherin were significantly elevated in the NA-DKD group (Figure 5(a)). Similar to unmatched data, urinary NGAL and RBP showed negative correlations with eGFR ($r = -0.256$, $p = 0.003$ and $r = -0.403$, $p < 0.001$, respectively) (Figure 5(b)). These results indicate that urinary NGAL and RBP can serve as biomarkers in age-matched T2DM patients with normoalbuminuric renal insufficiency.

4. Discussion

In this study, we found that age, plasma TNF-α, and 8-OHdG were independent risk factors for renal insufficiency in T2DM patients with normoalbuminuria. In addition, levels of urinary NGAL and RBP were elevated in patients with renal insufficiency and negatively related to eGFR in T2DM patients with normoalbuminuria. Furthermore, urinary NGAL and RBP were independently associated with eGFR, suggesting that urinary NGAL and RBP are biomarkers for T2DM patients with normoalbuminuric renal insufficiency.

Diabetic kidney disease is the most common cause of ESRD, the primary clinical characteristics of which are progressive proteinuria and renal failure [31]. However, a portion of patients with T2DM follows a nonalbuminuric pathway to renal impairment that may be misdiagnosed. A previous cross-sectional survey including 301 T2DM patients showed that the prevalence of GFR < 60 ml/min per 1.73 m^2 and normoalbuminuria was 23.3% [6], which is highly consistent with the prevalence in our study. Studies have reported that aging, rising blood pressure, and intrarenal vascular disease may play pathogenic roles in nonalbuminuric

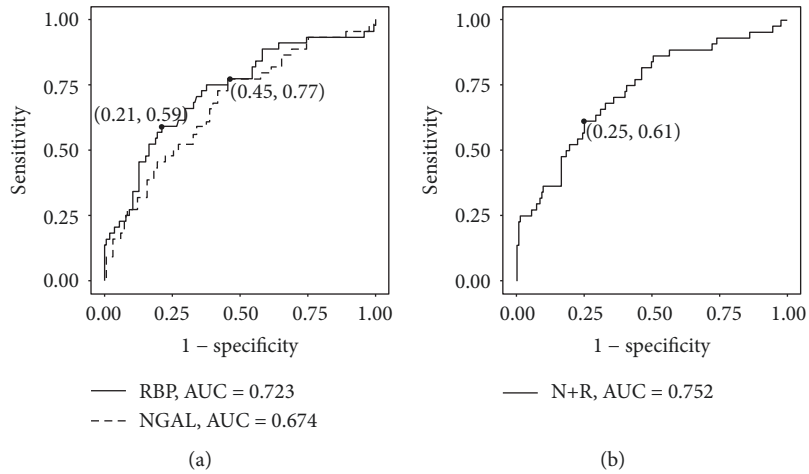

Figure 4: ROC analyses of urinary NGAL and RBP for renal insufficiency in T2DM patients with normoalbuminuria. (a) ROC curve for the ability of NGAL and RBP to identify cases with eGFR < 60 ml/min per 1.73 m^2 among patients with normoalbuminuria. (b) ROC curve for the combined detection of urinary NGAL and RBP (N+R) to identify cases with eGFR < 60 ml/min per 1.73 m^2 among patients with normoalbuminuria. ROC: receiver operating characteristic; AUC: area under the ROC curve; N+R: combined detection of urinary NGAL and RBP.

Table 2: Clinical characteristics of the matched patients.

	NO-CKD ($N = 88$)	NA-DKD ($N = 44$)	p values
Age (years)	63.5 ± 10.5	66.4 ± 11.7	0.141
Gender (male/female)	56/32	28/16	0.578
Diabetes duration (years)	10.9 ± 6.1	10.9 ± 6.2	0.968
BMI (kg/m^2)	23.10 ± 3.51	23.25 ± 3.07	0.803
SBP (mmHg)	129.4 ± 17.0	136.8 ± 20.9	0.033
DBP (mmHg)	78.8 ± 10.6	82.2 ± 13.2	0.108
HB (g)	129.9 ± 15.8	121.2 ± 26.7	0.051
HbA1C (%)	8.15 (6.90-10.0)	8.00 (7.33-9.00)	0.839
FBS (mmol/l)	8.24 ± 3.25	7.98 ± 3.28	0.667
TC (mmol/l)	4.21 ± 1.10	4.10 ± 1.33	0.621
TG (mmol/l)	1.36 (0.85-2.48)	1.67 (0.98-2.50)	0.447
HDL (mmol/l)	1.06 ± 0.27	1.06 ± 0.32	0.902
LDL (mmol/l)	2.05 ± 0.82	2.04 ± 0.79	0.944
ALB (g/l)	37.5 ± 5.5	37.7 ± 6.3	0.868
BUN (mmol/l)	5.55 (4.62-7.02)	8.21 (6.72-10.61)	<0.001
CR (mmol/l)	72.5 (60.0-84.0)	121.0 (86.0-169.5)	<0.001
UA (μmol/l)	310.2 ± 105.0	393.1 ± 139.6	<0.001
CYSC (mg/l)	0.81 (0.64-0.93)	1.40 (1.26-1.67)	<0.001

renal insufficiency [6] [15], which might explain why the patients with nonalbuminuric renal insufficiency in our study had higher age and SBP values than others.

Inflammation appears to associated with renal function decline in normoalbuminuric renal insufficiency [32]. Our previous study confirmed that the level of TNF-α was increased in T2DM patients [33], and the current study showed levels of plasma TNF-α and IL-6 were elevated in T2DM patients with renal insufficiency and were inversely related to the eGFR. Generally, diabetic nephropathy is believed to be a microvascular complication of DM, while studies have indicated that macroangiopathy was more prevalent in patients with normoalbuminuric renal insufficiency, which was usually accompanied by significant cardiovascular disease burden [8, 11, 12]. As a sensitive biomarker of intracellular oxidative stress, 8-OHdG was shown to be more highly expressed in a high intima media thickness (IMT) group than in a normal IMT group, and 8-OHdG was also correlated positively with coronary heart disease risk scores [34], suggesting that 8-OHdG is a useful biomarker of

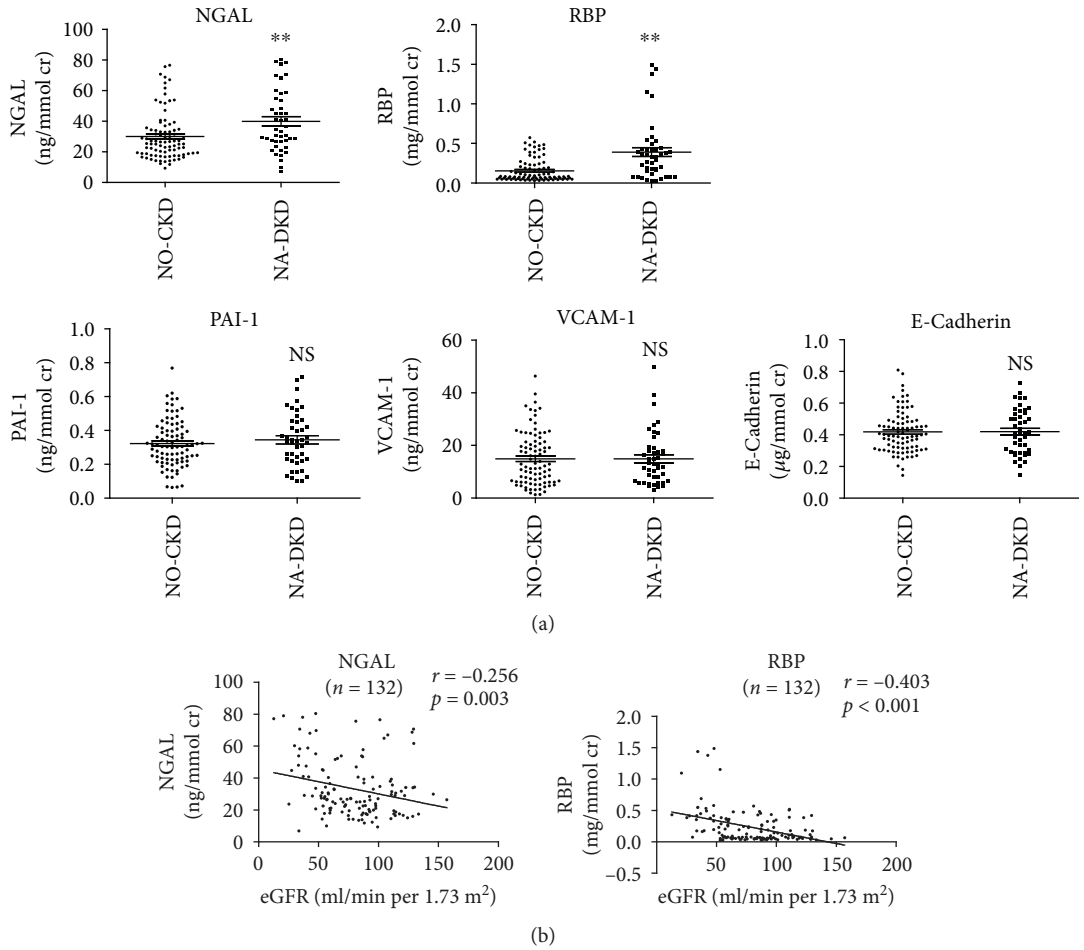

Figure 5: Correlations between urinary NGAL, RBP, PAI-1, VCAM-1, and E-cadherin with eGFR in matched T2DM patients with normoalbuminuria. (a) Levels of urinary NGAL, RBP, PAI-1, VCAM-1, and E-cadherin in matched patients with normoalbuminuria with/without renal insufficiency. (b) Single linear regression analysis of urinary NGAL, RBP, and eGFR in matched T2DM patients with normoalbuminuria. $^{**}p < 0.01$ vs. the NO-CKD group. NS: no significant.

macrovascular complications in patients with T2DM. Our results showed that 8-OHdG was an independent risk factor for renal insufficiency in T2DM patients with normoalbuminuria. ET-1 is a potent vasoconstrictor mainly produced by mesangial cells in the kidneys, and renal microcirculation is particularly susceptible to ET-1 [35], which may explain why plasma ET-1 levels were found to be elevated in diabetic patients with microalbuminuria [36], but not elevated in our patients with normoalbuminuric renal insufficiency. These results indicate that inflammation and oxidative stress may be factors contributing to the pathogenesis of normoalbuminuric renal insufficiency, which seems more relevant to macroangiopathy of T2DM.

In diabetic patients with proteinuria, the increase in interstitial fibrosis correlates with renal function decline, and this decline is independent of albuminuria, indicating that interstitial injury partly contributes to the declining eGFR in DM [37]. In patients with normoalbuminuric renal insufficiency, interstitial or vascular changes are observed more frequently than the renal structural change typical of diabetic nephropathy [15], which suggests that tubulointerstitial damage may be involved in the development of normoalbuminuric renal insufficiency. NGAL and RBP, tubular damage biomarkers, have low molecular weights which are filtered by glomeruli and reabsorbed by proximal tubules [38]. Injured tubules reduce reabsorption and thus increase their urinary excretion in T2DM patients with normoalbuminuric renal insufficiency. In previous studies, NGAL expression increased in patients with T1DM before the diagnosis of microalbuminuria [39] and increased progressively from UACR < 10 mg/g to 10-30 mg/g to >30 mg/g in T2DM patients [40]. Urinary RBP had been identified as a biomarker of proximal tubular dysfunction and had good diagnostic value in diabetic patients with macroalbuminuria [41]. Our present study showed that levels of NGAL and RBP were increased in T2DM patients with normoalbuminuric renal insufficiency and weakly but significantly correlated with eGFR, which may be caused by inflammation and oxidative stress, which can cause tubular damage [42]. Both urinary NGAL and RBP are correlated positively with plasma IL-6 and 8-OHdG in our study. Although tubulointerstitial damage is common with older age [43], our study showed

urinary NGAL and RBP were elevated in patients with declined kidney function and correlated negatively with eGFR in age-matched patients.

Our study has some limitations. First of all, this cross-sectional study only provided the basis for associations, and a longitudinal study is needed to confirm the value of these biomarkers. Besides, eGFR was calculated based on CKD-EPI-combined creatinine-cystatin C equation, which is not the "gold standards." In addition, further mechanism research is necessary to verify the roles of NGAL and RBP in normoalbuminuric renal insufficiency.

Taken together, our results reveal that urinary NGAL and RBP are biomarkers for normoalbuminuric renal insufficiency in T2DM, which may be caused by inflammation and oxidative stress. It is necessary to detect urinary NGAL and RBP in T2DM patients, especially elderly individuals.

Abbreviations

T2DM: Type 2 diabetes mellitus
DN: Diabetic nephropathy
NGAL: Neutrophil gelatinase-associated lipocalin
RBP: Retinol-binding protein
PAI-1: Plasminogen activator inhibitor-1
VCAM-1: Vascular cell adhesion molecule-1
ESRD: End-stage renal disease
UACR: Urinary albumin/creatinine ratio
EMT: Epithelial-mesenchymal transition
eGFR: Estimated glomerular filtration rate
HB: Hemoglobin
HbA1c: Hemoglobin A1c
FBS: Fasting blood glucose
TC: Total cholesterol
TG: Triglyceride
HDL: High-density lipoprotein
LDL: Low-density lipoprotein
ALB: Serum albumin
BUN: Blood urea nitrogen
CR: Creatinine
UA: Uric acid
CYSC: Cystatin C
8-OHdG: 8-Hydroxydeoxyguanosine
ET-1: Endothelin-1
ROC: Receiver operating characteristic
AUC: Area under the ROC curve
BMI: Body mass index
SBP: Systolic blood pressure
DBP: Diastolic blood pressure
IMT: Intima media thickness.

Data Availability

The data used to support the findings of this study are included within the article.

Conflicts of Interest

All authors declare that they have no conflicts of interest, financial, or otherwise.

Acknowledgments

We thank all of the patients for their participation in this study. This study was funded by the National Natural Science Foundation of China (No. 81470961 and No. 81870498).

Supplementary Materials

Table S1: clinical characteristics of the T2DM patients. Figure S1: associations between urinary biomarkers with UACR in T2DM patients. A: levels of urinary biomarkers in T2DM patients with/without albuminuria. B: relationship between urinary biomarkers and UACR in T2DM patients. $^{**}p < 0.01$ vs. the normoalbuminuria group. NGAL: neutrophil gelatinase-associated lipocalin; RBP: retinol-binding protein; PAI-1: plasminogen activator inhibitor-1; VCAM-1: vascular cell adhesion molecule-1. *(Supplementary Materials)*

References

[1] M. Afkarian, M. C. Sachs, B. Kestenbaum et al., "Kidney disease and increased mortality risk in type 2 diabetes," *Journal of the American Society of Nephrology*, vol. 24, no. 2, pp. 302–308, 2013.

[2] Z. H. Liu, "Nephrology in China," *Nature Reviews Nephrology*, vol. 9, no. 9, pp. 523–528, 2013.

[3] KDOQI, "KDOQI clinical practice guidelines and clinical practice recommendations for diabetes and chronic kidney disease," *American Journal of Kidney Diseases*, vol. 49, no. 2, pp. S12–154, 2007.

[4] H. J. Kramer, Q. D. Nguyen, G. Curhan, and C. Y. Hsu, "Renal insufficiency in the absence of albuminuria and retinopathy among adults with type 2 diabetes mellitus," *JAMA*, vol. 289, no. 24, pp. 3273–3277, 2003.

[5] A. X. Garg, B. A. Kiberd, W. F. Clark, R. B. Haynes, and C. M. Clase, "Albuminuria and renal insufficiency prevalence guides population screening: results from the NHANES III," *Kidney International*, vol. 61, no. 6, pp. 2165–2175, 2002.

[6] R. J. MacIsaac, C. Tsalamandris, S. Panagiotopoulos, T. J. Smith, K. J. McNeil, and G. Jerums, "Nonalbuminuric renal insufficiency in type 2 diabetes," *Diabetes Care*, vol. 27, no. 1, pp. 195–200, 2004.

[7] R. Retnakaran, C. A. Cull, K. I. Thorne, A. I. Adler, R. R. Holman, and for the UKPDS Study Group, "Risk factors for renal dysfunction in type 2 diabetes: U.K. Prospective Diabetes Study 74," *Diabetes*, vol. 55, no. 6, pp. 1832–1839, 2006.

[8] G. Penno, A. Solini, E. Bonora et al., "Clinical significance of nonalbuminuric renal impairment in type 2 diabetes," *Journal of Hypertension*, vol. 29, no. 9, pp. 1802–1809, 2011.

[9] S. De Cosmo, O. Lamacchia, A. Pacilli et al., "Normoalbuminuric renal impairment and all-cause mortality in type 2 diabetes mellitus," *Acta Diabetologica*, vol. 51, no. 4, pp. 687–689, 2014.

[10] G. Penno, A. Solini, E. Orsi et al., "Non-albuminuric renal impairment is a strong predictor of mortality in individuals with type 2 diabetes: the Renal Insufficiency And Cardiovascular Events (RIACE) Italian multicentre study," *Diabetologia*, vol. 61, no. 11, pp. 2277–2289, 2018.

[11] J. H. An, Y. M. Cho, H. G. Yu et al., "The clinical characteristics of normoalbuminuric renal insufficiency in Korean type 2 diabetic patients: a possible early stage renal complication,"

Journal of Korean Medical Science, vol. 24, Suppl 1, pp. S75–S81, 2009.

[12] M. Boronat, C. Garcia-Canton, V. Quevedo et al., "Non-albuminuric renal disease among subjects with advanced stages of chronic kidney failure related to type 2 diabetes mellitus," *Renal Failure*, vol. 36, no. 2, pp. 166–170, 2014.

[13] T. W. C. Tervaert, A. L. Mooyaart, K. Amann et al., "Pathologic classification of diabetic nephropathy," *Journal of the American Society of Nephrology*, vol. 21, no. 4, pp. 556–563, 2010.

[14] G. Mazzucco, T. Bertani, M. Fortunato et al., "Different patterns of renal damage in type 2 diabetes mellitus: a multicentric study on 393 biopsies," *American Journal of Kidney Diseases*, vol. 39, no. 4, pp. 713–720, 2002.

[15] E. I. Ekinci, G. Jerums, A. Skene et al., "Renal structure in normoalbuminuric and albuminuric patients with type 2 diabetes and impaired renal function," *Diabetes Care*, vol. 36, no. 11, pp. 3620–3626, 2013.

[16] P. Du, B. Fan, H. Han et al., "NOD2 promotes renal injury by exacerbating inflammation and podocyte insulin resistance in diabetic nephropathy," *Kidney International*, vol. 84, no. 2, pp. 265–276, 2013.

[17] J. M. Forbes, M. T. Coughlan, and M. E. Cooper, "Oxidative stress as a major culprit in kidney disease in diabetes," *Diabetes*, vol. 57, no. 6, pp. 1446–1454, 2008.

[18] Z. Lu, N. Liu, and F. Wang, "Epigenetic regulations in diabetic nephropathy," *Journal Diabetes Research*, vol. 2017, pp. 1–6, 2017.

[19] D. Umapathy, E. Krishnamoorthy, V. Mariappanadar, V. Viswanathan, and K. M. Ramkumar, "Increased levels of circulating (TNF-α) is associated with (-308G/A) promoter polymorphism of TNF-α gene in Diabetic Nephropathy," *International Journal of Biological Macromolecules*, vol. 107, pp. 2113–2121, 2018.

[20] R. Wu, X. Liu, J. Yin et al., "IL-6 receptor blockade ameliorates diabetic nephropathy via inhibiting inflammasome in mice," *Metabolism*, vol. 83, pp. 18–24, 2018.

[21] G. M. Hargrove, J. Dufresne, C. Whiteside, D. A. Muruve, and N. C. W. Wong, "Diabetes mellitus increases endothelin-1 gene transcription in rat kidney," *Kidney International*, vol. 58, no. 4, pp. 1534–1545, 2000.

[22] M. Sanchez, R. Roussel, S. Hadjadj et al., "Plasma concentrations of 8-hydroxy-2′-deoxyguanosine and risk of kidney disease and death in individuals with type 1 diabetes," *Diabetologia*, vol. 61, no. 4, pp. 977–984, 2018.

[23] D. Spires, B. Poudel, C. A. Shields et al., "Prevention of the progression of renal injury in diabetic rodent models with preexisting renal disease with chronic endothelin A receptor blockade," *American Journal of Physiology. Renal Physiology*, vol. 315, no. 4, pp. F977–F985, 2018.

[24] T. Tomohiro, T. Kumai, T. Sato, Y. Takeba, S. Kobayashi, and K. Kimura, "Hypertension aggravates glomerular dysfunction with oxidative stress in a rat model of diabetic nephropathy," *Life Sciences*, vol. 80, no. 15, pp. 1364–1372, 2007.

[25] L. A. Inker, C. H. Schmid, H. Tighiouart et al., "Estimating glomerular filtration rate from serum creatinine and cystatin C," *The New England Journal of Medicine*, vol. 367, no. 1, pp. 20–29, 2012.

[26] J. Wu, X. Shao, K. Lu et al., "Urinary RBP and NGAL levels are associated with nephropathy in patients with type 2 diabetes," *Cellular Physiology and Biochemistry*, vol. 42, no. 2, pp. 594–602, 2017.

[27] K. Al-Rubeaan, K. Siddiqui, M. A. Al-Ghonaim, A. M. Youssef, A. H. Al-Sharqawi, and D. AlNaqeb, "Assessment of the diagnostic value of different biomarkers in relation to various stages of diabetic nephropathy in type 2 diabetic patients," *Scientific Reports*, vol. 7, no. 1, p. 2684, 2017.

[28] A. Festa, K. Williams, R. P. Tracy, L. E. Wagenknecht, and S. M. Haffner, "Progression of plasminogen activator inhibitor-1 and fibrinogen levels in relation to incident type 2 diabetes," *Circulation*, vol. 113, no. 14, pp. 1753–1759, 2006.

[29] J. J. Liu, L. Y. Yeoh, C. F. Sum et al., "Vascular cell adhesion molecule-1, but not intercellular adhesion molecule-1, is associated with diabetic kidney disease in Asians with type 2 diabetes," *Journal of Diabetes and its Complications*, vol. 29, no. 5, pp. 707–712, 2015.

[30] K. Musial, A. Bargenda, and D. Zwolinska, "Urine survivin, E-cadherin and matrix metalloproteinases as novel biomarkers in children with chronic kidney disease," *Biomarkers*, vol. 20, no. 3, pp. 177–182, 2015.

[31] M. L. Gross, R. Dikow, and E. Ritz, "Diabetic nephropathy: recent insights into the pathophysiology and the progression of diabetic nephropathy," *Kidney International. Supplement*, vol. 67, pp. S50–S53, 2005.

[32] C. Chen, C. Wang, C. Hu et al., "Normoalbuminuric diabetic kidney disease," *Frontiers in Medicine*, vol. 11, no. 3, pp. 310–318, 2017.

[33] B. Yi, J. Huang, W. Zhang et al., "Vitamin D receptor downregulation is associated with severity of albuminuria in type 2 diabetes patients," *The Journal of Clinical Endocrinology and Metabolism*, vol. 101, no. 11, pp. 4395–4404, 2016.

[34] T. Nishikawa, T. Sasahara, S. Kiritoshi et al., "Evaluation of urinary 8-hydroxydeoxy-guanosine as a novel biomarker of macrovascular complications in type 2 diabetes," *Diabetes Care*, vol. 26, no. 5, pp. 1507–1512, 2003.

[35] F. C. Luft, "Proinflammatory effects of angiotensin II and endothelin: targets for progression of cardiovascular and renal diseases," *Current Opinion in Nephrology and Hypertension*, vol. 11, no. 1, pp. 59–66, 2002.

[36] G. De Mattia, M. Cassone-Faldetta, C. Bellini et al., "Role of plasma and urinary endothelin-1 in early diabetic and hypertensive nephropathy," *American Journal of Hypertension*, vol. 11, no. 8, pp. 983–988, 1998.

[37] J. L. Taft, C. J. Nolan, S. P. Yeung, T. D. Hewitson, and F. I. Martin, "Clinical and histological correlations of decline in renal function in diabetic patients with proteinuria," *Diabetes*, vol. 43, no. 8, pp. 1046–1051, 1994.

[38] D. R. Flower, "The lipocalin protein family: structure and function," *The Biochemical Journal*, vol. 318, no. 1, pp. 1–14, 1996.

[39] A. Lacquaniti, V. Donato, B. Pintaudi et al., ""Normoalbuminuric" diabetic nephropathy: tubular damage and NGAL," *Acta Diabetologica*, vol. 50, no. 6, pp. 935–942, 2013.

[40] J. A. M. de Carvalho, E. Tatsch, B. S. Hausen et al., "Urinary kidney injury molecule-1 and neutrophil gelatinase-associated lipocalin as indicators of tubular damage in normoalbuminuric patients with type 2 diabetes," *Clinical Biochemistry*, vol. 49, no. 3, pp. 232–236, 2016.

[41] S. M. Titan, J. M. Vieira Jr., W. V. Dominguez et al., "Urinary MCP-1 and RBP: independent predictors of renal outcome in

macroalbuminuric diabetic nephropathy," *Journal of Diabetes and its Complications*, vol. 26, no. 6, pp. 546–553, 2012.

[42] R. X. Li, W. H. Yiu, H. J. Wu et al., "BMP7 reduces inflammation and oxidative stress in diabetic tubulopathy," *Clinical Science (London, England)*, vol. 128, no. 4, pp. 269–280, 2015.

[43] A. D. Rule, H. Amer, L. D. Cornell et al., "The association between age and nephrosclerosis on renal biopsy among healthy adults," *Annals of Internal Medicine*, vol. 152, no. 9, pp. 561–567, 2010.

Hindawi
Journal of Immunology Research
Volume 2019, Article ID 9782594, 6 pages
https://doi.org/10.1155/2019/9782594

Research Article

Monocyte Subsets, Stanford-A Acute Aortic Dissection, and Carotid Artery Stenosis: New Evidences

Noemi Cifani,[1] Maria Proietta,[2] Maurizio Taurino,[3] Luigi Tritapepe,[4] and Flavia Del Porto[5]

[1]*Dipartimento di Medicina Clinica e Molecolare, Ospedale Sant'Andrea, Facoltà di Medicina e Psicologia, Ospedale Sant'Andrea, "Sapienza, " Università di Roma, Italy*
[2]*Dipartimento di Medicina Clinica e Molecolare, Ospedale Sant'Andrea, Facoltà di Medicina e Psicologia, Ospedale Sant'Andrea, UOS Aterosclerosi e Dislipidemia, "Sapienza, " Università di Roma, Italy*
[3]*Dipartimento di Medicina Clinica e Molecolare, Ospedale Sant'Andrea, Facoltà di Medicina e Psicologia, Ospedale Sant'Andrea, UOC Chirurgia Vascolare, "Sapienza, " Università di Roma, Italy*
[4]*Dipartimento di Scienze Anestesiologiche, Medicina Critica e Terapia del Dolore, Facoltà di Medicina e Odontoiatria, Policlinico Umberto I, "Sapienza, " Università di Roma, Italy*
[5]*Dipartimento di Medicina Clinica e Molecolare, Ospedale Sant'Andrea, Facoltà di Medicina e Psicologia, Ospedale Sant'Andrea, UOC Medicina Interna, "Sapienza, " Università di Roma, Italy*

Correspondence should be addressed to Flavia Del Porto; flavia.delporto@uniroma1.it

Received 21 February 2019; Revised 21 May 2019; Accepted 10 July 2019; Published 6 August 2019

Guest Editor: Mohammad A. Khan

Monocytes are a heterogeneous cell population distinguished into three subsets with distinctive phenotypic and functional properties: "classical" (CD14++CD16-), "intermediate" (CD14++CD16+), and "nonclassical" (CD14+CD16++). Monocyte subsets play a pivotal role in many inflammatory systemic diseases including atherosclerosis (ATS). Only a low number of studies evaluated monocyte behavior in patients affected by cardiovascular diseases, and data about their role in acute aortic dissection (AAD) are lacking. Thus, the aim of this study was to investigate CD14++CD16-, CD14++CD16+, and CD14+CD16++ cells in patients with Stanford-A AAD and in patients with carotid artery stenosis (CAS). *Methods*. 20 patients with carotid artery stenosis (CAS group), 17 patients with Stanford-A AAD (AAD group), and 17 subjects with traditional cardiovascular risk factors (RF group) were enrolled. Monocyte subset frequency was determined by flow cytometry. *Results*. Classical monocytes were significantly increased in the AAD group versus CAS and RF groups, whereas intermediate monocytes were significantly decreased in the AAD group versus CAS and RF groups. *Conclusions*. Results of this study identify in AAD patients a peculiar monocyte array that can partly explain depletion of T CD4+ lymphocyte subpopulations observed in patients affected by AAD.

1. Introduction

Atherosclerosis (ATS) is a multifactorial disease [1] characterized by an inflammatory remodeling of the arterial wall. Depending on size and site of vessels involved, ATS leads to a wide range of cardiovascular diseases (CVDs) [2], including ischemic heart disease, cerebrovascular disease, carotid artery stenosis (CAS), abdominal aortic aneurism (AAA), acute aortic dissection (AAD), and other conditions [3, 4]. Immune response strongly affects the outcome of intraparietal inflammation: T helper (Th) 1 lymphocytes have been mainly associated with plaque formation and Th2 lymphocytes with AAA, whereas macrophages have been related to AAD [1, 5, 6].

Monocytes represent the circulating precursor of tissue macrophages [7] and play an important role in atherogenesis, being rapidly attracted by activated endothelial cells [8]. During an atherosclerotic process, their differentiation into macrophages is associated with upregulation of phagocytic

activity leading to lipid accumulation and formation of typical foam cells [1]. Monocytes are a heterogeneous cell population distinguished by the expression of the surface markers CD14 (coreceptor for LPS) and CD16 (receptor for FcγRIII) [9] into three subsets: "classical" (CD14++CD16-), "intermediate" (CD14++CD16+), and "nonclassical" (CD14+ CD16++) [10]. Each monocyte subset possesses distinctive phenotypic and functional properties and displays different immune functions, distinguished by cytokine profiles and phagocytic activity [11]. A low number of studies evaluated monocyte behavior in patients affected by CVDs. Classical monocytes have been independently associated with cardiovascular events including death, myocardial infarction, and stroke [12, 13]. Furthermore, experimental evidences support the role of intermediate monocytes in atherooccclusive diseases [14], such as coronary artery disease (CAD) [15, 16], cardioembolic stroke [17], CAS [18], unstable angina [12, 18], and AAA [19]. However, to our knowledge, data about the role of monocyte subsets in AAD are still lacking.

Therefore, we evaluated CD14++CD16-, CD14++CD16+, and CD14+CD16++ cells in patients with Stanford-A AAD and in patients with CAS.

2. Materials and Methods

This was an observational retrospective study.

The population included in this study was composed of 17 patients undergoing Stanford-A AAD surgical repair at the Attilio Reale Heart and Great Vessels Department, Policlinico Umberto I, "Sapienza" University of Rome (AAD group). Patients were selected on the basis of the following inclusion criteria: (i) Stanford-A AAD; (ii) no history of neoplasm or autoimmune, infectious, or inflammatory systemic diseases; (iii) no presence of genetic syndromes known to be responsible for aortic disease; and (iv) no family history of aortic dissection or aneurysm.

A group of 20 patients with critical CAS (CAS group) was selected among those undergoing carotid thromboendo-arteriectomy (TEA) at the Department of Vascular Surgery, Sant'Andrea Hospital, "Sapienza" University of Rome. Patients were enrolled on the basis of the following inclusion criteria: (i) critical carotid stenosis, defined as a narrowing of the carotid lumen $\geq 70\%$ [20, 21]; (ii) no cardiac causes of stroke; (iii) no history of neoplasm or autoimmune or inflammatory systemic diseases; and (iv) no familiar or personal history of aneurysms/dissection. All patients underwent physical and neurological examinations, carotid artery ultrasound, and angiography by magnetic resonance imaging (MRI) or contrast tomography (CT).

Seventeen patients with traditional cardiovascular risk factors attending the Department of Atherosclerosis and Dyslipidemia, Sant'Andrea Hospital, "Sapienza" University of Rome, were used as the control group (RF group). Patients were selected on the basis of the following criteria: (i) no acute cerebrovascular symptoms or history of cardiovascular disease, (ii) no carotid stenosis > 20%, and (iii) no familiar or personal history of aneurysms/dissection.

No significant differences regarding age (mean age ± SD: 68.83 ± 4.11 years, 59.85 ± 11.01 years, and 62.59 ± 11.08 years for CAS, RF, and AAD, respectively), sex, diabetes, hypertension, dyslipidemia, and body mass index (BMI) were observed between CAS and RF groups.

AAD patients were matched with CAS and RF patients for age, sex, diabetes, and BMI but not for hypertension and dyslipidemia.

A venous blood sample was withdrawn from each patient (just before surgery) and from each control, in order to isolate peripheral blood mononuclear cells (PBMCs) by density gradient centrifugation (Lympholyte, Cedarlane, Hornby, CA). (Since Attilio Reale Heart and great Vessels Department is an hub reference center for AAD, all patients underwent to surgery within 6 hours from the onset of the symptoms and blood samples were collected within this time).

Monocyte subsets were analyzed by flow cytometry as previously described [22–24] using the following antibodies: CD14 FITC (BD Biosciences, San Jose, CA, USA), CD16 APC (BD Biosciences, San Jose, CA, USA), and HLA-DR PE (BD Biosciences, San Jose, CA, USA). Briefly, cells were first visualized on FSC vs. SSC, and an ample gate was drawn around the monocyte cloud to exclude the majority of debris and lymphocytes. These cells were then viewed on a CD14 vs. CD16 plot. Moreover, the presence of natural killer (NK) cells, most of which are CD16-positive and could interfere with CD16+ monocyte count, was checked by HLA-DR antibody; accordingly, HLA-DR-negative NK cells were excluded. Monocyte subsets CD14+CD16–, CD14+CD16+, and CD14+CD16++ were, therefore, defined according to the surface expression of CD14 and CD16 [23, 9] (Figure 1).

On the basis of the number of PBMC available, it was possible to test also CD4+ T lymphocytes in 6 patients of the CAS group, in 6 with RF, and in 10 with AAD. In the 10 AAD patients, immunohistochemistry of aortic specimens collected during surgery was performed as previously described [25].

FACS analysis was performed using a FACSCalibur cytometer (Becton-Dickinson) equipped with Cell Quest software. Isotype controls were used as compensation controls and to confirm antibody specificity.

All the statistical procedures were performed by GraphPad Prism 4 software (GraphPad Software Inc.).

The study was performed according to the principles of the Declaration of Helsinki and was approved by the ethics committee of the Faculty of Medicine.

Written informed consent was obtained from each patient or from an authorized family member.

3. Results and Discussion

3.1. Results

3.1.1. Monocytes. Classical monocytes were significantly increased in the AAD group versus CAS and RF groups ($p = 0.0342$ and $p = 0.0422$, respectively), whereas intermediate monocytes were significantly decreased in the AAD group versus CAS and RF groups ($p = 0.0494$ and $p = 0.0211$, respectively). In particular, both intermediate and

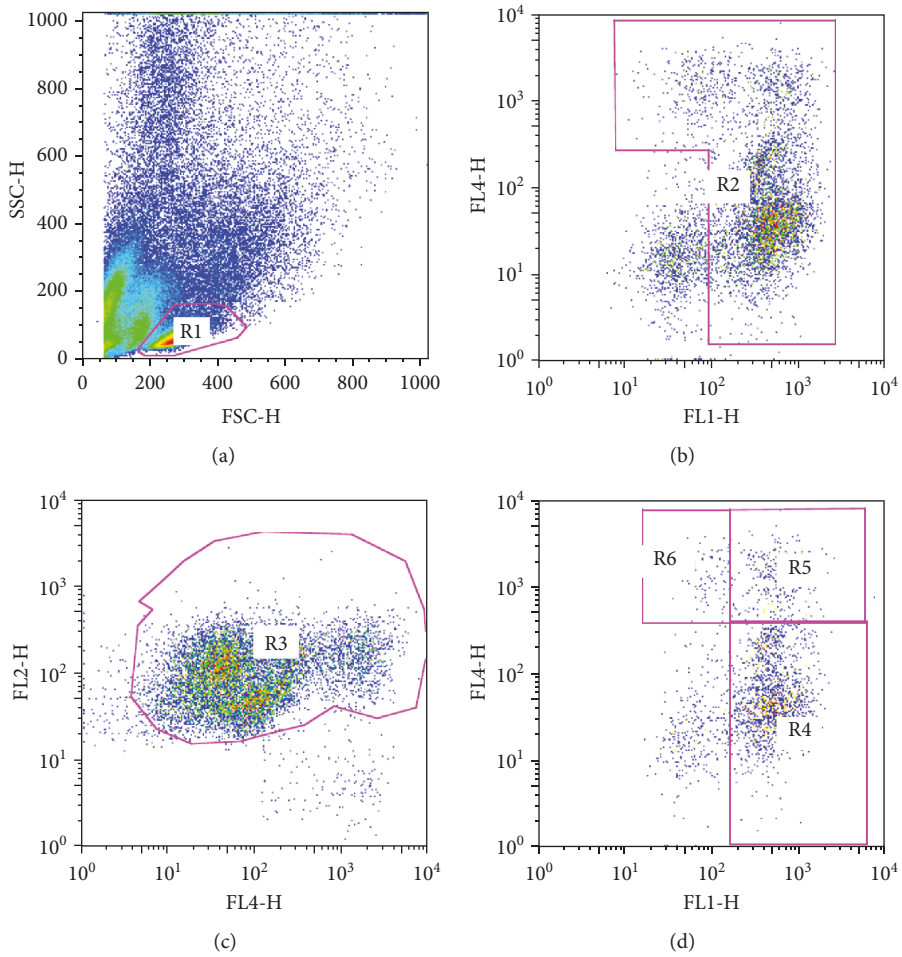

Figure 1: Representative flow cytometry strategy. Cells are visualized on FSC vs. SSC, and gate R1 is drawn around the monocyte cloud (a). These cells are then viewed on a CD14 (FITC, FL1-H) vs. CD16 (APC, FL4-H) plot, and gate R2 is drawn around the monocyte cloud (b). Gate R2 cells are viewed on a CD16 (APC, FL4-H) vs. HLA-DR (PE, FL2-H) plot, and HLA-DR-negative NK cells were excluded drawing R3 gate (c). Then, R3 monocyte population is viewed again on a CD14 (FITC, FL1-H) vs. CD16 (APC, FL4-H) plot, and CD14++CD16- (gate R4), CD14++CD16+ (gate R5), and CD14+CD16++ (gate R6) cells are defined according to the surface expression of CD14 and CD16 (d).

Table 1: Percentage of monocyte subsets in CAS, AAD, and RF groups.

	Group CAS ($n = 20$) Mean ± SD	M	Group AAD ($n = 17$) Mean ± SD	M	Group RF ($n = 17$) Mean ± SD	M
Classical monocytes	93.05 ± 4.21	93.74	95.37 ± 4.04	97.11	91.11 ± 7.68	92.67
Intermediate monocytes	5.78 ± 3.59	5.45	3.69 ± 3.23	2.89	6.99 ± 4.96	7.25
Nonclassical monocytes	1.17 ± 1.20	0.65	0.94 ± 1.19	0.45	1.90 ± 3.84	0.54

nonclassical monocytes progressively increased from AAD to RF, although any significant difference was observed regarding the nonclassical subset (Table 1, Figure 2). No significant differences were observed between CAS and RF groups for all monocyte subsets.

3.1.2. Lymphocyte Subpopulations. A significant decrease of CD4+ T lymphocyte percentage ($p = 0.05$) was observed in AAD (mean ± SD: 31.04 ± 17.92; median: 30.00) versus CAS (mean ± SD: 50.63 ± 19.34; median: 55.35). No significant differences were observed between CAS and RF (mean ± SD38.43 ± 14.36; median 39.00) and between AAD and RF.

3.1.3. Immunohistochemistry. Data regarding immunohistochemistry are reported in Table 2. In 8/10 AAD samples, an inflammatory infiltrate was observed within the aortic wall. In 7/8 samples, macrophages were the main population infiltrating the arterial wall, whereas only in one patient was observed a low infiltrate of T CD4+ lymphocytes.

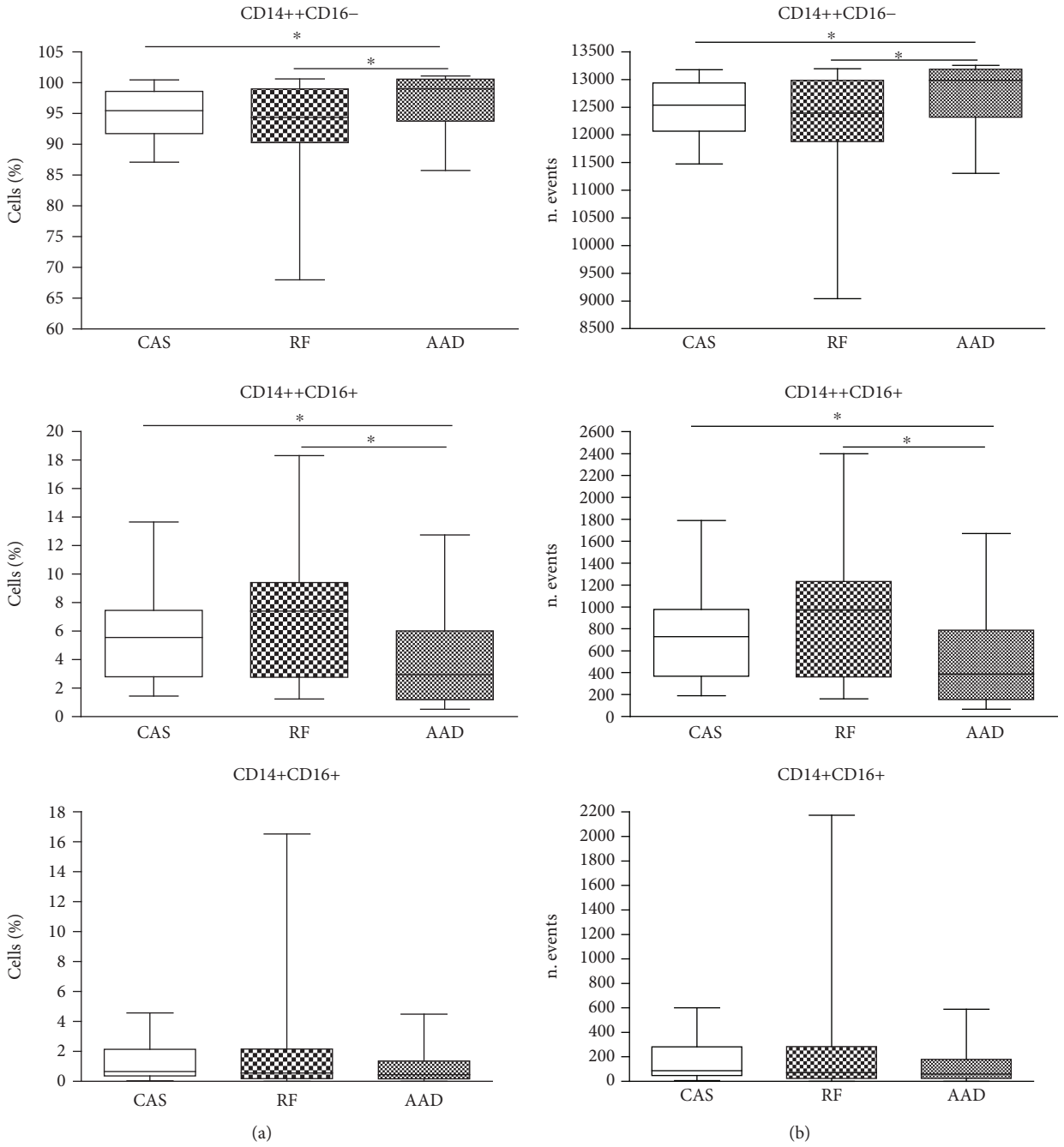

Figure 2: FACS analysis of monocyte subsets in CAS, RF, and AAD groups. Data were expressed as the percentage of cells (a) and the number of events (b). The 25 and 75 percentiles, median, minimal, and maximal are shown. Statistical analysis: Mann–Whitney nonparametric test. $^{*}p < 0.05$.

3.2. Discussion. Our results demonstrated that patients affected by AAD show a peculiar monocyte pattern characterized by elevated classic and reduced intermediate cell subsets, which predispose them to a prevalent natural immune response. Moreover, we observed that CAS and AAD patients displayed an opposite monocyte array, confirming that immune response plays a pivotal role in driving atherosclerotic parietal remodeling toward occlusion or rupture. In this field, it has been demonstrated that a prevalent CD4+ immune response directs subintimal inflammation toward plaque formation, whereas a prevalent innate macrophage activation underlies medial degeneration and aortic rupture in Stanford-A AAD patients with no genetic predisposition [1, 6].

We, indeed, considered AAD and asymptomatic critical CAS as the opposite sides of the same ATS diseases, in which immune response drives parietal remodeling toward rupture or stable occlusion.

Table 2: Immune infiltrate within the aortic wall.

Sample	Macrophages (CD68+)	Lymphocytes (CD4+)
1	—	1
2	1	1
3	1	—
4	—	—
5	3	—
6	—	—
7	2	—
8	3	1
9	3	2
10	1	—

Monocytes represent a systemic reservoir of myeloid precursors for renewal of tissue macrophages and dendritic cells, but they also exert effector/antigen-presenting cell and regulatory functions. Macrophages are the main cells involved in the innate immune response and play a crucial role in the inflammatory process underlying ATS [26]. These cells, indeed, express an array of inflammatory factors, as well as matrix metalloproteinases (MMPs), which are responsible for maintaining intraparietal inflammation and degrading extracellular matrix [27]. Their activation has been related to myocardial infarction, stroke, and CAS [28]. Moreover, several studies indicated, both in mice and in humans, that macrophage recall and their activation represent key events in the early phases of AAD [6].

Interestingly, monocytes are able to trigger and polarize T cell-mediated immune response [29–31]. In particular, intermediate monocytes exert proinflammatory actions [10, 32] and have been reported to favor T cell differentiation toward Th1 and Th17 [33].

Experimental evidences support the role of intermediate monocytes in atheroocclusive diseases [22–24], such as symptomatic and asymptomatic CAS, cardioembolic stroke, and unstable angina [12, 17, 18]. Our results confirmed a high percentage of intermediate monocytes in CAS patients, whereas such subset was decreased in the AAD group versus both CAS and RF. This suggests that such depletion is specifically related to aortic rupture and can at least in part explain the lack of T CD4+ subpopulations which characterizes Stanford-A AAD [6, 34]. We, indeed, confirm that CD4+ T lymphocytes are significantly reduced in peripheral blood of AAD patients in comparison with CAS [6]. Moreover, a prevalent macrophage infiltrate was found within the tunica media in aortic samples, whereas T CD4+ lymphocytes were poorly represented.

In the AAD group, a significant increase of classic monocytes was documented versus both CAS and RF. Monocyte CD14++CD16- are mainly involved in natural response against pathogens. Furthermore, this subset has been related to the inflammatory process occurring in ATS [35]. The increase of such pattern in Stanford-A AAD patients strongly confirms that inflammation underlies also ascending aortic wall rupture in patients with no genetic predisposition and supports the hypothesis of a microbial contribution to AAD [36].

4. Conclusion

This study seems of particular interest, since to our knowledge, it is the first report about monocyte subsets in AAD. We found that Stanford-A AAD patients with no genetic predisposition display a peculiar monocyte pattern, which strongly differs from that observed in the CAS group. We, therefore, can speculate that monocytes, particularly CD14++CD16+ cells, can represent the link between innate and adaptive immunity and can contribute to drive immune response toward a matrix degrading natural response.

Data Availability

The data used to support the findings of this study are available from the corresponding author upon request.

Conflicts of Interest

The authors have no conflict of interest including specific financial interest and relationships and affiliations relevant to the subject matter or materials discussed in the manuscript.

Acknowledgments

The authors thank Paola Del Porto for advice and support with flow cytometry and Cira Di Gioia for immunohistochemistry. This work was supported by the "Sapienza" University of Rome, financing for Research Project 2016.

References

[1] G. K. Hansson, "Inflammation, atherosclerosis, and coronary artery disease," *The New England Journal of Medicine*, vol. 352, no. 16, pp. 1685–1695, 2005.

[2] P. Zhong, D. Wu, X. Ye et al., "Secondary prevention of major cerebrovascular events with seven different statins: a multitreatment meta-analysis," *Drug Design, Development and Therapy*, vol. 11, pp. 2517–2526, 2017.

[3] N. Cifani, M. Proietta, L. Tritapepe et al., "Stanford-A acute aortic dissection, inflammation, and metalloproteinases: a review," *Annals of Medicine*, vol. 47, no. 6, pp. 441–446, 2015.

[4] N. D. Wong, "Epidemiology and prevention of cardiovascular disease," in *Oxford Textbook of Global Public Health*, R. Detels, M. Gulliford, Q. A. Karim, and C. C. Tan, Eds., Oxford University Press, 2015.

[5] E. M. Isselbacher, "Thoracic and abdominal aortic aneurysms," *Circulation*, vol. 111, no. 6, pp. 816–828, 2005.

[6] F. Del Porto, M. Proietta, L. Tritapepe et al., "Inflammation and immune response in acute aortic dissection," *Annals of Medicine*, vol. 42, no. 8, pp. 622–629, 2010.

[7] W. Wiktor-Jedrzejczakabd and S. Gordon, "Cytokine regulation of the macrophage (M phi) system studied using the colony stimulating factor-1-deficient op/op mouse," *Physiological Reviews*, vol. 76, no. 4, pp. 927–947, 1996.

[8] J. Jongstra-Bilen, M. Haidari, S. N. Zhu, M. Chen, D. Guha, and M. I. Cybulsky, "Low-grade chronic inflammation in regions of the normal mouse arterial intima predisposed to atherosclerosis," *The Journal of Experimental Medicine*, vol. 203, no. 9, pp. 2073–2083, 2006.

[9] B. Passlick, D. Flieger, and H. W. Ziegler-Heitbrock, "Identification and characterization of a novel monocyte subpopulation in human peripheral blood," *Blood*, vol. 74, pp. 2527–2534, 1989.

[10] L. Ziegler-Heitbrock, P. Ancuta, S. Crowe et al., "Nomenclature of monocytes and dendritic cells in blood," *Blood*, vol. 116, no. 16, pp. e74–e80, 2010.

[11] E. Idzkowska, A. Eljaszewicz, P. Miklasz, W. J. Musial, A. M. Tycinska, and M. Moniuszko, "The role of different monocyte subsets in the pathogenesis of atherosclerosis and acute coronary syndromes," *Scandinavian Journal of Immunology*, vol. 82, no. 3, pp. 163–173, 2015.

[12] K. S. Rogacev, B. Cremers, A. M. Zawada et al., "CD14++CD16+ monocytes independently predict cardiovascular events: a cohort study of 951 patients referred for elective coronary angiography," *Journal of the American College of Cardiology*, vol. 60, no. 16, pp. 1512–1520, 2012.

[13] K. E. Berg, I. Ljungcrantz, L. Andersson et al., "Elevated CD 14++CD 16- monocytes predict cardiovascular events," *Circulation: Cardiovascular Genetics*, vol. 5, no. 1, pp. 122–131, 2012.

[14] K. A. Krychtiuk, S. P. Kastl, S. L. Hofbauer et al., "Monocyte subset distribution in patients with stable atherosclerosis and elevated levels of lipoprotein(a)," *Journal of Clinical Lipidology*, vol. 9, no. 4, pp. 533–541, 2015.

[15] K. A. Krychtiuk, S. P. Kastl, S. Pfaffenberger et al., "Association of small dense LDL serum levels and circulatingmonocyte subsets in stable coronary artery disease," *PLoS One*, vol. 10, no. 4, article e0123367, 2015.

[16] K. A. Krychtiuk, S. P. Kastl, S. Pfaffenberger et al., "Small high-density lipoprotein is associated with monocyte subsets in stable coronary artery disease," *Atherosclerosis*, vol. 237, no. 2, pp. 589–596, 2014.

[17] G. M. Grosse, W. J. Schulz-Schaeffer, O. E. Teebken et al., "Monocyte subsets and related chemokines in carotid artery stenosis and ischemic stroke," *International Journal of Molecular Sciences*, vol. 17, no. 4, p. 433, 2016.

[18] S. Zeng, X. Zhou, L. Ge et al., "Monocyte subsets and monocyte-platelet aggregates in patients with unstable angina," *Journal of Thrombosis and Thrombolysis*, vol. 38, no. 4, pp. 439–446, 2014.

[19] G. Ghigliotti, C. Barisione, S. Garibaldi et al., "$CD16^{+}$ monocyte subsets are increased in large abdominal aortic aneurysms and are differentially related with circulating and cell-associated biochemical and inflammatory biomarkers," *Disease Markers*, vol. 34, pp. 131–142, 2013.

[20] C. S. Kidwell and S. Warach, "Acute ischemic cerebrovascular syndrome. Diagnostic criteria," *Stroke*, vol. 34, no. 12, pp. 2995–2998, 2003.

[21] G. Raman, D. Moorthy, N. Hadar et al., "Management strategies for asymptomatic carotid stenosis: a systematic review and meta-analysis," *Annals of Internal Medicine*, vol. 158, no. 9, pp. 676–685, 2013.

[22] R. D. Abeles, M. J. McPhail, D. Sowter et al., "CD14, CD16 and HLA-DR reliably identifies human monocytes and their subsets in the context of pathologically reduced HLA-DR expression by $CD14^{hi}/CD16^{neg}$ monocytes: expansion of $CD14^{hi}/CD16^{pos}$ and contraction of $CD14^{lo}/CD16^{pos}$ monocytes in acute liver failure," *Cytometry Part A*, vol. 81A, no. 10, pp. 823–834, 2012.

[23] L. Ziegler-Heitbrock and T. P. Hofer, "Toward a refined definition of monocyte subsets," *Frontiers in Immunology*, vol. 4, p. 23, 2013.

[24] G. P. Fadini, R. Cappellari, M. Mazzucato, C. Agostini, S. Vigili de Kreutzenberg, and A. Avogaro, "Monocyte–macrophage polarization balance in pre-diabetic individuals," *Acta Diabetologica*, vol. 50, no. 6, pp. 977–982, 2013.

[25] F. Del Porto, N. Cifani, M. Proietta et al., "Regulatory T CD4 + CD25+ lymphocytes increase in symptomatic carotid artery stenosis," *Annals of Medicine*, vol. 49, no. 4, pp. 283–290, 2017.

[26] M. S. Elkind, P. Ramakrishnan, Y. P. Moon et al., "Infectious burden and risk of stroke: the northern Manhattan study," *Archives of Neurology*, vol. 67, no. 1, pp. 33–38, 2010.

[27] Z. S. Galis, G. K. Sukhova, R. Kranzhöfer, S. Clark, and P. Libby, "Macrophage foam cells from experimental atheroma constitutively produce matrix-degrading proteinases," *Proceedings of the National Academy of Sciences of the United States of America*, vol. 92, no. 2, pp. 402–406, 1995.

[28] O. M. Pello, C. Silvestre, M. De Pizzol, and V. Andrés, "A glimpse on the phenomenon of macrophage polarization during atherosclerosis," *Immunobiology*, vol. 216, no. 11, pp. 1172–1176, 2011.

[29] N. V. Serbina, T. Jia, T. M. Hohl, and E. G. Pamer, "Monocyte-mediated defense against microbial pathogens," *Annual Review of Immunology*, vol. 26, no. 1, pp. 421–452, 2008.

[30] H. G. Evans, N. J. Gullick, S. Kelly et al., "In vivo activated monocytes from the site of inflammation in humans specifically promote Th17 responses," *Proceedings of the National Academy of Sciences of the United States of America*, vol. 106, no. 15, pp. 6232–6237, 2009.

[31] I. Avraham-Davidi, S. Yona, M. Grunewald et al., "On-site education of VEGF-recruited monocytes improves their performance as angiogenic and arteriogenic accessory cells," *Journal of Experimental Medicine*, vol. 210, no. 12, pp. 2611–2625, 2013.

[32] M. Hristov and C. Weber, "Differential role of monocyte subsets in atherosclerosis," *Thrombosis and Haemostasis*, vol. 106, no. 11, pp. 757–762, 2011.

[33] H. Zhong, W. Bao, X. Li et al., "CD16+ monocytes control T-cell subset development in immune thrombocytopenia," *Blood*, vol. 120, no. 16, pp. 3326–3335, 2012.

[34] M. Proietta, L. Tritapepe, N. Cifani, L. Ferri, M. Taurino, and F. Del Porto, "MMP-12 as a new marker of Stanford-A acute aortic dissection," *Annals of Medicine*, vol. 46, no. 1, pp. 44–48, 2014.

[35] J. Rojas, J. Salazar, M. S. Martínez et al., "Macrophage heterogeneity and plasticity: impact of macrophage biomarkers on atherosclerosis," *Scientifica*, vol. 2015, Article ID 851252, 17 pages, 2015.

[36] R. H. Mehta, R. Manfredini, F. Hassan et al., "Chronobiological patterns of acute aortic dissection," *Circulation*, vol. 106, no. 9, pp. 1110–1115, 2002.

Hindawi
Journal of Immunology Research
Volume 2019, Article ID 8535273, 12 pages
https://doi.org/10.1155/2019/8535273

Research Article

Promiscuous Chemokine Antagonist (BKT130) Suppresses Laser-Induced Choroidal Neovascularization by Inhibition of Monocyte Recruitment

Shira Hagbi-Levi,[1] Michal Abraham,[2] Liran Tiosano,[1] Batya Rinsky,[1] Michelle Grunin,[1] Orly Eizenberg,[2] Amnon Peled,[2,3] and Itay Chowers[1]

[1]*Department of Ophthalmology, Hadassah-Hebrew University Medical Center, Jerusalem 91120, P.O.B 12000, Israel*
[2]*Biokine Therapeutics Ltd., Science Park, Ness Ziona, Israel*
[3]*Goldyne Savad Institute of Gene Therapy, Hadassah-Hebrew University Medical Center, Jerusalem 91120, P.O.B 12000, Israel*

Correspondence should be addressed to Itay Chowers; chowers@hadassah.org.il

Received 7 January 2019; Revised 5 June 2019; Accepted 10 July 2019; Published 5 August 2019

Guest Editor: Heather Medbury

Background. Age-related macular degeneration (AMD), the most common cause of blindness in the developed world, usually affects individuals older than 60 years of age. The majority of visual loss in this disease is attributable to the development of choroidal neovascularization (CNV). Mononuclear phagocytes, including monocytes and their tissue descendants, macrophages, have long been implicated in the pathogenesis of neovascular AMD (nvAMD). Current therapies for nvAMD are based on targeting vascular endothelial growth factor (VEGF). This study is aimed at assessing if perturbation of chemokine signaling and mononuclear cell recruitment may serve as novel complementary therapeutic targets for nvAMD. *Methods.* A promiscuous chemokine antagonist (BKT130), aflibercept treatment, or combined BKT130+aflibercept treatment was tested in an *in vivo* laser-induced model of choroidal neovascularization (LI-CNV) and in an ex vivo choroidal sprouting assay (CSA). Quantification of CD11b+ cell in the CNV area was performed, and mRNA levels of genes implicated in CNV growth were measured in the retina and RPE-choroid. *Results.* BKT130 reduced the CNV area and recruitment of CD11b+ cells by 30-35%. No effect of BKT130 on macrophages' proangiogenic phenotype was demonstrated ex vivo, but a lower *VEGFA* and *CCR2* expression was found in the RPE-choroid and a lower expression of *TNFα* and *NOS1* was found in both RPE-choroid and retinal tissues in the LI-CNV model under treatment with BKT130. *Conclusions.* Targeting monocyte recruitment via perturbation of chemokine signaling can reduce the size of experimental CNV and should be evaluated as a potential novel therapeutic modality for nvAMD.

1. Introduction

Dysregulation of the complement and systemic immune systems has been associated with the pathogenesis of age-related macular degeneration (AMD). Genetic, histological, and biochemical studies have associated the alternative complement pathway with the disease [1–8]. Lymphocytes, mononuclear cells, and particularly monocytes and macrophages were also implicated in AMD [3, 9–23]. In fact, infiltration of monocytes to the retina was found to be essential for the development of choroidal neovascularization (CNV) [18, 24]. Increased numbers of CD56+ T cells have been detected in the blood of AMD patients when compared to age-matched controls [25], and the interaction of T cells and M1 macrophages was reported during the stages of AMD [23]. Once recruited to the eye, monocytes differentiate to macrophages that can exert a proangiogenic effect in the context of neovascular AMD (nvAMD), an effect that may be exacerbated in aging [17, 18, 22, 26–31]. Activated macrophages from nvAMD patients might exert a more significant proangiogenic effect compared with macrophages from age-matched controls [22]. Several macrophage-derived cytokines,

in addition to VEGF, can mediate CNV growth [32, 33]. Accordingly, perturbation of monocyte recruitment and/or function may potentially result in suppression of CNV growth that may potentially complement anti-VEGF-based therapies.

Chemokines and their receptors play a critical role in the progression of autoimmune and inflammatory diseases such as AMD. Multiple chemokines were found to be involved in the development of this pathology [34–38]. For example, a transcriptome-wide analysis of the AMD donor retinas suggested that CCL2, IP-10, MIG, and I-TAC are upregulated in all forms of the disease [39]. CXCR3 is one of the mammalian chemokine receptors, promoting chemotaxis and cell proliferation. This receptor binds to three major chemokine ligands: IP-10, MIG, and I-TAC. CXCR3 expression and IP-10 were elevated in the RPE-choroid fractions of the laser-induced CNV eyes compared with nontreated fellow eyes [40]. Our group has reported an increased expression of other chemokine receptors, namely, CCR1 and CCR2, in the CD14+CD16+ subset of monocytes from neovascular AMD (nvAMD) patients [41]. CCR2 is a major chemokine receptor that is also potentially involved in macrophage activation and recruitment in AMD [32]. In accordance with the high levels of MCP-1, the ligand for CCR2 was detected in the aqueous humor of patients with AMD [42, 43], and macrophages have been found in the vicinity of drusen areas of retinal pigment epithelium (RPE) atrophy, Bruch's membrane rupture, and choroidal neovascularization (CNV) in histological sections from AMD eyes [44–49].

Targeting a single chemokine, or its receptor, in an attempt to reduce macrophage recruitment to the retina was contemplated as a potential treatment for AMD. This approach is limited by the redundancy of the chemokine signaling system and by the nonexclusive nature of ligand-receptor interactions which characterizes it [50–52]. Here, we suggest an alternative approach involving antagonizing multiple chemokine signaling pathways simultaneously. Accordingly, a recent study demonstrated the efficiency of a broad-spectrum chemokine inhibitor (NR58-3.14.3) in modulating macrophage-mediated inflammation in light-induced retina injury [53].

BKT130 is a novel promiscuous chemokine-binding peptibody which has the ability to bind and inhibit multiple inflammatory chemokines, such as CCL2 (ligand for CCR2), CCL5 (binding CCR5), IP-10, MIG, and I-TAC (binding to CXCR3) [54]. This novel peptibody was already proven to have a therapeutic effect in autoimmune and inflammatory pathologies by inhibition of the recruitment of immune cells, inflammation, and disease progression in rodent models for rheumatoid arthritis (RA) and multiple sclerosis (MS) [54]. BKT130 was also found to inhibit melanoma and pancreatic tumor cell growth in mice [54]. In this study, we assessed the effect of this chemokine antagonist in a rodent model for laser injury-induced CNV and in complementary *in vitro* experiments.

2. Materials and Methods

2.1. Laser-Induced Model of CNV (LI-CNV) and Experimental Groups. LI-CNV was generated in adult Long-Evans rats (8-12 weeks old). Animals were treated in accordance with the guidelines of the Association for Research in Vision and Ophthalmology (ARVO). Experiments were conducted with the approval of the institutional animal care ethics committee. Before each procedure, rats were anesthetized by intraperitoneal injections of a mixture of 85% ketamine (Bedford Laboratories, Bedford, OH) and 15% xylazine (VMD, Arendonk, Belgium). Local anesthesia using oxybuprocaine HCL 0.4% (Localin) drops (Fisher Pharmaceuticals, Tel-Aviv, Israel) was applied to each eye 10 minutes before intravitreal injections or laser photocoagulation.

Laser burns (5-7 burns per eye) were generated as previously described [55]. Intravitreal injections were performed using a PLI-100 Pico-Injector (Medical System Corp., Greenvale, NY) as we have previously described [22]. Intravitreal injections of either 4 μl of 5 mg/ml BKT130 (Biokine, Ness Ziona, Israel) ($n = 9$ eyes), 1 μl of 40 mg/ml aflibercept (Bayer Pharma AG, Berlin, Germany) ($n = 8$), a combination of 4 μl BKT130 and 1 μl of aflibercept ($n = 8$), or 4 μl of PBS solution ($n = 10$) were provided. BKT130 dosage was according to a previous study which tested dose response and kinetic analysis in vivo [54], and aflibercept dosage was according to that used in human eyes which was adjusted according to the size of the rat eye. All intravitreal injections were performed at the time of the laser burn injury and 5 days later. Antibiotic ointment (5% Synthomycine) was applied after the injection. RPE-choroid flat mounts were dissected and processed for isolectin staining 10 days following the laser injury as we have previously described [22]. The contralateral retina of the same rat was homogenized and frozen at -80 for RNA extraction using TRI-Reagent (Sigma-Aldrich, Munich, Germany).

2.2. CNV Quantification. RPE-choroid flat mounts were fixated for one hour in 4% PFA and suspended overnight in isolectin solution (GS-Ib4 Alexa 594 staining solution, Molecular Probes, Eugene, Oregon) containing 200 mM NaN_3 and 1 mM $CaCl_2$. Flat mounts were then washed 6 times for 20 minutes in PBS and embedded on a slide with a mounting medium. Isolectin images of the RPE-choroid flat mounts were viewed using a fluorescent microscope (Olympus BX41, Tokyo, Japan). Background was controlled by setting the exposure parameters as such so that they provided no detectable signal for the control nonimmune serum-stained rat flat mount. These same parameters were maintained while capturing all images from the test sections. Images were photographed with an Olympus DP70 digital camera.

The CNV area around each laser injury was measured using the ImageJ software [56]. The optic disc was removed to avoid autofluorescence from background counts. The scale was set to translate pixels into mm^2, threshold was set on an unstained negative control, and these settings were used as background for all images. In order to calculate the average area of each CNV, we calculated the stained area of particles above the size of 60 pixels and divided it by the number of laser burns in the eye. The average CNV area of each eye was then calculated, and the mean CNV area of the four groups was compared.

2.3. Immunohistochemistry. Immunohistochemistry of the fixed retinas was performed for mononuclear phagocyte (CD11b+) cell count. In brief, mouse monoclonal anti-CD11b (Abcam, ab78457, 1 : 100) was used as the primary antibody for the rat mononuclear phagocytes. A donkey anti-mouse (Abcam, ab150110, 1 : 100) was used as the secondary antibody. Retinal flat mounts were first permeabilized and blocked for 3 hours at room temperature (RT) with blocking solution containing 0.1% Triton-X, 10% Normal Donkey Serum (NDS, Millipore S30, Temecula, CA, USA), 3% albumin bovine (BSA; Amresco Inc., Solon, OH, USA) in PBS. Primary antibody was added overnight in 4°C on shaker. Samples were then washed for 20 minutes six times in PBS at RT, and secondary antibodies were added for 2 hours on a shaker at RT. Samples were placed on slides with mounting medium after 4′,6′-diamidino-2-phénylindole (DAPI) (Enzo LifeScience Exeter, UK) staining, for cell nucleus identification. Flat mounts of eyes with LI-CNV and without primary antibodies served as negative controls, which defined our background for the microscopy.

Immunofluorescence analysis was performed using a Zeiss LSM 710 confocal laser scanning system (Carl Zeiss MicroImaging GmbH, Jena, Germany) with 25X oil objective and a tile scan. Background was controlled by setting the exposure parameters as described above. These same parameters were maintained while capturing images from the test sections. CD11b+ cells which were found in the laser injury site, at the sub retinal space, were counted by a masked observer, using ImageJ software. The perimeter of the laser injury site was determined based on the absence of nearby photoreceptor cells as identified via DAPI staining, surrounding the laser injury (Figure 1(a)). Results are presented as the mean number of cells per laser-treated area of each experimental group ± SEM.

2.4. Quantitative Real-Time PCR (QPCR). Total RNA was extracted from the flash-frozen retinas using TRI Reagent (Sigma-Aldrich), according to the manufacturer's instructions, and treated with DNase (TURBO DNA-free, Ambion, Austin, TX). Reverse transcriptase polymerase chain reaction was performed using the High Capacity cDNA Reverse Transcription Kits (Applied Biosystems, Foster City, CA) and anchored oligo dT primers on 1 μg total RNA in a volume of 20 μl.

Quantitative real-time PCR (QPCR) was performed using the SYBR Green technique to measure mRNA levels of genes involved in angiogenesis, inflammation, mononuclear cell marker, macrophage polarization, and monocyte recruitment. Oligonucleotide primers for genes of interest [*CCL2*, *CCR2*, *CCL5*, *VEGFA*, *IL1β*, *TNFα*, *NAP-2*, *MIP-2*, *CD11b*, *CD163*, *MRC1* (*CD206*), and *N0S1*] and for an endogenous control gene (*β-actin*) were designed for QPCR using Primer-Blast (https://www.ncbi.nlm.nih.gov/tools/primer-blast/). These genes were selected as they are related with chemokine signaling or with proangiogenic function of macrophages. All primers were purchased from Sigma-Aldrich (primer sequences are presented in Supplement Table 1). Measurement of the mRNA levels was performed on the retinas and RPE-choroid tissues, separately, 10 days after injections, in each experimental group ($n = 9$ eye samples in each group: PBS, BKT130, aflibercept, and, BKT130+aflibercept). Measurement of *β-actin* mRNA levels served as endogenous controls. All reactions were carried out in triplicate, using 384-well plates, at a total volume of 10 μl. Wells contained 20 ng (for *CCL2*, *CCR2*, *CCL5*, *MRC1*, *CD163*, *VEGFA*, *CD11b*, *NOS1*, and *IL1β*) or 100 ng (for *TNFα*, *NAP-2*, and *MIP-2*) cDNA template, 5 μl of SYBR Green FastMix (Quanta Biosciences), and 0.5 μl forward and reverse primers (10 mM) for each gene. Signal amplification was measured throughout 38 cycles of 60°C for 20 seconds, followed by 95°C for 20 seconds. To confirm the amplification of a specific cDNA, the dissociation temperature was examined and compared with the calculated melting temperature for each amplified product. The amplified products were also examined by

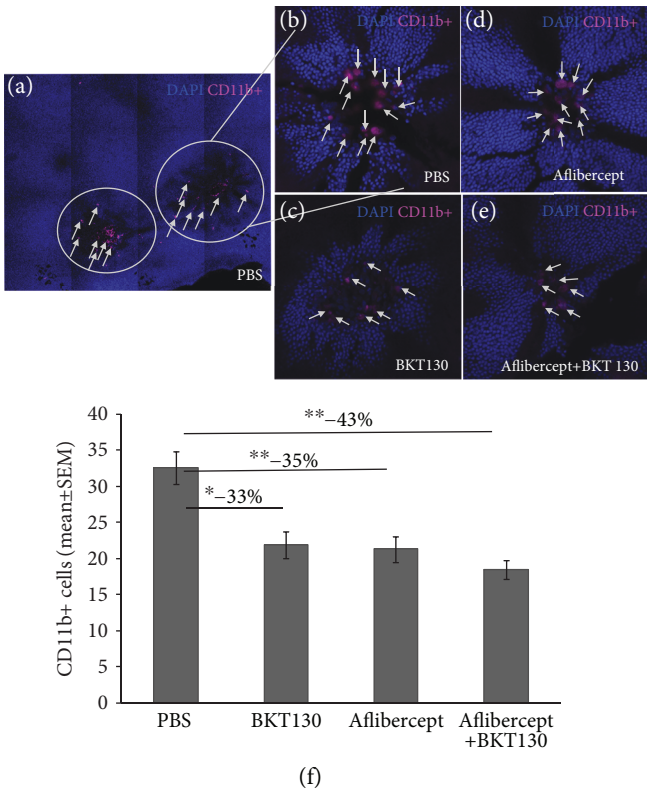

Figure 1: BKT130 reduces CD11b+ cell migration to the laser-treated area. Rat retinal flat mounts were prepared 10 days following laser injury and intravitreal injections. Flat mounts were observed using a confocal laser scanning system. CD11b-positive cells were observed in the center of the laser-treated areas (a). Each laser-treated area was observed in a 40x lens, and the macrophages (magenta) were counted (b–e). The eyes injected with BKT130, aflibercept, or BKT130+aflibercept demonstrated less CD11b-positive cells ((d) and (e), respectively) compared with PBS-injected eyes (b). A comparison between the amounts of cells found in laser-treated areas in each group is provided in (f). The *Y*-axis presents the mean (±SEM) number of CD11b+ cells found in each laser-treated area, in either BKT130 (number of laser burns = 19), aflibercept ($n = 25$ laser injury areas), BKT130+aflibercept ($n = 41$), or control PBS-injected group ($n = 24$). $^{*}P < 0.05$ and $^{**}P < 0.005$.

agarose gel electrophoresis. Fluorescent signals were measured by the CFX384, C1000 touch thermal cycler (Bio-Rad) and analyzed using the spreadsheet software (Excel; Microsoft, Redmond, WA). Expression levels of each gene were compared across the samples by using the expression levels of the endogenous control according to the standard $2^{(-\Delta\Delta CT)}$ calculation [57], giving results as relative quantification and fold change ± standard error of the mean (SEM).

2.5. Choroid Sprouting Assay (CSA). Blood samples (20 ml) were collected from 6 nvAMD patients (3 females, 3 males, mean age ± SEM: 70.8 ± 2.3 years, range: 64-81) in EDTA tubes (BD Bioscience). Patients were recruited from the retina clinic of the Department of Ophthalmology at the Hadassah-Hebrew University Medical Center. The criteria for the inclusion of nvAMD patients included the following: age over 55 years, diagnosis of AMD according to the AREDS criteria [58], and diagnosis of CNV according to fluorescein angiogram and optical coherence tomography. All patients signed an informed consent form, and the study was approved by the institutional ethics committee (see Ethical Approval). Monocytes were isolated from the whole blood, differentiated into macrophages (M0), and activated into M1- and M2a-like phenotypes, as we and others have previously described [22, 59, 60].

An ex vivo angiogenesis assay was performed as previously described [22, 61], to evaluate the effect of BKT130 on the macrophages' proangiogenic phenotype. Briefly, the supernatant from human-activated and human-polarized macrophages that were treated with 50 μg/ml BKT130 or untreated control macrophages was collected at day 7 of monocyte cell culture and kept in -20°C until use. Treatment with BKT130 took place at the day of macrophage polarization or at day 5 for the nonactivated macrophages (M0).

Adult C57BL6J mice, which were treated in accordance with the guidelines of the Association for Research in Vision and Ophthalmology (ARVO), were utilized for CSA experiments. Experiments were conducted with the approval of the institutional animal care ethics committee (see Ethical Approval). Mice were anesthetized with ketamine, checked for responses, and euthanized by cervical dislocation. The eyes were immediately enucleated and kept in ice-cold ECGS medium containing 1/100 penicillin-streptomycin and 1/100 glutamine before dissection. A choroid-sclera complex from the mice was gently dissected along with retinal pigment epithelium (RPE). The complex was cut into 5-6 1 mm long pieces. Fragments were embedded in 30 μl of growth factor-reduced Matrigel™ (BD Biosciences, Cat. 354230) in 24-well plates. The thickness of the Matrigel™ was approximately 0.4 mm. Plates were then incubated for 10 minutes in 37°C, in a 5% CO_2 cell culture incubator without medium to solidify the Matrigel™. Medium (250 μl) containing ECGM (C-22010, PromoCell, Germany), 2.5% supplement mix (C-9215, PromoCell, Germany), 5% FCS, 1/100 penicillin-streptomycin, and 1/100 glutamine was added to each well. 250 μl of the macrophages' supernatant or 250 μl of medium only was added to each well in duplicates. In addition, BKT130 was added directly to another group of CSA wells with the supernatant of untreated polarized M0 and M1 macrophages from 5 other nvAMD patients (4 female, 1 male, mean age ± SEM: 77.8 ± 3.9 years, range: 64-87), to assess the effect of BKT130 directly on the supernatant without its potential effect on the macrophages' phenotype. Medium was changed every 3 days, and the cultures were fixed with 4% PFA after 8 days. Cultures were viewed with an inverted phase-contrast CKX41 Olympus microscope, and images were photographed with an Olympus DP70 digital camera (Olympus, Tokyo, Japan).

ImageJ software was used to quantify the sprouting area. The scale was set to convert pixels to mm^2. Each image was converted to an 8-bit format to obtain a binary image. Sprouting area quantification and analysis were performed in duplicates for each sample.

2.6. Statistical Analysis. Data was processed using the biostatistical package InStat (GraphPad, San Diego, CA). $P < 0.05$ was considered to indicate the statistical significance. Values over two standard deviations from the average were excluded from the statistical analysis. Appropriate statistical tests were applied according to the results of a normalcy test, sample distribution, and nature of the parameters.

3. Results

3.1. BKT130 Suppresses Laser-Induced Model of CNV (LI-CNV). The LI-CNV rat was utilized to evaluate the *in vivo* effect of BKT130 on CNV growth (Figure 2). The CNV area was measured 10 days after the induction of LI-CNV and commencement of intravitreal therapy in the rat eyes. BKT130 treatment ($n = 9$ eyes) was associated with a 36.8% reduction in the CNV area [mean area $(mm^2) \pm$ SEM] as compared with control ($n = 10$) PBS-injected eyes (0.036 ± 0.005 vs. 0.057 ± 0.004, respectively; $P = 0.005$, ANOVA). Aflibercept treatment ($n = 8$) was associated with a 68.4% reduction of the CNV area as compared with controls (0.018 ± 0.001, $P = 0.0001$). Injection of both aflibercept and BKT130 ($n = 8$) resulted in a 70.2% smaller CNV area (0.017 ± 0.001, $P = 0.0001$). CNV was 50% smaller in aflibercept-treated eyes compared with BKT130-treated eyes ($P = 0.0003$) and 52.8% smaller in aflibercept+BKT130-treated eyes ($P = 0.0003$).

3.2. BKT130 Inhibits Mononuclear Phagocyte Recruitment to a LI-CNV. Immunostaining for CD11b+ cells was performed on the photoreceptor side of the retina flat mounts to assess their recruitment to the LI-CNV (Figure 1). CD11b+ cells were found beneath the photoreceptors (between retinal and RPE cells) overlying the laser injury site (Figure 1(a)). Laser injury sites were of similar size across the experimental groups, while the number of CD11b+ cells was associated with the specific treatment provided (Figure 1(a)). The lowest CD11b+ cell count (43% reduction) was found in the aflibercept+BKT130 (number of laser-treated areas = 41; mean cell count in each laser-treated area ± SEM: 18.51 ± 1.26) as compared with the control PBS-treated eyes ($n = 24$ laser injury areas, mean cell count = 32.63 ± 2.23; $P < 0.001$; ANOVA). A reduction in the number of CD11b+ cells was also found in BKT130-treated eyes ($n = 19$, cell

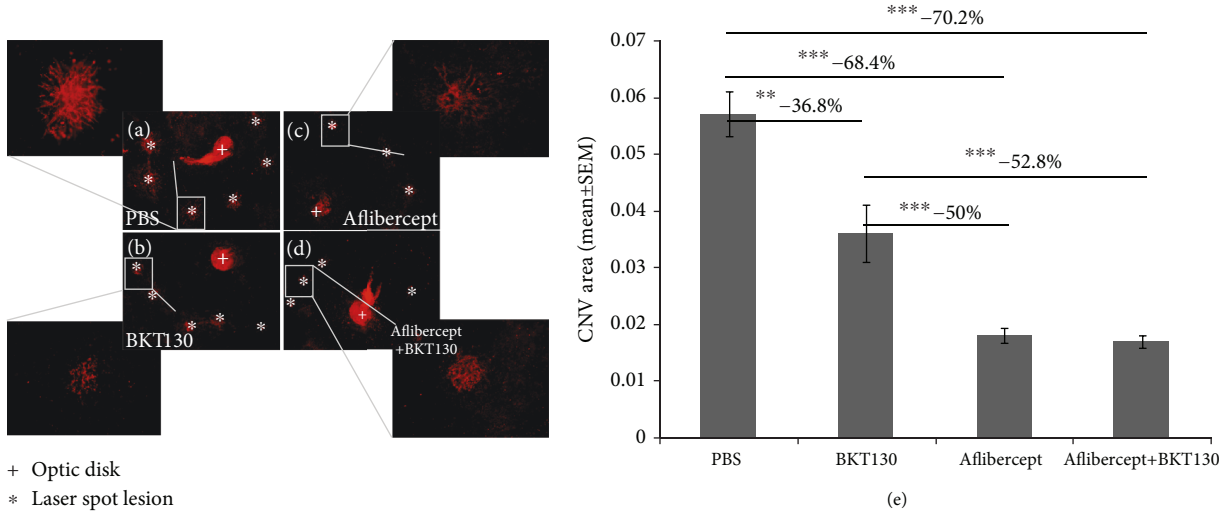

FIGURE 2: *In vivo* assessment of BKT130's effect in a rodent model of LI-CNV. BKT130 was injected intravitreally in a rat model of LI-CNV ($n = 9$ eyes). The eyes injected with PBS served as a negative control ($n = 10$), while intravitreal injections of aflibercept served as the positive control ($n = 8$). BKT130 was also injected with aflibercept to assess an additive effect ($n = 8$). CNV was identified and quantified using a fluorescent microscope in isolectin-stained RPE-choroid flat mounts (a–d). Each laser treated area was observed in a 20x lens and the whole flat mount in 4x lens. The CNV area was measured and compared between treatments and between PBS-injected eyes (e). The *Y*-axis presents the averaged (±SEM) CNV area (mm^2) of treated and PBS-injected control eyes. $^{**}P < 0.005$ and $^{***}P < 0.0005$.

count = 21.89 ± 1.85; $P < 0.01$; ANOVA) and in aflibercept-treated eyes ($n = 25$, 21.36 ± 1.78; $P < 0.001$; ANOVA) as compared to PBS-treated eyes. No difference in the mean cell number was found among BKT130, aflibercept, and combined aflibercept+BKT130-treated eyes.

3.3. BKT130 Treatment Affects Gene Expression Profile in the Eyes with LI-CNV. The mRNA expression profile of several genes evaluated with QPCR was associated with the specific treatments provided, as well as the tissue tested (retina and RPE-choroid; Figure 3).

Mean RPE-choroid *CCR2* expression (RQ ± SEM) was 2-fold lower in the BKT130-treated eyes ($n = 9$ eyes, 1.3 ± 0.26) as compared with PBS ($n = 9$, 2.56 ± 0.37, $P = 0.02$, *t*-test) and 1.8-fold lower from aflibercept+BKT130-treated eyes ($n = 9$, 2.35 ± 0.37, $P = 0.05$, *t*-test) (Figure 3(a)). Multivariate analysis for CCR2 mRNA levels in the RPE-choroid across the four groups did not disclose a difference ($P = 0.2$, Kruskal-Wallis test).

CCL5 mRNA levels in the RPE-choroid was 2-fold higher in BKT130-treated eyes (0.9 ± 0.14, $P = 0.03$, *t*-test) and 3-fold higher in aflibercept-treated eyes ($n = 9$, 1.37 ± 0.36, $P = 0.04$, *t*-test), as compared to the eyes injected with PBS (0.45 ± 0.09; Figure 3(b)). Multivariate analysis for *CCL5* mRNA levels across the four groups in the RPE-choroid did not disclose a difference ($P = 0.15$, Kruskal-Wallis test).

CCR2 and *CCL5* expression in the retinal tissue was similar among the experimental groups.

TNFα expression was 2.25-fold lower in RPE-choroid (0.8 ± 0.17) and 2.7-fold lower in retinal (1.05 ± 0.28) tissues of BKT130-treated eyes as compared to the PBS-treated eyes (1.8 ± 0.28, $P = 0.03$, Mann–Whitney test; 2.83 ± 0.67, $P = 0.05$, *t*-test, respectively) (Figures 3(c)–3(e)). A multivariate test for retinal *TNFα* expression across the four groups confirmed variable expression levels among the groups ($P = 0.04$, Kruskal-Wallis test). A multivariate test for RPE-choroid *TNFα* expression across the four groups did not disclose a difference ($P = 0.1$, Kruskal-Wallis test), yet when we pooled the two groups that were treated with BKT130 (BKT130 and aflibercept+BKT130), the multivariate test for RPE-choroid *TNFα* expression across the three groups confirmed variable expression levels among the groups ($P = 0.04$, Kruskal-Wallis test).

Retinal *VEGFA* expression was 1.8-fold lower in aflibercept-treated eyes (0.32 ± 0.03) as compared to PBS-treated eyes (0.59 ± 0.05, $P = 0.0003$, *t*-test). BKT130 treatment was associated with 3.2-fold reduced expression of *VEGFA* in the RPE-choroid (0.42 ± 0.12) as compared to PBS-treated eyes (1.34 ± 0.28, $P = 0.02$, *t*-test). The combination of aflibercept+BKT130 was associated with lower *VEGFA* expression by 1.25-fold in retinal tissue (0.47 ± 0.04) and 2.6-fold reduced levels in RPE-choroid tissue (0.52 ± 0.12) as compared with the PBS-treated group (0.59 ± 0.05, $P = 0.05$, *t*-test; 1.34 ± 0.28, $P = 0.01$, *t*-test, respectively) (Figures 3(d)–3(f)). A multivariate test for *VEGFA* expression across the four groups disclosed variable expression levels ($P = 0.03$ in the retina and $P = 0.004$ in the RPE-choroid, Kruskal-Wallis test).

A multivariate test for *CD11b* expression in the retina across the four groups disclosed variable expression levels ($P = 0.003$, Kruskal-Wallis test). Univariate analysis suggested that *CD11b* expression in the retina was decreased by 14-fold following BKT130 (0.026 ± 0.01) treatment and by 10-fold following aflibercept treatment (0.03 ± 0.01) as compared with PBS- (0.4 ± 0.1) treated eyes ($P = 0.02$, *t*-test; $P = 0.02$, *t*-test, respectively) (Figure 3(g)). No change was measured in *CD11b* expression in the RPE-choroid tissue.

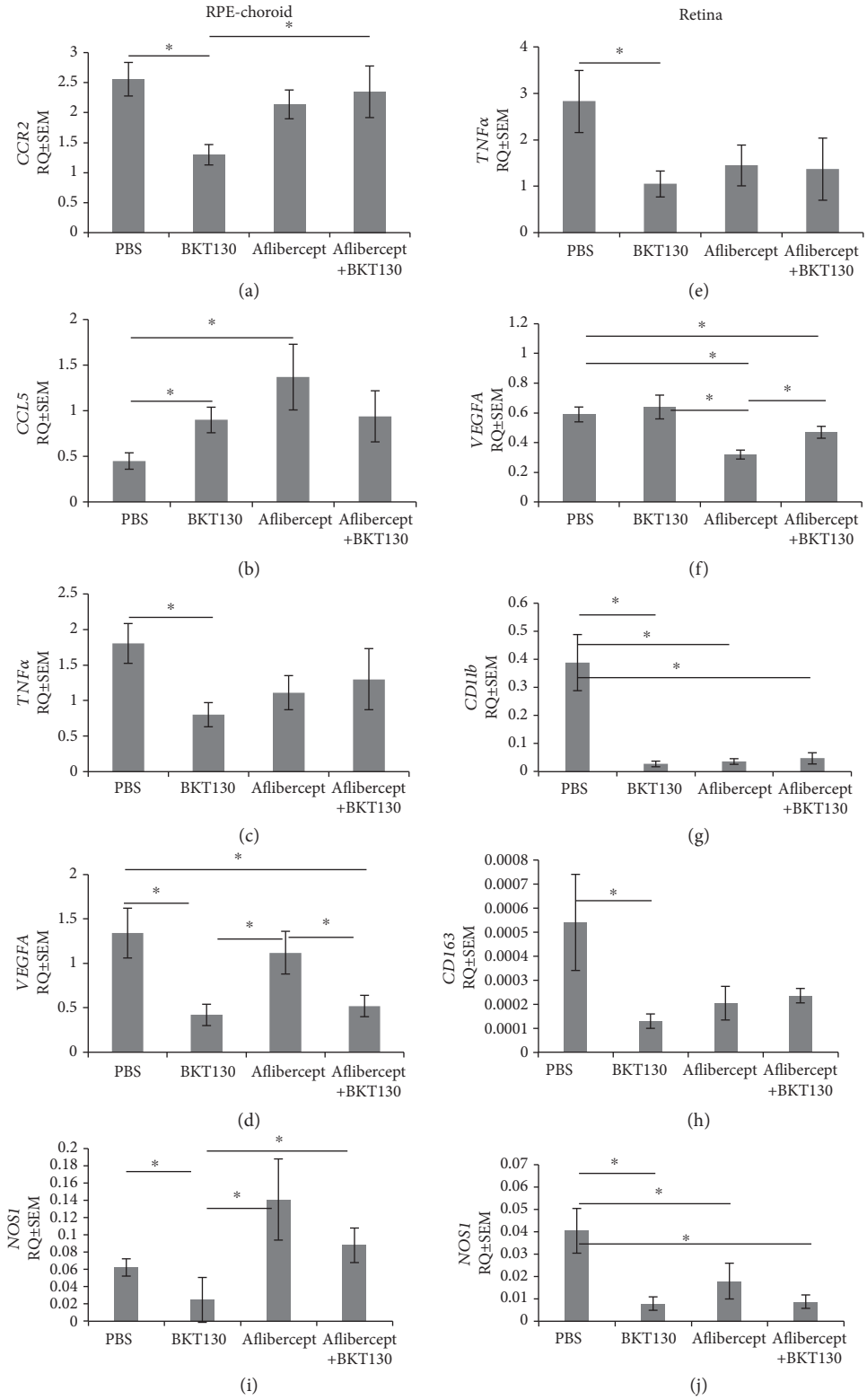

Figure 3: Gene expression profile of the retinas and RPE-choroid following treatment. mRNA expression levels of genes related to angiogenesis (*VEGFA*, *IL1β*, and *TNFα*), inflammation (*CCL2*, *CCR2*, *CCL5*, *TNFα*, *NAP-2*, and *MIP-2*), mononuclear cell markers (*NOS1*, *CD163*, and *CD11b*), and macrophage recruitment (*CCL2*, *CCR2*, *NAP-2*, and *MIP-2*) were evaluated in the RPE-choroid (a–d) and in the retinas (e–h) of rats via QPCR ($n = 9$ eyes in each group: PBS, BKT130, aflibercept, and BKT130+aflibercept). Presented are the genes that significantly changed after treatment. The Y-axis indicates RQ ± SEM. $^{*}P < 0.05$.

A multivariate test for *CD163* expression in the retina across the four groups did not disclose a difference ($P = 0.1$, Kruskal-Wallis test). Univariate analysis demonstrated that BKT130 treatment was associated with a 4.17-fold reduction of *CD163* (an M2 macrophage biomarker) expression in the retina (0.0005 ± 0.0002 and 0.0001 ± 0.00003, $P = 0.03$, t-test, respectively) (Figure 3(h)). No change was measured in *CD163* expression in the RPE-choroid tissue.

In univariate analysis, BKT130 treatment was associated with reduced *NOS1* (an M1 macrophage biomarker) expression in the RPE-choroid and in the retina, respectively (RPE-choroid: BKT130—0.02 ± 0.02, PBS—0.06 ± 0.01, $P = 0.05$; retina: BKT130—0.008 ± 0.003, PBS—0.04 ± 0.01, $P = 0.01$, t-test). Aflibercept monotherapy was not associated with altered *NOS1* expression in the choroid or the retina tissues. The combination therapy of aflibercept+BKT130 was associated with reduced NOS1 levels in the retina (aflibercept +BKT130: 0.008 ± 0.003, PBS: 0.04 ± 0.01, $P = 0.02$, t-test), but not in the RPE-choroid. A multivariate test for *NOS1* expression in the retina and in the RPE-choroid across the four groups disclosed variable expression levels ($P = 0.04$ for both tissues, Kruskal-Wallis test) (Figures 3(i) and 3(j)).

No difference in the expression levels of *MRC1*, *CCL2*, *IL1β*, *NAP-2*, and *MIP-2* in the retina or in the RPE-choroid was identified across the treatment groups (data not shown).

3.4. BKT130 Does Not Affect Macrophages' Proangiogenic Phenotype or Function. An ex vivo CSA was conducted to evaluate the effect of BKT130 on macrophage's proangiogenic phenotype and the function of the secreted proteins. No difference in the sprouting area was detected among wells treated with the supernatant of macrophages that were incubated with or without BKT130 ($n = 6$ in each group, mean of CSA area in $mm^2 \pm$ SEM, M0: untreated $1.72\,mm^2 \pm 0.32$ vs. treated $1.64\,mm^2 \pm 0.32$, $P = 0.7$; M1: untreated $2.2\,mm^2 \pm 0.34$ vs. treated 2.2 ± 0.35, $P = 0.4$; M2: untreated $1.62\,mm^2 \pm 0.34$ vs. treated $1.54\,mm^2 \pm 0.25$, $P = 0.6$; paired t-test). In addition, the sprouting area was not affected by the addition of BKT130 to the CSA wells treated with macrophage's culture media in each macrophage subtype tested (mean of CSA area in $mm^2 \pm$ SEM, M0: without BKT130 $1.4\,mm^2 \pm 0.6$ vs. with BKT130 $1.12\,mm^2 \pm 0.6$, $P = 0.8$; M1: without BKT130 $2.2\,mm^2 \pm 0.9$ vs. with BKT130 $1.36\,mm^2 \pm 0.5$, $P = 0.5$, paired t-test) (Figure 4).

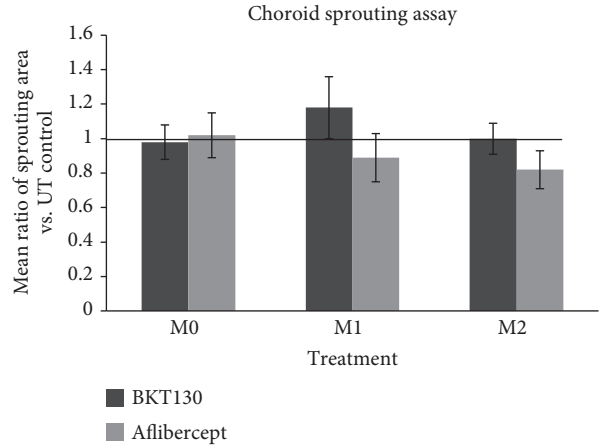

Figure 4: Choroid sprouting assay.

4. Discussion

We describe the effect of a novel promiscuous chemokine antagonist (BKT130) in the rat model of LI-CNV. Application of this compound via the intravitreal route was associated with a reduction in the recruitment of CD11b+ cells to the proximity of CNV lesions, a reduction of CNV size, and suppression of the expression of chemokines and cytokines, including the major monocyte receptor—CCR2—in the RPE-choroid tissue. Despite the fact that BKT130 inhibits chemokines which are expressed not only by the inflamed tissue but also by M1 and M2 macrophages, ex vivo treatment with BKT130 in CSA or treatment of cultured macrophages with BKT130 failed to suppress choroidal sprouting.

These data suggest that BKT130's favorable *in vivo* effect is mediated via perturbation of chemokine signaling and monocyte recruitment to the laser-injured area. Recently, it was suggested that microglia are resident macrophages of the retina that are derived from embryonic yolk sac progenitors during development, while nonresident bone marrow-derived macrophages may be recruited into the retina from the vasculature in pathology [62]. Therefore, any additional CD11b+ cells found in the retina are likely to represent recruited macrophages rather than resident microglia [63]. Macrophages were implicated in the pathogenesis of AMD based on multiple studies, among them are the presence of macrophages in the vicinity of AMD lesions [44, 45, 64, 65], proangiogenic human and rodent macrophages' effect in vitro and in the rodent model of LI-CNV [18, 22, 66], and the reduced size of experimental CNV following inhibition of the CCR-CCL2 signaling pathway and monocyte recruitment [30, 67].

BKT130 suppresses LI-CNV via antagonizing multiple chemokines, thereby indirectly suppressing the expression of VEGF and other proinflammatory and proangiogenic cytokines. In the present study, anti-VEGF therapy was also associated with reduced macrophage recruitment, conceivably, through a PGF trap which inhibits subretinal phagocyte accumulation and other different mechanisms [68–70].

Macrophages may mediate CNV progression via cytokine production. TNFα-expressing macrophages were previously detected in CNVs excised from AMD patients [71]. Our previous study showed that M1 macrophages from nvAMD, which had a proangiogenic effect in the rat model of LI-CNV, also produce considerable amounts of TNFα [22]. In addition, it has been previously suggested that macrophages secreting TNFα in CNV stimulate RPE expression of *VEGF* [71, 72] and that TNFα increases the secretion of VEGF A and C and leads to the upregulation of *VEGF* expression by human RPE cells and choroidal fibroblasts [73, 74]. Our current results showed approximately 60% reduction in *TNFα* expression in both retinal and RPE-choroidal tissues following BKT130 treatment. In addition,

we found reduced expression of *CD11b* and *NOS1* in both retinal and RPE-choroid tissues following BKT130 treatment which suggest reduced mononuclear phagocyte recruitment and reduced polarization towards the M1 macrophage phenotype. Interestingly, aflibercept, while suppressing macrophage recruitment as evident by reduced *CD11b* expression in the retina, did not suppress *TNFα, NOS1*, or *CCR2* expression suggesting that it did not affect macrophage polarization or polarized macrophages' recruitment. Thus, our findings support a potential suppression of M1 macrophages' polarization by BKT130 while aflibercept may potentially suppress the recruitment mononuclear cells but not polarization to the M1 phenotype and therefore may have a different mechanism of action on CNV growth. These results are in accordance with a recent report of higher expression of M1 markers in the RPE-choroid of a mouse following laser-induced CNV as compared to M2 macrophages' markers which were increased in the retina [75]. M1 macrophage activation and M1-dominant polarization profile of microglia were also recently described in the degenerative retina of rd1 mice [76].

VEGF immunoreactivity was previously found to be greater in inflammatory and active CNV and was found in the RPE to a greater extent than found in macrophages [77]. In addition to the RPE [78] and macrophages, at least six more retinal cell types have the capacity to produce and secrete VEGF including astrocytes [79], Müller cells [80], endothelial cells [81], microglia [77], pericytes [82], and ganglion cells [83]. BKT130 downregulated *VEGFA* expression in the RPE-choroid, but not in the retina. By contrast, aflibercept downregulated *VEGFA* expression in the retina and not in the RPE-choroid. Interestingly, combining aflibercept with BKT130 treatments caused downregulation of *VEGFA* expression both in retina and in RPE-choroid tissues. These results may reflect the variable mechanism of VEGF suppression associated with the two compounds and suggest a potential complementary effect of the combined therapy.

Caveats of the current study include the fact that LI-CNV in rat is a wound-healing reaction that follows an insult at the level of Bruch's membrane and relies heavily on inflammation [18, 19] and that it does not directly reflect nvAMD. In addition, because of the absence of a defined macula in rodents, this rodent model does not fully mimic the complexity of human pathology [84]. However, this model was proven to be suitable for testing the efficacy of new drugs through systemic or intraocular administration and has shown a predictive value for drug effects in patients with AMD, for example, with aflibercept [85, 86]. In addition, while we observed a trend towards enhanced suppression of CNV in the combination arm of aflibercept+BKT130, this arm did not show a smaller CNV size as compared with aflibercept monotherapy. Yet in the LI-CNV model, application of aflibercept essentially eliminated the neovascular tufts, thereby, resulting in a ceiling effect that does not allow for a functional effect of the combined therapy to be apparent. Such complete elimination of the CNV lesion is not usually achieved in nvAMD following anti-VEGF therapy. Thus, in the human pathology, there is a need for supplementing the effect of available therapies. Finally, the lower injection volume used in the aflibercept monotherapy group as compared to other groups may theoretically interact with CNV size. Yet our control group was injected with 4 μl of PBS, similar to the BKT130 group which was the main focus of this research. Furthermore, the highest injection volume was used in the 1 μl + 4 μl of the BKT130+aflibercept group, and this group yielded suppression of CNV.

5. Conclusion

Intravitreal delivery of a promiscuous chemokine antagonist, BKT130, inhibited the recruitment of monocytes to the laser injury area, reduced CNV area in the LI-CNV rat model, and decreased expression of *VEGFA* and *CCR2* in RPE-choroid and *TNFα* in both RPE-choroid and retinal tissues. Reduction in *TNFα* and *NOS1* with BKT130 but not with aflibercept might suggest a different macrophage subtype inhibition and therefore an additional effect on different patients. Additionally, a combination therapy with BKT130 and anti-VEGF had an additive effect on *VEGFA* expression in the eyes of rats with LI-CNV. Future studies should evaluate if perturbation of chemokine signaling may serve as a novel therapeutic option in nvAMD to supplement anti-VEGF therapy.

Abbreviations

AMD: Age-related macular degeneration
nvAMD: Neovascular stage of AMD
RPE: Retinal pigment epithelium
CNV: Choroidal neovascularization
LI-CNV: Laser-induced model of choroidal neovascularization
CSA: Choroid sprouting assay
FCS: Fetal calf serum
VEGF: Vascular endothelial growth factor.

Data Availability

We are happy to provide any relevant raw data, to any scientist who wishes to use them. For more information, please contact the corresponding author at chowers@hadassah.org.il.

Ethical Approval

Ethical approval for all protocols involving animals was approved by the Authority for Biological and Biomedical Models (ABBM) and the University Ethics Committee for the Care and Use of Laboratory Animals in Hebrew University, which is certified by the Association for Assessment and Accreditation of Laboratory Animal Care (AAALAC) (ethical approval number MD-16-14796-3, NIH approval number OPRR-A01-5011). All researchers working with laboratory animals underwent approval by the ethics committee of the ABBM to allow them to ethically work with laboratory animals. All guidelines with regard to humane and ethical treatment of laboratory animals (from ARVO) were followed to the utmost, and all methods used in this

study were carried out in accordance with the approved guidelines for the study.

Disclosure

The funders had no role in study design, data collection and analysis, decision to publish, or preparation of the manuscript.

Conflicts of Interest

SHL, LT, BR, MG, and IC declare no actual or potential conflicts of interest. MA and OE are employees of Biokine Therapeutics Ltd. AP serves as a consultant to Biokine Therapeutics Ltd. OE and AP are shareholders of Biokine Therapeutics Ltd.

Authors' Contributions

SHL conceived the study, carried out all experiments, analyzed the data, and wrote the manuscript. MA reviewed the manuscript. LT, BR, and MG participated in conducting the experiments. OE designed and produced the compound BKT130. AP conceived the study, obtained funding for the research, and coordinated it. IC conceived the study, analyzed the data, and participated in writing the manuscript. AP, MA, SHL, IC, and OE all participated in the study design, but none of them, except SHL, conducted the experiment or participated in the data analysis and/or results. All experiments are carried out in the lab of IC and by his students SHL, MG, BR, and LT. All authors read and approved the final manuscript.

Acknowledgments

This work was supported by a grant from Biokine Therapeutics Ltd. (#6037411) (AP).

Supplementary Materials

Appendix Table 1: mRNA primers for QPCR. *(Supplementary Materials)*

References

[1] D. H. Anderson, M. J. Radeke, N. B. Gallo et al., "The pivotal role of the complement system in aging and age-related macular degeneration: hypothesis re-visited," *Progress in Retinal and Eye Research*, vol. 29, no. 2, pp. 95–112, 2010.

[2] The AMD Gene Consortium, "Seven new loci associated with age-related macular degeneration," *Nature Genetics*, vol. 45, no. 4, pp. 433–439, 2013.

[3] H. P. N. Scholl, P. C. Issa, M. Walier et al., "Systemic complement activation in age-related macular degeneration," *PLoS One*, vol. 3, no. 7, article e2593, 2008.

[4] B. E. K. Klein, C. E. Myers, K. P. Howard, and R. Klein, "Serum lipids and proliferative diabetic retinopathy and macular edema in persons with long-term type 1 diabetes mellitus," *JAMA Ophthalmology*, vol. 133, no. 5, pp. 503–510, 2015.

[5] R. Klein, S. M. Meuer, C. E. Myers et al., "Harmonizing the classification of age-related macular degeneration in the three-continent AMD consortium," *Ophthalmic Epidemiology*, vol. 21, no. 1, pp. 14–23, 2014.

[6] R. Klein, C. E. Myers, G. H. S. Buitendijk et al., "Lipids, lipid genes, and incident age-related macular degeneration: the three continent age-related macular degeneration consortium," *American Journal of Ophthalmology*, vol. 158, no. 3, pp. 513–524.e3, 2014.

[7] R. Klein, C. E. Myers, K. J. Cruickshanks et al., "Markers of inflammation, oxidative stress, and endothelial dysfunction and the 20-year cumulative incidence of early age-related macular degeneration: the Beaver Dam Eye Study," *JAMA Ophthalmology*, vol. 132, no. 4, pp. 446–455, 2014.

[8] R. Klein, C. E. Myers, and B. E. K. Klein, "Vasodilators, blood pressure-lowering medications, and age-related macular degeneration: the Beaver Dam Eye Study," *Ophthalmology*, vol. 121, no. 8, pp. 1604–1611, 2014.

[9] M. Grunin, S. Hagbi-Levi, and I. Chowers, "The role of monocytes and macrophages in age-related macular degeneration," *Advances in Experimental Medicine and Biology*, vol. 801, pp. 199–205, 2014.

[10] A. O. Edwards and G. Malek, "Molecular genetics of AMD and current animal models," *Angiogenesis*, vol. 10, no. 2, pp. 119–132, 2007.

[11] J. L. Haines, M. A. Hauser, S. Schmidt et al., "Complement factor H variant increases the risk of age-related macular degeneration," *Science*, vol. 308, no. 5720, pp. 419–421, 2005.

[12] X. L. Tian, R. Kadaba, S. A. You et al., "Identification of an angiogenic factor that when mutated causes susceptibility to Klippel–Trenaunay syndrome," *Nature*, vol. 427, no. 6975, pp. 640–645, 2004.

[13] J. B. Maller, J. A. Fagerness, R. C. Reynolds, B. M. Neale, M. J. Daly, and J. M. Seddon, "Variation in complement factor 3 is associated with risk of age-related macular degeneration," *Nature Genetics*, vol. 39, no. 10, pp. 1200-1201, 2007.

[14] R. Zhang, K. G. Hadlock, H. Do et al., "Gene expression profiling in peripheral blood mononuclear cells from patients with sporadic amyotrophic lateral sclerosis (sALS)," *Journal of Neuroimmunology*, vol. 230, no. 1-2, pp. 114–123, 2011.

[15] S. H. Sarks, D. Van Driel, L. Maxwell, and M. Killingsworth, "Softening of drusen and subretinal neovascularization," *Transactions of the Ophthalmological Societies of the United Kingdom*, vol. 100, no. 3, pp. 414–422, 1980.

[16] D. H. Anderson, R. F. Mullins, G. S. Hageman, and L. V. Johnson, "A role for local inflammation in the formation of drusen in the aging eye," *American Journal of Ophthalmology*, vol. 134, no. 3, pp. 411–431, 2002.

[17] R. S. Apte, J. Richter, J. Herndon, and T. A. Ferguson, "Macrophages inhibit neovascularization in a murine model of age-related macular degeneration," *PLoS Medicine*, vol. 3, no. 8, article e310, 2006.

[18] D. G. Espinosa-Heidmann, I. J. Suner, E. P. Hernandez, D. Monroy, K. G. Csaky, and S. W. Cousins, "Macrophage depletion diminishes lesion size and severity in experimental choroidal neovascularization," *Investigative Ophthalmology & Visual Science*, vol. 44, no. 8, pp. 3586–3592, 2003.

[19] E. Sakurai, A. Anand, B. K. Ambati, N. van Rooijen, and J. Ambati, "Macrophage depletion inhibits experimental choroidal neovascularization," *Investigative Ophthalmology & Visual Science*, vol. 44, no. 8, pp. 3578–3585, 2003.

[20] K. Kataoka, K. M. Nishiguchi, H. Kaneko, N. van Rooijen, S. Kachi, and H. Terasaki, "The roles of vitreal macrophages

and circulating leukocytes in retinal neovascularization," *Investigative Ophthalmology & Visual Science*, vol. 52, no. 3, pp. 1431–1438, 2011.

[21] M. J. Robertson, L. P. Erwig, J. Liversidge, J. V. Forrester, A. J. Rees, and A. D. Dick, "Retinal microenvironment controls resident and infiltrating macrophage function during uveoretinitis," *Investigative Ophthalmology & Visual Science*, vol. 43, no. 7, pp. 2250–2257, 2002.

[22] S. Hagbi-Levi, M. Grunin, T. Jaouni et al., "Proangiogenic characteristics of activated macrophages from patients with age-related macular degeneration," *Neurobiology of Aging*, vol. 51, pp. 71–82, 2017.

[23] F. Cruz-Guilloty, A. M. Saeed, S. Duffort et al., "T cells and macrophages responding to oxidative damage cooperate in pathogenesis of a mouse model of age-related macular degeneration," *PLoS One*, vol. 9, no. 2, article e88201, 2014.

[24] A. Caicedo, D. G. Espinosa-Heidmann, Y. Pina, E. P. Hernandez, and S. W. Cousins, "Blood-derived macrophages infiltrate the retina and activate Muller glial cells under experimental choroidal neovascularization," *Experimental Eye Research*, vol. 81, no. 1, pp. 38–47, 2005.

[25] C. Faber, A. Singh, M. Krüger Falk, H. B. Juel, T. L. Sørensen, and M. H. Nissen, "Age-related macular degeneration is associated with increased proportion of $CD56^+$ T cells in peripheral blood," *Ophthalmology*, vol. 120, no. 11, pp. 2310–2316, 2013.

[26] A. Mantovani, A. Sica, and M. Locati, "Macrophage polarization comes of age," *Immunity*, vol. 23, no. 4, pp. 344–346, 2005.

[27] R. S. Apte, "Regulation of angiogenesis by macrophages," *Advances in Experimental Medicine and Biology*, vol. 664, pp. 15–19, 2010.

[28] S. Zandi, S. Nakao, K. H. Chun et al., "ROCK-isoform-specific polarization of macrophages associated with age-related macular degeneration," *Cell Reports*, vol. 10, no. 7, pp. 1173–1186, 2015.

[29] A. Sene, A. A. Khan, D. Cox et al., "Impaired cholesterol efflux in senescent macrophages promotes age-related macular degeneration," *Cell Metabolism*, vol. 17, no. 4, pp. 549–561, 2013.

[30] C. Tsutsumi, K. H. Sonoda, K. Egashira et al., "The critical role of ocular-infiltrating macrophages in the development of choroidal neovascularization," *Journal of Leukocyte Biology*, vol. 74, no. 1, pp. 25–32, 2003.

[31] L. Li, P. Heiduschka, A. F. Alex, D. Niekämper, and N. Eter, "Behaviour of CD11b-positive cells in an animal model of laser-induced choroidal neovascularisation," *Ophthalmologica*, vol. 237, no. 1, pp. 29–41, 2017.

[32] C. N. Nagineni, V. K. Kommineni, N. Ganjbaksh, K. K. Nagineni, J. J. Hooks, and B. Detrick, "Inflammatory cytokines induce expression of chemokines by human retinal cells: role in chemokine receptor mediated age-related macular degeneration," *Aging and Disease*, vol. 6, no. 6, pp. 444–455, 2015.

[33] Y. F. Feng, H. Guo, F. Yuan, and M. Q. Shen, "Lipopolysaccharide promotes choroidal neovascularization by up-regulation of CXCR4 and CXCR7 expression in choroid endothelial cell," *PLoS ONE*, vol. 10, no. 8, article e0136175, 2015.

[34] M. Rutar, R. Natoli, R. X. Chia, K. Valter, and J. M. Provis, "Chemokine-mediated inflammation in the degenerating retina is coordinated by Müller cells, activated microglia, and retinal pigment epithelium," *Journal of Neuroinflammation*, vol. 12, no. 1, p. 8, 2015.

[35] M. Rutar, R. Natoli, and J. M. Provis, "Small interfering RNA-mediated suppression of Ccl2 in Müller cells attenuates microglial recruitment and photoreceptor death following retinal degeneration," *Journal of Neuroinflammation*, vol. 9, no. 1, p. 221, 2012.

[36] F. M. Mo, A. D. Proia, W. H. Johnson, D. Cyr, and K. Lashkari, "Interferon γ–inducible protein-10 (IP-10) and eotaxin as biomarkers in age-related macular degeneration," *Investigative Ophthalmology & Visual Science*, vol. 51, no. 8, pp. 4226–4236, 2010.

[37] V. Torraca, C. Cui, R. Boland et al., "The CXCR3-CXCL11 signaling axis mediates macrophage recruitment and dissemination of mycobacterial infection," *Disease Models & Mechanisms*, vol. 8, no. 3, pp. 253–269, 2015.

[38] D. Petrovic-Djergovic, M. Popovic, S. Chittiprol, H. Cortado, R. F. Ransom, and S. Partida-Sánchez, "CXCL10 induces the recruitment of monocyte-derived macrophages into kidney, which aggravate puromycin aminonucleoside nephrosis," *Clinical and Experimental Immunology*, vol. 180, no. 2, pp. 305–315, 2015.

[39] A. M. Newman, N. B. Gallo, L. S. Hancox et al., "Systems-level analysis of age-related macular degeneration reveals global biomarkers and phenotype-specific functional networks," *Genome Medicine*, vol. 4, no. 2, p. 16, 2012.

[40] S. Fujimura, H. Takahashi, K. Yuda et al., "Angiostatic effect of CXCR3 expressed on choroidal neovascularization," *Investigative Ophthalmology & Visual Science*, vol. 53, no. 4, pp. 1999–2006, 2012.

[41] M. Grunin, T. Burstyn-Cohen, S. Hagbi-Levi, A. Peled, and I. Chowers, "Chemokine receptor expression in peripheral blood monocytes from patients with neovascular age-related macular degeneration," *Investigative Opthalmology & Visual Science*, vol. 53, no. 9, article 5292, 2012.

[42] M. Kramer, M. Hasanreisoglu, A. Feldman et al., "Monocyte chemoattractant protein-1 in the aqueous humour of patients with age-related macular degeneration," *Clinical & Experimental Ophthalmology*, vol. 40, no. 6, pp. 617–625, 2012.

[43] J. B. Jonas, Y. Tao, M. Neumaier, and P. Findeisen, "Cytokine concentration in aqueous humour of eyes with exudative age-related macular degeneration," *Acta Ophthalmologica*, vol. 90, no. 5, pp. e381–e388, 2012.

[44] P. L. Penfold, M. C. Killingsworth, and S. H. Sarks, "Senile macular degeneration: the involvement of immunocompetent cells," *Graefe's Archive for Clinical and Experimental Ophthalmology*, vol. 223, no. 2, pp. 69–76, 1985.

[45] M. C. Killingsworth, J. P. Sarks, and S. H. Sarks, "Macrophages related to Bruch's membrane in age-related macular degeneration," *Eye*, vol. 4, no. 4, pp. 613–621, 1990.

[46] S. Cherepanoff, P. McMenamin, M. C. Gillies, E. Kettle, and S. H. Sarks, "Bruch's membrane and choroidal macrophages in early and advanced age-related macular degeneration," *The British Journal of Ophthalmology*, vol. 94, no. 7, pp. 918–925, 2010.

[47] X. Cao, D. Shen, M. M. Patel et al., "Macrophage polarization in the maculae of age-related macular degeneration: a pilot study," *Pathology International*, vol. 61, no. 9, pp. 528–535, 2011.

[48] P. L. Penfold, J. G. Wong, J. Gyory, and F. A. Billson, "Effects of triamcinolone acetonide on microglial morphology and quantitative expression of MHC-II in exudative age-related macular degeneration," *Clinical & Experimental Ophthalmology*, vol. 29, no. 3, pp. 188–192, 2001.

[49] F. Sennlaub, C. Auvynet, B. Calippe et al., "CCR2(+) monocytes infiltrate atrophic lesions in age-related macular disease and mediate photoreceptor degeneration in experimental subretinal inflammation in Cx3cr1 deficient mice," *EMBO Molecular Medicine*, vol. 5, no. 11, pp. 1775–1793, 2013.

[50] S. J. Allen, S. E. Crown, and T. M. Handel, "Chemokine: receptor structure, interactions, and antagonism," *Annual Review of Immunology*, vol. 25, no. 1, pp. 787–820, 2007.

[51] H. Kohno, T. Maeda, L. Perusek, E. Pearlman, and A. Maeda, "CCL3 production by microglial cells modulates disease severity in murine models of retinal degeneration," *Journal of Immunology*, vol. 192, no. 8, pp. 3816–3827, 2014.

[52] S. Joly, M. Francke, E. Ulbricht et al., "Cooperative phagocytes: resident microglia and bone marrow immigrants remove dead photoreceptors in retinal lesions," *The American Journal of Pathology*, vol. 174, no. 6, pp. 2310–2323, 2009.

[53] N. Fernando, R. Natoli, K. Valter, J. Provis, and M. Rutar, "The broad-spectrum chemokine inhibitor NR58-3.14.3 modulates macrophage-mediated inflammation in the diseased retina," *Journal of Neuroinflammation*, vol. 13, no. 1, p. 47, 2016.

[54] M. Abraham, H. Wald, D. Vaizel-Ohayon et al., "Development of novel promiscuous anti-chemokine peptibodies for treating autoimmunity and inflammation," *Frontiers in Immunology*, vol. 8, article 1432, 2017.

[55] T. Tobe, N. Okamoto, M. A. Vinores et al., "Evolution of neovascularization in mice with overexpression of vascular endothelial growth factor in photoreceptors," *Investigative Ophthalmology & Visual Science*, vol. 39, no. 1, pp. 180–188, 1998.

[56] T. J. Collins, "ImageJ for microscopy," *BioTechniques*, vol. 43, 1 Supplement, pp. S25–S30, 2007.

[57] K. J. Livak and T. D. Schmittgen, "Analysis of relative gene expression data using real-time quantitative PCR and the $2^{-\Delta\Delta C}{}_{T}$ method," *Methods*, vol. 25, no. 4, pp. 402–408, 2001.

[58] The Age-Related Eye Disease Study Research Group, "The Age-Related Eye Disease Study (AREDS): design implications AREDS report no. 1," *Controlled Clinical Trials*, vol. 20, no. 6, pp. 573–600, 1999.

[59] A. Mantovani, S. Sozzani, M. Locati, P. Allavena, and A. Sica, "Macrophage polarization: tumor-associated macrophages as a paradigm for polarized M2 mononuclear phagocytes," *Trends in Immunology*, vol. 23, no. 11, pp. 549–555, 2002.

[60] F. O. Martinez, L. Helming, and S. Gordon, "Alternative activation of macrophages: an immunologic functional perspective," *Annual Review of Immunology*, vol. 27, no. 1, pp. 451–483, 2009.

[61] Z. Shao, M. Friedlander, C. G. Hurst et al., "Correction: choroid sprouting assay: an *ex vivo* model of microvascular angiogenesis," *PLoS One*, vol. 8, no. 8, article e69552, 2013.

[62] E. G. O'Koren, R. Mathew, and D. R. Saban, "Fate mapping reveals that microglia and recruited monocyte-derived macrophages are definitively distinguishable by phenotype in the retina," *Scientific Reports*, vol. 6, no. 1, article 20636, 2016.

[63] S. M. Hector and T. L. Sørensen, "Circulating monocytes and B-lymphocytes in neovascular age-related macular degeneration," *Clinical Ophthalmology*, vol. 11, pp. 179–184, 2017.

[64] P. Penfold, M. Killingsworth, and S. Sarks, "An ultrastructural study of the role of leucocytes and fibroblasts in the breakdown of Bruch's membrane," *Australian Journal of Ophthalmology*, vol. 12, no. 1, pp. 23–31, 1984.

[65] J. T. Rosenbaum, L. O'rourke, G. Davies, C. Wenger, L. David, and J. E. Robertson, "Retinal pigment epithelial cells secrete substances that are chemotactic for monocytes," *Current Eye Research*, vol. 6, no. 6, pp. 793–800, 1987.

[66] D. G. Espinosa-Heidmann, A. Caicedo, E. P. Hernandez, K. G. Csaky, and S. W. Cousins, "Bone marrow-derived progenitor cells contribute to experimental choroidal neovascularization," *Investigative Ophthalmology & Visual Science*, vol. 44, no. 11, pp. 4914–4919, 2003.

[67] P. Xie, M. Kamei, M. Suzuki et al., "Suppression and regression of choroidal neovascularization in mice by a novel CCR2 antagonist, INCB3344," *PLoS One*, vol. 6, no. 12, article e28933, 2011.

[68] M. Grunewald, I. Avraham, Y. Dor et al., "VEGF-induced adult neovascularization: recruitment, retention, and role of accessory cells," *Cell*, vol. 124, no. 1, pp. 175–189, 2006.

[69] E. C. Breen, "VEGF in biological control," *Journal of Cellular Biochemistry*, vol. 102, no. 6, pp. 1358–1367, 2007.

[70] S. Crespo-Garcia, C. Corkhill, C. Roubeix et al., "Inhibition of placenta growth factor reduces subretinal mononuclear phagocyte accumulation in choroidal neovascularization," *Investigative Ophthalmology and Visual Science*, vol. 58, no. 12, pp. 4997–5006, 2017.

[71] H. Oh, H. Takagi, C. Takagi et al., "The potential angiogenic role of macrophages in the formation of choroidal neovascular membranes," *Investigative Ophthalmology & Visual Science*, vol. 40, no. 9, pp. 1891–1898, 1999.

[72] A. Otani, H. Takagi, H. Oh, S. Koyama, M. Matsumura, and Y. Honda, "Expressions of angiopoietins and Tie2 in human choroidal neovascular membranes," *Investigative Ophthalmology and Visual Science*, vol. 40, no. 9, pp. 1912–1920, 1999.

[73] C. N. Nagineni, V. K. Kommineni, A. William, B. Detrick, and J. J. Hooks, "Regulation of VEGF expression in human retinal cells by cytokines: implications for the role of inflammation in age-related macular degeneration," *Journal of Cellular Physiology*, vol. 227, no. 1, pp. 116–126, 2012.

[74] H. Wang, X. Han, E. S. Wittchen, and M. E. Hartnett, "TNF-α mediates choroidal neovascularization by upregulating VEGF expression in RPE through ROS-dependent β-catenin activation," *Molecular Vision*, vol. 22, pp. 116–128, 2016.

[75] Y. Zhou, S. Yoshida, Y. Kubo et al., "Different distributions of M1 and M2 macrophages in a mouse model of laser-induced choroidal neovascularization," *Molecular Medicine Reports*, vol. 15, no. 6, pp. 3949–3956, 2017.

[76] T. Zhou, Z. Huang, X. Sun et al., "Microglia polarization with M1/M2 phenotype changes in rd1 mouse model of retinal degeneration," *Frontiers in Neuroanatomy*, vol. 11, 2017.

[77] H. E. Grossniklaus, J. X. Ling, T. M. Wallace et al., "Macrophage and retinal pigment epithelium expression of angiogenic cytokines in choroidal neovascularization," *Molecular Vision*, vol. 8, pp. 119–126, 2002.

[78] J. W. Miller, "Vascular endothelial growth factor and ocular neovascularization," *The American Journal of Pathology*, vol. 151, no. 1, pp. 13–23, 1997.

[79] J. Stone, A. Itin, T. Alon et al., "Development of retinal vasculature is mediated by hypoxia-induced vascular endothelial growth factor (VEGF) expression by neuroglia," *The Journal of Neuroscience*, vol. 15, no. 7, pp. 4738–4747, 1995.

[80] S. G. Robbins, J. R. Conaway, B. L. Ford, K. A. Roberto, and J. S. Penn, "Detection of vascular endothelial growth factor (VEGF) protein in vascular and non-vascular cells of the

normal and oxygen-injured rat retina," *Growth Factors*, vol. 14, no. 4, pp. 229–241, 1997.

[81] L. P. Aiello, R. L. Avery, P. G. Arrigg et al., "Vascular endothelial growth factor in ocular fluid of patients with diabetic retinopathy and other retinal disorders," *The New England Journal of Medicine*, vol. 331, no. 22, pp. 1480–1487, 1994.

[82] D. C. Darland, L. J. Massingham, S. R. Smith, E. Piek, M. Saint-Geniez, and P. A. D'Amore, "Pericyte production of cell-associated VEGF is differentiation-dependent and is associated with endothelial survival," *Developmental Biology*, vol. 264, no. 1, pp. 275–288, 2003.

[83] H. Ida, T. Tobe, H. Nambu, M. Matsumura, M. Uyama, and P. A. Campochiaro, "RPE cells modulate subretinal neovascularization, but do not cause regression in mice with sustained expression of VEGF," *Investigative Ophthalmology and Visual Science*, vol. 44, no. 12, pp. 5430–5437, 2003.

[84] J. W. Miller, "Age-related macular degeneration revisited – piecing the puzzle: the LXIX Edward Jackson memorial lecture," *American Journal of Ophthalmology*, vol. 155, no. 1, pp. 1–35.e13, 2013.

[85] J. S. Heier, D. M. Brown, V. Chong et al., "Intravitreal aflibercept (VEGF trap-eye) in wet age-related macular degeneration," *Ophthalmology*, vol. 119, no. 12, pp. 2537–2548, 2012.

[86] Y. Y. Saishin, Y. Y. Saishin, K. Takahashi et al., "VEGF-TRAPR1R2 suppresses choroidal neovascularization and VEGF-induced breakdown of the blood-retinal barrier," *Journal of Cellular Physiology*, vol. 195, no. 2, pp. 241–248, 2003.

Hindawi
Journal of Immunology Research
Volume 2019, Article ID 4197829, 10 pages
https://doi.org/10.1155/2019/4197829

Review Article

Functions of Exosomes in the Triangular Relationship between the Tumor, Inflammation, and Immunity in the Tumor Microenvironment

Tiantian Wang, Moussa Ide Nasser, Jie Shen, Shujuan Qu, Qingnan He, and Mingyi Zhao

Department of Pediatrics, The Third Xiangya Hospital, Central South University, Changsha, Hunan Province 410013, China

Correspondence should be addressed to Qingnan He; heqn2629@163.com and Mingyi Zhao; 36163773@qq.com

Received 12 April 2019; Accepted 11 July 2019; Published 1 August 2019

Guest Editor: Nivin Sharawy

Exosomes are extracellular vesicles that contain diverse components such as genetic materials, proteins, and lipids. Owing to their distinct derivation and tissue specificity, exosomes act as double-edged swords during the development of neoplasms. On the one hand, tumor-derived exosomes can modulate the immune system during tumorigenesis by regulating inflammatory cell infiltration and oxidative stress and by promoting epithelial-to-mesenchymal transition and immune-induced tumor dormancy. On the other hand, components of specific immune cell-derived exosomes may contribute to the efficacy of antitumor immunotherapy. In this review, we demonstrate the pivotal role of exosomes in the triangular relationship in the tumor microenvironment between the tumor, inflammation, and immunity, which may provide potential strategies for tumor immunotherapy at genetic and cellular levels.

1. Introduction

Exosomes are vesicles that contain genetic materials, lipids, and functional proteins, and exosomes secreted by cancer and immune cells contain cell-specific content. Owing to their widespread and stable existence in biological fluids, exosomes may act as useful biomarkers for detecting the progression of cancers [1]. Intriguingly, exosomes exert bidirectional effects on cancers as a result of their distinct origins and heterogeneity. For example, some tumor-derived exosomes (TDEs) act as tumor growth stimulators, activating the epithelial-to-mesenchymal transition (EMT) and tumor dormancy during cancer proliferation, invasion, and metastasis, whereas other exosomes that originate from specific immune cells act as inhibitors that interfere with cancer growth [2]. In addition, many studies have demonstrated the significance of inflammation in the initiation and development of tumors, and it has been shown that exosomes can affect the progression of inflammation in the tumor environment by initiating inflammatory pathways, activating neutrophils, and regulating oxidative stress. This review discusses the latest research on the functions of exosomes in the triangular relationship between the tumor, inflammation, and immunity in the tumor environment and provides a basis for the potential use of exosomes as vectors in tumor gene therapy and tumor immunotherapy.

2. Exosomes

2.1. Exosomes and Their Biological Characteristics. Extracellular vesicles (EVs) consist of three main subtypes based on their biogenesis: exosomes, microvesicles, and apoptotic bodies [3, 4]. Exosomes are vesicles 40–200 nm in diameter marked by tetraspanins, Alix, and TSG101. Microvesicles are around 200-2000 nm in size and are marked by integrins, selectins, and CD40. Apoptotic bodies are around 500-2000 nm in size and are marked by phosphatidylserines and genomic DNA [5]. Exosomes, which were first identified in sheep reticulocytes in 1985 [6], are double-layered lipid membrane-enclosed vesicles that are secreted by almost all viable cells under both normal and pathological conditions and are extensively present in body fluids, intercellular

spaces, and tissues [7]. Exosomes contain diverse proteins, lipids, and nucleic acids, such as microRNAs (miRNAs), long noncoding RNAs (lncRNAs), and circular RNAs (circRNAs). There are two types of proteins present in exosomes. The first type, which exists in most exosomes and can function as a marker, includes heat-shock proteins (HSPs), transmembrane 4 superfamily proteins, membrane transport proteins, and fusion proteins [8]. The second type, which is cell-specific and has heterogeneous functions, includes major histocompatibility complex II (MHCII) and fas ligand (FasL), which are present in exosomes from lymphoblastoid cells and induce apoptosis in $CD4^+$ T cells [9]. Exosomes are rich in cholesterol, glycosphingolipids, ether lipids, and phosphatidylserine, which participate in both biogenesis and structural maintenance [10–12]. The first release of the exosome database included 58,330 circRNAs, 15,501 lncRNAs, and 18,333 mRNAs, which suggests a sophisticated genetic control system [13]. These functional RNAs can affect biological activities and modulate cellular events such as cell proliferation, apoptosis, differentiation, and immunoregulation [14–16].

2.2. Exosomes and Intercellular Communication. Exosomes participate in intercellular communication. Tumor-derived exosomal lncRNAs have been implicated as signaling mediators that coordinate the functions of neighboring tumor cells. Interestingly, some exosomal RNAs from donor cells can function in recipient cells and are called "exosomal shuttle RNAs," suggesting a role in genetic exchange between cells [17]. For example, after stimulation with arsenite, exosomes derived from hepatic epithelial cells can transfer circRNA_100284 to surrounding cells, which increases the expression of enhancer zeste homolog 2 (EZH2) and cyclin-D1 and subsequently promotes the G1/S transition [18]. This finding demonstrates the oncogenic capacity of exosomes. Through intercellular communication, changes in an individual cell may influence the course of tumor proliferation and metastasis on a macroscale. In fact, in epithelial ovarian cancer, tumor-secreted exosomes transfer miR-99a-5p to adjacent human peritoneal mesothelial cells (HPMCs), resulting in increased levels of fibronectin and vitronectin, extracellular matrix components that are closely associated with tumor invasion [19].

2.3. Exosomes and Inflammation. Another vital function of exosomes that is related to disease progression is the modulation of inflammation [20, 21]. Exosomes can promote or inhibit the development of inflammation. Hypoxia-induced delivery of miR-23a from exosomes secreted by tubular epithelial cells was shown to promote macrophage activation and trigger tubulointerstitial inflammation [22]. Similarly, miR-150-5p and miR-142-3p from dendritic cell- (DC-) released exosomes can be transferred to regulatory T cells (Tregs), resulting in an increase in interleukin 10 (IL-10) expression and a decrease in IL-6 expression [23]. Choroid plexus epithelial cells can release exosomes that contain miR-146a and miR-155, which upregulate the expression of inflammatory cytokines in astrocytes and microglia [24]. Another type of exosome exhibits protective effects against inflammation-related diseases [25]. In endometriosis, exosomal miR-138 can protect against inflammation by decreasing the expression level of nuclear factor-κB (NF-κB), a transcription factor that regulates inflammatory cytokines, such as tumor necrosis factor-α (TNF-α) and IL-18 [26]. In addition, a study showed that exosomes secreted by bone marrow mesenchymal stem cells (BMSCs) can attenuate inflammatory changes in a rat model of experimental autoimmune encephalomyelitis by modulating microglial polarization and maintaining the balance between M2-related and M1-related cytokines [27]. Another study revealed that exosomal miR-181c suppressed Toll-like receptor 4 (TLR-4) expression and subsequently lowered TNF-α and IL-1β levels in burn-induced inflammation [28]. Treg-derived exosomes containing miR-Let-7d affected T helper cell 1 (Th1) cell growth and inhibited IFN-γ secretion to inhibit inflammation [29]. Exosomal miR-155 from bone marrow cells (BMCs) was shown to enhance the innate immune response in chronic inflammation by increasing TNF-α levels [30]. These findings provide a basis for investigating the role of inflammation in the tumor microenvironment, as well as the possibility of utilizing exosomes as a carrier to attenuate inflammation and restore impaired immune responses in cancer.

3. The Function of Exosomes in the Tumor Microenvironment and Metabolism

3.1. Exosomes Are Involved in Immune Activities during Tumorigenesis. Tumor occurrence is strongly correlated with a failure in immune surveillance, and surprisingly, the translocation of tumor-derived exosomes may assist in immune escape by interfering with cellular events, such as immune cell differentiation and cytokine secretion. One study showed that exogenous circRNAs activate the expression of retinoic-acid-inducible gene-I (*RIG-I*) and initiate innate immunity [31]. This study clearly demonstrated that foreign genes could affect the endogenous genes in cells and induce an immune reaction. Zhou et al. showed that the melanoma-derived exosomal miRNA-Rab27a could be taken up by $CD4^+$ T cells and may accelerate mitochondrial apoptosis and upregulate the expression of B-cell lymphoma-2 (BCL-2) and B-cell lymphoma-extra large (BCL-xL), which are antiapoptotic proteins [32] (Figure 1). This result demonstrates the interaction between tumor cells and immune cells. This finding is not unique, and other studies have reported similar results. For example, Ning et al. showed that exosomes from lung carcinoma or breast cancer cells could block the differentiation of $CD4^+$IFN-γ^+ Th1 cells, inhibit the maturation and migration of DCs, and induce apoptosis to promote the immunosuppressive effect of DCs [33]. Head and neck cancer cell- (HNCC-) derived exosomes affect $CD8^+$ T cells by inducing a loss of CD27/CD28, accompanied by decreased levels of the antitumor cytokine IFN-γ [34] (Figure 1). miR-29a-3p and miR-21-5p in tumor-related macrophage-derived exosomes inhibit the STAT3 signaling pathway and increase the Treg/T helper cell 17 (Th17) ratio in epithelial ovarian cancer, which may lead to poor patient outcomes [35]. Human hepatocellular carcinoma- (HCC-) derived exosomes containing high mobility group box 1

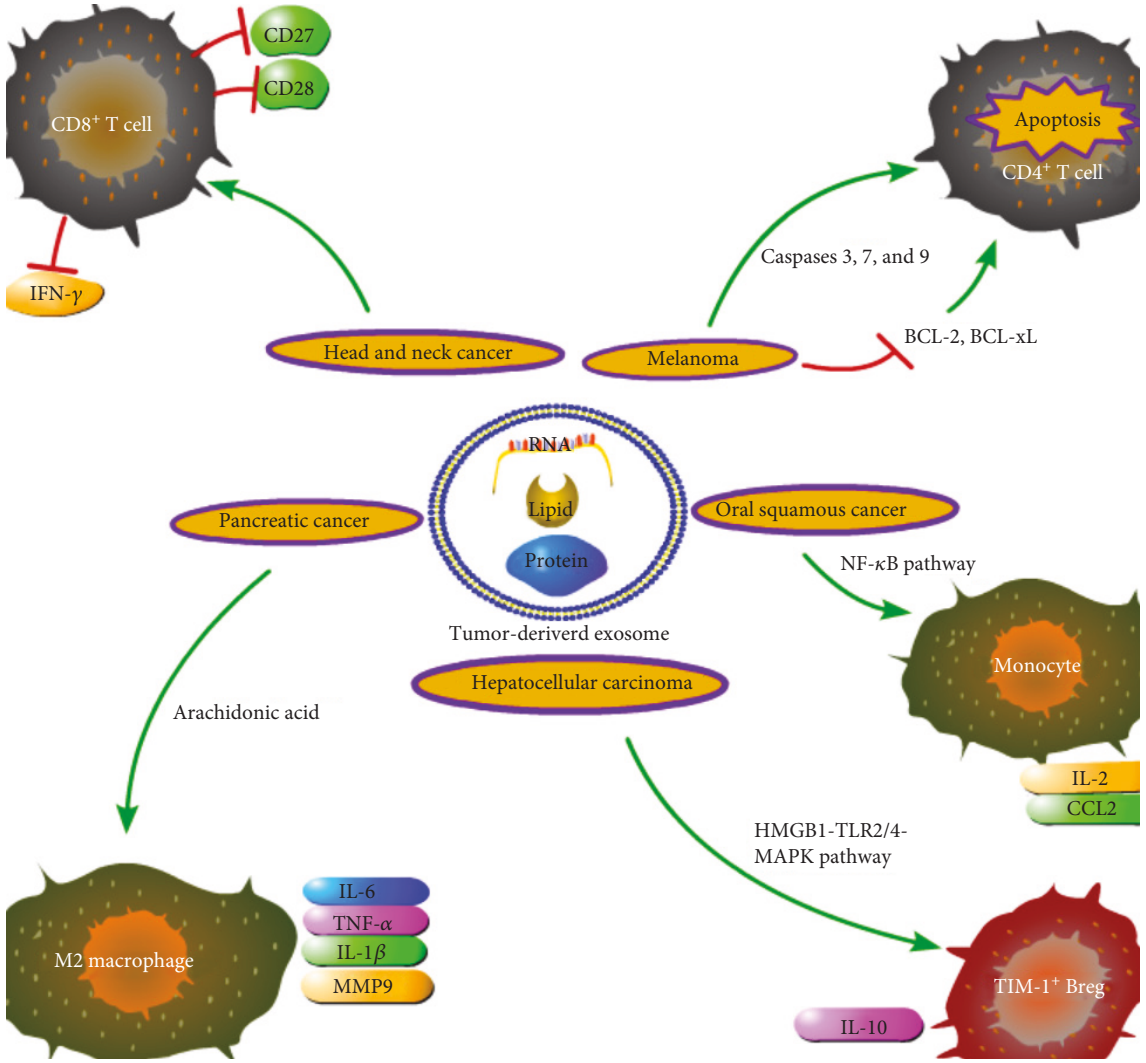

Figure 1: Various effects of tumor-derived exosomes on the immune system and possible associated pathways in the tumor microenvironment.

(HMGB1) promote the proliferation of the T cell immunoglobulin domain and mucin domain protein-1 positive regulatory B (TIM-1^+ Breg) cells by inducing the Toll-like receptor/mitogen-activated protein kinase (TLR/MAPK) pathway and the production of IL-10, an immunosuppressive cytokine, thus working against $CD8^+$ T cells through the TLR2/4-MAPK pathway and leading to immune surveillance failure [36] (Figure 1). These findings demonstrate that TDEs are involved in generating an immunosuppressive microenvironment that promotes the progression of solid tumors. In addition, exosomes may also promote tumor progression in hematological cancers. For example, elevated levels of the lncRNA HOX transcript antisense (HOTAIR) can lead to decreased T-lymphocyte proliferation as well as reduced immunoglobulin production and a reversed ratio of $CD4^+/CD8^+$ T cell subsets through the Wnt/β-catenin pathway, which may eliminate the immunologic rejection of leukemia cells [37]. Exosomal circRNAs from tumor cells play a crucial role in poor prognosis in cancer [38]; however, few studies have examined their interaction with the immune system. The immunosuppressive role of tumor-secreted exosomes suggests their potential in tumor therapy, as blockage of tumor-secreted exosomes may enhance the antitumor effects of tumor-related T cells and inhibit the silencing of these cells [39]. However, specific immune cell-derived exosomes may also be conducive to tumor development. In colorectal cancer, macrophage-derived exosomes containing miR-21-5p and miR-155-5p can regulate the Brahma-related gene 1 (*BRG1*) coding sequence to promote the metastasis of cancer cells (Table 1) [40].

3.2. Exosomes, Oxidative Stress, and Inflammation during Tumor Progression. A sustained oxidative stress state may trigger chronic inflammation through activation of inflammatory pathways [41]. During chronic inflammation, slow release of reactive oxygen species (ROS) can cause genetic mutations in nearby cells, promote the proliferation of malignantly transformed cells, and inhibit apoptosis [41, 42]. For example, pancreatic cancer cell-derived exosomes have been shown to regulate STAT3 signaling in monocytes and induce

Table 1: Exosome functions in the tumor microenvironment: effects on the tumor, immunity, and inflammation.

Tumor type	Exosome content	Exosome origin	Effector cells	Effector components
Melanoma	miR-Rab27a	Tumor	$CD4^+$ T cells	BCL-2, BCL-xL
LC, breast cancer	/	Tumor	$CD4^+IFN\text{-}\gamma^+$ Th1 cells, DCs	/
HNC	/	Tumor	$CD8^+$ T cells	CD27/CD28, IFN-γ
EOC	miR-29a-3p, miR-21-5p	Macrophage	Treg/Th17 cells	STAT3 signaling, Treg/Th17 ratios
HCC	*HMGB1*	Tumor	T cells, TIM-1^+ Breg cells, $CD8^+$ T cells	TLR/MAPK pathway, IL-10
Leukemia	lncRNA HOTAIR	Tumor	T lymphocytes, $CD4^+/CD8^+$ T cells	Wnt/β-catenin axis, Ig
CRC	miR-21-5p, miR-155-5p	Macrophage	Tumor cells	*BRG1*
PC	/	Tumor	Macrophages	IL-6, IL-1β, and TNF-α
OC	/	Tumor	Monocytes	NF-κB pathway, IL-6, MMP9
HCC	lncRNA TUC339	Tumor	Macrophages	Costimulatory molecules
CC	miR-1246	Tumor	Macrophages	TGF-β
GC	/	Tumor	Neutrophils	HMGB1/TLR4/NF-κB
PC	/	Tumor	Monocytes	STAT3 signaling, arginase, ROS
Leukemia	/	Tumor	Macrophages, BM-MSCs	TNF-α, IL-10, ROS
EC	*Ecrg-4* mRNA	Tumor	/	Inflammation-related genes
Breast cancer	/	Camel milk	Tumor cells, CD 4^+ T cells, $CD8^+$ T cells	Tumor cell apoptosis, ROS
Glioma	miR-10a, miR-21	Tumor	MDSCs	ROS, IL-10, TGF-β
LC	KIT	Mast cell	Tumor cells	KIT/SCF pathway

Tumor abbreviations: LC: lung cancer; HNC: head and neck cancer; EOC: epithelial ovarian cancer; CRC: colorectal cancer; EC: esophageal cancer; PC: pancreatic cancer; OC: oral cancer; CC: colon cancer; and GC: gastric cancer. "/" means "not mentioned".

the expression of arginase and ROS [43]. In contrast, leukemic cell-derived exosomes increase the levels of inflammatory mediators such as TNF-α and IL-10 in macrophages but decrease ROS levels in BMSCs, thus turning the local bone marrow into a leukemia-friendly microenvironment [44]. These results reflect the different ROS states in solid and nonsolid tumors.

Chronic inflammation can initiate cellular activities that contribute to the malignant transformation of cells, particularly DNA damage and genetic instability [45, 46]. TDEs may accelerate tissue damage and inflammation during tumor progression. In pancreatic cancer, macrophages treated with TDEs secreted a greater amount of inflammatory molecules, including IL-6, IL-1β, and TNF-α [47] (Figure 1). Additionally, in oral cancer, monocytes can take up extracellular vesicles, which promote the activation of NF-κB and the establishment of a proinflammatory milieu marked by increased levels of IL-6 and matrix metallopeptidase 9 (MMP9) [48] (Figure 1). HCC cell-derived exosomes containing abundant *lncRNA TUC339* cause a reduction in the levels of proinflammatory mediators, expression of costimulatory molecules, and phagocytosis activity in macrophages [49], resulting in the inhibition of immune activity. Colon cancer cells secrete exosomes containing *miR-1246* that can reprogram macrophages to promote the generation of an anti-inflammatory environment via increased expression of TGF-β [50]. Additionally, neutrophils, a signature of inflammation, can regulate immunosuppression to promote tumor progression via suppression of natural killer cell activity [51]. Zhang et al. showed that gastric cancer cell-derived exosomes increase the number of inflammatory factors and activate neutrophils in an HMGB1/TLR4/NF-κB axis-dependent manner, which can promote tumor metastasis [52].

Nevertheless, exosomes can also be ideal tools to slow tumor progression. Mao et al. reported that exosomes could carry *esophageal cancer-related gene-4* (*Ecrg-4*) mRNA and inhibit the expression of genes related to angiogenesis and inflammation [53]. Interestingly, camel milk-derived exosomes can slow the development of breast cancer by inducing tumor cell apoptosis, reducing oxidative stress and the release of inflammatory cytokines, and activating the immune response by increasing the numbers of CD 4^+ and $CD8^+$ T cells (Table 1) [54].

3.3. Exosomes, Inflammation, and Immunity in the Tumor Microenvironment. Chronic inflammation may act as a negative mediator in tumor immunity through myeloid-derived suppressor cells (MDSCs), which are precursors of immune cells such as macrophages, DCs, and granulocytes. A recent report showed that increased levels of the inflammatory cytokine IFN-γ can disrupt the differentiation of MDSCs and thus interfere with antigen presentation in tumors [55]. TDEs may be involved in this process of immune suppression. In a mouse model of glioma, TDEs containing *miR-10a and miR-21* can be engulfed by MDSCs and affect their development to produce immunosuppressive molecules [56]. Similarly, mast cells (MCs) can be considered the bridge between inflammation and immunity in the tumor and may participate in angiogenesis and lymphangiogenesis

[57]. The function of TDEs on mast cells is not clear and requires further investigation. On the other hand, lung cancer cells can take up MC-derived exosomes containing the protein KIT and attain rapid growth [58]. In this way, MC-derived exosomes could be a key target for tumor immunotherapy. One report has shown that exosomes from mast cells processed by hepatitis C virus E2 (HCV-E2) can block HCC metastasis [59].

3.4. Exosomes and Immune Tolerance. It has been shown that the lncRNA-SNHG14 can enhance the efficiency of trastuzumab in breast cancer by targeting the B-cell lymphoma-2/B-cell lymphoma-2 associated X (Bcl-2/Bax) signaling pathway, which regulates apoptosis [60]. In esophageal squamous cell carcinoma (ESCC), elevated levels of exosomal lncRNA *prostate androgen-regulated transcript 1* (*PART1*) caused resistance to gefitinib by binding to miR-129 and increasing the expression of Bcl-2 [61]. Similarly, for melanoma patients with no reaction to immunization therapy, exosomal PD-L1 derived from melanoma cells was shown to interfere with the antitumor activity of immune cells by binding to $CD8^+$ T cells, inhibiting the proliferation of tumor-infiltrating $CD8^+$ T lymphocytes (TILs) and reducing the production of IFN-γ and IL-2 [62]. Kanlikilicer et al. showed that exosomes from paclitaxel-resistant ovarian cancer (OC) cells could transfer miR-1246 to M2-type macrophages, allowing miR-1246 to bind to the 3′UTR of caveolin-1 (*Cav1*) and function through platelet-derived growth factor receptor (PDGFR) tyrosine signaling to inhibit cell proliferation [63]. Amazingly, exosomes could be used as a tool to overcome the problem of drug resistance. A silencing RNA-(siRNA-) targeting GRP78 (siGRP78) contained in exosomes from BMCs was able to impede tumor cell proliferation, invasion, and metastasis in HCC [64]. Gene silencing could also be applied to other chemotherapy-tolerant cancers, as long as the genetic mechanism underlying the effects of the exosomes is known.

3.5. Exosomes and EMT. EMT initiates the conversion of malignant tumor epithelial cells to an interstitial phenotype, which can promote invasion and metastasis. A recent study showed that BMSCs in a hypoxic state transferred exosomal-derived miR-193a-3p, miR-210-3p, and miR-5100 to activate signal transducer and activator of transcription 3 (STAT3) signaling in lung cancer cells and also led to an increase in the levels of vimentin and N-cadherin, two mesenchymal markers [65]. These results strongly suggest that TDEs are involved in tumor EMT progression. Following pretreatment with TGF-β, an inflammatory cytokine, exosomal-derived *lnc-MMP2-2* was shown to promote the expression of matrix metalloproteinase-2 (MMP2), an important EMT marker, to regulate the dissemination of lung cancer cells through the vasculature [66]. This demonstrates the participation of the immune system in EMT. Furthermore, *Snail*, an EMT transcriptional factor, was shown to activate the M1 macrophage- (M1 MΦ-) M2 macrophage (M2 MΦ) transition by increasing TDEs-miR-21 and transferring TDEs to $CD14^+$ human monocytes, which promotes the advancement of HNC [67]. Therefore, the import of exosomal siRNAs into tumor cells may be an effective tumor gene and immunotherapy method to suppress the expression of target mRNAs [68]. Interestingly, the impact of exosomes on EMT is not completely one-sided. For example, exosomes containing miR-128-3p block EMT by inhibiting the mRNA expression of B-cell-specific Moloney murine leukemia virus integration site 1 (*Bmi1*) in CRC [69]. Additionally, cancer-associated fibroblasts (CAFs) can secrete exosomes lacking miR-148b that are transferred to endometrial cancer cells (ECCs) and modulate EMT by relieving the suppression of DNA (cytosine-5)-methyltransferase 1 (*DNMT1*) [70]. *miR-155-5p* in exosomes derived from gastric cancer cells induced a mesenchymal-like morphological change and increased the levels of E-cadherin and vimentin as well as resistance to paclitaxel, a classical chemotherapy medicine [71]. These studies demonstrate the significance of exosomes in the modulation of gene expression, components of the extracellular matrix, basement membrane remodeling, and tumor chemotherapy (Table 2).

3.6. Exosomes and Tumor Dormancy. Immune-induced tumor dormancy refers to the phenomenon of cell cycle arrest, downregulation of proliferation-related genes, and slowing of metabolism in tumor cells, which is regulated by the immune system. This quiescent state may be reversed through interactions between exosomes and tumor cells. It has been reported that miR-93 and miR-193 act to decrease cyclin D1 and induce quiescence in glioblastoma multiforme (GBM), which leads to a lower percentage of cycling cells [72]. In addition, increased levels of miR-23b in breast cancer cells transferred from exosomes suppressed the expression of *MARCKS*, which encodes a protein that facilitates cell cycling [73]. However, in the bone marrow of bladder cancer patients, M1 MΦ-derived exosomes may convert quiescent tumor cells into cycling cells through NF-κB, while M2 MΦ-derived exosomes may contribute to dormancy [74]. This finding exhibits the diverse immunoregulatory roles of immune cells during tumor progression (Table 2).

4. Exosomes in Tumor Immunotherapy

4.1. Exosomes and the Immune Checkpoint Protein PD-1. Programmed death-1 (PD-1), which is expressed on the surface of immune cells, and its ligand programmed cell death-1 ligand 1 (PD-L1), which is expressed in various tumor tissues, are significant immunosuppressive molecules, and their interaction can induce T cell apoptosis and inhibit T cell proliferation, promoting tumor progression. Therefore, inhibitors of PD-1 and PD-L1 are ideal antitumor immune sentinel-related drugs. Recent studies have revealed that exosomes may participate in PD-1-related anti- or protumorigenesis effects. The main obstacle to successful immunotherapy is immunosuppression, and the accumulation of MDSCs is the main mechanism of immunosuppression. It has been reported that oral squamous cell carcinoma-(OSCC-) derived exosomes can regulate MDSCs through the miR-21/PTEN/PD-L1 pathway and suppress the cytotoxicity of $\gamma\delta$ T cells [75]. Chronic lymphocytic leukemia-(CLL-) derived exosomes containing the noncoding Y

Table 2: Exosomes, EMT, and tumor dormancy.

Function	Tumor	Exosome contents	Exosome origin	Effector
EMT	LC	miR-193a-3p, miR-210-3p, miR-5100	BMSCs	STAT3 signaling, vimentin, N-cadherin
	LC	lnc-MMP2-2	/	MMP2
	HNC	miR-21	Tumor	Snail, $CD14^+$ human monocytes
	CRC	miR-128-3p	/	Bmi1/E-cadherin, MRP5
	EC	Lacking miR-148b	CAFs	*DNMT1*
	GC	miR-155-5p	Tumor	E-cadherin, vimentin
Tumor dormancy	GBM	miR-93, miR-193	Tumor	Cyclin D1
	Bladder cancer	/	M1 MΦs	NF-κB p65
	Breast cancer	miR-23b	BMSCs	*MARCKS*

Tumor-type abbreviations: LC: lung cancer; HNC: head and neck cancer; EC: endometrial cancer; CRC: colorectal cancer; GBM: glioblastoma multiforme; GC: gastric cancer. "/" means "not mentioned".

Table 3: Exosomes and immunotherapy.

Tumor type	Exosome contents	Exosome origin	Effector cells	Active components
OSCC	miR-21	Tumor	MDSCs	PTEN/PD-L1
CLL	Y RNA hY4	Tumor	Monocytes	TLR7/CCL2, CCL4, IL-6
HNSCC	PD-L1(+)	Tumor	$CD8^+$ T cells	CD69
HCC	PD-1 antibody	Tumor	DCs	PD-1^+ $CD8^+$ T cells
	miR-138	γδ T cell	$CD8^+$ T cells	PD-1, CTLA-4
	14-3-3ζ	Tumor	TILs	Cell proliferation
	/	DCs	Naive T cells, CTLs	Cell proliferation
Glioblastoma melanoma	/	NK cells	Tumor cells	TNF-α, granzyme B
Neuroblastoma	miR-186	NK cells	Tumor cells	*MYCN*, *TGFBR1*

Tumor-type abbreviations: OSCC: oral squamous cell carcinoma; HCC: hepatocellular carcinoma; HNSCC: head and neck squamous cell carcinoma; CLL: chronic lymphocytic leukemia. "/" means "not mentioned".

RNA hY4 can turn monocytes into procarcinogenic cells through Toll-like receptor 7 (TLR7) signaling, and these cells may release tumor-related cytokines such as C-C motif chemokine ligand 2 (CCL2), CCL4, and IL-6 to generate an inflammatory environment and increase the expression of PD-L1 on the surface of tumor cells to induce immune escape [76]. In addition, exosomes can alter the tumor microenvironment by enveloping PD-L1. Theodoraki et al. showed that PD-L1(+) exosomes in the plasma of patients with HNSCC could inhibit the expression of CD69 on $CD8^+$ T cells, which is a signature of activated T cells [77]. In immunotherapy, treatment with dendritic cells pulsed with TDEs in combination with the PD-1 antibody was shown to enhance the effect of sorafenib, leading to an increased number of PD-1^+ $CD8^+$ T cells, and was more efficient than sorafenib alone [78]. In addition, plasma-derived exosomes containing PD-L1 mRNA may enhance the efficiency of nivolumab and pembrolizumab for the treatment of melanoma and non-small cell lung cancer (NSCLC) [79]. γδT cell-derived exosomes containing miR-138 have potential as a drug delivery system targeting PD-1 and CTLA-4 in $CD8^+$ T cells to increase their cytotoxicity in OSCC [80]. However, more evidence for the feasibility of TDE use for clinical applications is needed (Table 3).

4.2. Exosomes and Adoptive Cell Transfer. Adoptive cell transfer (ACT) therapy uses effector cells and immune molecules to directly attack tumor cells and is called "passive" immunotherapy. One of the main players in ACT therapy is tumor-infiltrating lymphocytes (TILs). TILs are a group of heterogeneous antitumor lymphocytes present in tumor tissues that include $CD8^+$ T cells, some $CD4^+$ T cells, a small number of B cells, NK cells, macrophages, DCs, MDSCs, and Tregs. Recent studies have shown that exosomes are involved in TIL-related immunotherapy. For example, exosomal 14-3-3 protein zeta (14-3-3ζ) shed from HCC cells can be transferred to TILs and interfere with their antitumorigenesis function [81]. In contrast, Li et al. showed that exosomes derived from DCs can boost the proliferation of naive T cells, subsequently increase the number of cytotoxic T lymphocytes (CTLs), and initiate an immune reaction against HCC [82]. In addition, exosomes released by NK cells can function as fuel for the immune killing machines against various tumors, including glioblastoma, melanoma, and other cancers, in a TNF-α- and granzyme B-related manner [83–85]. NK cell-derived exosomes containing miR-186 exert their cytotoxic effects against neuroblastoma by inhibiting the expression of *MYCN* and *TGFBR1* [86]. These findings suggest that immune cell-derived exosomes may contribute

to immune activation against tumors by functioning as unmanned vehicles (Table 3).

5. Summary and Perspectives

Exosomes are attracting increasing interest owing to their significant heterogeneity and their ability to regulate the tumor immune microenvironment. Specifically, tumor cell-derived exosomes may accelerate tumor progression by enhancing immunosuppression and inflammation, increasing oxidative stress, inducing EMT, and regulating tumor dormancy, which may lead to a poor prognosis. In contrast, specific immune cell-derived exosomes can act as tumor inhibitors, suggesting their immense potential for use in cancer immunotherapy. However, various possible strategies for their use remain to be validated. At the gene level, some ncRNAs, including miRNAs, circRNAs, and lncRNAs, have been suggested to be closely associated with carcinogenesis. Therefore, if an siRNA can be transferred to tumors via exosomes, it may be able to subsequently downregulate target mRNA expression and inhibit tumor invasion [87]. From the perspective of cell therapy, the interactions between immune cells and tumor cells via exosomes may allow us to modulate immune reactions against cancers. For example, overexpression of protective contents in immune cell-secreted exosomes may assist in killing the tumor cell. In addition, exosomes can be used as carriers for gene therapy and immune therapy to deliver specific tumor-related molecules, such as PD-1 [88]. However, one obstacle preventing the widespread use of exosomes in clinical practice is that the yield of exosomes from traditional culture is low. Additionally, the methods used for the separation and purification of exosomes, namely, ultracentrifugation and sucrose density gradient centrifugation, are time-consuming and laborious. Further studies on exosomes and modifications are needed to solve these problems and facilitate the clinical application of exosomes as drug carriers in antitumor immunotherapy.

Conflicts of Interest

The authors declare no conflicts of interest.

Authors' Contributions

Tiantian Wang collected the literature and drafted the manuscript. Jie Shen assisted with preparing the figures and tables. Moussa Ide Nasser revised and edited the manuscript. Qingnan He and Mingyi Zhao conceptualized and guaranteed the review. All authors approved the final manuscript as submitted and agree to be accountable for all aspects of the work.

Acknowledgments

This study was funded by grants from the New Xiangya Talent Project of the Third Xiangya Hospital of Central South University (JY201524).

References

[1] W. Tang, K. Fu, H. Sun, D. Rong, H. Wang, and H. Cao, "circRNA microarray profiling identifies a novel circulating biomarker for detection of gastric cancer," *Molecular Cancer*, vol. 17, no. 1, p. 137, 2018.

[2] F. A. Alzahrani, M. A. El-Magd, A. Abdelfattah-Hassan et al., "Potential effect of exosomes derived from cancer stem cells and MSCs on progression of DEN-induced HCC in rats," *Stem Cells International*, vol. 2018, Article ID 8058979, 17 pages, 2018.

[3] T. Huang, C. Song, L. Zheng, L. Xia, Y. Li, and Y. Zhou, "The roles of extracellular vesicles in gastric cancer development, microenvironment, anti-cancer drug resistance, and therapy," *Molecular Cancer*, vol. 18, no. 1, article 62, 2019.

[4] B. Basu and M. K. Ghosh, "Extracellular vesicles in glioma: from diagnosis to therapy," *BioEssays*, vol. 41, no. 7, article 1800245, 2019.

[5] H. Shao, H. Im, C. M. Castro, X. Breakefield, R. Weissleder, and H. Lee, "New technologies for analysis of extracellular vesicles," *Chemical Reviews*, vol. 118, no. 4, pp. 1917–1950, 2018.

[6] B. T. Pan, K. Teng, C. Wu, M. Adam, and R. M. Johnstone, "Electron microscopic evidence for externalization of the transferrin receptor in vesicular form in sheep reticulocytes," *The Journal of Cell Biology*, vol. 101, no. 3, pp. 942–948, 1985.

[7] M. R. Ward, A. Abadeh, and K. A. Connelly, "Concise review: rational use of mesenchymal stem cells in the treatment of ischemic heart disease," *Stem Cells Translational Medicine*, vol. 7, no. 7, pp. 543–550, 2018.

[8] R. J. Simpson, S. S. Jensen, and J. W. E. Lim, "Proteomic profiling of exosomes: current perspectives," *Proteomics*, vol. 8, no. 19, pp. 4083–4099, 2008.

[9] M. W. Klinker, V. Lizzio, T. J. Reed, D. A. Fox, and S. K. Lundy, "Human B cell-derived lymphoblastoid cell lines constitutively produce Fas ligand and secrete $MHCII^{+}FasL^{+}$ killer exosomes," *Frontiers in Immunology*, vol. 5, p. 144, 2014.

[10] S. Phuyal, T. Skotland, N. P. Hessvik et al., "The ether lipid precursor hexadecylglycerol stimulates the release and changes the composition of exosomes derived from PC-3 cells," *The Journal of Biological Chemistry*, vol. 290, no. 7, pp. 4225–4237, 2015.

[11] J. Bergan, T. Skotland, T. Sylvänne, H. Simolin, K. Ekroos, and K. Sandvig, "The ether lipid precursor hexadecylglycerol causes major changes in the lipidome of HEp-2 cells," *PLoS One*, vol. 8, no. 9, article e75904, 2013.

[12] G. N. Shenoy, J. Loyall, C. S. Berenson et al., "Sialic acid-dependent inhibition of T cells by exosomal ganglioside GD3 in ovarian tumor microenvironments," *Journal of Immunology*, vol. 201, no. 12, pp. 3750–3758, 2018.

[13] S. Li, Y. Li, B. Chen et al., "exoRBase: a database of circRNA, lncRNA and mRNA in human blood exosomes," *Nucleic Acids Research*, vol. 46, no. D1, pp. D106–D112, 2018.

[14] L. Huang, X. Zhang, M. Wang et al., "Exosomes from thymic stromal lymphopoietin-activated dendritic cells promote Th2 differentiation through the OX40 ligand," *Pathobiology*, vol. 86, no. 2-3, pp. 111–117, 2019.

[15] C. Li, D. R. Liu, G. G. Li et al., "CD97 promotes gastric cancer cell proliferation and invasion through exosome-mediated MAPK signaling pathway," *World Journal of Gastroenterology*, vol. 21, no. 20, pp. 6215–6228, 2015.

[16] E. J. Park, O. Prajuabjinda, Z. Y. Soe et al., "Exosomal regulation of lymphocyte homing to the gut," *Blood Advances*, vol. 3, no. 1, pp. 1–11, 2019.

[17] H. Valadi, K. Ekström, A. Bossios, M. Sjöstrand, J. J. Lee, and J. O. Lötvall, "Exosome-mediated transfer of mRNAs and microRNAs is a novel mechanism of genetic exchange between cells," *Nature Cell Biology*, vol. 9, no. 6, pp. 654–659, 2007.

[18] X. Dai, C. Chen, Q. Yang et al., "Exosomal circRNA_100284 from arsenite-transformed cells, via microRNA-217 regulation of EZH2, is involved in the malignant transformation of human hepatic cells by accelerating the cell cycle and promoting cell proliferation," *Cell Death & Disease*, vol. 9, no. 5, p. 454, 2018.

[19] A. Yoshimura, K. Sawada, K. Nakamura et al., "Exosomal miR-99a-5p is elevated in sera of ovarian cancer patients and promotes cancer cell invasion by increasing fibronectin and vitronectin expression in neighboring peritoneal mesothelial cells," *BMC Cancer*, vol. 18, no. 1, p. 1065, 2018.

[20] D. Xu, M. Song, C. Chai et al., "Exosome-encapsulated miR-6089 regulates inflammatory response via targeting TLR4," *Journal of Cellular Physiology*, vol. 234, no. 2, pp. 1502–1511, 2019.

[21] Q. Yang, G. K. Nanayakkara, C. Drummer et al., "Low-intensity ultrasound-induced anti-inflammatory effects are mediated by several new mechanisms including gene induction, immunosuppressor cell promotion, and enhancement of exosome biogenesis and docking," *Frontiers in Physiology*, vol. 8, p. 818, 2017.

[22] Z. L. Li, L. L. Lv, T. T. Tang et al., "HIF-1α inducing exosomal microRNA-23a expression mediates the cross-talk between tubular epithelial cells and macrophages in tubulointerstitial inflammation," *Kidney International*, vol. 95, no. 2, pp. 388–404, 2019.

[23] S. L. Tung, D. A. Boardman, M. Sen et al., "Regulatory T cell-derived extracellular vesicles modify dendritic cell function," *Scientific Reports*, vol. 8, no. 1, p. 6065, 2018.

[24] S. Balusu, E. van Wonterghem, R. de Rycke et al., "Identification of a novel mechanism of blood-brain communication during peripheral inflammation via choroid plexus-derived extracellular vesicles," *EMBO Molecular Medicine*, vol. 8, no. 10, pp. 1162–1183, 2016.

[25] L. Chen, F. B. Lu, D. Z. Chen et al., "BMSCs-derived miR-223-containing exosomes contribute to liver protection in experimental autoimmune hepatitis," *Molecular Immunology*, vol. 93, pp. 38–46, 2018.

[26] A. Zhang, G. Wang, L. Jia, T. Su, and L. Zhang, "Exosome-mediated microRNA-138 and vascular endothelial growth factor in endometriosis through inflammation and apoptosis via the nuclear factor-κB signaling pathway," *International Journal of Molecular Medicine*, vol. 43, no. 1, pp. 358–370, 2018.

[27] Z. Li, F. Liu, X. He, X. Yang, F. Shan, and J. Feng, "Exosomes derived from mesenchymal stem cells attenuate inflammation and demyelination of the central nervous system in EAE rats by regulating the polarization of microglia," *International Immunopharmacology*, vol. 67, pp. 268–280, 2019.

[28] X. Li, L. Liu, J. Yang et al., "Exosome derived from human umbilical cord mesenchymal stem cell mediates miR-181c attenuating burn-induced excessive inflammation," *eBioMedicine*, vol. 8, pp. 72–82, 2016.

[29] I. S. Okoye, S. M. Coomes, V. S. Pelly et al., "MicroRNA-containing T-regulatory-cell-derived exosomes suppress pathogenic T helper 1 cells," *Immunity*, vol. 41, no. 3, p. 503, 2014.

[30] M. Alexander, A. G. Ramstead, K. M. Bauer et al., "Rab27-dependent exosome production inhibits chronic inflammation and enables acute responses to inflammatory stimuli," *Journal of Immunology*, vol. 199, no. 10, pp. 3559–3570, 2017.

[31] Y. G. Chen, M. V. Kim, X. Chen et al., "Sensing self and foreign circular RNAs by intron identity," *Molecular Cell*, vol. 67, no. 2, pp. 228–238.e5, 2017.

[32] J. Zhou, Y. Yang, W. W. Wang et al., "Melanoma-released exosomes directly activate the mitochondrial apoptotic pathway of CD4(+) T cells through their microRNA cargo," *Experimental Cell Research*, vol. 371, no. 2, pp. 364–371, 2018.

[33] Y. Ning, K. Shen, Q. Wu et al., "Tumor exosomes block dendritic cells maturation to decrease the T cell immune response," *Immunology Letters*, vol. 199, pp. 36–43, 2018.

[34] B. T. Maybruck, L. W. Pfannenstiel, M. Diaz-Montero, and B. R. Gastman, "Tumor-derived exosomes induce CD8(+) T cell suppressors," *Journal for Immunotherapy of Cancer*, vol. 5, no. 1, p. 65, 2017.

[35] J. Zhou, X. Li, X. Wu et al., "Exosomes released from tumor-associated macrophages transfer miRNAs that induce a Treg/Th17 cell imbalance in epithelial ovarian cancer," *Cancer Immunology Research*, vol. 6, no. 12, pp. 1578–1592, 2018.

[36] L. Ye, Q. Zhang, Y. Cheng et al., "Tumor-derived exosomal HMGB1 fosters hepatocellular carcinoma immune evasion by promoting TIM-1(+) regulatory B cell expansion," *Journal for Immunotherapy of Cancer*, vol. 6, no. 1, p. 145, 2018.

[37] G. J. Li, H. Ding, and D. Miao, "Long-noncoding RNA HOTAIR inhibits immunologic rejection of mouse leukemia cells through activating the Wnt/β-catenin signaling pathway in a mouse model of leukemia," *Journal of Cellular Physiology*, vol. 234, no. 7, pp. 10386–10396, 2019.

[38] H. Zhang, T. Deng, S. Ge et al., "Exosome circRNA secreted from adipocytes promotes the growth of hepatocellular carcinoma by targeting deubiquitination-related USP7," *Oncogene*, vol. 38, no. 15, pp. 2844–2859, 2019.

[39] G. N. Shenoy, J. Loyall, O. Maguire et al., "Exosomes associated with human ovarian tumors harbor a reversible checkpoint of T-cell responses," *Cancer Immunology Research*, vol. 6, no. 2, pp. 236–247, 2018.

[40] J. Lan, L. Sun, F. Xu et al., "M2 macrophage-derived exosomes promote cell migration and invasion in colon cancer," *Cancer Research*, vol. 79, no. 1, pp. 146–158, 2019.

[41] S. Reuter, S. C. Gupta, M. M. Chaturvedi, and B. B. Aggarwal, "Oxidative stress, inflammation, and cancer: how are they linked?," *Free Radical Biology & Medicine*, vol. 49, no. 11, pp. 1603–1616, 2010.

[42] K. L. Cheung, J. H. Lee, T. O. Khor et al., "Nrf2 knockout enhances intestinal tumorigenesis in $Apc^{min/+}$ mice due to attenuation of anti-oxidative stress pathway while potentiates inflammation," *Molecular Carcinogenesis*, vol. 53, no. 1, pp. 77–84, 2014.

[43] N. Javeed, M. P. Gustafson, S. K. Dutta et al., "Immunosuppressive CD14+HLA-$DR^{lo/neg}$ monocytes are elevated in pancreatic cancer and "primed" by tumor-derived exosomes," *OncoImmunology*, vol. 6, no. 1, article e1252013, 2016.

[44] N. Jafarzadeh, Z. Safari, M. Pornour, N. Amirizadeh, M. Forouzandeh Moghadam, and M. Sadeghizadeh, "Alteration

of cellular and immune-related properties of bone marrow mesenchymal stem cells and macrophages by K562 chronic myeloid leukemia cell derived exosomes," *Journal of Cellular Physiology*, vol. 234, no. 4, pp. 3697–3710, 2019.

[45] M. Cai, R. Shen, L. Song et al., "Bone marrow mesenchymal stem cells (BM-MSCs) improve heart function in swine myocardial infarction model through paracrine effects," *Scientific Reports*, vol. 6, no. 1, article 28250, 2016.

[46] M. Murata, R. Thanan, N. Ma, and S. Kawanishi, "Role of nitrative and oxidative DNA damage in inflammation-related carcinogenesis," *Journal of Biomedicine & Biotechnology*, vol. 2012, Article ID 623019, 11 pages, 2012.

[47] S. S. Linton, T. Abraham, J. Liao et al., "Tumor-promoting effects of pancreatic cancer cell exosomes on THP-1-derived macrophages," *PLoS One*, vol. 13, no. 11, article e0206759, 2018.

[48] F. Momen-Heravi and S. Bala, "Extracellular vesicles in oral squamous carcinoma carry oncogenic miRNA profile and reprogram monocytes via NF-κB pathway," *Oncotarget*, vol. 9, no. 78, pp. 34838–34854, 2018.

[49] X. Li, Y. Lei, M. Wu, and N. Li, "Regulation of macrophage activation and polarization by HCC-derived exosomal lncRNA TUC339," *International Journal of Molecular Sciences*, vol. 19, no. 10, article 2958, 2018.

[50] T. Cooks, I. S. Pateras, L. M. Jenkins et al., "Mutant p53 cancers reprogram macrophages to tumor supporting macrophages via exosomal miR-1246," *Nature Communications*, vol. 9, no. 1, p. 771, 2018.

[51] A. Spiegel, M. W. Brooks, S. Houshyar et al., "Neutrophils suppress intraluminal NK cell-mediated tumor cell clearance and enhance extravasation of disseminated carcinoma cells," *Cancer Discovery*, vol. 6, no. 6, pp. 630–649, 2016.

[52] X. Zhang, H. Shi, X. Yuan, P. Jiang, H. Qian, and W. Xu, "Tumor-derived exosomes induce N2 polarization of neutrophils to promote gastric cancer cell migration," *Molecular Cancer*, vol. 17, no. 1, p. 146, 2018.

[53] L. Mao, X. Li, S. Gong et al., "Serum exosomes contain ECRG4 mRNA that suppresses tumor growth via inhibition of genes involved in inflammation, cell proliferation, and angiogenesis," *Cancer Gene Therapy*, vol. 25, no. 9-10, pp. 248–259, 2018.

[54] A. A. Badawy, M. A. El-Magd, and S. A. AlSadrah, "Therapeutic effect of camel milk and its exosomes on MCF7 cells in vitro and in vivo," *Integrative Cancer Therapies*, vol. 17, no. 4, pp. 1235–1246, 2018.

[55] M. D. Sharma, P. C. Rodriguez, B. H. Koehn et al., "Activation of p53 in immature myeloid precursor cells controls differentiation into Ly6c$^+$CD103$^+$ monocytic antigen-presenting cells in tumors," *Immunity*, vol. 48, no. 1, pp. 91–106.e6, 2018.

[56] X. Guo, W. Qiu, Q. Liu et al., "Immunosuppressive effects of hypoxia-induced glioma exosomes through myeloid-derived suppressor cells via the miR-10a/Rora and miR-21/Pten pathways," *Oncogene*, vol. 37, no. 31, pp. 4239–4259, 2018.

[57] G. Sammarco, G. Varricchi, V. Ferraro et al., "Mast cells, angiogenesis and lymphangiogenesis in human gastric cancer," *International Journal of Molecular Sciences*, vol. 20, no. 9, p. 2106, 2019.

[58] H. Xiao, C. Lässer, G. Shelke et al., "Mast cell exosomes promote lung adenocarcinoma cell proliferation – role of KIT-stem cell factor signaling," *Cell Communication and Signaling*, vol. 12, no. 1, p. 64, 2014.

[59] L. Xiong, S. Zhen, Q. Yu, and Z. Gong, "HCV-E2 inhibits hepatocellular carcinoma metastasis by stimulating mast cells to secrete exosomal shuttle microRNAs," *Oncology Letters*, vol. 14, no. 2, pp. 2141–2146, 2017.

[60] H. Dong, W. Wang, R. Chen et al., "Exosome-mediated transfer of lncRNA-SNHG14 promotes trastuzumab chemoresistance in breast cancer," *International Journal of Oncology*, vol. 53, no. 3, pp. 1013–1026, 2018.

[61] M. Kang, M. Ren, Y. Li, Y. Fu, M. Deng, and C. Li, "Exosome-mediated transfer of lncRNA PART1 induces gefitinib resistance in esophageal squamous cell carcinoma via functioning as a competing endogenous RNA," *Journal of Experimental & Clinical Cancer Research*, vol. 37, no. 1, p. 171, 2018.

[62] G. Chen, A. C. Huang, W. Zhang et al., "Exosomal PD-L1 contributes to immunosuppression and is associated with anti-PD-1 response," *Nature*, vol. 560, no. 7718, pp. 382–386, 2018.

[63] P. Kanlikilicer, R. Bayraktar, M. Denizli et al., "Exosomal miRNA confers chemo resistance via targeting Cav1/p-gp/M2-type macrophage axis in ovarian cancer," *eBioMedicine*, vol. 38, pp. 100–112, 2018.

[64] H. Li, C. Yang, Y. Shi, and L. Zhao, "Exosomes derived from siRNA against GRP78 modified bone-marrow-derived mesenchymal stem cells suppress sorafenib resistance in hepatocellular carcinoma," *Journal of Nanobiotechnology*, vol. 16, no. 1, article 103, 2018.

[65] X. Zhang, B. Sai, F. Wang et al., "Hypoxic BMSC-derived exosomal miRNAs promote metastasis of lung cancer cells via STAT3-induced EMT," *Molecular Cancer*, vol. 18, no. 1, p. 40, 2019.

[66] D. M. Wu, S. H. Deng, T. Liu, R. Han, T. Zhang, and Y. Xu, "TGF-β-mediated exosomal lnc-MMP2-2 regulates migration and invasion of lung cancer cells to the vasculature by promoting MMP2 expression," *Cancer Medicine*, vol. 7, no. 10, pp. 5118–5129, 2018.

[67] C. H. Hsieh, S. K. Tai, and M. H. Yang, "Snail-overexpressing cancer cells promote M2-like polarization of tumor-associated macrophages by delivering MiR-21-abundant exosomes," *Neoplasia*, vol. 20, no. 8, pp. 775–788, 2018.

[68] C. Wang, L. Chen, Y. Huang et al., "Exosome-delivered TRPP2 siRNA inhibits the epithelial-mesenchymal transition of FaDu cells," *Oncology Letters*, vol. 17, no. 2, pp. 1953–1961, 2019.

[69] T. Liu, X. Zhang, L. Du et al., "Exosome-transmitted miR-128-3p increase chemosensitivity of oxaliplatin-resistant colorectal cancer," *Molecular Cancer*, vol. 18, no. 1, article 43, 2019.

[70] B. L. Li, W. Lu, J. J. Qu, L. Ye, G. Q. Du, and X. P. Wan, "Loss of exosomal miR-148b from cancer-associated fibroblasts promotes endometrial cancer cell invasion and cancer metastasis," *Journal of Cellular Physiology*, vol. 234, no. 3, pp. 2943–2953, 2018.

[71] M. Wang, R. Qiu, S. Yu et al., "Paclitaxel-resistant gastric cancer MGC-803 cells promote epithelial-to-mesenchymal transition and chemoresistance in paclitaxel-sensitive cells via exosomal delivery of miR-155-5p," *International Journal of Oncology*, vol. 54, no. 1, pp. 326–338, 2018.

[72] J. L. Munoz, N. D. Walker, S. Mareedu et al., "Cycling quiescence in temozolomide resistant glioblastoma cells is partly explained by microRNA-93 and -193-mediated

decrease of cyclin D," *Frontiers in Pharmacology*, vol. 10, p. 134, 2019.

[73] M. Ono, N. Kosaka, N. Tominaga et al., "Exosomes from bone marrow mesenchymal stem cells contain a microRNA that promotes dormancy in metastatic breast cancer cells," *Science Signaling*, vol. 7, no. 332, p. ra63, 2014.

[74] N. D. Walker, M. Elias, K. Guiro et al., "Exosomes from differentially activated macrophages influence dormancy or resurgence of breast cancer cells within bone marrow stroma," *Cell Death & Disease*, vol. 10, no. 2, p. 59, 2019.

[75] L. Li, B. Cao, X. Liang et al., "Microenvironmental oxygen pressure orchestrates an anti- and pro-tumoral γδ T cell equilibrium via tumor-derived exosomes," *Oncogene*, vol. 38, no. 15, pp. 2830–2843, 2019.

[76] F. Haderk, R. Schulz, M. Iskar et al., "Tumor-derived exosomes modulate PD-L1 expression in monocytes," *Science Immunology*, vol. 2, no. 13, 2017.

[77] M. N. Theodoraki, S. S. Yerneni, T. K. Hoffmann, W. E. Gooding, and T. L. Whiteside, "Clinical significance of PD-L1(+) exosomes in plasma of head and neck cancer patients," *Clinical Cancer Research*, vol. 24, no. 4, pp. 896–905, 2018.

[78] S. Shi, Q. Rao, C. Zhang, X. Zhang, Y. Qin, and Z. Niu, "Dendritic cells pulsed with exosomes in combination with PD-1 antibody increase the efficacy of sorafenib in hepatocellular carcinoma model," *Translational Oncology*, vol. 11, no. 2, pp. 250–258, 2018.

[79] M. Del Re, R. Marconcini, G. Pasquini et al., "PD-L1 mRNA expression in plasma-derived exosomes is associated with response to anti-PD-1 antibodies in melanoma and NSCLC," *British Journal of Cancer*, vol. 118, no. 6, pp. 820–824, 2018.

[80] L. Li, S. Lu, X. Liang et al., "γδTDEs: an efficient delivery system for miR-138 with anti-tumoral and immunostimulatory roles on oral squamous cell carcinoma," *Molecular Therapy - Nucleic Acids*, vol. 14, pp. 101–113, 2019.

[81] X. Wang, H. Shen, G. Zhangyuan et al., "14-3-3ζ delivered by hepatocellular carcinoma-derived exosomes impaired anti-tumor function of tumor-infiltrating T lymphocytes," *Cell Death & Disease*, vol. 9, no. 2, article 159, 2018.

[82] J. Li, S. Huang, Z. Zhou et al., "Exosomes derived from rAAV/AFP-transfected dendritic cells elicit specific T cell-mediated immune responses against hepatocellular carcinoma," *Cancer Management and Research*, vol. 10, pp. 4945–4957, 2018.

[83] A. Shoae-Hassani, A. A. Hamidieh, M. Behfar, R. Mohseni, S. A. Mortazavi-Tabatabaei, and S. Asgharzadeh, "NK cell-derived exosomes from NK cells previously exposed to neuroblastoma cells augment the antitumor activity of cytokine-activated NK cells," *Journal of Immunotherapy*, vol. 40, no. 7, pp. 265–276, 2017.

[84] L. Zhu, X. J. Li, S. Kalimuthu et al., "Natural killer cell (NK-92MI)-based therapy for pulmonary metastasis of anaplastic thyroid cancer in a nude mouse model," *Frontiers in Immunology*, vol. 8, p. 816, 2017.

[85] L. Zhu, S. Kalimuthu, P. Gangadaran et al., "Exosomes derived from natural killer cells exert therapeutic effect in melanoma," *Theranostics*, vol. 7, no. 10, pp. 2732–2745, 2017.

[86] P. Neviani, P. M. Wise, M. Murtadha et al., "Natural killer–derived exosomal miR-186 inhibits neuroblastoma growth and immune escape mechanisms," *Cancer Research*, vol. 79, no. 6, pp. 1151–1164, 2019.

[87] T. Yang, B. Fogarty, B. LaForge et al., "Delivery of small interfering RNA to inhibit vascular endothelial growth factor in zebrafish using natural brain endothelia cell-secreted exosome nanovesicles for the treatment of brain cancer," *The AAPS Journal*, vol. 19, no. 2, pp. 475–486, 2017.

[88] N. Arrighetti, C. Corbo, M. Evangelopoulos, A. Pasto, V. Zuco, and E. Tasciotti, "Exosome-like nanovectors for drug delivery in cancer," *Current Medicinal Chemistry*, vol. 25, 2018.